uOttawa

L'Université canadienne
Canada's university

FACULTÉ DES ÉTUDES SUPÉRIEURES ET POSTOCTORALES

uOttawa

L'Université canadienne
Canada's university

FACULTY OF GRADUATE AND POSDOCTORAL STUDIES

Soroush Sorourian
AUTEUR DE LA THÈSE / AUTHOR OF THESIS

M.A.Sc. (Civil Engineering)
GRADE / DEGREE

Department of Civil Engineering
FACULTÉ, ÉCOLE, DÉPARTEMENT / FACULTY, SCHOOL, DEPARTMENT

Modelling of Wave and Current Induced Concentration of Cohesive Sediments

TITRE DE LA THÈSE / TITLE OF THESIS

Dr. I. Nistor
DIRECTEUR (DIRECTRICE) DE LA THÈSE / THESIS SUPERVISOR

Dr. R. Townsend
CO-DIRECTEUR (CO-DIRECTRICE) DE LA THÈSE / THESIS CO-SUPERVISOR

EXAMINATEURS (EXAMINATRICES) DE LA THÈSE / THESIS EXAMINERS

Dr. C. Rennie

Dr. S. Vanapalli

Dr. P. Van Geel

Gary W. Slater
Le Doyen de la Faculté des études supérieures et postdoctorales / Dean of the Faculty of Graduate and Postdoctoral Studies

MODELLING OF WAVE AND CURRENT INDUCED CONCENTRATION OF COHESIVE SEDIMENTS

by

Soroush Sorourian

A thesis

submitted under the supervision of

Dr. Ioan Nistor

Dr. Ronald Townsend

In fulfillment of the

requirements for the degree of

Master of Applied Science

in

Civil Engineering

Department of Civil Engineering

University of Ottawa

Ottawa, Canada

K1N 6N5

May, 2007

Your file Votre référence
ISBN: 978-0-494-34111-7
Our file Notre référence
ISBN: 978-0-494-34111-7

ABSTRACT

The current research deals with the numerical modelling of cohesive sediment transport under the action of waves in coastal regions. A new mathematical model for the simulation of mud concentration profiles is proposed and developed. The model aims to improve the prediction of cohesive sediment transport compared to the very few mud transport models currently available, by incorporating several new physical phenomena, such as electrochemical particle cohesion, in the calculation of sediment entrainment, transport and deposition.

Cohesive sediments are also important in terms of environmental impacts, particularly due to their association with contaminants that attach to them. Processes that govern the behaviour of cohesive sediments differ significantly from those governing non-cohesive sediments. In addition to the physical complexities of cohesive sediment processes, chemical aspects must be considered as well. In this sense, the electrochemical behaviour of cohesive sediments plays an important role as a stabilizing force against the eroding shear force. All of these factors point to the need for a multi-disciplinary approach in dealing with cohesive sediments.

Several theoretical concepts were incorporated in order to better estimate the sediment erosion process and enhance the accuracy of the suspended sediment concentration prediction. Firstly, unlike the case of any previous models, the electrochemical force between cohesive sediment particles has been considered. Secondly, a new approach was used to relate bed resistance to soil characteristics. Thirdly, the prediction of the bed shear stress was refined by relating the wave friction factor to parameters of the model such as bed roughness and median grain diameter. Relating the wave friction factor to grain diameter is incorporated for the first time in cohesive sediment transport models. Fourthly, the time-dependent erosion rate was also considered for the first time in cohesive sediment transport models.

The numerically simulated suspended sediment concentration profiles were compared with experimental data. The results of the proposed model agree well with the experimental data, as soon as a steady state condition is achieved. The results of the new numerical models

provide a better estimation of the suspended sediment concentration profile compared to the initial model.

To

the Baha'i youth in Iran

who are deprived of higher education

ACKNOWLEDGEMENTS

I would like to express my deepest appreciation to Dr. Ioan Nistor and Dr. Ronald Townsend, for their unflagging, and supportive guidance, suggestions, stimulating discussion and inspiration. Their constant patience and invaluable help, combined with a high level of generosity and intelligence, made their contributions to the present thesis unaccountable. They guided the author's steps into the world of scientific research.

I wish to acknowledge my heartfelt gratitude to the Baha'i community of Canada. I am deeply indebted to a large group of people who supported and assisted me with their unsurpassed love, enthusiasm, optimism and confidence. This study could not have been done without such high quality support. Space prevents me from listing all of them, but a few stand out as worthy of mention: Mrs. Sherri Yazdani and Mr. Ted Slavin.

The author would also like to thank Dr. Ashish J. Mehta for his continuously great advice, support and assistance. Appreciation is extended to all the members, colleagues and academic staff of Water Resources, Department of Civil Engineering of the University of Ottawa. The author would also like to extend deep thanks to all other members of the University of Ottawa, both staff and students with whom he came into contact, for their constant assistance, patience and inspiration.

Finally yet importantly, the author is unable to befittingly thank his family for their most sincere and loving support and encouragement. Accomplishment of this study would have been impossible without their gracious and selfless assistance.

TABLE PF CONTENTS

LIST OF FIGURES

LIST OF TABLES

LIST OF SYMBOLS

Symbol	Description
a_b	water particle excursion
a_r	empirical coefficient
b_r	empirical coefficient
$c(z,t), c$	suspended sediment concentration
c_1	minimum concentration for flocculation settling
c_2	maximum concentration for flocculation settling
c_3	maximum concentration for hindered settling
C_D	drag coefficient
c_u	sediment remoulded shear stress
c_w	wave celerity
c_v	consolidation coefficient
d_0	near-bed orbital diameter of wave motion
D_d	dimensionless grain diameter
d_f	floc diameter
D_m	molecular diffusion coefficient
d_s	median particle diameter
E	erosion rate
E'	erosion velocity

E_*	non-dimensional entrainment rate
E_0	erosion constant
E_A	attractive inter-particle energy
E_R	repulsive inter-particle energy
E_T	total potential energy
F	mass flux of sediment
f_c	current friction factor
F_A	attractive cohesion force
F_R	repulsive cohesion force
F_T	total cohesion force
F_n	net resuspension flux
f_w	wave friction factor
g	gravitational acceleration
G	elastic modulus
G_1	elastic modulus
G_2	elastic modulus
H	wave height
h	water depth
H_b	interface amplitude
h_b	mud height
h_p	plunk constant
k	wave number

k_b	Boltzmann constant
k_1	empirical coefficient
k_2	empirical coefficient
k_3	empirical coefficient
k_s	Nikuradse roughness coefficient
k_y	yield strength
L	wave length
m	empirical coefficient
M	erosion constant
m_s	eroded mass
M_1	erosion constant
M_2	erosion constant
n	Manning coefficient
Q	non-dimensional buoyancy flux
R_i	gradient Richardson number
R_{ic}	critical Richardson number
R_{ig}	global Richardson number
R_w	wave Reynolds number
S	relative density of sediment
s	empirical parameter
$s_{\max}$	empirical coefficient
T	wave period

t	time
t_0	initial time
t_{total}	total simulation time
u	velocity component in x-direction
$\overline{u}$	time-averaged velocity in x-direction
$\widetilde{u}$	wave oscillating velocity in x-direction
u'	turbulent fluctuation velocity in x-direction
U	depth-averaged current velocity
u_b	maximum orbital velocity
u_e	downward propagation of velocity
u_*	maximum bed shear velocity
U_{wcr}	critical peak near-bottom orbital velocity
v	horizontal velocity in y-direction
$\overline{v}$	time-averaged velocity in y-direction
$\widetilde{v}$	wave oscillating velocity in y-direction
v'	turbulent fluctuation velocity in y-direction
w	horizontal velocity in z-direction
W	water content
$\widetilde{w}$	wave oscillating velocity in y-direction
w'	turbulent fluctuation velocity in y-direction
W_{ds}	dimensionless settling velocity
W_L	liquid limit of mud
w_s	sediment settling velocity

w_{s2}	maximum settling velocity
W_{sf}	free settling velocity
x	horizontal coordinate in wave direction
y	horizontal coordinate perpendicular to wave direction
z	vertical coordinate
α	empirical coefficient
α_0	stratified damping coefficient
α_1	empirical coefficient
α_4	entrainment coefficient
α_c	empirical coefficient
α_w	non-dimensional wave diffusion constant
χ	electrochemical anchoring coefficient
β	Shield parameter
β_0	stratified damping coefficient
β_1	stratified damping coefficient
β_4	empirical coefficient
β_c	stratified damping coefficient
β_e	local erosion coefficient
γ	rate of increase of resistance with respect to depth
γ_0	shear strain amplitude
γ_1	empirical coefficient
γ_s	shear strain

δ	boundary layer thickness
δ_1	empirical coefficient
Δb	buoyancy step across mud water interface
ε_{sn}	neutral diffusion coefficient
ε_{nw}	neutral diffusion coefficient due to wave motion
ε_{nc}	neutral diffusion coefficient due to current motion
ε_s, ε_{sz}	diffusion coefficient in z-direction
ε_{sx}	diffusion coefficient in x-direction
ε_{sy}	diffusion coefficient in y-direction
ζ_1	non-dimensional bed-dependent constant
η_*	non-dimensional viscosity of mud
η_1	water surface elevation
η_2	mud surface elevation
θ	absolute temperature
θ_{wc}	dimensionless critical near-bottom orbital velocity
κ	von Karman's constant
μ, μ_1	water dynamic viscosity
μ'	dynamic viscosity
μ''	second dynamic viscosity
μ^*	complex dynamic viscosity
μ_2	mud dynamic viscosity
μ_p	apparent viscosity

ν	fluid kinematic viscosity
ν_e	equivalent kinematic viscosity
ν_t	fluid turbulent eddy viscosity coefficient
ξ_1	non-dimensional bed-dependent constant
Π_D	second invariant of shear strain
ρ	water density
ρ_D	bed dry density
ρ_f	floc density
ρ_m	density of fluid mud
ρ_s	sediment granular density
ρ_s'	excess density of sediment
σ	wave frequency
τ	applied stress
τ_0	amplitude of applied stress
τ_b	bed shear stress
τ_{bw}	amplitude of oscillatory bed shear due to waves
τ_{bc}	amplitude of oscillatory bed shear due to current
τ_c	critical shear stress for erosion
τ_{c0}	bed shear strength at $t=t_0$
τ_{dep}	characteristic deposition shear stress
τ_m	mean bed shear stress for combined wave-current system

τ_{max}	maximum bed shear stress for combined wave-current system
τ_{rms}	root-mean square bed shear stress for combined wave-current system
τ_y	vane shear strength
ϕ	solid volume fraction
Φ	density stratification correction factor
ϕ_0	phase shift
ϕ_1	bed packing angle
ϕ_c	critical solid volume fraction

1 INTRODUCTION

A large part of the earth is covered with cohesive sediments or mud. Cohesive sediments are important for a number of reasons:

- Cohesive sediments are a valuable resource. Great civilizations formed and flourished in fertile lands, due to deposits of natural cohesive sediments by rivers along their flood plain. The civilizations of Egypt along the Nile River, Mesopotamia along the Euphrates and Tigris, India along the Indus, and China along the Yellow River are all illustrative examples. Even today, the most fertile and productive areas are the ones formed around river deltas such as the Mississippi delta.
- Cohesive sediments are also an important construction material. Materials such as plaster and brick are made of these types of sediments.
- In recent decades, association of contaminants with cohesive sediments has been a growing concern. Organic and inorganic pollutants can easily adhere to clay particles, and be transported or accumulated, causing damage to entire ecosystems.
- Cohesive sediments are easily transported in suspension and tend to accumulate in still water regions, such as navigation channels and harbour basins, in thick layers, up to several meters. This can cause severe management problems by burying benthic communities, impeding navigation, reducing water quality and contributing to eutrophication. Maintenance and dredging of navigation channels are costly, especially when the sediments to be removed are contaminated. For example, the Port of Rotterdam has to dredge about 10 million cubic meter annually to safeguard navigation (Winterwerp and van Kesteren, 2003). In some ports and channels, the accumulation of mud is so rapid that it exceeds the capacity of the available dredges, such in the case of Savannah Port, United States (CTH, 1971); Europoort, the Netherlands (Parker and Kirby, 1982) and Atchafalaya Bar Channel, Louisiana (Teeter *et al.*, 2003). The accumulation of organic contaminants in estuaries like St. Lucia Estuary, Florida is considered to be the main cause of water quality reduction in this area (SFWMD, 2004).

- Thick layers of cohesive sediments are also found on the slopes of continental shelves. These layers can become mobile because of natural events (such as earthquakes and tsunami's) or human disturbance (i.e. pipelines), and can cause serious hazards such as damaging pipelines and deep-sea cables.

1.1 Significance of the Study

Cohesive sediments are those in which attractive forces, such as electrochemical forces, dominate the gravity force in resisting against suspension (CEM, 2002). Size, composition and plasticity are the factors by which these sediments are recognized. The cohesive nature of sediments appears at the grain size of about 0.074 mm (74 μm; φ>3.76) (Dean and Dalrymple, 2002). The cohesive behaviour of fine sediments becomes very important for grain sizes of less than 0.02 mm (Taki, 2001; Mehta and Li, 2003). However, even a small percentage of clay in the bed material is enough for cohesion to dominate (10% according to Raudkivi, 1998 and 25% according to Torfs, 1997).

In coastal studies and management, numerous phenomena have to be considered. However, as Kamphuis (2000) states, "...the most important consideration and ultimate design criterion in a design for the coastal zone is often the movement of sediment". Sediment transport causes erosion or accretion of a beach, which may alter its bathymetric profile. These processes significantly affect the appearance of a beach and, in particular, its infrastructure: warehouses, hotels, etc. This effect may lead to the need to design and construct costly structures such as breakwaters in order to protect the beach against erosion. Sediment transport in coastal areas is still an ongoing challenge for researchers to overcome. The main reasons for this challenge include the following elements.

Firstly, sediment transport is closely related to the time-dependent velocity field, including the turbulent characteristics of the surf zone. Time-averaged or depth-integrated equations, which are most commonly used to compute the velocity field, are still employed in many of the sediment transport models. However, erroneous prediction of the flow-induced sediment transport emphasises the need for more accurate numerical models. Furthermore, theoretical difficulties in formulating, solving and modelling turbulence makes this problem even more complex.

Secondly, the nature of waves is irregular. However, most of the sediment transport models consider wave input to be in the form of regular waves. These models tend to give good results in the case of comparisons with laboratory data in which regular waves are used. However, the use of such models is limited when it comes to practical applications since wave randomness, the true state of the ocean waves, is often not included. Incorporating complicated random wave models with hydrodynamic models is difficult due to the theoretical and computational complexities involved.

The processes that govern the behaviour of cohesive sediments differ significantly from those governing non-cohesive sediments, making the understanding and prediction of sediment transport even more complicated. Cohesive sediments usually flocculate, whereas non-cohesive sediments travel as individual particles. Therefore, unlike non-cohesive particles, the size and specific weight of cohesive sediments are functions of the flow field (van Leussen 1988; Krishnappan *et al.* 1992; Lau and Krishnappan 1994; Krishnappan and Engel 1997). Moreover, the transport of silt and clay also interacts with the movement of sand through the same area, making sediment transport in such areas very complex (Kamphuis, 2000). In addition to the physical complexities of cohesive sediment processes, chemical aspects must be considered as well. The electrochemical forces between sediment particles play an important role as a stabilizing force against the eroding shear force. On the other hand, cohesive sediments are important in terms of environmental impacts due to their association with contaminants. All of these factors point to the need for a multi-disciplinary approach in studies that seek a better understanding of these phenomena.

Physical modelling is expensive, particularly for the case of cohesive sediments. Moreover, proper material can not be easily provided in order to simulate cohesive sediments at a smaller scale. Therefore, especial attention is given to numerical modelling.

The above-mentioned challenges have been the motivation for the present study dealing with the transport of cohesive sediments. However, the existing numerical models are empirical in form and are often site-specific at the present stage. The present models also lack the interdisciplinary aspect of cohesive sediment behaviour, such as chemical and biological processes. This emphasises the importance of incorporating these new aspects in order to reduce the dependence of the present models on the site-specific empiricism.

1.2 Objectives of the Study

The purpose of the current research is to better estimate the non-equilibrium suspended cohesive sediment concentration profiles under waves and currents by a newly proposed numerical model. This model includes both a cohesive sediment concentration model and a wave-mud interaction model. The erosion, deposition, diffusion and entrainment processes are also included in the model. Special attention is focused on modeling of the erosion process of cohesive sediments. The objectives of the present study are:

1. To improve the estimation of sediment concentration under waves and currents by incorporating the effect of electrochemical forces between cohesive sediment particles during the erosion process.
2. To employ a new formulation to relate the critical shear strength of the bed to the vane shear stress, which is easier to define.
3. To improve the accuracy of the calculated bed shear stress under waves, by incorporating the wave friction factor.
4. To improve the rate of cohesive sediment transport by applying a time-dependent concept in the formulation of the erosion rate under waves and currents.

1.3 Scope of the Study

The present research encompasses the following assumptions:

- The linear wave theory is used in this study.
- The model is 1-D (one-dimensional) and it is wave-averaged.
- The initial bed is assumed horizontal.

1.4 Organization of Dissertation

The present thesis has been organized in four chapters. A brief description of the content, structured on the chapters, is presented below.

Chapter 1 describes the general framework of the thesis, explains the significance of the study and establishes the research objectives and the scope of the research.

Chapter 2 reviews the state-of-the-art knowledge on cohesive sediment transport in coastal areas. An extensive literature review is conducted on the major issues addressed by the present work. Several theoretical concepts and explanations are presented: properties of cohesive sediments, suspended sediment concentration theory, the cohesive sediment processes, as well as explanations on the bed shear stress, mud rheology and on the wave-mud interaction.

Chapter 3 describes the suspended sediment concentration mathematical and numerical model formulation, and the wave-mud interaction mathematical and numerical model. This chapter includes the bulk of the research contributions for improvement of the model as well. Details of the laboratory and field data are also explained in this chapter.

Chapter 4 includes comparisons between results of the numerical model and of the available experimental data. A summary of the present study, as well as conclusions and recommendations for further studies conclude this chapter.

2 LITERATURE REVIEW

2.1 Cohesive sediments

2.1.1 Sediment properties

Cohesive sediments can be categorized according to their grain size, composition, and plasticity. The first two properties are particularly important for coastal and estuarine studies (Mehta and Li, 2003). Table 2.1 shows a classification of the fine-grained sediments with respect to grain size.

Table 2.1 Size and textural classification of sediments and their relation to cohesion (Mehta and Li, 2003).

SIZE RANGE (*mm*)	TEXTURAL DESCRIPTION	DESCRIPTION	CHARACTERISTICS
>0.062	Coarse-grained	Very fine sand	Cohesionless
0.062 to 0.040	Fine-grained	Coarse silt	Practically cohesionless
0.040 to 0.020	Fine-grained	Medium silt	Cohesion increasingly important with decreasing size
0.020 to 0.002	Fine-grained	Fine silt/ very fine silt/ clay	Cohesion important
0.002>	Fine-grained	clay	Cohesion very important

From the point of view of their composition, three major factors are important when defining cohesive sediments: inorganic mineral content, organic content, and biochemicals (Mehta, 1991).

The inorganic part of fine sediments can be constituted of clay or non-clay minerals. Clays are crystal-shaped minerals that consist of silica (SiO_2), alumina (Al_2O_3), iron, alkalis (Na^+, K^+) and alkalines (Ca^{++}, Mg^{++}) and they have ability to absorb certain anions and cations (Mehta and Li, 2003). Usually cohesion of clays is defined in terms of the cation exchange capacity (CEC), which is milliequivalants of Na^+ in terms of Na_2O per 100 gram of clay (Grim, 1968). Another important factor for clay is its critical salinity. If the water's salinity exceeds the sediment critical salinity, the floc size, density, and strength change as well (Ariathurani *et al.* 1977). The CEC and the critical salinity of three types of sediments are provided in Table 2.2. However, salinity higher than 10% does not change the properties of the floc significantly (Krone, 1962).

Table 2.2 Three common clay minerals, CEC and critical salinity for flocculation (Mehta and Li, 2003).

CLAY MINERAL	CEC (MEQ/100G)	CRITICAL SALINITY (PPT)
Kaolinite	3-15	0.6
Illite	10-40	1.1
Smectite (or Montmorillonite)	80-150	2.4

For non-clay materials in coastal areas, Mehta and Li (2003) mentioned quartz and carbonate to be the most significant ones in terms of sediment transport under waves and currents.

2.1.2 Suspended sediment concentration profile

The qualitative description of the suspended sediment concentration profile of cohesive sediments is presented in Figure 2.1. In this description, the term "mobile" is used to mean moving horizontally. The upper layer is called "mixed layer mobile suspension". In this layer, the concentration is so low that the water-sediment mixture can be expressed in the form of a Newtonian fluid. The turbulent mass diffusion is neutral, i.e., the vertical diffusion

of sediments is not damped by the negative buoyancy due to the concentration gradient (Mehta, 1989). The settling velocity is independent of the sediment concentration, i.e., the *free settling* mode dominates.

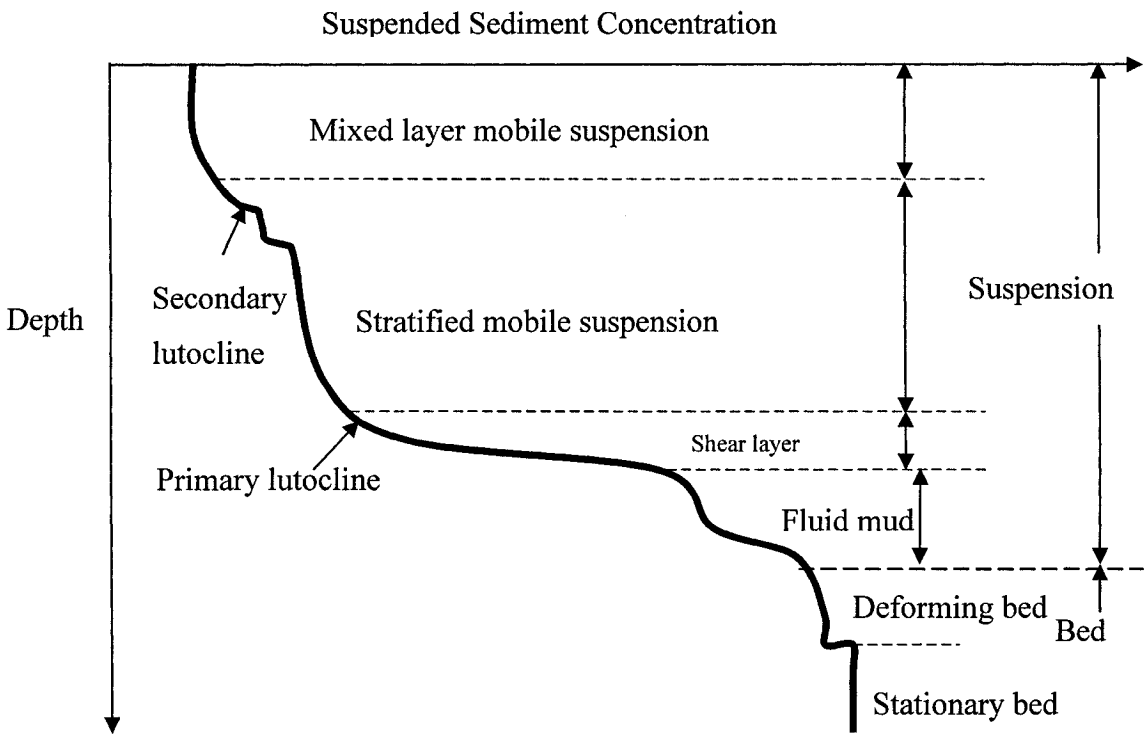

Figure 2.1 Vertical mixture density profile classification (after Mehta and Li, 2003).

In the "stratified mobile layer", the non-Newtonian behaviour of water-sediment mixture increases with an increase in sediment concentration. Moreover, the increase in concentration leads to more inter-particle collisions and, therefore, generates larger flocs. The size and density of flocs increases with depth and the *flocculation settling* mode is dominating in this layer. As a result of interaction between diffusion and settling velocity of particles, horizontal gradients are formed, known as *secondary lutoclines* (Mehta and Li, 2003).

Below the stratified layer, a sudden increase in the concentration of sediments within a relatively thin shear layer is observed, known as the *primary lutocline*. Unlike secondary lutoclines, the primary lutocline is observed even under significant flow-induced forcing. The

reason is that the sharp concentration gradient enhances the buoyancy stabilization and prevents the turbulent flow from dissipating the lutocline.

Below the primary lutocline, the settling velocity decreases rapidly due to *hindered settling*. Hindered settling occurs when sediment concentration exceeds about 20 kg/m^3 and the pore water becomes entrapped in the sediment network and cannot escape upward easily. Moreover, the presence of mucous diatoms, which lubricate the sediments, block the passage of pore water and prevent further consolidation (Willis and Krishnappan, 2004). Fluid mud tends to move horizontally due to wave or gravity forces in the form of a completely non-Newtonian fluid. During the flow, the friction between the lower and upper layers of mud provides drainage opportunities, which can lead to consolidation or resuspension of sediments (Willis and Krishnappan, 2004).

The lowest layer, below the fluid mud, can be assumed to be the stationary bed; based on its possibility of deformation, this layer can be divided into two sub-layers. Sediment concentration in these sub-layers does not significantly change with respect to an increase in depth. In the bed deforming bed layer, the consolidation process dominates the fluidization.

2.2 Cohesive sediment transport processes

A general scheme of the concentration and with respect to depth is depicted in Figure 2.2.

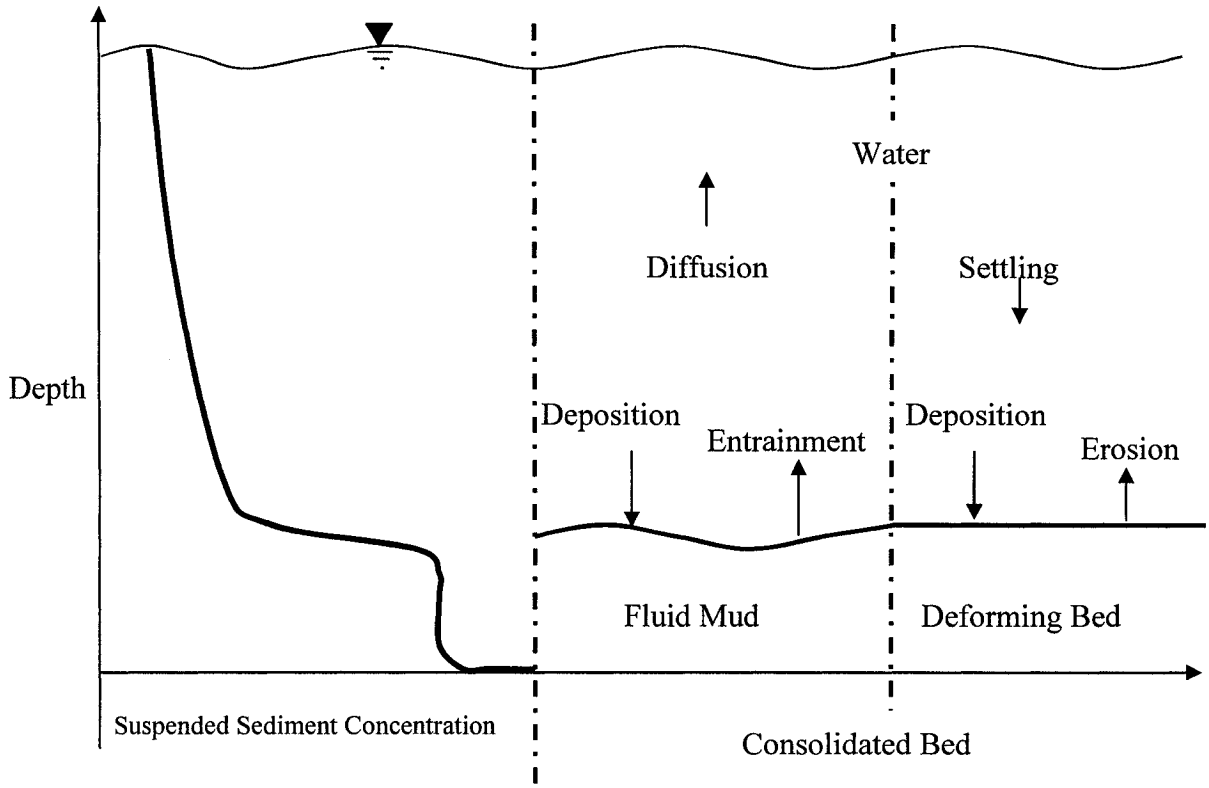

Figure 2.2 Sediment transport flux determining sediment concentration profile dynamics.

The first phenomena to be considered are entrainment and deposition, which occur at the boundary of fluid mud and water-sediment mixture. Entrainment of the fluid mud depends on the turbulence caused by eddies and the sediments are carried above the luctoline layer by turbulent diffusion. When all the fluid mud layers get entrained, erosion occurs right from the stable (stationary) bed. Erosion can happen either gradually or abruptly, due to failure of the bed layer.

Deposition is the opposite mechanism of erosion. Deposition flux depends on the settling velocity, the concentration of sediment in suspension and the bed shear stress. For a specific concentration and settling velocity, the highest deposition rate is observed in the absence of the flow field and diminishes with an increase in flow (Mehta and Li, 2003).

The last process to be discussed is the "fluidization". It occurs due to the weakening of the bed due to wave forces. By an increase in wave forces, the magnitude of shear stress increases and effective normal stress decreases and finally becomes zero at the fluidization

point (Mehta and Li, 2003). However, after wave action stops, a dewatering process starts as a function of the weight of the layers and cohesive forces. This process is called consolidation.

2.3 Erosion rate and resuspension

Erosion is one of the major factors in sediment resuspension, sediment transport and beach deformation of cohesive beaches. It is also one of the most studied aspects of the cohesive sediment transport. Some researchers employed theoretical approaches in order to formulate this phenomenon (like Dade *et al.*, 1992); some researchers used *in-situ* flume studies (Maa and Lee, 1997; Maa *et al.*, 1998,) or laboratory flume studies (van Leussen and Winterwerp, 1990; Maa and Mehta, 1986; Sheng, 1986; Sheikh *et al.*, 1998), while others used observations of suspended sediment variability in order to examine the factors controlling the rate of erosion (Sanford and Helka, 1993; Sanford *et al.*, 1991).

Erosion of cohesive sediments occurs when hydrodynamic erosive forces exceed gravitational, cohesive or frictional forces. This phenomenon is called **surface erosion**. The second condition, when flow-induced shear stress exceeds bed bulk shear stress, is called **mass erosion** (Mehta, 1986). Therefore, shear stress generated by waves or currents is the preeminent factor in the bed erosion. Other factors, such as electrochemical force, density, water content and particle size contribute to the resistance against erosion.

The mathematical explanation of the erosion rate of cohesive sediments can be categorized into three categories:

2.3.1 Power law formulations

The general form of power law equations is as follows:

$$E = M[\tau_b - \tau_c(z)]^n \qquad (2.1)$$

in which E is the erosion rate, τ_b is the bed shear stress, τ_c is the critical shear stress, M is the erosion rate constant and n is an exponent. This type of formula is used to describe depth-limited type of erosion in which bed strength increases with depth and ultimately halts

the erosion process. Some of the proposed equations for erosion rate under this category are provided for reference:

Amos *et al.*, (1992) conducted some experiments on Bay of Fundy and proposed the following formula for erosion rate (r^2=0.69, n=72):

$$E = 4.9\times10^{-4}\left(\tau_b - \tau_c(z)\right)^{0.81} \qquad (2.2)$$

Jepsen *et al.*, (1997) reported the erosion rate to be a function of the bulk density:

$$E = A\rho_m^m \tau_b^n \qquad (2.3)$$

in which A, m and n are empirical coefficients, ρ_m is the bed bulk density defined in terms of water content as:

$$\rho_m = \frac{\rho_s \rho_w}{\rho_w + (\rho_s - \rho_w)W} \qquad (2.4)$$

in which ρ_m is the bed bulk density, ρ_w is the water density, ρ_s is the sediment density and W is the water content defined as the ratio of mass of the water over mass of the grains. Coefficients A, n and m for some rivers are provided by the author in the following table:

Table 2.3 Erosion Parameters for some Rivers (Jepsen *et al.*, 1997).

	n	*m*	**A**
Detroit River	2.23	-56	$3.65*10^3$
Fox River	1.89	-95	$2.69*10^6$
Santa Barbara	2.10	-45	$4.15*10^5$

Maa *et al.* (1998) conducted series of *in situ* experiments on Baltimore Harbour, MR, and reported erosion rate to be:

$$E = m(\tau_b - \tau_c)^n \qquad (2.5)$$

in which m and n are empirical coefficients. The authors gave these values for the coefficients at the sites they studied:

Table 2.4 Results of erosion rate parameters from in-situ measurements (Maa *et al.*, 1998)

	FORT MCHENRY	ANCHORAGE 5	WHITE ROCK	PARADISE
τ_c (N/m^2)	0.05	0.1	0.04	0.11
m	0.0266	0.2013	0.5149	0.5564
n	1.513	2.708	2.374	3.626

Roberts *et al.* (1998) expressed erosion rate in terms of the mud bulk density and the bed shear stress in the following way:

$$E = C\tau_b^n e^{k\rho_m} \qquad (2.6)$$

where k is a constant, which depends on the type of sediment, while C and n are empirical coefficients.

2.3.2 Exponential formulations

These types of equations are usually used for depth-limited erosion. The general form is expressed as follows:

$$E = E_0 \exp\left(\alpha[\tau_b - \tau_c(z)]^\beta\right) \qquad (2.7)$$

in which E is the erosion rate, E_0 is the erosion constant, usually referred to as the "floc constant", α and β are empirical coefficients and τ_b and τ_c are the applied stress and depth-dependant critical shear stress, respectively.

Gularte *et al.* (1980) presented this formula for erosion rate:

$$E = E_0 \frac{k_b \theta}{h_p} \exp\left(-\frac{\dot{E}}{R\theta}\right) \qquad (2.8)$$

where E is the erosion rate, E_0 is a constant, k_b is the Boltzmann constant, θ is the absolute temperature, h_p is the Plank constant, and $\dot{E}$ is the exponential activation energy.

Parchure and Mehta (1985) proposed:

$$E = E_0 \exp\left[\alpha(\tau_b - \tau_c)^{1/2}\right] \qquad (2.9)$$

in which E_0 ranges from 0.0833 to 0.533 kg/m^2/s while α ranges from 4.2 to 25.6 m/N$^{1/2}$.

Mehta (1988) developed the following equation for the erosion rate of cohesive sediments:

$$E = E_0 \exp\left(-a_r \tau_c^{b_r}\right)(\tau_b - \tau_c) \qquad (2.10)$$

where a_r, b_r are sediment dependant coefficients.

Amos *et al.* (1992) expressed the rate of erosion in this form:

$$E = E_0 \exp\left(\alpha[\tau_b - \tau_c(z)]^{0.5}\right) \qquad (2.11)$$

From regression analysis, they reported E_0 and α to be 5.1×10^{-5} and 1.62, respectively.

Sanford and Helka (1993) used Equation (2.11) and defined:

$$E = E_0 \exp\left\{\alpha\sqrt{\tau_c(z)}\left(\frac{\tau_b}{\tau_c(z)} - 1\right)^{0.5}\right\} \qquad (2.12)$$

Usually, $0 < \tau_b/\tau_c - 1 < 10$, and since for 0<x<10, $1.3\ln(x+1) \approx x^{0.5}$, they further obtained:

$$E = E_0 \exp\left\{1.3\alpha\sqrt{\tau_c(z)}\ln\left(\frac{\tau_b}{\tau_c(z)}\right)\right\} \qquad (2.13)$$

The above equation can be simplified to:

$$E = \frac{E_0}{\tau_c(z)^{1.3\alpha\sqrt{\tau_c(z)}}}\tau_b^{1.3\alpha\sqrt{\tau_c(z)}} \qquad (2.14)$$

which is in the form of a power equation.

2.3.3 Linear formulations:

These formulations are the simple form of Power law equations with n = 1. These kind of equations are usually used for unlimited erosion in which erosion rate does not decrease with depth:

$$E = M(\tau_b - \tau_c) \qquad (2.15)$$

where E is the erosion rate, M is a constant, τ_b bed shear stress, and τ_c is the critical shear stress. Ariathurani and Arulandanan (1978) proposed the following relationship:

$$E = M_1\frac{(\tau_b - \tau_c)}{\tau_c} \qquad (2.16)$$

where E is in kg/m^2/sec and M_1 is 0.009

Thorn and Parsons (1980) modified the previous equation and recommended:

$$E = M_2(\tau_b - \tau_c) \qquad (2.17)$$

where $M_2 = 9.73\times10^{-8}$.

Mei *et al.*, (1997) used the following equation in their model:

$$E = E_0|\tau_b| \qquad (2.18)$$

Winterwerp and van Kesteren (2004) proposed this relationship for rate of erosion:

$$E = \frac{c_v \phi_{s,0}(z) \rho_{dry}(z)}{10 D_{50} c_u(z)} (\tau_b - \tau_c) \qquad (2.19)$$

in which $\rho_{dry}(z)$ is the dry bulk density of bed, c_v is the consolidation coefficient in the vertical direction, $\phi_{s,0}$ is the volume concentration $(= 1/(1 + W_0 \rho_s / \rho_w))$, D_{50} is the median floc diameter, and c_u is the sediment remoulded shear strength.

2.3.4 Conceptual and interpretational difficulties

Not only are all of the equations used to model the rate of erosion empirical and calibrated with either laboratory, *in situ* tests or large scale observational data, but also the interpretation of data is often subjective (Sanford and Maa, 2001). Some of the researchers define τ_c as the stress at which initiation of first motion occurs (Young and Southard, 1978). Some researchers define it by extrapolating the erosion rate versus stress data, back to zero erosion (Partheniades, 1965; Sanford *et al.*, 1991; Sanford and Helka, 1993; Ravens and Gschwend; 1999; Tolhurst et al, 2000b). Some other researchers define it as the stress at which significant erosion first occurs (Gust and Morris, 1989; Maa and Lee, 1997; Maa et al, 1998; Roberts *et al.*, 1998) while some define an entire depth sequence of increasing critical stresses (Parchure and Mehta, 1985; Mehta, 1988; Kuijper *et al.*, 1989; Amos *et al.*, 1992; Amos *et al.*, 1997; Zerik *et al.*, 1998; Piedra-Cueva and Mory, 2001).

Similarly, with respect to the erosion rate at a specific value of the shear stress, some researchers defined it as the initial erosion rate after the application of new stresses (e.g. Maa *et al.*, 1998). Other papers defined it as the rate of erosion after the passing of the initial response period (e.g. Ravens and Gschwend, 1999). Another concept was to consider it as the average erosion rate during the entire period of stress application (e.g. Tolhurst *et al.*, 2000a).

Lack of consensus in explaning and interpreting the erosion process, may be because of the lack of proper understanding of physical phenomena. This leads to differences in the derived parameters, even when the same type of sediment is being used (Tolhurst, 2001a).

Moreover, all of the aforementioned formulas are empirical, site-specific and vary also from one wave condition to another (Sanford and Maa, 2001; Willis and Krishnappan, 2004). Generally, if erosion rate formulas are used for the limited range of the same experimental data, they turn out to be almost equivalent (Hayter, 1983; Sanford and Helka, 1993), but they are erroneous if used for out-of-range extrapolated conditions (Kuijper *et al.*, 1989).

2.3.5 Time-dependent erosion rate

Piredra-Cueva and Mory (2001) found that the linear approach might be used for depth-limited type of erosion as well, by simply allowing τ_c to increase with depth.

The idea of the time-dependent erosion rate proposed in the present work is based on the study of Sanford and Maa (2001) who extended the standard linear erosion formulation to incorporate both depth limited (Type I) or unlimited (Type II) erosions. The authors' basic assumptions were as follows:

1. The erosion constant is proportional to sediment concentration at the water-mud interface.
2. Critical shear stress increases locally at a constant rate with depth.

Sanford and Maa (2001) predicted the decay rate to be proportional to the rate of erosion per excess stress times the rate of increase in critical stress with depth. They found that, if the time scale of change in shear stress is long compared to sediment depletion, the depth change will control the phenomena and erosion will be halted after a while (Type I). However, if the time scale in shear stress change is short, Type II erosion occurs and erosion will be controlled by the instantaneous difference between the bottom shear stress and the critical shear stress. Finally, their approach was verified using *in-situ* erosion tests that were conducted in Baltimore Harbour, MD.

Sanford and Maa (2001) applied their model for the case of variable bed shear stresses as well. Their efforts in this case included a bed with a constant and sinusoidal rate of increase in bed shear stress.

Sanford and Maa (2001) chose the linear erosion rate formula for their study expressed as:

$$E(z,t) = M(z)[\tau_b(t) - \tau_c(z)] \qquad (2.20)$$

where M varies with depth. Therefore, erosion rate depends on both time and depth. They further assumed that:

$$M(z) = \rho_s \phi_s(z) \beta_e \qquad (2.21)$$

where ρ_s is the sediment density, $\phi_s(z) = 1 - \phi(z)$ is the volume fraction of sediment, and β_e is a local constant. Dividing both sides by $\rho_s \phi_s(z)$ and differentiating with respect to time yields the following governing equation:

$$\frac{dE'}{dt} + \beta_e \gamma E' = \beta_e \frac{d\tau_b}{dt} \qquad (2.22)$$

where $E' = E[\rho_s \phi_s(z)]^{-1} = dz/dt$ is the erosion velocity, $\gamma = \frac{d\tau_c}{dz}$ that is the rate of increase in resistance against erosion with respect to depth that is assumed to be locally constant.

The homogeneous solution of the above-mentioned governing equation $(d\tau_b/dt = 0)$ is incorporated in the present study. Considering this condition, the following solution is obtained:

$$E' = \beta_e(\tau_b - \tau_{c0})\exp[-\gamma\beta_e(t - t_0)] \qquad (2.23)$$

where τ_{c0} is the critical shear stress when τ_b is first applied at $t = t_0$. The details of equations used in the current study are provided in Section 3.1.11.

The model of Sanford and Maa (2001) showed reasonable results in comparison with *in-situ* data, except in predicting the erosion constant for large eroded masses. Their results stimulated Aberle *et al.* (2004) to pursue their initial idea . Their contribution was to calibrate the local erosion constant in Sanford and Maa's model in order to get more accurate results.

Aberle *et al.* (2004) conducted an *in-situ* experiment with straight benthic flume in freshwater and saltwater environments in order to measure the erosion rate. They used Equation (2.23) to analyse their data and also used two methods to calibrate the equation:

the "bulk density" method and "last step" method. They found that the erosion constant, M, increases linearly with bulk density. They also reported that the value of β_e is dependent on the dry bulk density, salinity and on the sand content. They found that β_e decreases with an increase in dry bulk density. However, they noticed discrepancies in three sites analyzed and attributed them to the existence of fibrous organic material such as decomposing leaves, root systems, etc. (Aberle *et al.*, 2004). The relation between β_e and bed bulk density is included in the present study and is discussed in Section 3.1.11.

2.4 Critical bed shear resistance

"In coastal engineering terms, the principal indicator of the cohesive sediment behaviour is critical shear stress for erosion of bed sediment, τ_c" (CEM, 2002). The critical shear stress is difficult to measure directly. Therefore, correlation methods have been developed in order to relate the critical shear stress and other properties that can be measured in an easier way (Dean and Darlymple, 2002).

2.4.1 Critical shear stress in terms of bulk density

One of the approaches is to define τ_c in terms of the bed bulk density that has been commonly used in numerical models (Willis and Krishnappan, 2004). The general form of these types of equations is as follows:

$$\tau_c = m\rho_m^n \qquad (2.24)$$

in which ρ_m is the bulk density and n and m are empirical constants. Studies by Mehta, (1985), van Rijn (1989) and Mehta (1989) confirmed this formulation.

2.4.2 Critical shear stress in terms of vane shear stress

Another common approach is to correlate the critical shear stress to the vane shear stress of the bed material. In order to do so, a vane is inserted into a sample from the same soil as the bed material. A gradual torque is applied until the sediment cylinder fails to prevent the vain from twisting. Finally, the critical shear stress is obtained in terms of the measured torque.

Dunn (1959) presented this relationship:

$$\tau_c = 0.01\tau_y \qquad (2.25)$$

in which τ_c is the critical shear stress and τ_y is the vane shear stress. Magniot (1968) identified the critical shear stress as:

$$\begin{cases} \tau_c = 0.25\tau_y & \tau_y > 1.6Pa \\ \tau_c = \sqrt{0.1\tau_y} & \tau_y < 1.6Pa \end{cases} \qquad (2.26)$$

Dade and Nowell (1991) developed a more complicated formula for expressing the critical shear stress:

$$\tau_c = \frac{40\rho\nu^2}{\tan\phi_1 d_s^2}\left\{\sqrt{\frac{g\rho_s' d_s^3 \tan^2\phi_1}{240\rho\nu^2}\left[1+3(1-\cos\phi_1)\frac{\tau_y}{g\rho_s' d_s}\right]}+1-1\right\} \qquad (2.27)$$

in which d_s is the particle diameter, ρ is the fluid density, ρ_s' is excess density of the sediment, ν is the kinematic viscosity, and ϕ_1 is the bed-packing angle of bed with recommended value of 65°

When the magnitude of τ_y is greater than 0.7 Pa, Equation (2.27) can be reduced to:

$$\tau_c = 0.31\tau_y \qquad (2.28)$$

which is relevantly close to Migniot's (1968) formula.

2.4.3 Incorporating the electrochemical resistance of cohesive sediments

When the size of sediment particles is smaller than 20 microns, the electrochemical resistance force - induced by the surface electrical charge acting on each particle - becomes more important than the gravitational and friction forces (Taki, 1986). Moreover, the viscosity of the fluid mud strongly depends on the surface electrical charge of particles (Taki, 1986). This charge ranges approximately between -20 mV to +20 mV and is an accurate indicator of the coagulation of particles (Overbeek, 1991).

Ito and Matsui (1975) related surface charge to the yield stress of mud and found a strong relation between these two elements, especially when water content ratio is higher than two. Based on the previous studies of Kitahara *et al.* (1971) and Hunter (1981), Taki (2001) developed an equation for the formulation of the critical shear stress by incorporating the "electrochemical anchoring force theory", in which Van der Waals forces and surface charge of particles equalize the shear induced by the flow.

Taki (2001) expressed the total potential energy, E_T, as a result of the combination of the attractive (E_A) and repulsive (E_R) potential energies between two sediment particles. Cohesion, F_c, was introduced as an equilibrium term between the attractive and repulsive forces, i.e., $dE_T/dx = 0$. The attractive, repulsive, as well as the total electrochemical forces are depicted in Figure 2.3.

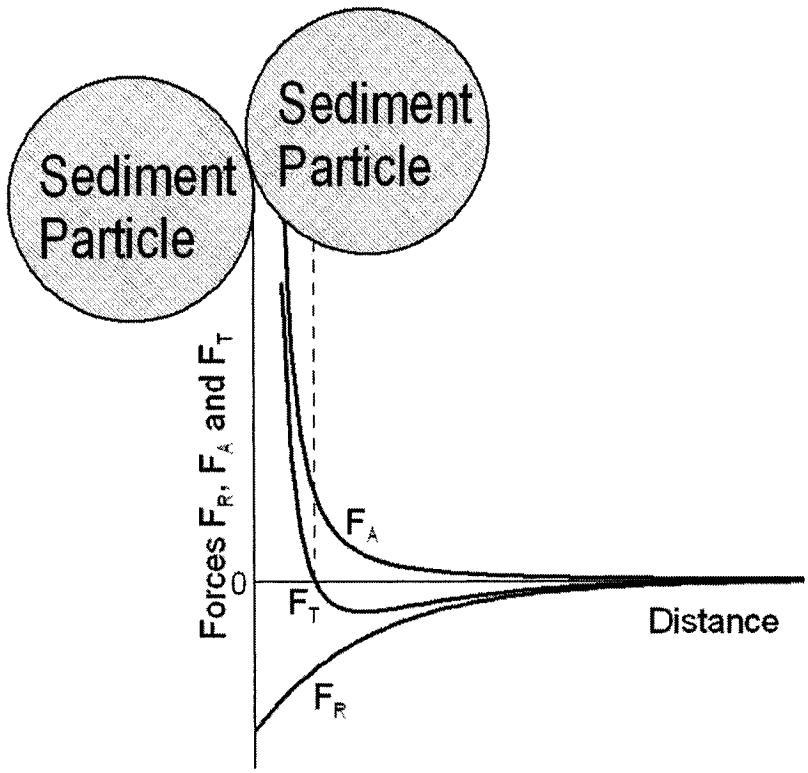

Figure 2.3 Attractive force, F_A, repulsive force, F_R, and combined electrochemical force, F_T at the particle interface.

Finally, the critical shear stress was found to be:

$$\tau_c = 0.05 + \chi\left[\frac{1}{\left\{(\pi/6)\left(1+32sW_L\eta_*^{-0.4}\right)\right\}^{1/3}-1}\right]^2 \qquad (2.29)$$

in which χ is the electrochemical anchoring coefficient, W_L is the liquid limit of mud, s is the specific weight of the mud particle and η_* is the degree of resistance of a particle deposited on the mud layer. The parameter η_* is defined as (Taki, 1991):

$$\eta_* = \nu_b / \left\{(s-1)gd_s^3\right\}^{1/2} \qquad (2.30)$$

where d_s is the equivalent spherical diameter of the particle, and ν_b is the kinematic viscosity of mud.

Taki (2001)found that the coefficient χ ranges between 0.1 and 2.0. The mean value of χ used in his experiments was 0.3.

2.5 Fluid mud entrainment

The mechanism of entrainment of fluid mud is different from the erosion of settled mud that has a structural matrix (Mehta and Srinivas, 1994; Kranenburg, 1994). This entrainment occurs when mechanical mixing energy dominates the potential energy stored in density stratification, which causes the breakup of the fluid mud-water interface and mass erosion of sediments (Scarlatos and Mehta, 1993; Mehta and Srinivas, 1993; Winterwerp *et al.*, 1993), while surface erosion typically occurs over harder cohesive beds (Taki, 1990; Parchure and Mehta, 1985) (Figure 2.4).

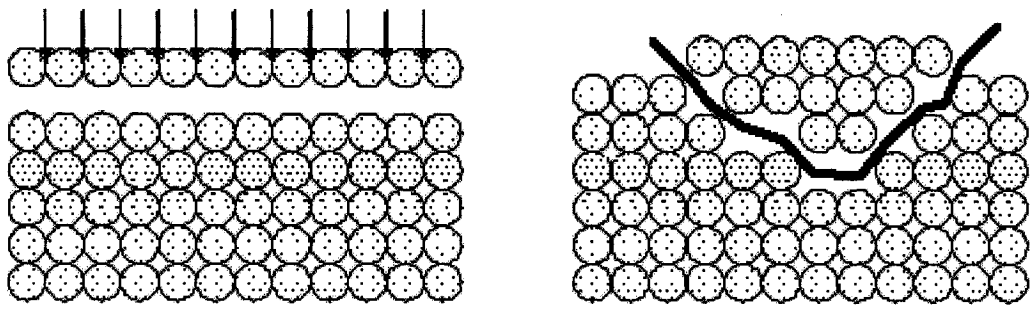

(a) Surface Erosion **(b) Mass Erosion**

Figure 2.4 Surface erosion and mass erosion.

Particularly for the case of wave action, inter-particle bonds break up under cycle loading and the bed becomes fluidized. The resulting fluidized bottom is subjected to further bulk entrainment. For example, in the case of Lake Okeechobee located in south-central Florida, a relatively dense mud bottom stays permanently fluidized by wind-generated waves (Kirby *et al.*, 1994).

The first studies dealing with the development of mathematical formulations for mud entrainment came from the studies for entrainment of salt-stratified layers. Kato and Phillips (1969) conducted a laboratory experiment with a flume containing initially stratified fluid. A constant shear stress was applied and finally, an upper homogeneous layer and a lower stratified fluid with a buoyancy step of Δb across the interface were obtained during experiments. The entrainment rate was expressed as follows:

$$F_{n*} = \frac{u_e}{u_*} = k_3 Ri_*^n \qquad (2.31)$$

where F_{n*} represents the non-dimensional entrainment rate, u_e is the rate of downward propagation of the interface, u_* is the friction velocity, $Ri_* = h\Delta b/u_*^2$ is the Richardson number, h is the depth of the upper homogeneous layer, k_3 is an empirical coefficient and $n = -1$. Li (1996) noted that in Equation (2.31), the upward flux of sediment mass at low values of Ri_* is proportional to the cube of the mean mixed layer velocity. In contrast, this

rate depends on U^2 in turbulent flows (Partheniades, 1965; Mehta, 1989). Moore and Long (1971) conducted a two layer experiment with uniform longitudinal density and velocity profiles that lead them to find the relation between non-dimensional buoyancy flux and the global Richardson number as:

$$Q \sim Ri_g^{-1} \qquad (2.32)$$

where $Q = q/\Delta b(2\Delta U)$ is the non-dimensional buoyancy flux, $2\Delta U$ is the velocity difference between the two layers, $Ri_g = \hat{H}\Delta b/(2\Delta U)$ is the global Richardson number and $\hat{H}$ is the total depth. After reviewing some experimental results, Christodoulou (1986) found that parameter n mentioned in Eq. (2.31) can take values of 0, 0.5, 1 and 1.5 as Ri_g increases from 10^{-2} to greater than 1. They attributed each value of the constant n to a specific mode of entrainment (1986).

Atkinson (1988) noted that molecular diffusion of particles becomes important when the Richardson number is of the order of 10^2. By incorporating this factor, he introduced the following expression:

$$F_n = \frac{A - BRiPe^{-1/2}}{C + Ri} \qquad (2.33)$$

where A, B and C are empirical coefficients and $Pe = Uh/k$ is the Peclet number and k is the salt's molecular diffusivity.

Srinivas and Mehta (1989) conducted an experiment in a race track-shaped flume, used for commercial kaolinite and bentonite for fluid mud and applied Equation (2.31). They found that $n = 1$, for $4 < Ri < 7$. However, as Ri increases, n also increases, although, with less entrainment rate than salt. Using regression analysis, they proposed the following expression:

$$F_n = \frac{ARi^{-0.9}}{\left(B^2 + Ri^2\right)^C} \qquad (2.34)$$

where A, B and C are empirical coefficients.

Scarlatos and Mehta (1993) approximated the mud-water system by a two-layered, slightly viscous, horizontal system with water flowing over the fluid mud. Due to the motion of water over stationary fluid mud, a steep velocity gradient along the lutocline developed. That resulted in the generation of a vortex sheet. By introducing a slight disturbance along the interface, the vortex sheet initially developed a wave-like pattern, and then it was stretched, folded and eventually caused thickening and vigorous mixing of the water-mud interface. It was concluded that the dynamic behaviour of the vortex sheet is controlled by the velocity and gradients of density across the water-mud interface.

Mehta and Srinivas (1993) extended the formula of Atkinson (1988) by applying the turbulent energy balance for the horizontally homogeneous boundary layer above the fluid mud layer with mean flow in the longitudinal direction. The non-dimensional formula for entrainment rate in terms of global Richardson number was then obtained as:

$$F_n = \alpha_4 Ri_g^{-1} - \beta_4 Ri_g \qquad (2.35)$$

where $F_n = u_e/U$, $Ri_g = \delta \Delta b / U^2$, Δb is the jump across the water-fluid mud interface, U is the mean mixed layer velocity, δ is the mixed layer thickness, and α_4 and β_4 are experimentally determined coefficients. The first term on the right hand side of Equation (2.35) is an indicator of the interaction between the mechanical mixing energy and potential energy stored through density stratification. The second term on the right hand side of Equation (2.35) summarizes the effect of other factors such as cohesion, settling velocity and the viscosity difference between water and mud.

Experiments of Winterwerp (1994) also demonstrated the dependence of entrainment rate on the global Richardson number. The non-dimensional entrainment rate was related to $Ri_*^{-1/2}$ for small Ri_* and to Ri_*^{-1} for large Ri_*.

Kranenburg (1994), Kranenburg and Winterwerp (1997), and Bruens (2003) derived an entrainment model for two conditions: (a) Case I in which the fluid mud layer is entrained by the turbulent water layer above it; (b) Case II in which the turbulence is generated by the fluid mud layer due to shear stress at the bottom of the fluid mud layer. In this latter case, water entrainment downward into the fluid mud layer increased the depth of the fluid mud.

Such behaviour has also been reported by Wolanski *et al.*, (1988) and Le Hir (1994, 1997) for river channels and in sub-marine turbidity currents.

Li (1996) extended the formula of Mehta and Srinivas (1993) (Equation 2.35) by introducing the critical Richardson number, Ri_c, above which entrainment occurs, ignoring molecular diffusion. Li (1996) expressed the entrainment rate as:

$$F_n = \rho_m u_b \alpha_4 \left(R_{ic}^2 R_{ig}^{-1} - R_{ig} \right) \qquad (2.36)$$

where u_b is the maximum wave-induced horizontal velocity just outside the bottom wave boundary layer. In order to determine the critical Richardson number, Li (1996) used three sets of data and predicted the value of Ri_c at which no or very small entrainment occurred. He attributed the small entrainment to molecular diffusion which was ignored in his formulation. The first set of data used to compare his results was provided by measurements in the Changjiang River by Ren and Jang (1986) and Li (1989). A value of 0.043 was found for Ri_c, with an experimental range of 100~350 for Reynolds number. The second data set was based on the Maa (1986) experiments and a value of 0.05 was found while the last data set was from Miamura (1993) in which a mean value of 0.053 was obtained.

2.6 Flocculation

Cohesive sediments tend to agglomerate together. This process is called flocculation and the resulting particle is called "floc". Floc size is different, which complicates the prediction of their deposition. Flocs are typically shaped like flakes, i.e., their thickness is much smaller than their other two dimensions.

Flocculation occurs as sediment particles strike each other. Collision and cohesion are two important factors in flocculation (Krone, 1962).

Cohesion is due to the inter-particle electrochemical forces described in Section 2.4.3. Particles cohere if attractive short-range forces dominate repulsive forces generated by the clouds of cations around particles. The strength of the repulsive forces depends on the

surface charge of the particles, which is governed by the particle mineralogy and the types of cations present in the surrounding fluid (Whitehouse *et al.*, 2000).

Collision of particles is directly related to internal shear forces in the water (Krone, 1972). Internal shearing promotes flocculation by bringing particles close enough to each other such that the inter-particle attractive forces dominate the repulsive forces so that particles bond together in the form of flocs. On the other hand, internal shearing limits the size of the flocs. The inter-particle bonds in macroflocs are weaker and can easily break up under internal shear stress. Therefore, macroflocs (up to 1 mm diameter) are observed in high concentration and low shear environments (Dyer and Manning, 1999). Moreover, as the size of floc increases the amount of water in it increases as well. Thus, density of flocs decreases. As a result, these large flocs can be resuspended as they try to pass a maximum shear stress region before being deposited.

The size and settling velocity of flocs are much larger than the individual particles. Migniot (1968) studied the relationship between the settling velocity of flocs with respect to the median grain size diameter of particles. In this study, Migniot introduced the flocculation factor as the ratio of the fall velocity of the flocculated particles to that of the individual particles. From this study, it was found that the flocculation factor is in the order of 10^4 for particles with a median diameter of 0.1 microns. This factor decreases as the median particle diameter increases and reaches unity for particles with a diameter of about 60 microns. This indicates that there is little flocculation for particles with a median diameter greater than 60 microns and therefore the cohesive behaviour of sediment ceases for particles larger than this size.

Flocculation promotes deposition. The settling velocity of flocs increases as their size increase (Fennessy *et al.*, 1994; Dyer and Manning, 1999; Whitehouse *et al.*, 2000). However, some of the studies indicate that as the amount of water in flocs increases with the increase in their size, the density of flocs decreases and tends to approach the density of the water. Hence, flocs' behavior become similar to that of fluid particles. Therefore, after passing a maximum floc size, the settling velocity of flocs decreases (Krishnappan, 2000; Willis and Krishnappan, 2004). McAnally and Mehta (2002) stated that the flocculation

process does not have significant effect on the rate of deposition of medium cohesion sediments but dominates the high cohesion sediment deposition.

The maximum floc size also depends on the following parameters: mineralogy, organic content, pH and ionic strength of the mud, the chemical composition of the pore water and suspending water; and other hydrodynamic parameters of the flow such as water temperature and salinity (Whitehouse *et al.*, 2000).

The densest and largest flocs are found in the fluid mud where the concentration is high and turbulence is highly damped. As fluid mud is generated, collision increases due to the increase in concentration but declines as turbulence is damped and settling is hindered (McAnally, 2000).

2.7 Settling velocity

Settling velocity (also called "fall velocity") of cohesive sediments varies between 10^{-5} to 10^{-2} ms^{-1}. Settling velocity depends on the sediment grain size, its shape, specific weight, surface roughness and fluid properties (McAnally *et al.*, 2007). Fall velocity summarizes those properties and its measurement is simple (Willis and Krishnappan, 2004). Settling velocity of fine sediments - especially the cohesive ones - strongly depends on the concentration (Mehta, 1988).

Fall velocity of cohesive sediments is usually divided into four regions: Free settling, flocculation settling, hindered settling, and negligible settling as indicated in Figure 2.5.

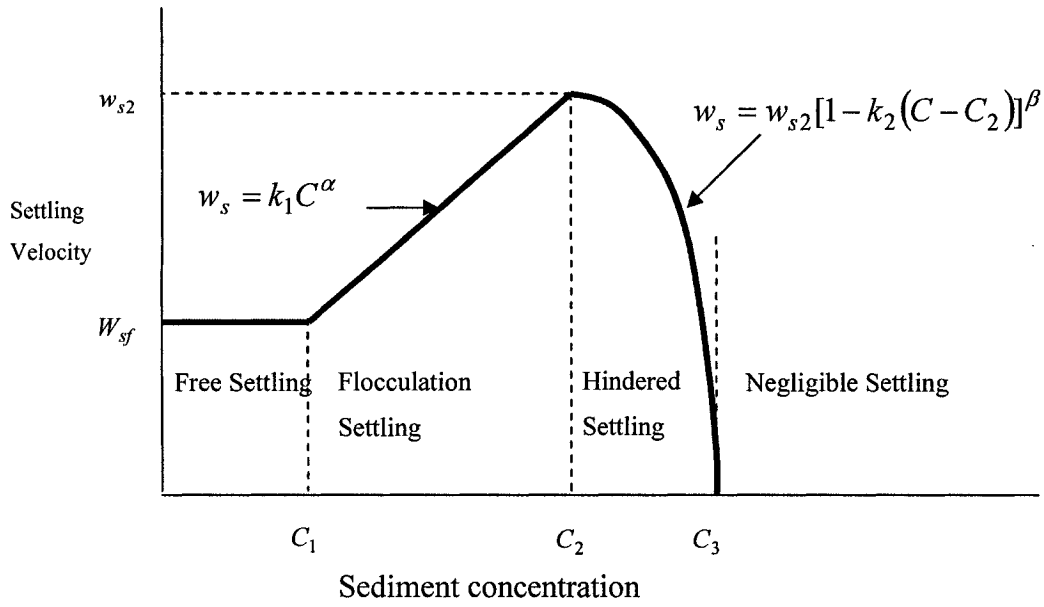

Figure 2.5 Variation of the average settling velocity with concentration (adapted from Mehta, 1991).

In the free settling domain, the settling velocity is independent of the sediment concentration due to low values of sediment concentration. The upper limit of concentration for this region, known as C_1, is considered to vary between 0.1 and 0.3 kg/m^3 (Mehta, 1988). The settling velocity can be calculated using Stokes' Law as:

$$W_{sf} = \sqrt{\frac{4}{3C_D}\left(\frac{\rho_f - \rho}{\rho}\right) g d_f} \qquad (2.37)$$

where ρ_f is the bulk density of the flocs, ρ is the density of water, g is the gravitational acceleration, C_D is the drag coefficient and d_f is a representative floc diameter. Under the free settling condition, d_f , C_D and ρ_f remain practically constant during the settling process, so that W_{sf} is also constant. However, the values of ρ_f, C_D and d_f are difficult to obtain. It is therefore recommended to obtain W_{sf} from the settling column measurement rather than from Equation (2.37) (Vanoni, 1975). Lau and Krishnapan (1994), studied the variation of floc density with respect to floc diameter for the case of Fraser River (Canada) and derived the following formula:

$$\rho_f - \rho = \rho_s \exp(-bd_f^c) \qquad (2.38)$$

in which d_f is floc diameter, and b and c are empirical constants determined to be $b = 0.0015$ and $c = 1.7$.

In the flocculation region, settling velocity increases with an increase in sediment concentration, due to formation of flocs. The following equation has been proposed to describe the relationship between the settling velocity and the sediment concentration in this range (e.g. Raudkivi, 1998; Mehta and Li, 2003):

$$W_s = k_1 C^{\alpha} \qquad (2.39)$$

in which α is (theoretically) equal to 1.33, but may actually vary between about 0.8 and 2.0 (Krone, 1962; Mehta, 1988) while k_1 is a proportionality coefficient which depends on sediment composition. Burt and Stevenson (1983) reported values of 1.341 and 1.37 for k_1 and α, respectively. Thorn (1981) found 0.513 for k_1 and 1.29 for α, based on data collected in the Severn Estuary (UK). Delo and Burt (1986) reported a value of $\alpha = 0.61$ for the Humber Estuary.

Finally, in the hindered settling region, the high concentration of sediment flocs creates a "net" that entraps water and prevents the upward transport of sediment particles (Willis and Krishnappan, 2004) and decreases their fall velocity. The general equation for this case is (Mehta and Li, 2003):

$$w_s = w_{s2}[1 - k_2(C - C_2)]^{\beta} \qquad (2.40)$$

where β is typically equal to 5.0 (Richardson and Zaki, 1954), by definition $w_{s2} = w_s\big|_{C=C_2}$ and k_2 is a coefficient dependent on sediment properties. The study of Thorn (1981) indicated a value of $\beta = 4.65$ for the Severn Estuary.

Some researchers attempted to propose a general combined settling velocity formula which would account for for both flocculation and hindered settling regions. Hwang (1989) proposed the following formulation:

$$w_s = \begin{cases} \dfrac{\alpha_1 c_1^{\beta_1}}{\left(c_1^2 + \gamma_1^2\right)^{\delta_1}} = W_{sf} & c \le c_1 \\ \dfrac{\alpha_1 c^{\beta_1}}{\left(c^2 + \gamma_1^2\right)^{\delta_1}} & c > c_1 \end{cases} \qquad (2.41)$$

where $\alpha_1, \beta_1, \delta_1$ and γ_1 are empirical constants. Wolasnki *et al.* (1992) found that these constants depend on sediment properties and the rate of shearing due to turbulence. c_1 represents the minimum concentration for the flocculation settling region.

The study of Lau and Krishnappan (1994) for the Fraser River (British Columbia) resulted in the following formulation for the settling velocity:

$$w_s = (1.65/18)\exp\left(-0.0015 d_f^{1.7}\right) g\, d_f^2 / \nu \qquad (2.42)$$

The maximum floc size was found to be 55 μm. Figure 2.6 provides the variation of floc density and fall velocity with respect to floc size.

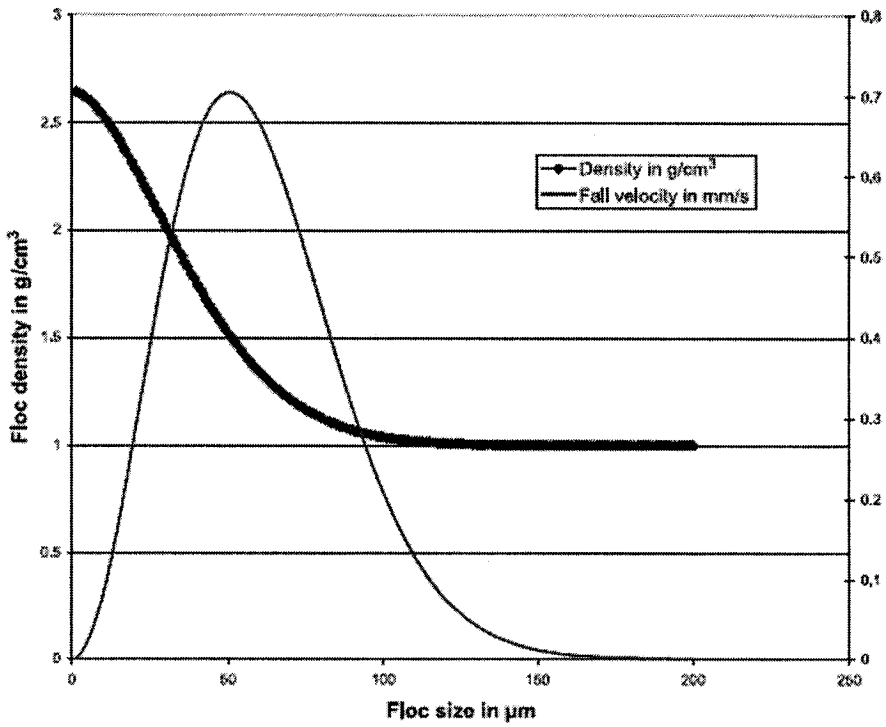

Figure 2.6 Floc density and fall velocity versus floc size (adapted from Willis and Krishnappan, 2004).

You (2004) reported concentrations of 0.3 kg/m^3 for the free settling region, $0.3 < C < 4.3$ kg/m^3 for the flocculation region and $C > 4.3$ kg/m^3 for the hindered settling region. From this study, the following equation for calculating the sediment settling velocity was proposed:

$$w_s = w_{sf} \exp\left(0.9779C - 0.1080C^2\right) \qquad (2.43)$$

2.8 Bed shear stress under waves and combined waves and currents

The most important hydrodynamic property of sediment transport under wave action and the preeminent factor in the erosion process under oscillatory flow is the bed shear stress (Maa, 1986; Sawaragi, 1995; Whitehouse *et al.*, 2000). Unlike the case of steady flow conditions, for smooth beds where the ratio of bed roughness to excursion distance outside the boundary layer is less than 0.01, the wave bed shear stress has the same period as the wave period (Maa, 1986). However, for rough beds, where $k_s/a_b > 0.01$ r, the rhythmic formation and release of vortices may induce higher order harmonics (Loftquist, 1980). Sawaragi (1995) classified the investigations on the boundary layer and the bottom shear stress in the following categories:

1. Direct measurement of near bottom water particle velocity. The calculation of the flow field within the boundary layer and the associated bed resistance is based on the collected data;
2. Direct measurement of the bottom shear stress (e.g. Reidel, 1973; Kamphuis, 1975);
3. Determination of the flow structure and of the shear stress within the boundary layer using the boundary layer equations (e.g. Kijiura, 1964,1968; Johns, 1968; Asano and Iwagaki, 1983).

Following the first approach, Jonsson (1963) proposed the resistance law by formulating the logarithmic distribution of velocity. He measured the velocity on a fixed roughness using a propeller velocimeter. He then expressed the amplitude of the bottom shear stress, τ_b as:

$$\tau_b = \frac{1}{2} f_w \rho u_b^2 \qquad (2.44)$$

where u_b is the amplitude of water orbital velocity and f_w is the wave friction factor. This formula was applied for both laminar and turbulent flows using different expressions of the wave friction factor. This is presented and discussed later in this chapter. The most intense disturbance of sediments occurs under breaking waves. However, most of the existing theoretical studies apply non-breaking wave conditions to the breaking wave case since this theoretical approach is simpler (Whitehouse *et al.*, 2000). Deigaard *et al.* (1991) supported this idea by showing that the average of shear stress in the surf zone (breaking wave area) is not significantly different then the one corresponding to the unbroken offshore waves condition. However, neglecting wave breaking may cause underestimation of sediment concentration, especially in the upper half of the suspended sediment column in the surf zone, where wave breaking-induced turbulence is the dominating factor in sediment transport.

Whitehouse *et al.* (2000) stated that if current and wave velocities over a smooth bed are sufficiantly small so that flow remains basically laminar, the combined wave-current shear stress can be represented by the scalar addition of both the wave and current-induced stresses. However, in the case of turbulent flow, the high nonlinearity generated by turbulence in the current and wave boundary layer makes this approach erroneous. A number of studies have been dedicated to study the wave-current coexisting systems and their interaction. The first among them was conducted by Bowen (1969) and Longuet-Higgins (1970), both of whom introduced the theory of the wave-induced current. They proposed the time-averaged bottom shear as a resistance force against spatial variation of radiation stress. This idea was further pursued and developed by other researchers such as Liu and Dalrymple (1976), Sawaragi *et al.* (1978) and Nishimura (1982). The difference between their models lies only in the way they evaluate the friction factor and define the time variation of the bottom shear stress.

Soulsby *et al.* (1993) proposed a specific pattern for turbulent flow conditions which is schematically shown in Figure 2.7.

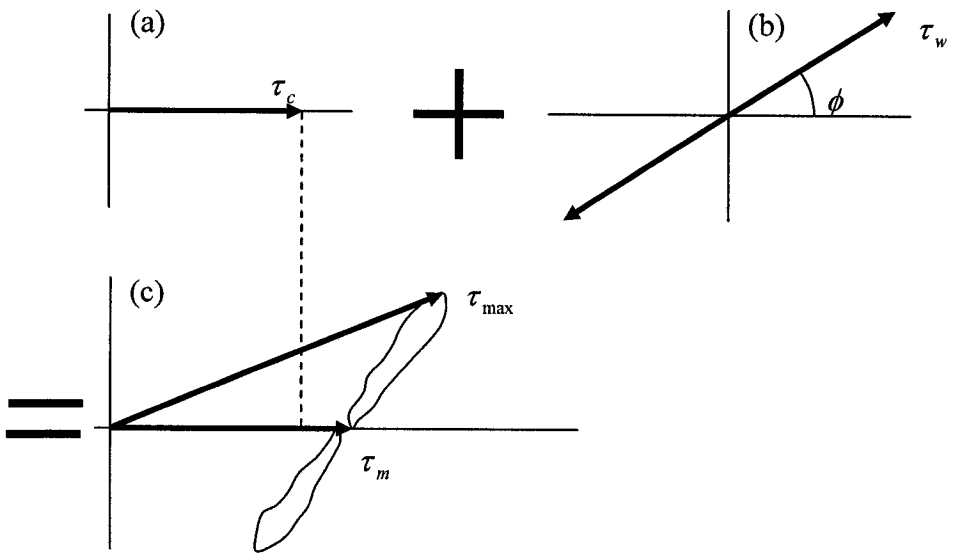

Figure 2.7 Schematic pattern of bed shear stress. (a) The bed shear stress due to current alone (τ_c), (b) the wave-alone stress (amplitude = τ_w), and combined wave-current interaction bed shear stress with mean value of τ_m and maximum of τ_{max} (adapted from Soulsby, 1993).

Three important factors to be determined are: (1) the mean combined shear over one wave period, τ_m, that is used to determine the friction governing the current and the diffusion of the sediment in the outer flow; (2) the maximum bed shear stress over one wave period, τ_{max}, that is used to determine the threshold of sediment motion and diffusion nearing the vicinity of the bed (Whitehouse *et el.*, 2000); and (3) the root-mean-square value of the shear stress over one wave period, τ_{rms} which is particularly of interest for the case of random waves.

For the case of a rough bed, Soulsby *et al.* (1993) compared eight different models and found that the models of Fredsøe (1984) and Grant and Madsen (1979) performed best. Based on their results, Soulsby (1995) proposed the following equations developed as a result of the best fit analysis for 61 laboratory and 70 field measurements data sets for the mean shear stress over a wave period for rough beds:

$$\tau_m = \tau_{bc}\left[1+1.2\left(\frac{\tau_{bw}}{\tau_{bc}+\tau_{bw}}\right)^{3.2}\right] \qquad (2.45)$$

in which τ_{bc} and τ_{bw} are the bed shear stresses that occur due to current alone and wave alone, respectively.

The maximum and root-mean-square stresses were likewise expressed as:

$$\tau_{\max} = \left[\left(\tau_m + \tau_{bw}\cos\phi\right)^2 + \left(\tau_{bw}\sin\phi\right)^2\right]^{1/2} \qquad (2.46)$$

$$\tau_{rms} = \left(\tau_m^2 + \frac{1}{2}\tau_{bw}^2\right)^{1/2} \qquad (2.47)$$

where ϕ is the angle between current direction and direction of wave propagation.

The model proposed by Soulsby is based on this assumption that the increase of the oscillatory component of the stress due to the turbulent current is negligible. Almost all of the aforementioned models were developed for rough-bed conditions. Soulsby *et al.* (1993) performed one laboratory experiment and studied the effect of combined waves and currents over a smooth bed. The authors reported a significant non-linear enhancement of τ_m in the case of wave-dominated conditions, but no enhancement for current-dominated conditions. They also found that the non-linear enhancement does not improve the prediction of $\tau_{\max}$ significantly. Moreover, their results showed the damping of current-generated turbulence by large waves. They further applied the theoretical model of Fredsøe (1984) and found poor agreement with experimental data. Soulsby (2000) modified Equation (2.45) for smooth-bed and proposed the following equation:

$$\tau_m = \tau_{bc}\left[1+9\left(\frac{\tau_{bw}}{\tau_{bc}+\tau_{bw}}\right)^{9}\right] \qquad (2.48)$$

2.9 Wave friction factor

Another approach towards the better calculation of shear stress under waves or co-existing systems of waves and currents was directed towards the better estimation of wave friction factor, f_w. This factor has been expressed in terms of the Nikuradse bed roughness, and either the wave orbital diameter or the boundary layer thickness, both of which are parameters that contain high levels of uncertainty. Moreover, some wave friction formulas were developed for various cases of flow: laminar, smooth turbulent or rough turbulent. However, the validity of the formulations between these flow regimes is poorly defined (Le Roux, 2003).

Jonsson, (1965) and Kamphuis (1975) proposed a diagram (shown in Figure 2.8) for the wave friction factor which is similar to the Moody diagram.

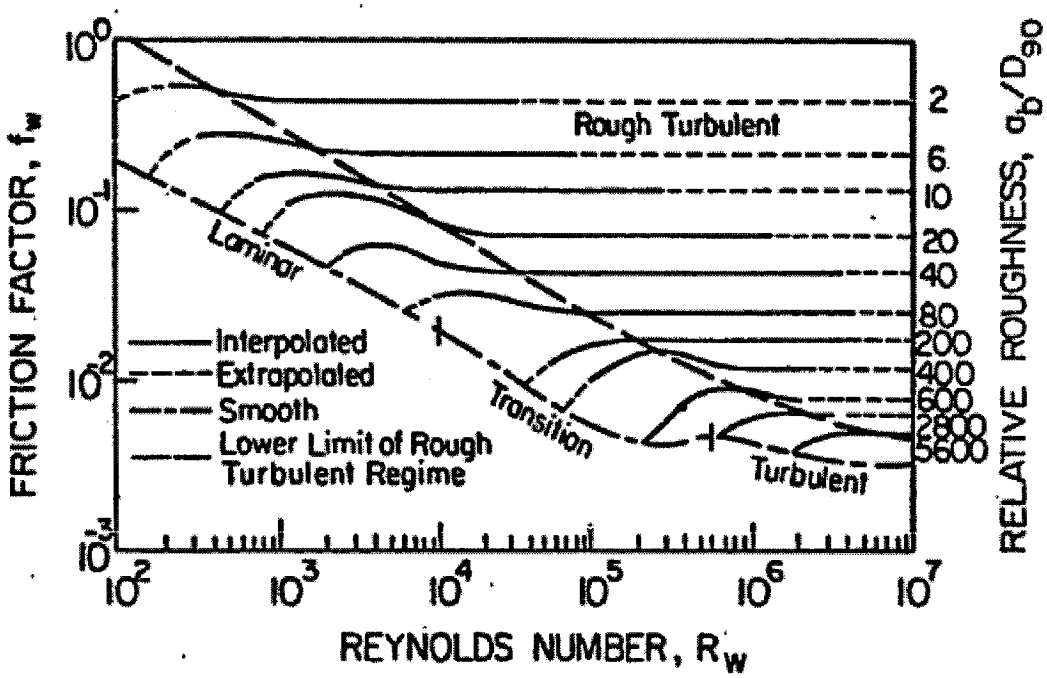

Figure 2.8 Wave friction factor diagram (Kamphuis, 1975).

For the case of laminar flow condition, the following equation was proposed (Jonsson ,1966; Schlichting, 1968):

$$f_w = 2/\sqrt{R_w} \qquad (2.49)$$

where R_w is the wave Reynolds number, which is less than $1.24\text{x}10^{-4}$ for the case of laminar flow. It is defined as:

$$R_w = \frac{u_b^2}{\nu\sigma} \qquad (2.50)$$

where u_b is the amplitude of the wave-induced orbital velocity, ν is the fluid kinematic viscosity and $\sigma = 2\pi/T$.

For the case of the smooth turbulent boundary layer, Jonsson (1965) introduced the following expression:

$$f_w = 2[\nu/(0.5U_{wcr}d_0)]^{0.5} \qquad (2.51)$$

where U_{wcr} is the critical wave orbital velocity and d_0 is the near-bed orbital diameter of wave motion. Soulsby (1997) presented a simpler formula, analogous to the equation developed for laminar flow condition as:

$$f_w = BR_w^{-N} \qquad (2.52)$$

where $B = 0.0521$ and $N = 0.187$. Other alternatives are $B = 0.035$, $N = 0.16$ (Fredsøe and Deigaard, 1992) and $B = 0.0450$, $N = 0.175$ (Myrhaug, 1995).

For rough turbulent boundary layers, Jonsson (1963) proposed the following equation:

$$\frac{1}{4\sqrt{f_w}} + \log\left(\frac{1}{4\sqrt{f_w}}\right) = -0.08 + \log\left(\frac{a_b}{k_s}\right) \qquad (2.53)$$

where k_s is the bed roughness and a_b is the water particle excursion defined as $a_b = u_b/\sigma$. The main problem with this equation is that it is a transcendence equation. Two approximations of this equation proposed by Jonsson (1963) and Swart (1974) are presented

here. These formulations are most widely used (Le Roux, 2003). Jonsson (1963) gave this approximation for the wave friction factor:

$$f_w = 0.0604/\left[\log(30\delta/k_s)^2\right] \qquad (2.54)$$

where δ is the boundary layer thickness. Difficulties in measuring the boundary layer thickeness is a challenge for this equation (Jonsson, 1963; Schichting, 1968). Teleki and Anderson (1970), reported that the following equation by Li (1954) is the best description for the boundary layer thickness:

$$\delta = 6.5\sqrt{(\mu T/2\rho\pi)} \qquad (2.55)$$

Swart (1974) proposed the following approximate expression of Jonnson's formula, which is valid within the range of $1 < a_b/k_s < 3000$:

$$f_w = \exp\left[-5.977 + 5.213(a_b/k_s)^{-0.194}\right] \qquad (2.56)$$

Kamphuis (1975) related f_w to a_b/k_s, based on measurement of bottom shear stress in rough turbulent region that is valid for $a_b/k_s < 100$:

$$f_w = 0.4(a_b/k_s)^{-0.75} \qquad (2.57)$$

Soulsby (1997) slightly modified this equation by fitting his proposed curve to 44 experimental (measured) values and proposed the following expression for the friction factor:

$$f_w = 0.237(a_b/k_s)^{-0.52} \qquad (2.58)$$

Myrhaug (1989) gave an implicit relationship for f_w that is valid for smooth, transitional and rough turbulent flows:

$$\left\{\ln\left(6.36\frac{a_b f_w^{1/2}}{k_s}\right)-\ln\left[1-\exp\left(-0.0262\frac{R_w f_w^{1/2}}{a_b/k_s}\right)\right]+\frac{4.71 a_b/k_s}{R_w f_w^{1/2}}\right\}^2 = \frac{0.32}{f_w}+1.64 \quad (2.59)$$

Neilson (1992) presented the following equation which is valid for all values of a_b/k_s :

$$f_w = \exp\left[5.5(a_b/k_s)^{-0.2}-6.3\right] \quad (2.60)$$

Soulsby (1997) performed an analysis and predicted errors generated by Equations (2.56), (2.58), (2.59) and (2.60) that is presented in Table 2.5. One can conclude - based on his analysis - that the formula of Soulsby (1997) provides better estimation of the wave friction factor than all other three equations.

Table 2.5 Performance of various wave friction formula preditions versus experimental data (adapted from Soulsby, 1997)

RESEARCHER	EQUATION	10%	20%	50%
Myrhaug (1989)	(2.59)	9	16	36
Swart (1974)	(2.56)	5	18	39
Neilson (1992)	(2.60)	15	23	37
Soulsby (1997)	(2.58)	19	27	42

Le Roux (2003) developed a formula that does not depend on the Nikuradse roughness or on the wave boundary layer thickness. He related the wave friction factor to the Shield parameter and stated that his method is capable of performing well under combined wave-current conditions as well. He expressed the wave friction factor as follows:

$$f_w = \frac{2\beta g(\rho_s - \rho)d_s}{U_{wcr}^2 \rho} \qquad (2.61)$$

where d_s is the median grain size diameter, U_{wcr} is the critical peak near bottom orbital velocity while β is the Shields parameter for unidirectional current defined as (Le Roux, 1998):

$$\begin{aligned} \beta &= -0.0717 \log W_{ds} + 0.0625 && 0.0625 < W_{ds} \leq 2.5 \\ \beta &= 0.0171 \log W_{ds} + 0.0272 && 2.5 < W_{ds} \leq 11 \\ \beta &= 0.045 && W_{ds} > 11 \end{aligned} \qquad (2.62)$$

where W_{ds} is the dimensionless settling velocity expressed as (Le Roux, 1992, 1998):

$$\begin{aligned} W_{ds} &= (0.2354 D_d)^2 && D_d < 1.2538 \\ W_{ds} &= (0.208 D_d - 0.0652)^{3/2} && 1.2538 \leq D_d < 2.9074 \\ W_{ds} &= 0.2636 D_d - 0.37 && 2.9074 \leq D_d < 22.9866 \\ W_{ds} &= (0.8255 D_d - 0.54)^{2/3} && 22.9866 \leq D_d < 134.92150 \\ W_{ds} &= (2.531 D_d + 160)^{1/2} && 134.92150 \leq D_d < 1750 \end{aligned} \qquad (2.63)$$

in which D_d is dimensionless grain size diameter expressed as follows:

$$D_d = d_s \sqrt[3]{\rho g(\rho_s - \rho) / \mu^2} \qquad (2.64)$$

and where μ is the dynamic viscosity of water.

Le Roux (2001) proposed the following formula to determine U_{wcr}:

$$U_{wcr} = -0.01\left[(\theta_{wc} g d_s \rho_\gamma)^2 / (\rho\mu/T)\right] + 1.3416\left[(\theta_{wc} g d_s \rho_\gamma) / (\rho\mu/T)^{0.5}\right] - 0.6485 \qquad (2.65)$$

in which θ_{wc} is the dimensionless critical near-bottom orbital velocity expressed by Le Roux (2001) as follows:

$$\theta_{wc} = 0.0246 W_{ds}^{-0.55} \qquad (2.66)$$

2.10 Mud rheology and wave-mud interaction

In order to compute the entrainment rate of mud, its rheological properties must be properly elucidated and understood. These properties govern the way fluid mud interacts with waves, the way that mud influences wave attenuation, wave energy dissipation, the vertical diffusion and settling of sediment particles, their deposition, etc. The rheologcal behaviour of mud largely depends on the concentration of the sediments, sediment and water salinity, the pH of mud, its mineralogical composition, and the proportion between solid particles and the organic matter contained in the mud (Whitehouse *et al.*, 2000).

Unlike sand beds, the mud bed is almost impermeable. Thus the later is usually considered as a single-phase continuum (Li, 1996). Mud rheology is the relation through which the applied load, in the form of wave-induced turbulence, is related to the structure of mud and its response. This relation will further help define the stress-strain relation that is used in the momentum and continuity equations (Chou, 1989).

The importance of mud rheology under oscillatory, wave-induced forcing factor was first emphasized by Mehta (1991b). Apart from the stress-strain relation, mud rheology is strongly dependent on load frequency (Jiang, 1993) and it may also be time-dependent (Williams and Williams, 1992). The general form of equation used to express mud rheology is the relation between applied stress and shear strain in the following form (Malvern, 1969):

$$\tau = f(\gamma) \qquad (2.67)$$

where τ is the applied stress and γ is the shear strain. A few models have been proposed to explain cohesive sediment rheology and several details pertaining to their characteristics are presented below.

2.10.1 Linear visco-elastic models

Linear visco-elastic models are usually expressed in the following form (Li, 1996):

$$\sum_{r=0}^{N} p_r \frac{\partial^r}{\partial t^r}(\tau) = \sum_{s=0}^{N'} q_s \frac{\partial^s}{\partial t^s}(\gamma) \qquad (2.68)$$

where subscripts r and s denote the order of partial differentiation, p_r and q_s are model parameters such as dynamic viscosity and elastic modulus, while N and N' are specified maximum differential order of the model. Some of the common models in this category are:

2.10.1.1 Newtonian Fluid

With $p_0 = 1$, $q_0 = 2\mu$, μ is the dynamic viscosity of mud and all other coefficients are zero. The constitutive equation for Newtonian fluid is (Dalrymple and Liu, 1978; Shibayama *et al.*, 1986):

$$\tau = 2\mu\dot{\gamma} \qquad (2.69)$$

where the dot denotes derivation with respect to time.

2.10.1.2 Elastic material

With $p_0 = 1$, $q_0 = 2G$, G is elastic modulus and all other coefficients set equal to zero. Thus the stress-strain relation becomes (Dawson, 1978; Foda, 1989):

$$\tau = 2G\gamma \qquad (2.70)$$

2.10.1.3 Maxwell model

With $p_0 = 1/2\mu$, $p_1 = 1/2G$, $q_1 = 1$ and all other coefficients set equal to zero. The general form of the equation is:

$$\frac{1}{2\mu}\tau + \frac{1}{2G}\dot{\tau} = \dot{\gamma} \qquad (2.71)$$

2.10.1.4 Voigt model

With $p_0 = 1$, $q_0 = 2G$, $q_1 = 2\mu$ and other coefficients set equal to zero. The constitutive equation for the Voigt model is (Hsiao and Shemdin, 1980; Macpherson, 1980; Maa, 1986; Sakakiyama and Bijker, 1989):

$$\tau = 2G\gamma + 2\mu\dot{\gamma} \qquad (2.72)$$

The concept of the Voigt and Maxwell models is schematically shown in Figure 2.9.

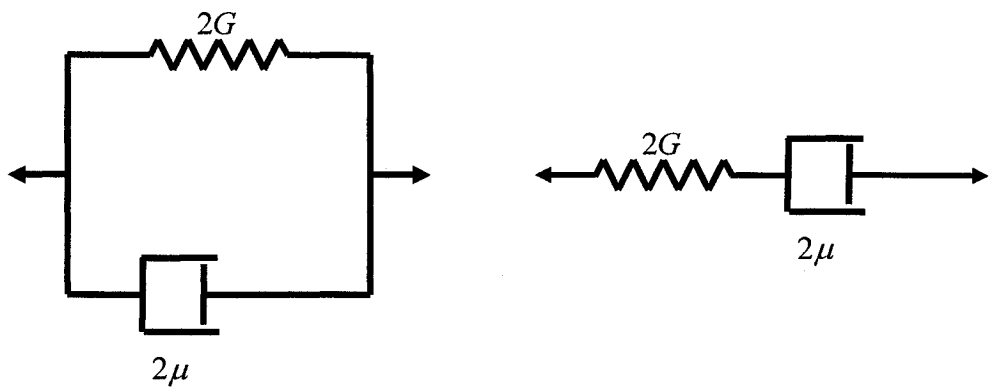

(a) Voigt Model (b) Maxwell Model

Figure 2.9 Two parameter visco-elastic models.

2.10.1.5 Jeffrey model or Standard Solid model

This three-parameter model was developed by combining the Maxwell and Voigt models. The constitutive parameters are: $p_0 = (G_1 + G_2)/\mu_2$, $p_1 = 1$, $q_0 = 2G_1G_2/\mu_2$, $q_1 = 2G_1$ and all other parameters set equal to zero. The general form of stress-strain relation of this type is written as follows (Keedwell, 1984; Jiang, 1993):

$$\frac{G_1 + G_2}{\mu_2}\tau + \dot{\tau} = \frac{2G_1G_2}{\mu_2}\gamma + 2G_1\dot{\gamma} \qquad (2.73)$$

Also, by combining the Maxwell and Jeffrey models, a new model was proposed (known as Jeffrey-Maxwell model). The coefficients of this model are: $p_0 = G_2/\mu_2$, $p_1 = 1$, $q_0 = 2G_1G_2/\mu_2$, $q_1 = 2(G_1 + G_2)$ and all other parameters set equal to zero. The constitutive equation for this model is:

$$\frac{G_1+G_2}{\mu_2}\tau+\dot{\tau}=\frac{2G_1G_2}{\mu_2}\gamma+2(G_1+G_2)\dot{\gamma} \qquad (2.74)$$

Jeffrey models are depicted schematically in Figure 2.10.

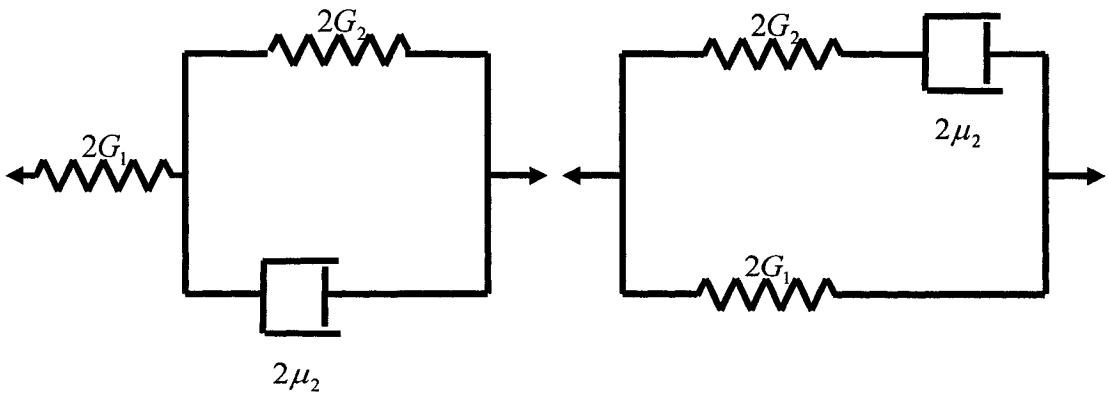

(a) Standard Solid Model (b) Jeffrey-Maxwell Model

Figure 2.10 Jeffrey models.

Under oscillatory forcing factors such as wave-induced loading, the shear stress and shear strain can be expressed in terms of the angular frequency of loading as:

$$\begin{aligned}\tau &= \tau_0 \exp(-i\sigma t)\\ \gamma &= \gamma_0 \exp[-i(\sigma t-\phi_0)]\end{aligned} \qquad (2.75)$$

where σ is the frequency of loading, ϕ_0 is the phase shift, and τ_0 and γ_0 are the maximum amplitudes of τ and γ, respectively. Therefore, the general stress-strain relation can be simplified to:

$$\tau=\frac{\sum_{s=0}^{N'} q_s(-i\sigma)^s}{\sum_{r=0}^{N} p_r(-i\sigma)^{r+1}}\dot{\gamma}=2(\mu'+i\mu'')\dot{\gamma}=2\mu^*\dot{\gamma} \qquad (2.76)$$

where μ^* is called complex dynamic viscosity, μ' is the dynamic viscosity and μ'' is called the second viscosity. The standard methodology used to determine the parameters of mud rheology is to conduct a set of experimental oscillatory tests (Chou, 1989; Jiang, 1993) and using the results of these tests, the complex viscosity can be determined. However, since none of the above-mentioned models fully describe the behaviour of mud under various types of loading, more terms and implicitly more complicated models are required in order to obtain more accurate results. Such an approach was proven to limit model applicability and complicates the experimental work (Li, 1996).

2.10.2 Nonlinear and time-dependent models

In the case of these models, the relation between applied stress and strain is non-linear. In some models, an initial resistance, known as yield stress, is considered for mud, since the structure of the soft mud can resist small shear stresses. These models are generally known as visco-plastic models (Engelund and Wan, 1984; Suhayda, 1986; Mei and Liu, 1987; Tsuruya, 1987; Liu and Mei, 1989; Shibayama *et al.*, 1990). For small strains, the general stress-strain relation can be expressed as follows:

$$\tau = \left(2\mu_p + \frac{\tau_y}{\sqrt{\Pi_D}} \right) \dot{\gamma} \qquad (2.77)$$

where μ_p is the apparent viscosity, τ_y is the yield strength and Π_D is the second invariant of $\dot{\gamma}$, which is expressed as:

$$\Pi_D = 2\left(\frac{\partial u}{\partial x} \right)^2 + 2\left(\frac{\partial w}{\partial z} \right)^2 + \left(\frac{\partial u}{\partial z} + \frac{\partial w}{\partial x} \right)^2 \qquad (2.78)$$

For the one-dimensional condition, Equation (2.77) can be simplified to (Wilkinson, 1960):

$$\tau = \tau_y + \mu_p \dot{\gamma} \qquad (2.79)$$

These types of models are referred to as Bingham plastic models (Whitehouse *et al.*, 2000).

The other type of non-linear models are known as shear thinning or pseudo-plastic models. In this case, the apparent viscosity decreases with an increase in the shear strain rate, under increasing applied shear stress. The general constitutive equation for this type of model is (Sisko, 1958; Feng, 1992; Whitehouse *et al.*, 2000):

$$\tau = \mu_\infty \dot{\gamma} + c\dot{\gamma}^n \qquad (2.80)$$

in which the apparent viscosity is $\mu_\infty + c\dot{\gamma}^{n-1}$, μ_∞ is the constant viscosity at the limit of high shear rate, c is the measure of consistency of the cohesive material and $n<1$ is a mud specific parameter. These types of models usually give satisfactory results for flocculated clay slurries (Whitehouse *et al.*, 2000).

Other types of non-linear models are known as shear thickening models that follow the same formulation as shear thinning models, with this difference of $n>1$. These models tend to give good results for concentrated deflocculated clay slurries (Whitehouse *et al.*, 2000).

Some of the researchers have tried to combine the linear visco-elastic and non-linear plastic models. These models are called visco-elastic-plastic models (Shibayama *et al.*, 1993; Soltanpour *et al.*, 2003; Oveisy and Soltanpour, 2005). Fluid mud is assumed to be visco-elastic when stress is less than yield stress and it is considered to be visco-plastic when applied stress is greater than yield stress. The constitutive equation for these models is expressed as:

$$\tau = 2\mu_p \dot{\gamma} \qquad (2.81)$$

$$\mu_p = \begin{cases} \mu_{2e} + \dfrac{iG}{\sigma} & \left(\frac{1}{2}\tau^2 \le \tau_y^2\right) \\ \mu_{2p} + \dfrac{\tau_y}{\sqrt{\Pi_D}} & \left(\frac{1}{2}\tau^2 > \tau_y^2\right) \end{cases} \qquad (2.82)$$

where μ_{2e} is the viscosity of mud in visco-elastic state and μ_{2p} is the viscosity of mud in the visco-plastic state.

3 SUSPENDED SEDIMENT CONCENTRATION MODEL

A new one-dimensional time-dependent model was developed by the author. The model is used to calculate the suspended sediment concentration of cohesive sediments. This model is based on the model developed by Mehta and Li (2003). This model assumes the presence of several combinations of hydrodynamic conditions: current, waves or wave plus weak current. A weak current is a condition in which wave-induced upward diffusion is modulated by the current, but the wave-induced flow field remains unchanged.

The model treats sediment concentration under two different mechanisms: (1) fluid mud resuspension and (2) bed resuspension. In the case of fluid mud, entrainment of fluid mud into the water column and its re-deposition can be simulated under conditions of waves or waves plus weak current. The existence of the current is not considered for fluid mud, since physically, it does not occur. The resuspension and re-deposition of sediments from the bed is simulated for current, waves, or waves plus weak current.

The developed model can compute the suspended sediment concentration from either an initial sediment concentration profile or from clear water conditions. The mathematical formulation of the model is presented herein.

3.1 Theoretical formulation of the suspended sediment concentration numerical model

The computational domain in the model is divided into two parts: *(1) the water layer* and *(2) the fluid mud,* or *the bed layer*. The physical domain of the numerical model is presented in Figure 3.1 schematically.

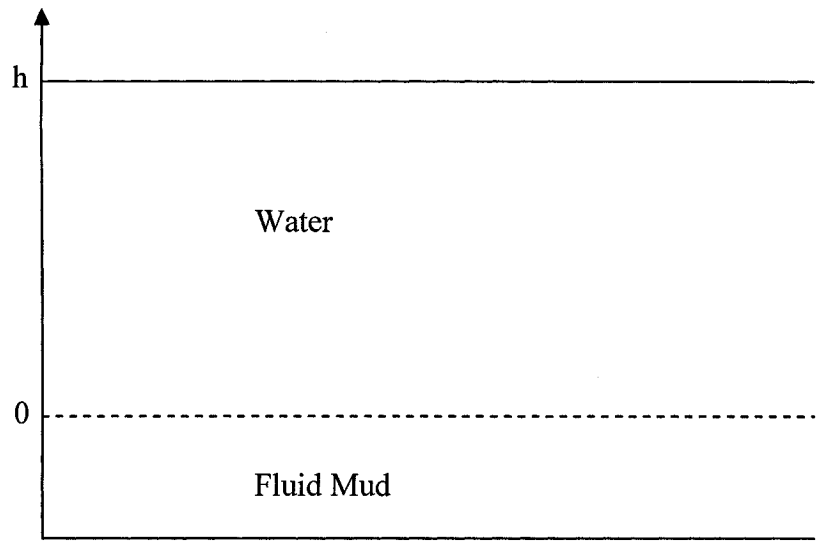

Figure 3.1 Water/Fluid mud or Water/Bed system.

3.1.1 Wave-averaged transport equation

The global advection-diffusion sediment transport is presented in this section. Due to the difficulty of modelling turbulence and boundaries, the simplified form of wave-averaged equation is used and the effect of turbulent and wave-induced transport are considered in diffusion coefficient. The temporal variation of the sediment concentration is equal to the gradient of the mass flux at each point in the water column and can be written as:

$$\frac{\partial c}{\partial t} = \nabla \cdot \vec{F} \qquad (3.1)$$

where c is sediment concentration and F is the sediment mass flux. Sediment flux consists of advective, diffusive and settling components. Therefore, assuming isotropic behaviour of sediments in space, Equation (3.1) can be expanded as:

$$\frac{\partial c}{\partial t} + \frac{\partial (uc)}{\partial x} + \frac{\partial (vc)}{\partial y} + \frac{\partial (wc)}{\partial z} = \frac{\partial}{\partial x}\left(D_m \frac{\partial c}{\partial x}\right) + \frac{\partial}{\partial y}\left(D_m \frac{\partial c}{\partial y}\right) + \frac{\partial}{\partial z}\left(D_m \frac{\partial c}{\partial z}\right) + \frac{\partial}{\partial z}(w_s c) \qquad (3.2)$$

where u, v, w are instantaneous flow velocities in the x, y, z-directions, D_m represents the molecular diffusion coefficient, and w_s represents the settling velocity. Due to their different time scales, each of the instantaneous velocities and concentrations can be decomposed into three components: *a wave-averaged one, a wave oscillating one* and *the turbulent fluctuation one*. Each of these components have different time scales: the turbulent fluctuation has a time scale of 0.0001~1 s (e.g. Hinze, 1959); the time scale for wave periods is around 0.1 ~ 30s (for the case of ultragravity and gravity waves, Kamphuis, 2000); the time scale for natural flows is much higher (about 12 hours in the case of tides, Kamphuis, 2000). Therefore, each velocity component can be written as:

$$u = \bar{u} + \tilde{u} + u',\ v = \bar{v} + \tilde{v} + v',\ w = \bar{w} + \tilde{w} + w',\ c = \bar{c} + \tilde{c} + c' \qquad (3.3)$$

where $\bar{u}$, $\bar{v}$, $\bar{w}$, and $\bar{c}$ are time-averaged values over one wave period, $\tilde{u}$, $\tilde{v}$, $\tilde{w}$ and $\tilde{c}$ are the wave oscillating components, while u', v', w' and c' are the turbulent fluctuation terms. Substituting Equation (3.3) in Equation (3.2) and time-averaging over one wave period, one obtains:

$$\begin{aligned}&\frac{\partial \bar{c}}{\partial t} + \frac{\partial(\overline{u\bar{c}})}{\partial x} + \frac{\partial(\overline{v\bar{c}})}{\partial y} + \frac{\partial(\overline{w\bar{c}})}{\partial z} + \frac{\partial(\overline{\tilde{u}\tilde{c}})}{\partial x} + \frac{\partial(\overline{\tilde{v}\tilde{c}})}{\partial y} + \\ &\frac{\partial(\overline{\tilde{w}\tilde{c}})}{\partial z} + \frac{\partial(\overline{u'c'})}{\partial x} + \frac{\partial(\overline{v'c'})}{\partial y} + \frac{\partial(\overline{w'c'})}{\partial z} = \\ &\frac{\partial}{\partial x}\left(D_m \frac{\partial \bar{c}}{\partial x}\right) + \frac{\partial}{\partial y}\left(D_m \frac{\partial \bar{c}}{\partial y}\right) + \frac{\partial}{\partial z}\left(D_m \frac{\partial \bar{c}}{\partial z}\right) + \frac{\partial}{\partial z}(w_s \bar{c})\end{aligned} \qquad (3.4)$$

in which the over-bar implies time-averaging.

As a closure model, by incorporating the eddy viscosity concept, turbulent stresses and wave oscillating stresses are expressed in terms of the diffusion coefficients as shown below:

$$-\overline{\tilde{u}\tilde{c}} - \overline{u'c'} = \varepsilon'_x \frac{\partial \bar{c}}{\partial x}, -\overline{\tilde{v}\tilde{c}} - \overline{v'c'} = \varepsilon'_y \frac{\partial \bar{c}}{\partial y}, -\overline{\tilde{w}\tilde{c}} - \overline{w'c'} = \varepsilon'_z \frac{\partial \bar{c}}{\partial z} \qquad (3.5)$$

where ε'_x, ε'_y and ε'_z are the diffusion coefficients due to the wave-induced and turbulent current-induced diffusion.

In the next step, molecular diffusions, wave-induced and turbulent diffusions are combined to form the general diffusion coefficient, that is:

$$\varepsilon_x = \varepsilon'_x + D_m \quad , \quad \varepsilon_y = \varepsilon'_y + D_m \quad , \quad \varepsilon_z = \varepsilon'_z + D_m \tag{3.6}$$

Therefore, the time-averaged mass transport becomes:

$$\frac{\partial \bar{c}}{\partial t} + \frac{\partial(\overline{u\bar{c}})}{\partial x} + \frac{\partial(\overline{v\bar{c}})}{\partial y} + \frac{\partial(\overline{w\bar{c}})}{\partial z} = \frac{\partial}{\partial x}\left(\varepsilon_x \frac{\partial \bar{c}}{\partial x}\right) + \frac{\partial}{\partial y}\left(\varepsilon_y \frac{\partial \bar{c}}{\partial y}\right) + \frac{\partial}{\partial z}\left(\varepsilon_z \frac{\partial \bar{c}}{\partial z}\right) + \frac{\partial}{\partial z}(w_s \bar{c}) \tag{3.7}$$

Ross (1988) stated that the horizontal gradient in the sediment concentration are three to four orders of magnitude smaller than the vertical sediment concentration gradient in the case of coastal zones, estuaries and shallow lakes. Therefore, the horizontal gradient terms are neglected in the present model and uniform variables were assumed in the horizontal directions. Moreover, as long as the linear waves are used in this study, $\bar{u} = \bar{v} = \bar{w} = 0$. Thus, the simplified one-dimensional governing equation for z-direction becomes:

$$\frac{\partial \bar{c}}{\partial t} = \frac{\partial}{\partial z}\left(\varepsilon_z \frac{\partial \bar{c}}{\partial z}\right) + \frac{\partial}{\partial z}(w_s \bar{c}) \tag{3.8}$$

For the case of simplicity, the over-bar is omitted from the expression of the sediment concentration throughout the rest of this chapter.

3.1.2 Vertical mass transport equation

Neglecting the horizontal convection and diffusion in the mass transport governing equation, the wave-average settling-diffusion equation can be expressed as:

$$\frac{\partial c}{\partial t} - \frac{\partial}{\partial z}\left(\varepsilon_s \frac{\partial c}{\partial z} + w_s c\right) = 0 \tag{3.9}$$

where c is sediment concentration in the water column, ε_s is the diffusion coefficient in z direction and w_s is the settling velocity. The boundary conditions of Equation (3.9) are:

1. No vertical sediment flux at water surface $(z = h)$:

$$\left(\varepsilon_s \frac{\partial c}{\partial z} + w_s c\right)\Big|_{z=h} = 0 \qquad (3.10)$$

2. The vertical sediment flux at water-mud interface $(z = 0)$ is equal to the net resuspension flux:

$$\left(\varepsilon_s \frac{\partial c}{\partial z} + w_s c\right)\Big|_{z=0} = -F_n \qquad (3.11)$$

in which F_n is the resuspension flux.

3.1.3 Settling velocity

Equation (3.9) is strongly dependent on the formulation of the settling velocity (Wolansky *et al.*, 1988; Hwang, 1989). The settling velocity in the proposed model is expressed as::

$$w_s = \begin{cases} \dfrac{\alpha_1 c_1^{\beta_1}}{\left(c_1^2 + \gamma_1^2\right)^{\delta_1}} = W_{sf} & c \le c_1 \\ \dfrac{\alpha_1 c^{\beta_1}}{\left(c^2 + \gamma_1^2\right)^{\delta_1}} & c > c_1 \end{cases} \qquad (3.12)$$

3.1.4 Vertical diffusion coefficient

The diffusion coefficient depends on the hydrodynamic field and on the sediment concentration gradient. Therefore, it can be expressed in terms of the neutral diffusion coefficient and the stratification factor as follows:

$$\varepsilon_s = \varepsilon_{sn} \Phi \qquad (3.13)$$

in which ε_{sn} is the neutral diffusion coefficient for non-stratified flows and Φ is the density stratification correction factor which increasingly reduces the ratio, $\varepsilon_s / \varepsilon_{sn}$, below unity as the concentration gradient increases in the water column; in other words, the flow energy

needed for particle entrainment decreases (Dyer, 1986). The density stratification correction factor is modeled using Munk and Anderson's formula (1948) which is used in combination with both Hwang (1989) and Ross (1988) formulae for simulating sediment-induced stratification. The equation is expressed as:

$$\Phi = \frac{1}{(1+\alpha_0 R_i)^{\beta_0}} \qquad (3.14)$$

in which α_0 and β_0 are non-dimensional empirical coefficients which depend on the effect of the suspended sediment on the turbulent mixing length, and R_i is the gradient Richardson number expressed as:

$$R_i = \left(\frac{g}{\rho}\right)\frac{-\partial\rho/\partial z}{(\partial u/\partial z)^2} \qquad (3.15)$$

where u is the horizontal velocity, ρ is the fluid density and g is the gravitational acceleration. It should be noted that Equation (3.15) is not valid in the case of uniform velocity conditions, since, for that case, $R_i \to \infty$.

In order to define the neutral diffusion coefficient under wave motion, the formulation of Hwang and Wang (1982) was adopted as follows:

$$\varepsilon_{nw} = \alpha_w H^2 \sigma \frac{\sinh^2 kz}{2\sinh^2 kh} \qquad (3.16)$$

where H is the wave height, α_w is a non-dimensional wave diffusion constant, $\sigma = 2\pi/T$ is the wave frequency, T is the wave period, $k = 2\pi/L$ is the wave number, and L is the wave length.

The wavelength is computed using linear wave theory as:

$$L = \frac{g}{2\pi} T^2 \tanh kh \qquad (3.17)$$

The neutral diffusion coefficient under current is expressed as (Vanoni, 1975):

$$\varepsilon_{nc} = \kappa u_* z\left(1-\frac{z}{h}\right) \qquad (3.18)$$

where κ is the von Karman Constant and u_* is friction velocity.

In the presence of waves and weak current conditions, cohesive sediments are entrained at a faster rate compared to the condition when only waves are present (Li, 1996). Therefore, the model uses the following equation for this case:

$$\varepsilon_s = (\varepsilon_{nw} + \varepsilon_{nc})\Phi \qquad (3.19)$$

3.1.5 Fluid mud entrainment rate

For the case of fluid mud, the rate of entrainment uses the concept of Li (1996) and it is expressed as:

$$F_n = \begin{cases} \rho_m u_b \alpha_4 \left(R_{ic}^2 R_{ig}^{-1} - R_{ig}\right) - w_s c\big|_{z=0} & \left(R_{ig} < R_{ic}\right) \\ -w_s c\big|_{z=0} & \left(R_{ig} \geq R_{ic}\right) \end{cases} \qquad (3.20)$$

where ρ_m is density of fluid mud, u_b is the amplitude of horizontal velocity just outside the bottom boundary layer, α_4 is a non-dimensional coefficient, R_{ig} is the global Richardson number and R_{ic} is the critical value for global Richardson number. The global Richardson number is defined as:

$$R_{ig} = \frac{\frac{\rho_m - \rho}{\rho} g\delta}{\Delta u_0^2} \qquad (3.21)$$

Where δ is the thickness of wave bottom boundary layer, ν is the kinematic viscosity of water, T is the wave period and Δu_0 is the magnitude of the maximum difference between velocities across the water-fluid mud interface. This velocity is obtained either by measurement or from the wave-mud interaction model, which is based on the study of Jiang (1993).

3.1.6 Wave-mud interaction model

3.1.6.1 Mud rheology

In order to use the wave-mud interaction model, the rheological description of the mud must be known. The model is capable of working with three rheological options. The first rheological model is a three parameter standard solid model initially developed by Jiang (1993). The general stress-strain relation is expressed as follows:

$$\frac{G_1 + G_2}{\mu_2}\tau + \dot{\tau} = \frac{2G_1 G_2}{\mu_2}\gamma + 2G\dot{\gamma} \qquad (3.22)$$

where τ is the applied shear stress, γ is the shear strain, G_1 and G_2 are the elastic moduli, μ_2 is the mud dynamic viscosity, and dots denote time derivatives. The model can be simplified to the Voigt model which is less accurate when $G_1 \to \infty$. The equation then becomes:

$$\tau = 2G_2\gamma + 2\mu_2\dot{\gamma} \qquad (3.23)$$

If $G_2 = 0$, Equation (3.23) further simplifies to approximate the behaviour of the mud-water mixture in the form of a Newtonian fluid:

$$\tau = 2\mu_2\dot{\gamma} \qquad (3.24)$$

The wave-mud interaction model is capable to work with any of the above-mentioned rheological options.

3.1.6.2 Wave-mud interaction modelling

The scheme of the physical domain used in the wave-mud interaction model is shown in Figure 3.2. Water surface elevation is represented as $\eta_1(x,t) = He^{i(kx-\sigma t)}$ and the interfacial elevation between the layers is represented as $\eta_2(x,t) = H_b e^{i(kx-\sigma t)}$. In this expressions, H is the wave height, H_b is the interfacial amplitude (complex), k is the wave number, σ is the wave frequency and $i = \sqrt{-1}$.

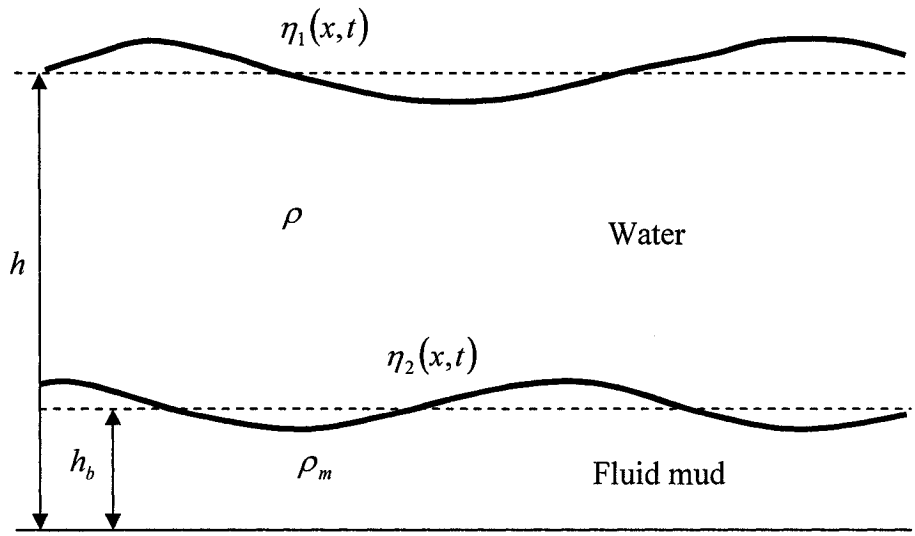

Figure 3.2 The physical domain for the wave-mud interaction model.

In the governing equations, convective acceleration terms for both water and mud are neglected. The governing equations for continuity and momentum are:

Continuity:
$$\frac{\partial \hat{u}_j}{\partial x} + \frac{\partial \hat{v}_j}{\partial y} = 0 \qquad (3.25)$$

$$\frac{\partial \hat{u}_j}{\partial t} = -\frac{1}{\rho_j}\frac{\partial \hat{P}_j}{\partial x} + \frac{\mu_{ej}}{\rho_j}\left(\frac{\partial^2 \hat{u}_j}{\partial x^2} + \frac{\partial^2 \hat{u}_j}{\partial z^2}\right) \qquad (3.26)$$

Momentum:
$$\frac{\partial \hat{v}_j}{\partial t} = -\frac{1}{\rho_j}\frac{\partial \hat{P}_j}{\partial x} + \frac{\mu_{ej}}{\rho_j}\left(\frac{\partial^2 \hat{v}_j}{\partial x^2} + \frac{\partial^2 \hat{v}_j}{\partial z^2}\right) \qquad (3.27)$$

Where $\hat{u}_j$ and $\hat{v}_j$ are the horizontal and vertical components of the wave orbital velocity vector, respectively, μ_{ej} is equivalent dynamic viscosity, subscript j refers to the water layer, $(j=1)$ and mud layer $(j=2)$ and $\hat{P}_j$ is the dynamic pressure defined as:

$$\hat{P}_j = \hat{P}_j^t + \rho_j g z + P_j^0 \tag{3.28}$$

where $\hat{P}_j^t$ is the total pressure and:

$$P_j^0 = \begin{cases} 0 & for \ \ j=1 \\ (\rho_2 - \rho_1)gh & for \ \ j=2 \end{cases} \tag{3.29}$$

in which ρ_1 is the density of water, and ρ_2 is the mud density.

For water,

$$\mu_{e1} = \mu_1 \tag{3.30}$$

For mud, if modeled as Newtonian fluid,

$$\mu_{e2} = \mu_2 \tag{3.31}$$

If modeled as a Voigt material,

$$\mu_{e2} = \mu_2 + i\frac{G_2}{\rho_2} \tag{3.32}$$

And if modeled as standard solid material,

$$\mu_{e2} = \frac{2G_1\left(\frac{G_1}{\mu_2}\right)}{\sigma^2 + \left(\frac{G_1+G_2}{\mu_2}\right)^2} + i\frac{\frac{2G_1}{\sigma}\left[\frac{(G_1+G_2)G_2}{\mu_2^2} + \sigma^2\right]}{\sigma^2 + \left(\frac{G_1+G_2}{\mu_2}\right)^2} \tag{3.33}$$

The boundary conditions used to solve the governing equations are:

1. At the fixed bed ($z = 0$), horizontal and vertical velocities are zero:

$$\hat{u}_2 = 0 \tag{3.34}$$

$$\hat{v}_2 = 0 \tag{3.35}$$

2. At the interface between the two layers, $z = h_b$, the kinematic and dynamic conditions are:

$$\hat{u}_1 = \hat{u}_2 \tag{3.36}$$

$$\hat{v}_1 = \hat{v}_2 \tag{3.37}$$

$$\frac{\partial \eta_2}{\partial t} = \hat{v}_1 = \hat{v}_2 \tag{3.38}$$

$$\mu_{e1}\left(\frac{\partial \hat{u}_1}{\partial z} + \frac{\partial \hat{v}_1}{\partial x}\right) = \mu_{e2}\left(\frac{\partial \hat{u}_2}{\partial z} + \frac{\partial \hat{v}_2}{\partial x}\right) \tag{3.39}$$

$$\hat{P}_1^t - 2\mu_{e1}\frac{\partial \hat{v}_1}{\partial z} = \hat{P}_2^t - 2\mu_{e2}\frac{\partial \hat{v}_2}{\partial z} \tag{3.40}$$

3. At the free water surface ($z = h$), the boundary conditions are:

$$\frac{\partial \eta_1}{\partial t} = \hat{v}_1 \tag{3.41}$$

$$\mu_{e1}\left(\frac{\partial \hat{u}_1}{\partial z} + \frac{\partial \hat{v}_1}{\partial x}\right) = 0 \tag{3.42}$$

No wind : $$\hat{P}_1^t - 2\mu_{e1}\frac{\partial \hat{v}_1}{\partial z} = 0 \tag{3.43}$$

The solutions of these equations for $\hat{u}_j$, $\hat{v}_j$ and $\hat{P}_j$ are assumed separable and periodic in time and in x-direction, i.e.:

$$\begin{aligned} \hat{u}_j(x,z,t) &= u_j(z)\exp[i(kx-\sigma t)] \\ \hat{v}_j(x,z,t) &= v_j(z)\exp[i(kx-\sigma t)] \\ \hat{P}_j(x,z,t) &= P_j(z)\exp[i(kx-\sigma t)] \end{aligned} \tag{3.44}$$

Now Equation (3.44) is further substituted into the governing equations (Equations 3.25~3.27). Subsequently, boundary conditions are also applied and the solutions for linear wave propagation over soft mud are obtained (Jiang, 1993). Mehta and Li (2003) recommended a value $G_2 = 100{,}000$ or more in Voigt model, in order to simulate rigid bed conditions.

3.1.7 Bed resuspension rate

In the case of the bed resuspension rate, for the boundary condition at the bed surface, the resuspension net sediment flux is expressed as:

$$F_n = \begin{cases} E_{dep} & \left(\tau_b \le \tau_{dep}\right) \\ 0 & \left(\tau_{dep} < \tau_b \le \tau_c\right) \\ E_c & \left(\tau_b > \tau_c\right) \end{cases} \qquad (3.45)$$

In which τ_b is the bed shear stress, τ_c is the bed shear strength for erosion, τ_{dep} is the critical shear stress for deposition, E_{dep} is the deposition rate and E_c is the erosion rate. The deposition rate is based on the formulation of Krone (1962):

$$E_{dep} = -w_s c\big|_{z=0}\left(1 - \frac{\tau_b}{\tau_{dep}}\right) \qquad (3.46)$$

The bed shear stress is calculated using the expression proposed by Jonnson (1963):

$$\tau_b = \frac{1}{2} f_w \rho u_b^2 \qquad (3.47)$$

where u_b is amplitude of the wave orbital velocity at the bed and f_w is the wave friction factor (Jonnson, 1966). For the case of currents, the bed shear stress is:

$$\tau_b = \frac{1}{2} f_c \rho U^2 \qquad (3.48)$$

in which U is the depth-averaged current velocity and f_c is the current friction coefficient and is expressed as (Vanoni, 1975):

$$f_c = 2g\frac{n^2}{h^{1/3}} \tag{3.49}$$

where n is the Manning's bed resistance coefficient.

The erosion rate is based on the formulation of Mehta (1988):

$$E_c = s(\tau_b - \tau_c) \tag{3.50}$$

in which s is an empirical parameter expressed as (Lee *et al.*, 1994):

$$s = s_{\max} e^{-a_r \tau_c^{b_r}} \tag{3.51}$$

where $s_{\max}, a_r$ and b_r are coefficients dependent on sediment properties .

In the original model of Mehta and Li (2003), the bed shear strength resistance is formulated as in the previous work of Mehta (1991):

$$\tau_c(z) = \alpha_e(\phi_s(z) - \phi_e)^{\beta_e} \tag{3.52}$$

where α_c and β_c are empirical coefficients, ϕ_s represents the solids volume fraction $\phi_s = \rho_D/\rho_s$ and ϕ_c is the critical solids volume fraction below which mud has fluid-like behaviour. Here, ρ_s is the sediment granular density and ρ_D represents the bed dry bulk density, expressed as (Mehta *et al.*, 1982):

$$\rho_D = \overline{\rho}_D \zeta \left(\frac{h_b - \Delta z}{h_b}\right)^{\xi} \tag{3.53}$$

where h_b is the bed depth, $\overline{\rho}_D$ is the bed average dry density, Δz is incremental depth from the bed surface, and ζ and ξ are non-dimensional coefficients dependent on sediment properties.

3.1.8 *Electrochemical anchoring resistance*

Following a detailed literature review previously presented and discussed in the thesis, the effect of electrochemical resistance of the cohesive sediments is incorporated in the formulation of the sediment entrainment rate. The approach used is based on the formula developed by Taki (2001):

$$\tau_c = 0.05 + \chi\left[\frac{1}{\left\{(\pi/6)\left(1+32SW_L\eta_*^{-0.4}\right)\right\}^{1/3}-1}\right]^2 \qquad (3.54)$$

in which χ the is electrochemical anchoring coefficient, W_L is liquid limit of mud, S is the specific weight of the sediment particle and η_* is the degree of resistance of a particle deposited on the mud. The parameter η_* is defined as:

$$\eta_* = \nu_b \Big/ \left\{(S-1)gd_s^3\right\}^{1/2} \qquad (3.55)$$

where d_s is equivalent spherical diameter of the particle, ν_b is the kinematic viscosity of mud.

3.1.9 *Defining shear resistance by including vane shear strength of bed*

In order to include vane shear strength of the bed, the formula proposed by Dade and Nowell (1991) is employed:

$$\tau_c = \frac{40\rho\nu^2}{\tan\phi_1 d_s^2}\left\{\sqrt{\frac{g\rho_s' d_s^3\tan^2\phi_1}{240\rho\nu^2}\left[1+3(1-\cos\phi_1)\frac{\tau_y}{g\rho_s' d_s}\right]}+1-1\right\} \qquad (3.56)$$

in which d_s is the sediment particle diameter, ρ is the fluid density, ρ_s' is excess density of the sediment, ν is the kinematic viscosity, and ϕ_1 is the bed-packing angle of bed.

3.1.10 *Wave friction factor formulation*

In order to study the effect of the wave friction factor on the vertical suspension of cohesive sediments, three methods were incorporated and compared with each other in order to estimate their accuracy.

3.1.10.1 Wave friction factor using Jonnson formula

First method is the one proposed by Jonnson (1963) in which the wave friction factor is expressed as:

$$f_w = 0.0604/\left[\log(30\delta/k_s)^2\right] \qquad (3.57)$$

where δ is the boundary layer thickness and k_s is the Nikuradse roughness coefficient. Based on the recommendation of Teleki and Anderson (1970), the following equation by Li (1954) was used to describe boundary layer thickness:

$$\delta = 6.5\sqrt{(\mu T/2\rho\pi)} \qquad (3.58)$$

3.1.10.2 Wave friction factor using Swart formula:

In this case, the wave friction factor is modeled from the equation of Swart (1974) expressed as:

$$f_w = \exp\left[-5.977 + 5.213(a_b/k_s)^{-0.194}\right] \qquad (3.59)$$

where k_s is the Nikuradse bed roughness and a_b is expressed as:

$$a_b = u_b/\sigma \qquad (3.60)$$

where u_b is the wave orbital velocity at the bed and $\sigma = 2\pi/T$ is the wave frequency.

3.1.10.3 Wave friction factor using Le Roux formula

The formula of Le Roux (2003) is used as follows:

$$f_w = \frac{2\beta g(\rho_s - \rho)d_s}{U_{wcr}^2 \rho} \qquad (3.61)$$

where d_s is the median grain size diameter, U_{wcr} is the critical peak near-bottom orbital velocity and β is the Shield parameter for unidirectional current defined as (Le Roux, 1998):

$$\begin{aligned} \beta &= -0.0717 \log W_{ds} + 0.0625 && 0.0625 < W_{ds} \le 2.5 \\ \beta &= 0.0171 \log W_{ds} + 0.0272 && 2.5 < W_{ds} \le 11 \\ \beta &= 0.045 && W_{ds} > 11 \end{aligned} \qquad (3.62)$$

where W_{ds} is the dimensionless settling velocity expressed as (Le Roux, 1992, 1998):

$$\begin{aligned} W_{ds} &= (0.2354 D_d)^2 && D_d < 1.2538 \\ W_{ds} &= (0.208 D_d - 0.0652)^{3/2} && 1.2538 \le D_d < 2.9074 \\ W_{ds} &= 0.2636 D_d - 0.37 && 2.9074 \le D_d < 22.9866 \\ W_{ds} &= (0.8255 D_d - 0.54)^{2/3} && 22.9866 \le D_d < 134.92150 \\ W_{ds} &= (2.531 D_d + 160)^{1/2} && 134.92150 \le D_d < 1750 \end{aligned} \qquad (3.63)$$

where D_d is the dimensionless grain size diameter as follows:

$$D_d = d_s \sqrt[3]{\rho g(\rho_s - \rho)/\mu^2} \qquad (3.64)$$

where μ is the dynamic viscosity of water.

Le Roux (2001) proposed the following formula to determine U_{wcr}:

$$U_{wcr} = -0.01\left[(\theta_{wc} g d_s \rho_\gamma)^2 / (\rho\mu/T)\right] + 1.3416\left[(\theta_{wc} g d_s \rho_\gamma)/(\rho\mu/T)^{0.5}\right] - 0.6485 \qquad (3.65)$$

in which θ_{wc} is the dimensionless critical near-bottom orbital velocity expressed by Le Roux (2001) as:

$$\theta_{wc} = 0.0246 W_{ds}^{-0.55} \qquad (3.66)$$

3.1.11 Time-dependent erosion rate

The development of Sanford and Maa (2001), who related the erosion rate to time is incorporated in the present study. The governing equation (2.22) is solved for the case of constant bed shear stress and is presented below:

$$E' = \beta_e(\tau_b - \tau_{c0})\exp[-\gamma\beta_e(t - t_0)] \qquad (3.67)$$

where $E' = E[\rho_s \phi_s(z)]^{-1} = dz/dt$ is the erosion velocity, ρ_s is the sediment density, $\phi_s(z) = 1 - \phi(z)$ is the volume fraction of sediment, τ_{c0} is the critical shear stress when τ_b is first applied at $t = t_0$, β_e is the local erosion coefficient and $\gamma = \frac{d\tau_c}{dz}$ is the rate of increase of bed resistance with respect to depth. Based on Equations (3.52) and (3.53) one obtains:

$$\gamma = \frac{d\tau_c}{dz} = -\alpha_e\beta_e\left(\frac{\overline{\rho}_D\zeta\xi}{\rho_s h_b}(1 - \Delta z/h_b)^{(\xi-1)}\right)\left(\frac{\rho(z)}{\rho_s} - \phi_e\right)^{(\beta_e-1)} \qquad (3.68)$$

Considering $\Delta z = 0$ for initial critical shear stress, one can write:

$$\tau_{c_0} = \alpha_e\left(\frac{\overline{\rho}_D}{\rho_s} - \phi_e\right)^{\beta_e} \qquad (3.69)$$

The value for β_e is calculated in terms of the bulk density of mud, based on the study of Aberle *et al.* (2004). The Richard's logistic model, commonly used to fit S-shaped curves, is adopted as the best fit for the present case. The general form of the equation and its parameters is:

$$y = \frac{a}{[1 + \exp(b - cx)]^{1/d}} \qquad (3.70)$$

where coefficients $a = 0.000821$, $b = -7.969$, $c = -0.0103$ and $d = 0.935$ provide the best match for the experimental data. The correlation was also found to be 0.934, a value which indicates good agreement with experimental data. The data of β_e versus bulk density and the best-fit curve is depicted in Figure 3.3.

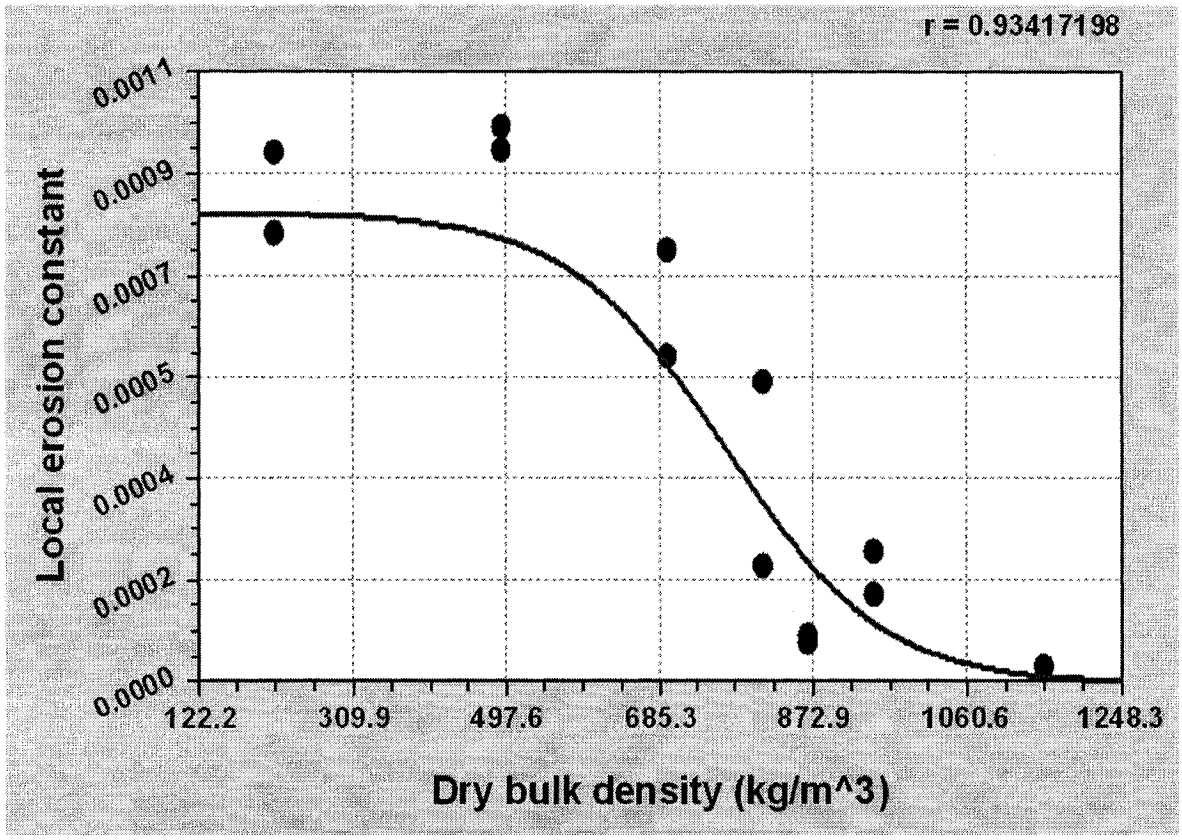

Figure 3.3 Variation of local erosion coefficient vs. bed bulk density (Data from Aberle *et al.*, 2004).

3.2 Program structure

The program uses the implicit finite difference scheme to solve the non-linear equation conservation of mass and momentum. The author has written the program in FORTRAN 90. The main program is called **VEST.FOR**. It consists of three modules: the first module is used to define and input data. This can either be done through file input or screen input. The second module is used to compute the suspended sediment concentration profiles. The last

module provides the output of the program. The developed program also includes fourteen subroutines.

Five of the subroutines are related to the calculation of the hydrodynamic parameters, two of which deal with the calculation of wave hydrodynamics for bed and fluid mud conditions. These subroutines compute wave frequency, wavelength, wave number, wave orbital velocity, Richardson number, neutral diffusivity coefficient and bed shear stress. One subroutine is developed for the case of current over the bed and is used to compute the bed shear stress, bed roughness, and neutral diffusivity coefficient. Two of the hydrodynamic subroutines deal with wave plus weak current for the case of bed and fluid mud.

Two sediment transport subroutines calculate the entrainment and resuspension fluxes for bed and fluid mud conditions. One subroutine is developed for diagonal matrix calculations and one is prepared for providing output of the model.

The last four subroutines deal with wave-mud interaction model which is necessary to calculate Δu^2 in the global Richardson number. These subroutines incorporate the concepts previously presented in the thesis (Section 3.1.6) which deal with mud rheology as well as with the calculation of the first and second order wave over soft mud, using the secant method.

The flowchart of the model is provided in Figure 3.4. Figure 3.5 presents the time-dependent bed flux subroutine.

Another program which is used to graphically display the results of the computation is written in MATLAB and is entitled **VESTG.M**. It has the capability to animate the time variation of suspended sediment concentration profiles.

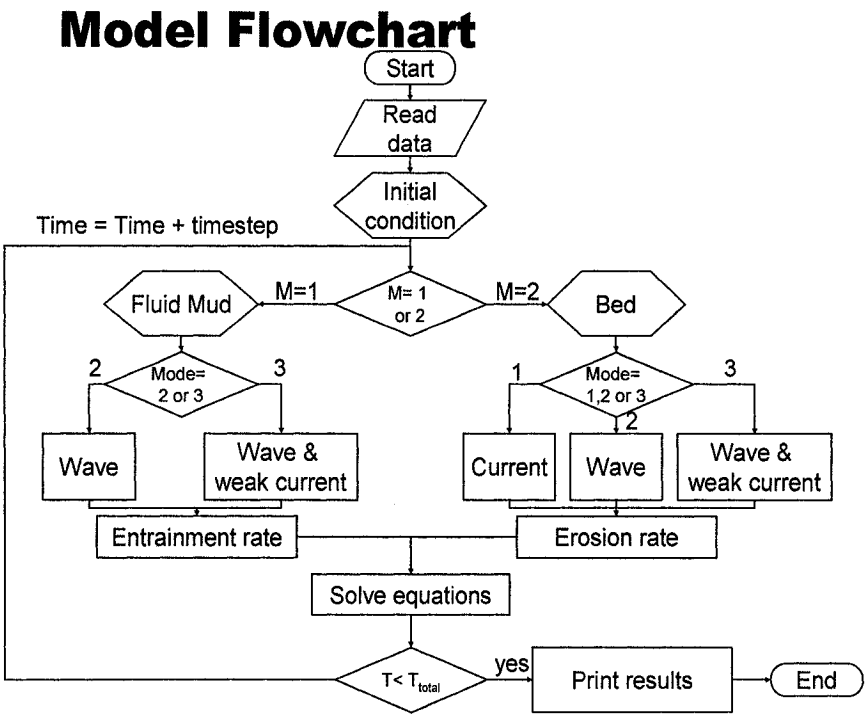

Figure 3.4 Flowchart of suspended sediment concentration profile model (adapted from Mehta and Li, 2003)

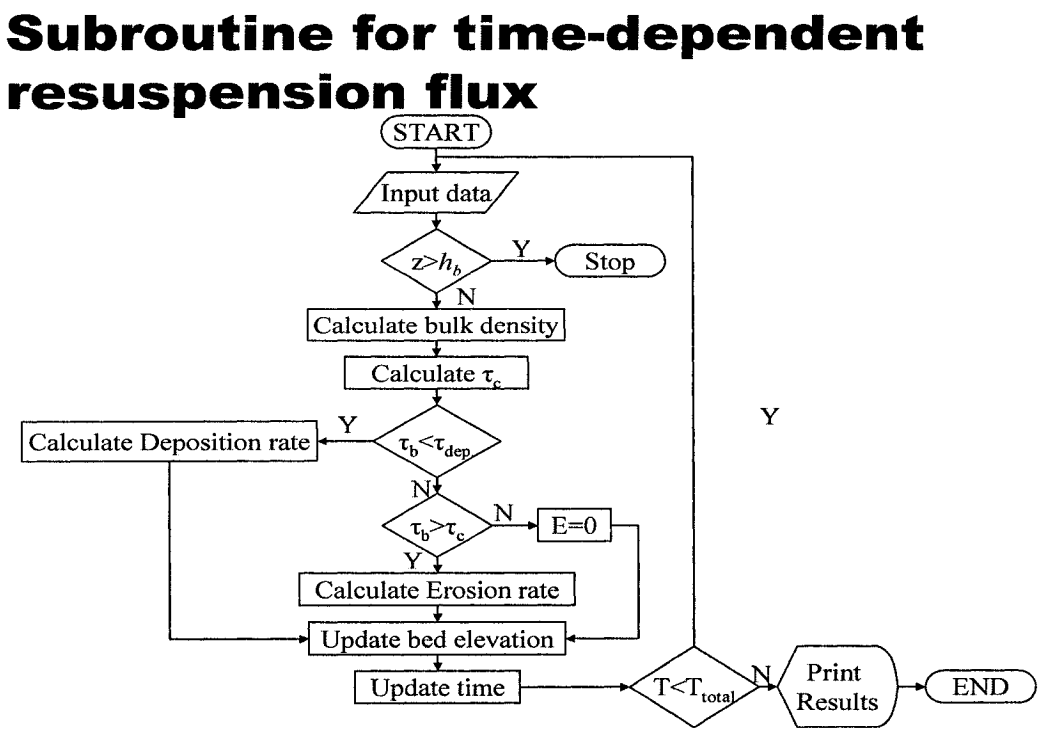

Figure 3.5 Flowchart fot time-dependent resuspension flux modelling

3.3 Description of the program input parameters

The input parameters of the model can be divided into six categories as follows:

1. Hydrodynamic parameters:
    a. Wave height [m] and wave period [s];
    b. Mean current velocity [m/s];
    c. Water depth [m];
    d. Water density [kg/m^3].
2. Sediment parameters:
    a. Sediment granular density [kg/m^3];
    b. Parameters for settling velocity [non-dimensional];
    c. Maximum free settling velocity [m/s];
    d. Median particle size D_{50} [m];
    e. Limit Concentration.
3. Diffusion related parameters:
    a. Empirical parameters for stabilized diffusivity [non-dimensional];
    b. Wave diffusion constant [non-dimensional].
4. Fluid mud characteristics:
    a. Mud bulk density [kg/m^3];
    b. Fluid mud depth [m];
    c. Mud rheological constants: G1 [Pa], G2 [Pa] and mu2 [Pa.s];
    d. Entrainment coefficient [non-dimensional].
5. Bed characteristics:
    a. Manning coefficient [$s/m^{1/3}$];
    b. Characteristic stress for deposition [Pa];

c. Depth averaged dry density [kg/m^3];

d. Bulk density coefficients, chi and zeta [non-dimensional];

e. Coefficients for erosion rate [non-dimensional];

f. Electrochemical anchoring coefficient [non-dimensional];

g. Mud dynamic viscosity (for electrochemical resistance method) [Pa.s];

h. Soil friction angle [Degrees] (for the case of vane shear method);

i. Wave friction factor (except for cases in which it is computed) [non-dimensional];

j. Local erosion constant (for time dependent erosion rate) [ms^{-1}Pa^{-1}];

k. Vane shear strength [Pa].

6. Other parameters:

   a. Initial values of sediment concentration and their elevation;

   b. Initial time [min], end time [min], and output time [min];

   c. Calculation time-step [s], and calculation grids .

3.4 Model application to laboratory experimental data:

Laboratory data for comparison are selected from runs 4, 5, and 6 of the experimental work conducted by Maa (1986). Maa (1986) used a horizontal plexiglass flume that was 20 m long, 0.458 m wide, and 0.45 m high (Figure 3.6). A plunging wave generator was added in the upstream with adjustable wave height and period. The tests were not done for the case of breaking waves. Two types of sediment, commercial kaolinite and estuarial mud from Cedar Keys (Florida) were used in the experiment which was carried out using monochromatic (sinusoidal) waves.

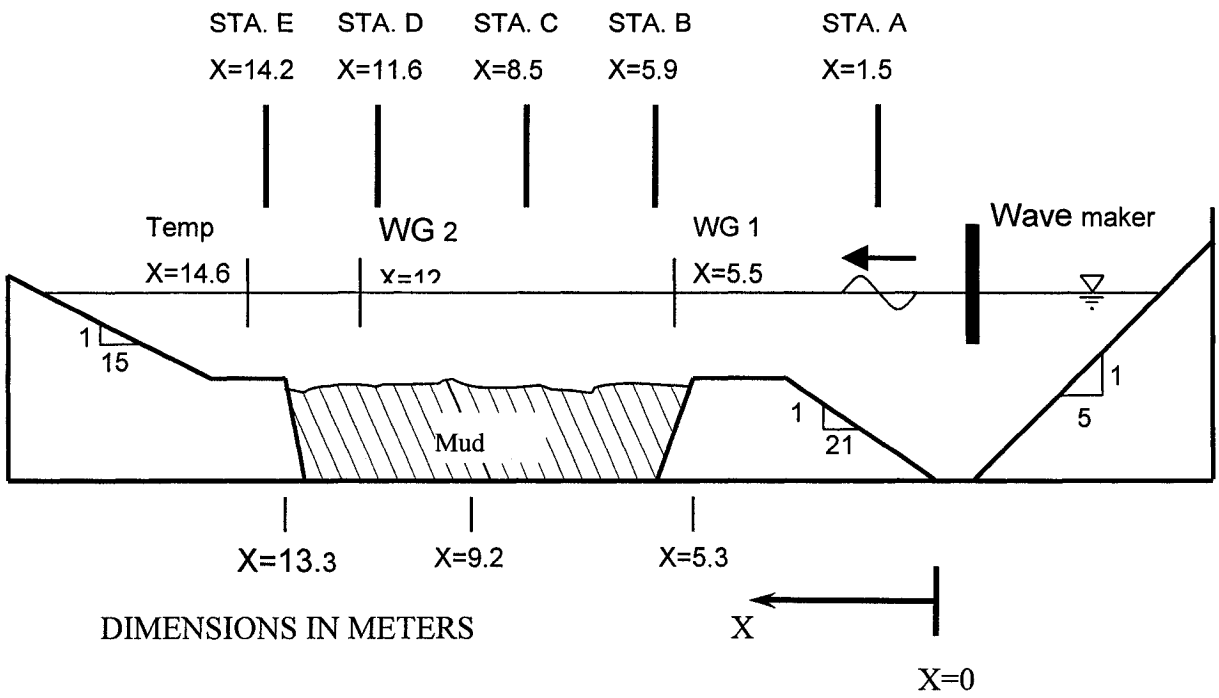

Figure 3.6 Experimental setup of Maa (1986).

The experiments started from initial concentration distribution, then the first hydrodynamic (wave) action was applied for 3 to 7 hours, then wave loading was increased in order to study the increase in applied bottom shear stress. This condition was maintained for the same period of time of 3 to 7 hours. In run 6, the hydrodynamic loading was also applied for a period of 4 hours. Suspended sediment concentration was measured at specific time intervals at three elevations inside of the flume. Wave height, wave period, bed bulk density, granular sediment and water density and vane shear stress were measured in the experiments. Based on further study of the wave induced resuspension study of Hwang (1989) and Ross (1988) and current induced resuspension modelling of Ross (1988), Li (1996) recommended the following parameters for the calculation of the settling velocity: $w_{sf} = 6.37 \times 10^{-7}\, m/s$, $c_1 = 0.1 kg/m^3$, $\alpha_1 = 0.01$, $\beta_1 = 1.33$ $\gamma_1 = 1.5$ and $\delta_1 = 9$. The stratification parameters, α_0 and β_0 were chosen to be 0.5 and 0.5, respectively. These values are within the range mentioned in the study of Ross (1988) who found α_0 to vary between 0.062 and 180 and β_0

to vary from 0.5 to 0.75. The other parameters are calibrated in the model and are presented, for each case, in Chapter 4.

3.5 Model application to field data

Field data from two experiments are used. The sites of the experiments are along the Louisiana coast (U.S.).

One of the experiments conducted along the Louisiana coast was performed by Kemp (1986). Data were collected as a winter cold front approached. Strong wind-induced waves resuspended bottom sediments. Data were measured at pre-frontal, frontal and post-frontal intervals of time.

The second data set collected along Louisiana coast was collected by Sheremet and Stone (2003) in July 2003, when Hurricane Claudette passed the Louisiana coast. Measurements were done before, during and after passing of the hurricane. Their study included the effect of wind and weak current. Wave and current conditions, as well as suspended sediment concentrations in terms of turbidity, were measured.

3.5.1 Field data from Vermilion Bay, Louisiana

The study site is 30 km of coastline, southwest of Vermilion Bay, on the eastern margin of the Louisiana Chenier Plain (Figure 3.7).

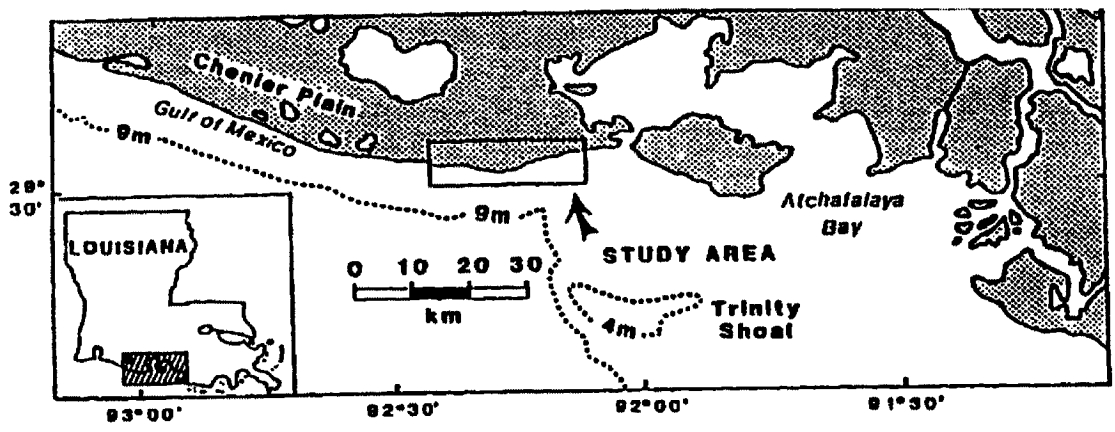

Figure 3.7 Location of field data study of Kemp (1986).

The sedimentation in the area is due to the Atchafalaya River, which is the largest distributary of the Mississippi River. The Atchafalaya conveys 30% of the Mississippi River's discharge, with the average value of 5,126 m^3/s. The average suspended sediment load of the Atchafalaya River is 84 million metric tons per year (compiled by U.S. Army Corps of Engineers, [Allison *et al.*, 2000]). The most significant sedimentation occurs during the spring flood, typically from December to April, due to superposition between high Atchafalaya discharge and intense cold frontal activity (Walker and Hammack, 2000). Wind-induced currents in this area reach values of up to 0.50 m/s and play a more significant role than tide-induced currents (Li, 1996). The bed material consists of about 50 to 80% clay, 20 to 50% silt and zero to 14 % sand. Clay minerals are mainly smectite (37%), illite (30%) and kaolinite (18%). The density of deposited mud varied between 1200 kg/m^3 at the surface to 1400 kg/m^3 at a meter below (Li, 1996).

The data were collected from December 10 to 13, 1982, when a cold front passed through the region. The data correspond to pre-frontal, frontal and post frontal periods and include wave characteristics and time series of suspended sediment concentrations. Table 3.1 provides more details on the wave and suspended sediment data. These data were collected every 20 minutes together with pressure records. During the pre-frontal period, spilling breakers were observed near the shoreline, but, at least in two subsequent conditions, waves were attenuated before reaching the shoreline. Li (1996) suggested that this was due to the formation of fluid mud in the frontal and post frontal periods that dissipated the wave energy and prevented it from further travelling towards shoreline. Table 3.1 also provides the data on the suspended sediment concentrations that ranged from 0.2 to 5.7 kg/m^3 and decreased with elevation above sea bottom. The maximum value for concentration was recorded at 0.1 m above the bed during the frontal period.

Table 3.1 Measured wave and suspended sediment data from Louisiana coast (adopted from Kemp, 1986).

TIME	WAVE HEIGHT [cm]	WAVE PERIOD [s]	SUSPENDED SEDIMENT CONCENTRATION (g/l) (DATUM IS THE MEAN SEA SURFACE)			
			-0.1 m	-0.25 m	-0.55 m	-0.8 m
Frontal, Dec. 11, 1982						
13:07	Average 11.7	Average 6.6	0.205	0.256	0.350	3.213
13:38			0.304	0.355	0.634	4.650
14:23			0.360	0.341	0.362	5.666
15:09			-	0.337	0.515	1.155
Post-Frontal, Dec., 13, 1982						
10:51	Average 5.2	Average 6.9	-	0.820	0.901	1.355
11:30			-	0.582	0.618	1.131
12:34			0.413	0.426	0.439	0.732
13:01			0.431	0.477	0.466	0.773

Measured water depth at the study location varied between 0.85 and 1.05 m. Mud depth was found to be 0.18 m by Li (1996). In his experiments, Kemp (1986) did not measure mud properties or the settling velocity parameters. Settling velocity parameters were taken from Hwang (1989), with $\beta_1 = 1.33, \gamma_1 = 1.5$ and $\delta_1 = 9.0$. Mud density was found to be 1,270 kg/m^3 and water density was considered to be 1,030 kg/m^3, a usual value for sea-water density in the region. The other coefficients used in the model are provided in Chapter 4.

3.5.2 *Field data from Atchafalaya Bay, Louisiana Coast*

This set of data was collected by using WAVCIS array ("Wave-Current-Surge Information System), discussed in detail in Stone *et al.* (2001). The observation site, depicted as CSI 3, is located approximately 20 km south of Marsh Island, as shown in Figure 3.8. The data is provided by Sheremet and Stone (2003), Sheremet *et al.* (2005) and Sheremet (2006), who all studied and compared the impact of short waves and their interaction with the muddy bed by comparing two sites with different characteristics (one muddy environment: CSI 3 and one sandy environment: CSI 5) located along the Louisiana coast during Hurricane Claudette in the Summer of 2003. The study site is located along the 5-m isobath, on a very mild sloping shelf (<0.001). Bed material is inorganic fine sediment with a median grain size of 6.34 μm.

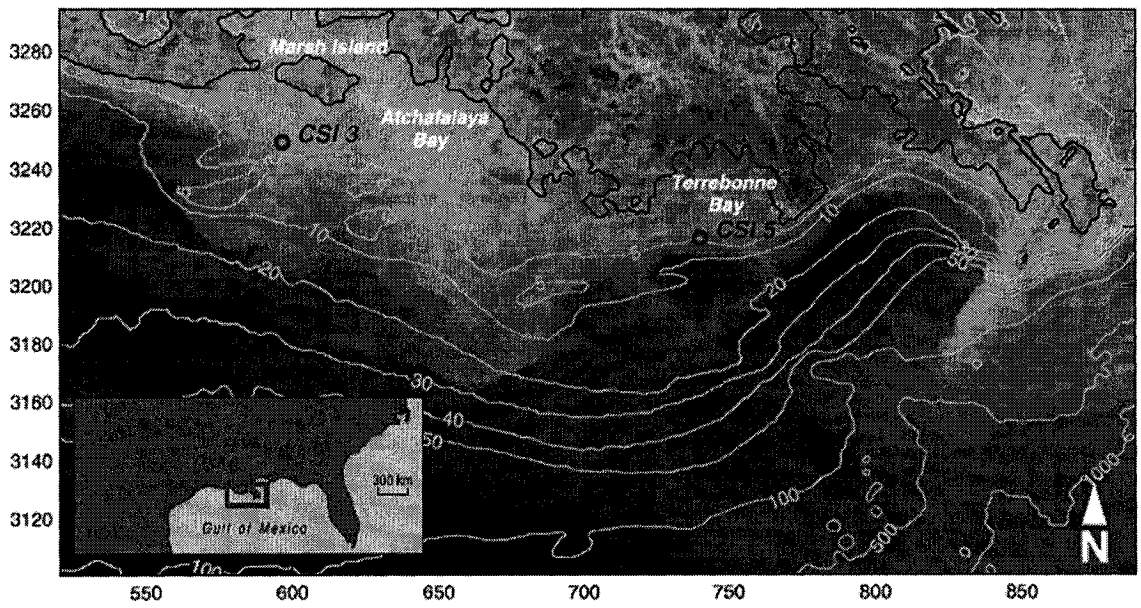

Figure 3.8 The satellite image of the Louisiana coast. (Sheremet and Stone, 2003). Bathymetric contours are in meters and the coordinates are in kilometres with respect to UTM 1983, Zone 15.

Sheremet (2006) provided the suspended sediment concentration data for CSI 3 between June 11 and June 16. Wave data were also made available by Sheremet *et al.* (2005) for the period between June 11 and June 18. During the experimental data collection, a sudden jump was

observed in the significant wave height starting with June 13. This was due to the hurricane and the phenomena related to sediment resuspension for these extreme conditions is beyond the scope of the current study. Hence, the mean significant wave height between June 11 and 13 was used. The data for significant wave height and its mean value before storm inception is shown in Figure 3.9. The mean significant wave height was found to be equal to 0.177 m.

Tides in the studied region are reported to be low with weak tidal currents (Wright *et al.*, 1997). However, the same approach used for waves was applied for recording the current. The mean value for the available data before hurricane inception, i.e., between June 11 and 13 was computed and extended for the whole period as mean current velocity (Figure 3.10). The estimated mean current velocity is 0.08 m/s.

The wave period was provided by Sheremet et Stone (2003). Based on Figure 3.11, the mean significant wave period of 3.17 seconds was used.

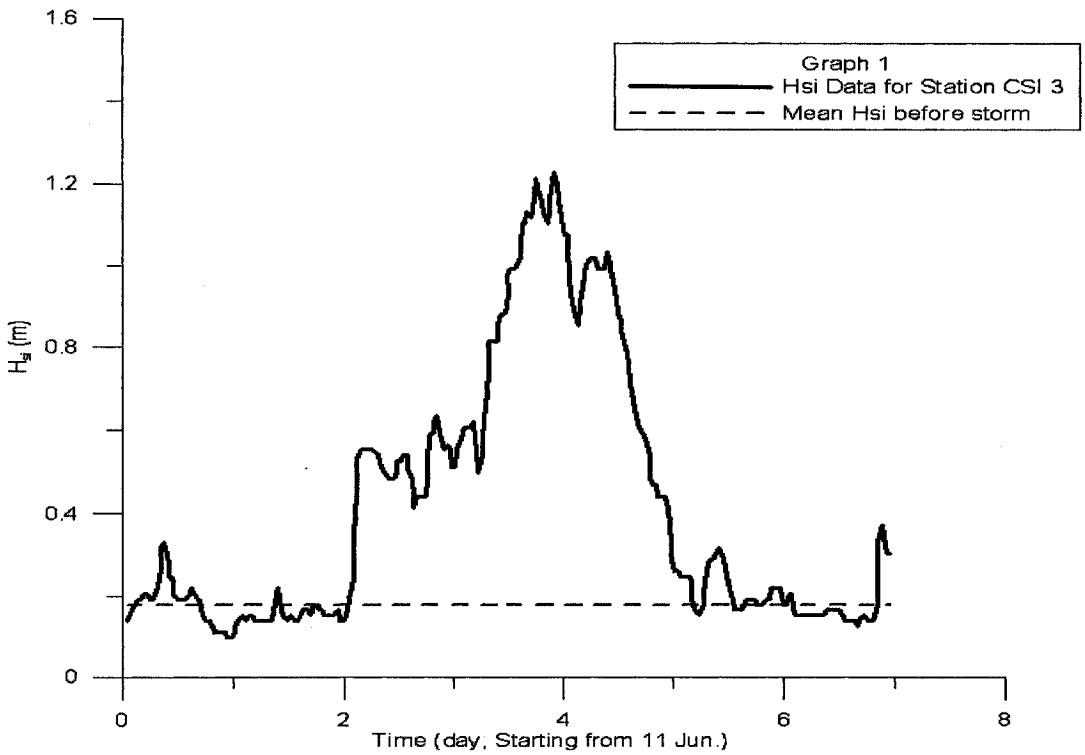

Figure 3.9 Time variation of the significant wave height for CSI 3 station and mean significant wave height before storm inception.

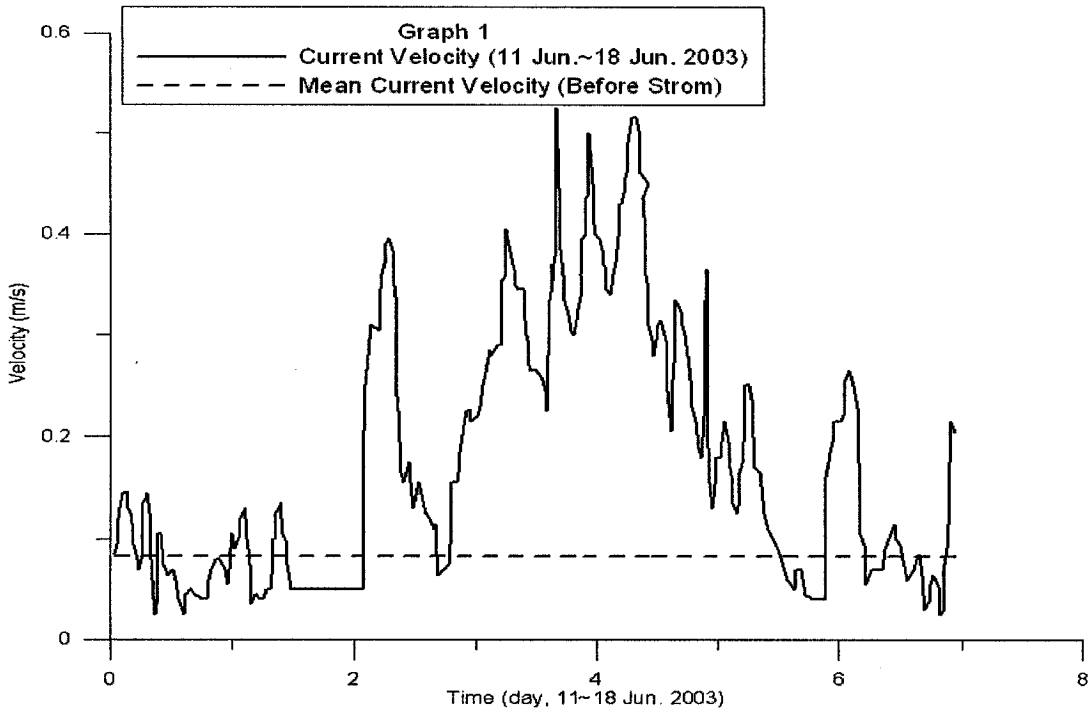

Figure 3.10 Time variation of the current velocity in CSI 3 station and mean current speed before storm inception.

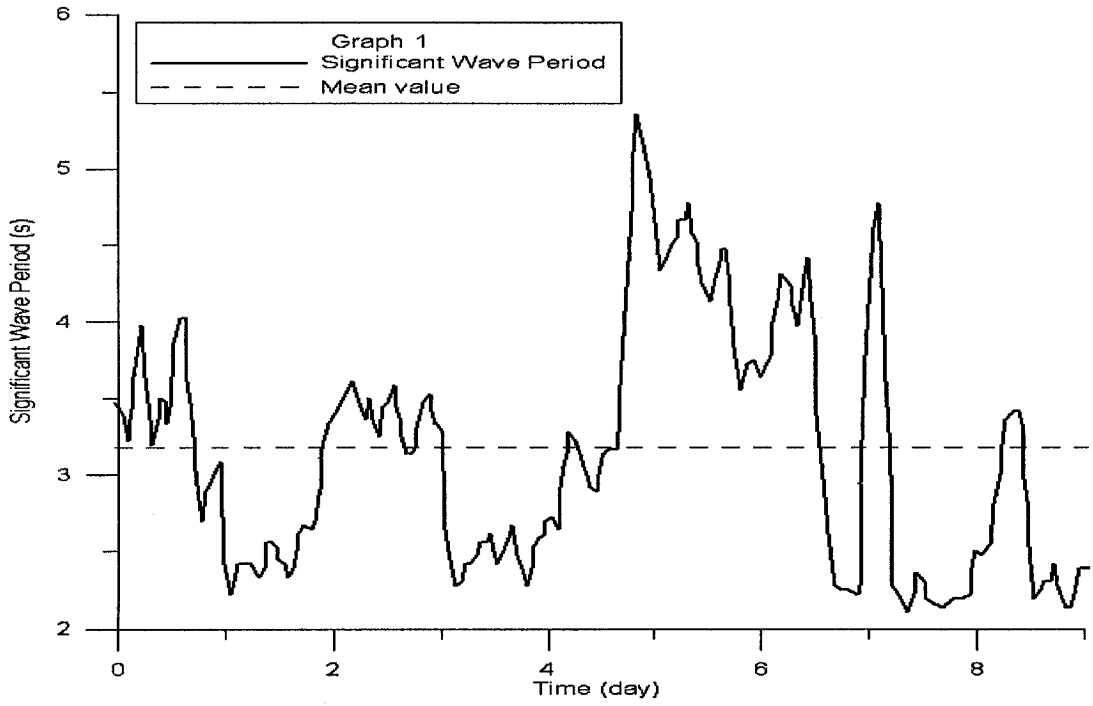

Figure 3.11 Significant wave period for station CSI 3.

In order to measure sediment concentration, optical backscatter sensors were used at 1, 2 and 3 m above the bottom. The sensors collected data every 20 minutes in terms of turbidity (Nephelometric Turbidity Units=NTU) and were calibrated to get equivalent values in kg/m^3. The calibration curve, based on the data of Sheremet (2006), is provided in Figure 3.12. However, the relation between NTU and the concentration tends to become nonlinear at values of NTU> 1400. Sheremet *et al.* (2005) also pointed out the high degree of nonlinearity with concentrations higher than 1.7 kg/m^3.

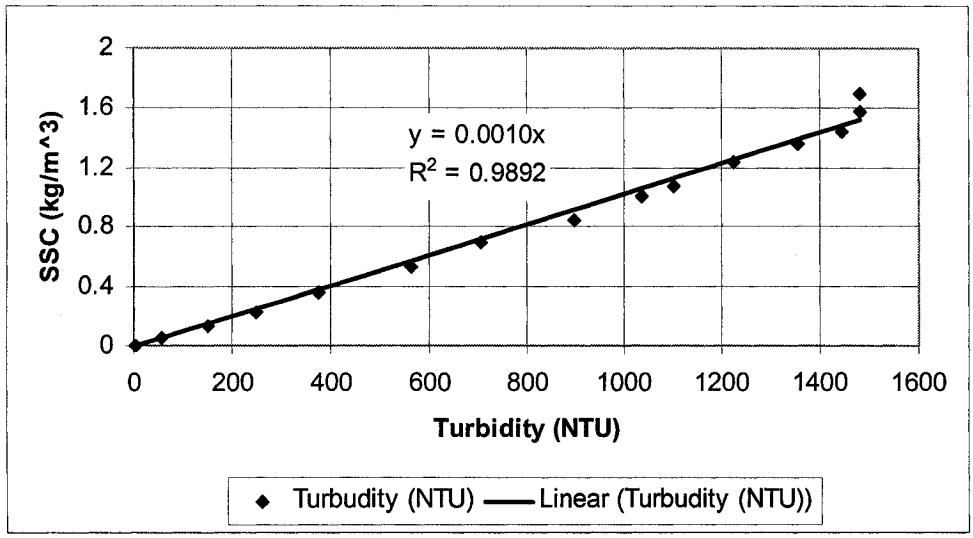

Figure 3.12 Calibration curve for converting turbidity (NTU) to suspended sediment soncentration (kg/m^3).

The settling velocity parameters were adopted from Sheremet *et al.* (2005) as follows: $c_1 = 1.78 kg/m^3$, $w_{sf} = 0.000022 m/s$, $\alpha_1 = 0.0037$, $\beta_1 = 1.33$, $\gamma_1 = 2.0$ and $\delta_1 = 1.5$. Other parameters were calibrated for the best fit and are provided in Chapter 4.

Table 3.2 Parameters for numerical modelling - Runs 4, 5 and 6 (Maa, 1986).

		RUN 4	RUN 5	RUN 6
Wave period [s], height [m] and duration [min]		1.6;3.4;0~285	1.7;3.2;0~230	1.8;3.5;0~180
		1.1;5.5;285~588	1.2;5.2;230~537	1.4;4.5;180~425
				1.0;5.3;425~670
Water depth [m]		0.264	0.197	0.274
Mud depth [m]		0.093	0.16	0.105
Mud density [kg/m^3]		1080	1080	1100
Settling velocity parameters [non-dimensional]	c_1 [kg/m^3]	0.1	0.1	0.1
	w_{sf} [m/s]	6.37x10^{-7}	6.37x10^{-7}	6.37x10^{-7}
	α_1	0.01	0.01	0.01
	β_1	1.33	1.33	1.33
	γ_1	9.0	9.0	9.0
	δ_1	1.5	1.5	1.5
Wave diffusion coefficient, α_w [non-dimensional]		0.19	0.5	0.8
Elevation of sediment sample below water surface [cm]	#1	-12.4	-8.3	-13.9
	#2	-20.7	-16.6	-22.2
	#3	-22.6	-18.5	-24.2

Table 3.3 Parameters for numerical modelling - Vermillion - Louisiana coast.

		FRONTAL	POST-FORNTAL
Wave period [s], height [m] and duration [min]		6.6;11.7;76 5.9;10.2;46	6.9;5.2;190
Water depth [m]		0.9	0.9
Mud depth [m]		0.18	0.18
Settling velocity parameters [non-dimensional]	c_1 [kg/m^3]	0.3	0.3
	w_{sf} [m/s]	1.9×10^{-6}	1.9×10^{-6}
	α_1	0.03	0.03
	β_1	1.33	1.33
	γ_1	9.0	9.0
	δ_1	1.5	1.5
Wave diffusion coefficient, α_w [non-dimensional]		0.3	0.3
Stratified damping coefficients [non-dimensional]	α_0	0.5	0.5
	β_0	0.33	0.33
Elevations of sediment sample below water surface [cm]	#1	-0.5	0.5
	#2	-25	-25
	#3	-55	-55
	#4	-80	-80

Table 3.4 Parameters for numerical modelling - Atchafalaya Bay, Louisiana coast.

INPUT DATA		VALUE
Wave Period [s], Height [m]		3.17;0.177
Water depth [m]		5
Mud depth [m]		60
Mean current velocity [m/s]		0.08
Settling velocity parameters	c_1 [kg/m^3]	1.78
	w_{sf} [m/s]	0.000022
	α_1 [non-dimensional]	0.0037
	β_1 [non-dimensional]	1.33
	γ_1 [non-dimensional]	2.0
	δ_1 [non-dimensional]	1.5
Wave diffusion coefficient, α_w [non-dimensional]		2
Elevations of sediment sample above bed [m]	#1	1
	#2	2
	#3	3

4 RESULTS

In this chapter, the numerical model results corresponding to each of the model developments are compared to the results of the numerical model of Mehta and Li (2003) and the experimental data. For each case, one set of results is provided while the rest of them are given in the thesis appendices.

4.1 Electrochemical anchoring resistance

Parameters used for modelling the flume experiments of Maa (1986) are presented in Table 4.1. Table 4.2 shows the same parameters for the field data of Vermilion Bay and Atchafalaya Bay, Louisiana. Some of the input parameters were discussed in the

previous chapter.

The results for simulation of the field data for Vermilion bay, Louisiana corresponding to the frontal period are provided in Figure 4.1. The original sediment concentration profiles are provided by Li (1996). It can be observed that by including the electrochemical force, the suspended sediment concentration (SSC) increases and the numerical model is capable of simulating the sediment concentration profile better than the model of Mehta and Li. Moreover, the numerical simulation shows better agreement with experimental data as we approach the steady state solution. However, the sediment concentration in the near-bed region is overestimated. This is due to the presence of lutocline that is not captured in the present model. The rest of simulation results are given in Appendix A.

Table 4.1 Parameters for numerical modelling - runs 4, 5 and 6 (Maa, 1986).

		RUN 4	RUN 5	RUN 6
Wave period [s], height [m] and duration [min]		1.6;3.4;0~285	1.7;3.2;0~230	1.8;3.5;0~180
		1.1;5.5;285~588	1.2;5.2;230~537	1.4;4.5;180~425
				1.0;5.3;425~670
Water depth [m]		0.264	0.197	0.274
Mud depth [m]		0.093	0.16	0.105
Settling velocity parameters [non-dimensional]	c_1 [kg/m^3]	0.1	0.1	0.1
	w_{sf} [m/s]	$6.37\text{x}10^{-7}$	$6.37\text{x}10^{-7}$	$6.37\text{x}10^{-7}$
	α_1	0.01	0.01	0.01
	β_1	1.33	1.33	1.33
	γ_1	9.0	9.0	9.0
	δ_1	1.5	1.5	1.5
Wave diffusion coefficient, α_w		0.19	0.5	0.8
Stratified diffusion coefficients [non-dimensional]	α_0	0.5	0.5	0.5
	β_0	0.4	0.45	0.45
Sediment granular density [kg/m^3]		2650	2650	2650
Bed bulk density [kg/m^3]		1080	1080	1100
Water density [kg/m^3]		1000	1000	1000
Bed density parameters [non-dimensional]	$\overline{\rho}_D$ [kg/m^3]	250.3	194.4	254
	ζ_1	0.797	0.797	0.797
	ξ_1	-0.45	-0.45	-0.45
Wave friction factor [non-dimensional]		0.03	0.025	0.025
Erosion rate parameters [nom-dimensional]	s_{max}	0.8	0.8	0.8
	a_r	8.0	8.0	8.0
	b_r	0.5	0.5	0.5

Median particle size [m]		2.1e-6	2.1e-6	2.1e-6
Mud dynamic viscosity [Pa.s]		0.014	0.014	0.014
Electrochemical anchoring coefficient [non dimensional]		0.255	1.15	0.2
Elevation of sediment sample below water surface [cm]	#1	-12.4	-8.3	-13.9
	#2	-20.7	-16.6	-22.2
	#3	-22.6	-18.5	-24.2

Table 4.2 Parameters for numerical modelling for the model including the electrochemical resistance forces - Vermilion Bay (Kemp, 1986) and Atchafalaya Bay (Sheremet *et al.*, 2005).

		VERMILION BAY, LOUISIANA (KEMP, 1986)		ATCHAFALAYA BAY, LOUISIANA (SHEREMET ET AL., 2005)
		Frontal	Post Frontal	
Wave period [s], height [m] and duration [min]		6.6;11.7;76	6.9;5.2;190	3.17;0.177;400
		5.9;10.2;46		
Water depth [m]		0.9	0.9	5.0
Mud depth [m]		0.18	0.18	0.6
Settling velocity parameters [non dimensional]	c_1 [kg/m^3]	0.3	0.3	1.78
	w_{sf} [m/s]	1.9×10^{-6}	1.9×10^{-6}	0.000022
	α_1	0.03	0.03	0.0037
	β_1	1.33	1.33	1.33
	γ_1	9.0	9.0	2.0
	δ_1	1.5	1.5	1.5
Wave diffusion coefficient, α_w		0.3	0.3	2
Stratified diffusion coefficients [non dimensional]	α_0	0.5	0.5	0.5
	β_0	0.33	0.33	0.2
Sediment granular density [kg/m^3]		2650	2650	2650
Bed bulk density [kg/m^3]		1270	1270	1270
Water density [kg/m^3]		1030	1030	1030
Bed density parameters [non-dimensional]	$\overline{\rho}_D$ [kg/m^3]	400	400	400
	ζ_1	0.797	0.797	0.797
	ξ_1	-0.45	-0.45	-0.45

Wave friction factor [non-dimensional]		0.03	0.03	0.03
Erosion rate parameters [non-dimensional]	s_{max}	0.8	0.8	0.8
	a_r	5	5	5
	b_r	0.5	0.5	0.5
Median particle size [m]		6e-5	6e-5	6.34e-6
Mud dynamic viscosity [Pa.s]		0.03	0.03	0.03
Electrochemical anchoring coefficient [non-dimensional]		0.15	0.30	0.18
Elevation of sediment sample above the bed [cm]	#1	80	80	100
	#2	55	55	200
	#3	25	25	300
	#4	0.5	0.5	

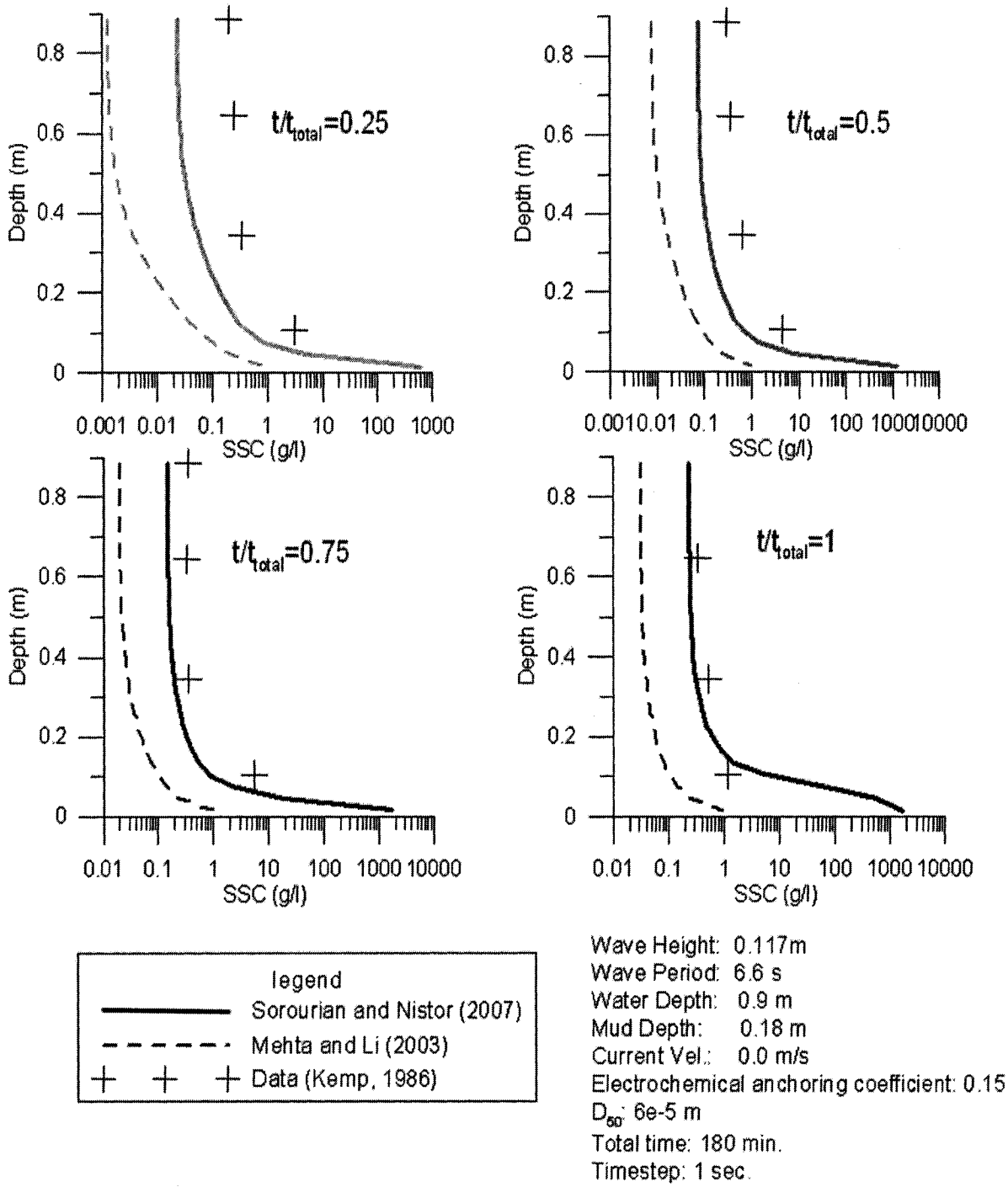

Figure 4.1 Comparison between the numerical model results and field data of Kemp (1986) - Model modified for including electrochemical resistance.

4.2 Defining shear resistance by including vane shear strength of bed

The measured values for flume and field experiments are summarized in Table 4.3 and Table 4.4. The results for the case of field data of Vermilion Bay, Louisiana, frontal period (Kemp, 1986) are presented in Figure 4.2. The rest of the figures are shown in Appendix A. In comparison with Mehta and Li (2003), model seems to provide better prediction for the sediment concentration over the entire period of the wave action. The results of original model is taken from Li (1996). However, there is an over-prediction of the sediment concentration in vicinity of the bed that is due to the presence of the lutocline.

Table 4.3 Parameters for numerical modelling for vane shear case - Run 4, 5, and 6 (Maa, 1896).

		RUN 4	RUN 5	RUN 6
Wave period [s], height [m] and duration [min]		1.6;3.4;0~285	1.7;3.2;0~230	1.8;3.5;0~180
		1.1;5.5;285~588	1.2;5.2;230~537	1.4;4.5;180~425
				1.0;5.3;425~670
Water depth [m]		0.264	0.197	0.274
Mud depth [m]		0.093	0.16	0.105
Settling velocity parameters [non-dimensional]	c_1 [kg/m^3]	0.1	0.1	0.1
	w_{sf} [m/s]	$6.37\text{x}10^{-7}$	$6.37\text{x}10^{-7}$	$6.37\text{x}10^{-7}$
	α_1	0.01	0.01	0.01
	β_1	1.33	1.33	1.33
	γ_1	9.0	9.0	9.0
	δ_1	1.5	1.5	1.5
Wave diffusion coefficient, α_w		0.19	0.5	0.8
Stratified diffusion coefficients [non-dimensional]	α_0	0.5	0.5	0.5
	β_0	0.4	0.45	0.45
Bed density parameters [non-dimensional]	$\overline{\rho}_D$ [kg/m^3]	250.3	194.4	254
	ζ_1	0.797	0.797	0.797
	ξ_1	-0.45	-0.45	-0.45
Sediment granular density [kg/m^3]		2650	2650	2650
Bed bulk density [kg/m^3]		1080	1080	1100
Water density [kg/m^3]		1000	1000	1000
Wave friction factor [non-dimensional]		0.03	0.025	0.025
Erosion rate parameters	s_{max}	0.8	0.8	0.8
	a_r	5	5	5

	b_r	1	1	1
Median particle size [m]		2.1e-6	2.1e-6	2.1e-6
Bed vane shear strength [Pa]		2.0	2.0	2.0
Bed friction angle (degrees)		65	65	65
Elevation of sediment sample below water surface [cm]	#1	-12.4	-8.3	-13.9
	#2	-20.7	-16.6	-22.2
	#3	-22.6	-18.5	-24.2

Table 4.4 Parameters for numerical modelling for vane shear case - Vermilion Bay (Kemp, 1986) and Atchafalaya Bay (Sheremet *et al.*, 2005).

		VERMILION BAY, LOUISIANA (KEMP, 1986)		ATCHAFALAYA BAY, LOUISIANA (SHEREMET *ET*
		Frontal	Post Frontal	
Wave period [s], height [m] and duration [min]		6.6;11.7;76	6.9;5.2;190	3.17;0.177;400
		5.9;10.2;46		
Water depth [m]		0.9	0.9	5.0
Mud depth [m]		0.18	0.18	0.60
Settling velocity parameters [non-dimensional]	c_1 [kg/m^3]	0.3	0.3	1.78
	w_{sf} [m/s]	$1.9\text{x}10^{-6}$	$1.9\text{x}10^{-6}$	0.000022
	α_1	0.03	0.03	0.0037
	β_1	1.33	1.33	1.33
	γ_1	9.0	9.0	2.0
	δ_1	1.5	1.5	1.5
Wave diffusion coefficient, α_w		0.3	0.3	2
Stratified diffusion coefficients [non-dimensional]	α_0	0.5	0.5	0.5
	β_0	0.33	0.33	0.2
Sediment granular density [kg/m^3]		2650	2650	2650
Bed bulk density [kg/m^3]		1270	1270	1270
Water density [kg/m^3]		1030	1030	1030
Wave friction factor [non-dimensional]		0.03	0.03	0.03
Erosion rate parameters	s_{max}	0.8	0.8	0.8
	a_r	5	5	5

	b_r	1	1	1
Bed density parameters [non-dimensional]	$\overline{\rho}_D$ [kg/m^3]	400	400	400
	ζ_1	0.797	0.797	0.797
	ξ_1	-0.45	-0.45	-0.45
Median particle size [m]		6e-5	6e-5	6.34e-6
Bed vane shear strength [Pa]		0.5	0.6	0.35
Bed friction angle (degrees)		65	65	65
Elevation of sediment sample above the bed [cm]	#1	85	85	100
	#2	55	55	200
	#3	25	25	300
	#4	0.5	0.5	

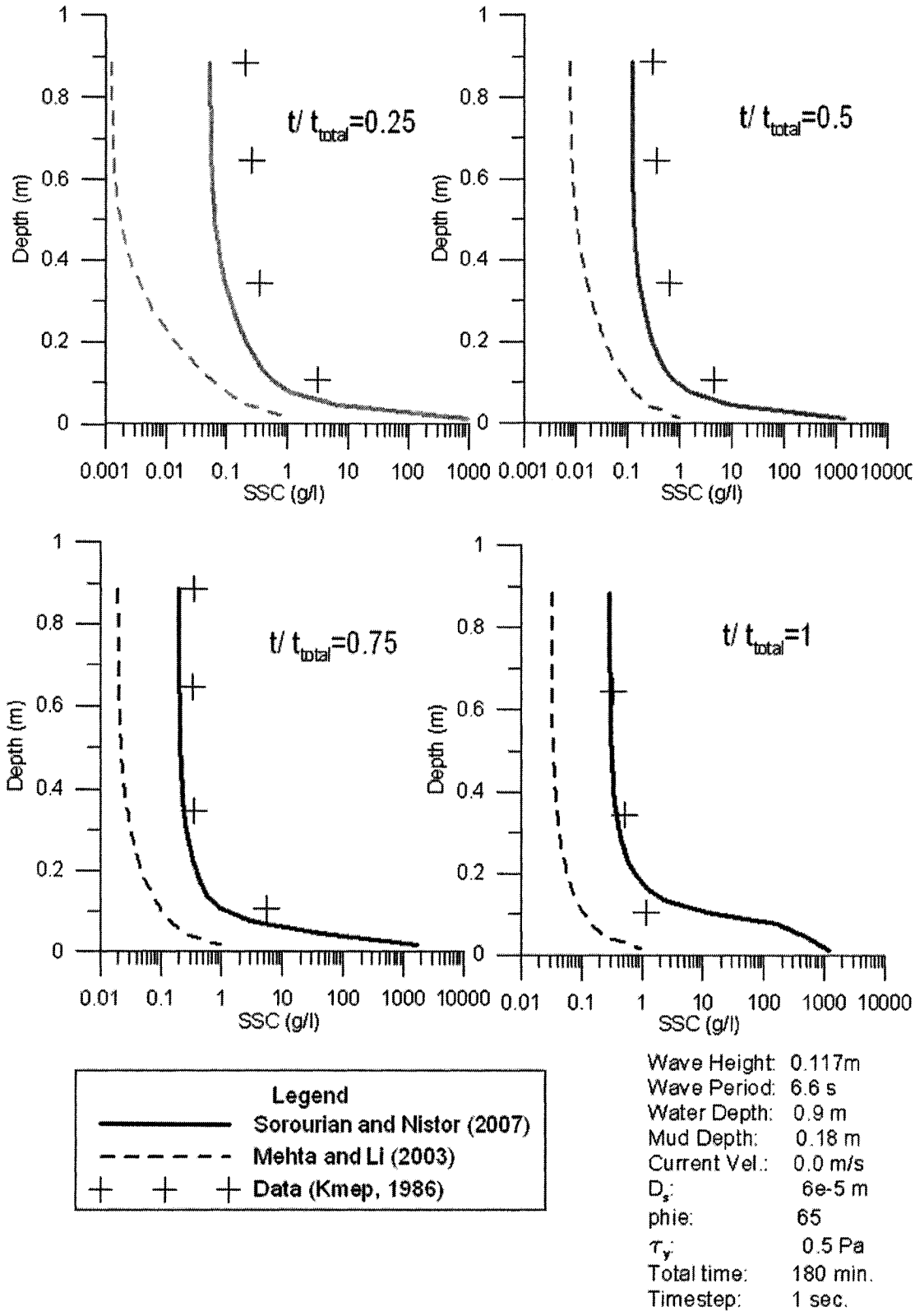

Figure 4.2 Comparison between the numerical model results and field data of Kemp (1986) - Model including the concept of the vane shear strength.

4.3 Wave friction factor

Result of model including the formulation of the wave friction factor are presented herein. Table 4.5 and Table 4.6 provide the input parameters used in the numerical model for both the available flume and field experiments. The reasons for the selection of these parameters are discussed in Chapter 3. Figure 4.3 to Figure 4.5 show the results of the comparison between numerical data and the experimental results for Vermilion Bay field data. The original numerical data are provided by Li (1996). The proposed model seems to successfully simulate the effect of the wave friction factor and, in comparison with the original model, results are in better agreement with the experimental data. The use of different formulation of the wave friction factor does not provide significant improvements when compared to each other, but the formula of La Roux (2003) seems to provide better prediction of the sediment concentration at near-bed level.

Table 4.5 Parameters for numerical modelling for wave friction factor cases - Runs 4, 5, and 6 (Maa, 1986).

		RUN 4	RUN 5	RUN 6
Wave period [s], height [m] and duration [min]		1.6;3.4;0~285	1.7;3.2;0~230	1.8;3.5;0~180
		1.1;5.5;285~588	1.2;5.2;230~537	1.4;4.5;180~425
				1.0;5.3;425~670
Water depth [m]		0.264	0.197	0.274
Mud depth [m]		0.093	0.16	0.105
Settling velocity parameters [non-dimensional]	c_1 [kg/m^3]	0.1	0.1	0.1
	w_{sf} [m/s]	$6.37\text{x}10^{-7}$	$6.37\text{x}10^{-7}$	$6.37\text{x}10^{-7}$
	α_1	0.01	0.01	0.01
	β_1	1.33	1.33	1.33
	γ_1	9.0	9.0	9.0
	δ_1	1.5	1.5	1.5
Wave diffusion coefficient, α_w		0.19	0.5	0.8
Stratified diffusion coefficients [non-dimensional]	α_0	0.5	0.5	0.5
	β_0	0.4	0.45	0.45
Bed density parameters [non-dimensional]	$\overline{\rho}_D$ [kg/m^3]	250.3	194.4	254
	ζ_1	0.797	0.797	0.797
	ξ_1	-0.45	-0.45	-0.45
Sediment granular density [kg/m^3]		2650	2650	2650
Bed bulk density [kg/m^3]		1080	1080	1100
Water density [kg/m^3]		1000	1000	1000
Erosion rate parameters [non-dimensional]	s_{max}	0.8	0.8	0.8
	a_r	5	5	5
	b_r	1	1	1
Median particle size [m]		2.1e-6	2.1e-6	2.1e-6

Roughness k_s [m]		0.05	0.05	0.05
Elevation of sediment sample below water surface [cm]	#1	-12.4	-8.3	-13.9
	#2	-20.7	-16.6	-22.2
	#3	-22.6	-18.5	-24.2

Table 4.6 Parameters for numerical modelling for the wave friction factor case - Vermilion Bay (Kemp, 1986) and Atchafalaya Bay (Sheremet *et al.*, 2005).

		VERMILION BAY, LOUISIANA (KEMP, 1986)		ATCHAFALAYA BAY, LOUISIANA (SHEREMET *ET AL.*, 2005)
		Frontal	Post Frontal	
Wave period [s], height [m] and duration [min]		6.6;11.7;76	6.9;5.2;190	3.17;0.177;-
		5.9;10.2;46		
Water depth [m]		0.9	0.9	5.0
Mud depth [m]		0.18	0.18	0.60
Settling velocity parameters [non-dimensional]	c_1 [kg/m^3]	0.3	0.3	1.78
	w_{sf} [m/s]	1.9×10^{-6}	1.9×10^{-6}	0.000022
	α_1	0.03	0.03	0.0037
	β_1	1.33	1.33	1.33
	γ_1	9.0	9.0	2.0
	δ_1	1.5	1.5	1.5
Wave diffusion coefficient, α_w [non-dimensional]		0.3	0.3	2
Stratified diffusion coefficients [non-dimensional]	α_0	0.5	0.5	0.5
	β_0	0.33	0.33	0.2
Sediment granular density [kg/m^3]		2650	2650	2650
Bed bulk density [kg/m^3]		1270	1270	1270
Water density [kg/m^3]		1030	1030	1030
Erosion rate parameters [non-dimensional]	s_{max}	0.8	0.8	0.8
	a_r	5	5	5
	b_r	1	1	1

Bed density parameters	$\overline{\rho}_D$ [kg/m^3]	400	400	400
	ζ_1	0.797	0.797	0.797
	ξ_1	-0.47	-0.47	-0.47
Median particle size [m]		6e-5	6e-5	6.34e-6
Roughness k_s [m]		0.05	0.05	0.05
Elevation of sediment sample above the bed [cm]	#1	80	80	100
	#2	55	55	200
	#3	25	25	300
	#4	0.5	0.5	

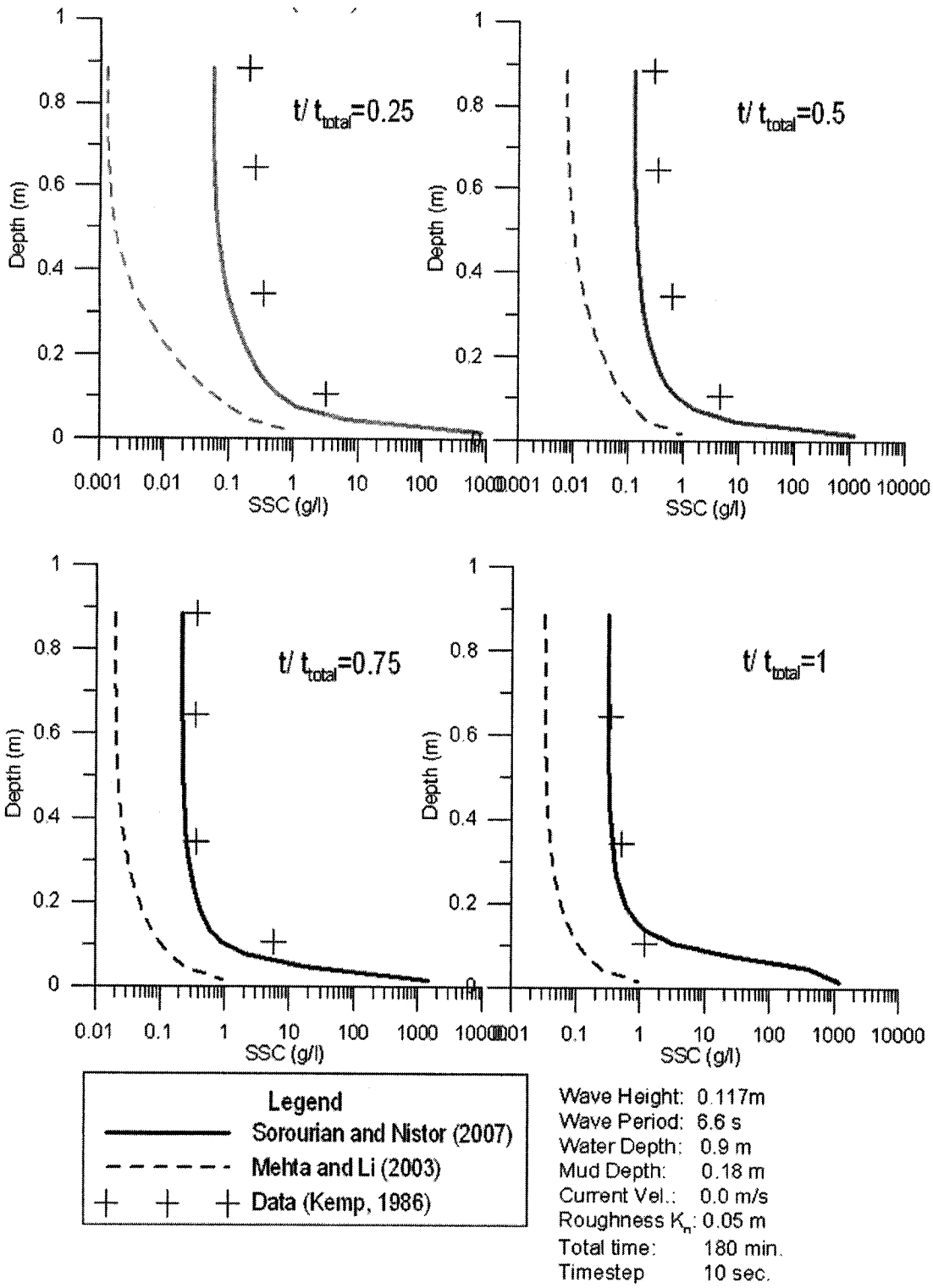

Figure 4.3 Comparison between the numerical model results and field data of Kemp (1986) - Model incorporating the wave friction factor using the formula of Jonsson (1963).

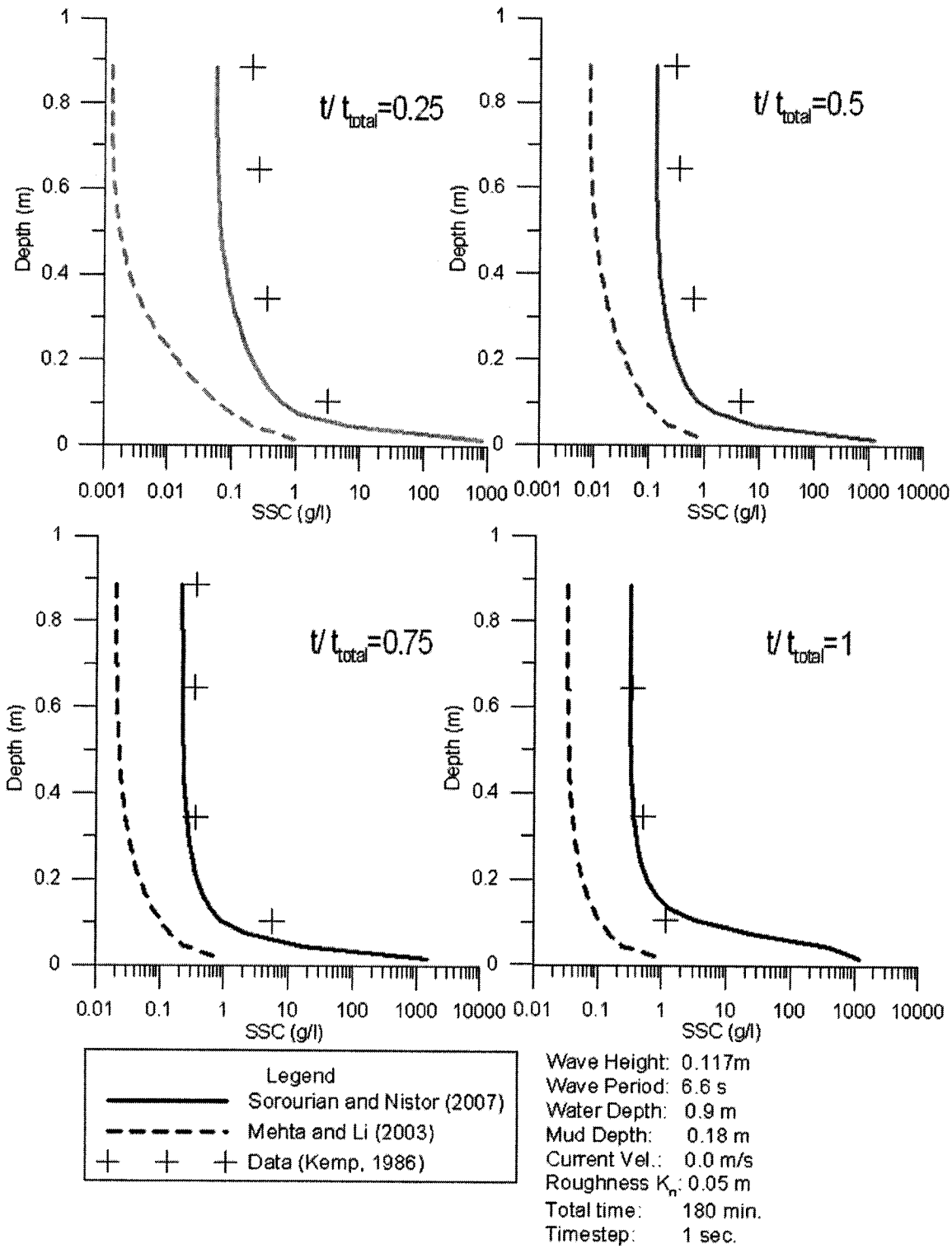

Figure 4.4 Comparison between the numerical model results and field data of Kemp (1986). - Model incorporating the wave friction factor using the formula of Swart (1974).

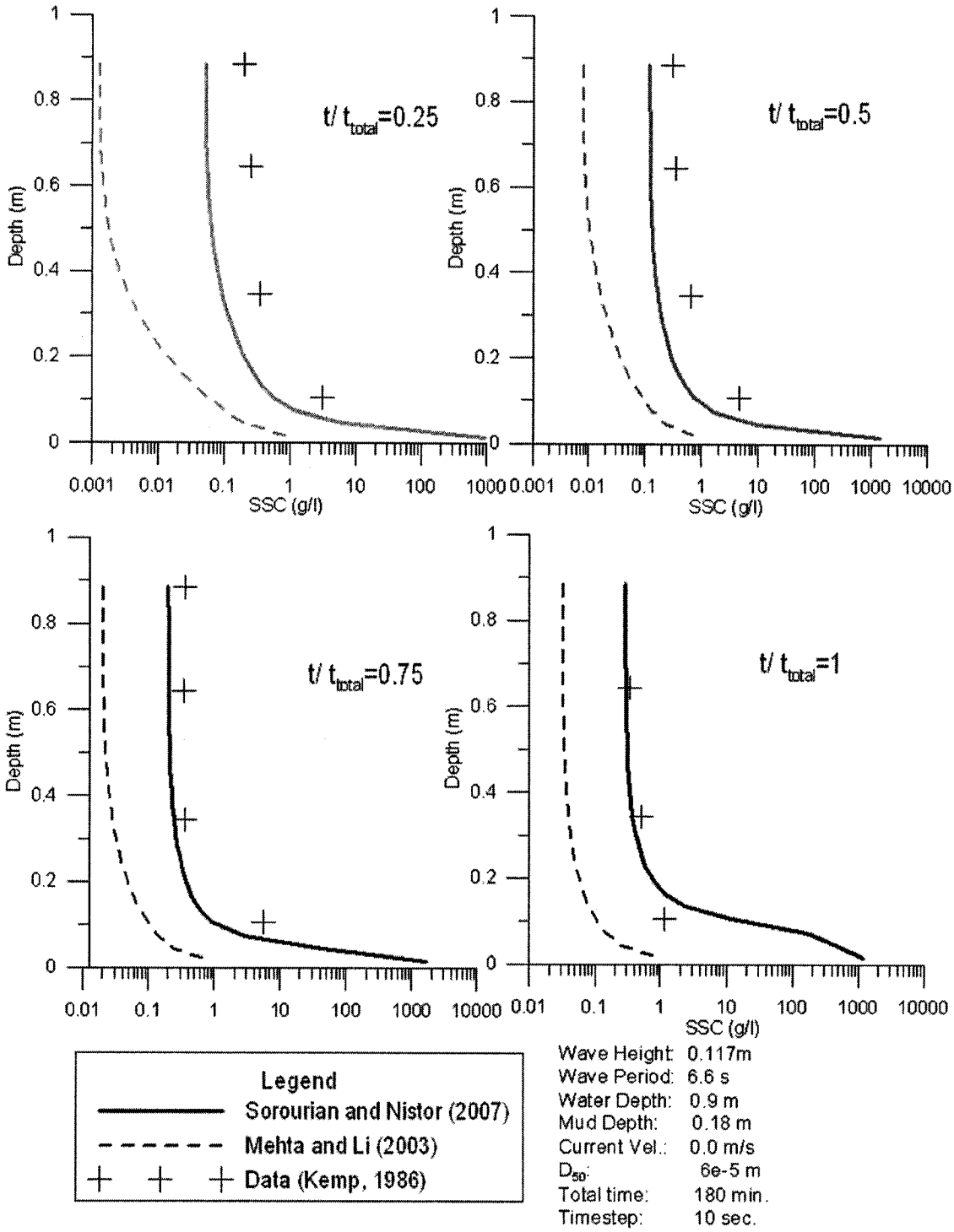

Figure 4.5 Comparison between the numerical model results and field data of Kemp (1986). - Model incorporating the wave friction factor using the formula of Le Roux (2003).

4.4 Time-dependent erosion rate

The input parameters for the time-dependent erosion rate, previously discussed in Chapter 3, are included in Table 4.7 and Table 4.8. The comparison of modified simulation results and the original model for Vermilion Bay field data is presented in Figure 4.6. The rest of the figures are presented in Appendix A. Results of original model are provided by Li (1996). Comparing to his model, the results of the suspended sediment obtained with the newly proposed model are in good agreement with the experimental data.

Table 4.7 Parameters for numerical modelling for the time-dependent erosion rate - Run 4, 5, and 6 (Maa, 1896).

		RUN 4	RUN 5	RUN 6
Wave period [s], height [m] and duration [min]		1.6;3.4;0~285	1.7;3.2;0~230	1.8;3.5;0~180
		1.1;5.5;285~588	1.2;5.2;230~537	1.4;4.5;180~425
				1.0;5.3;425~670
Water depth [m]		0.264	0.197	0.274
Mud depth [m]		0.093	0.16	0.105
Settling velocity parameters [non-dimensional]	c_1 [kg/m^3]	0.1	0.1	0.1
	w_{sf} [m/s]	6.37×10^{-7}	6.37×10^{-7}	6.37×10^{-7}
	α_1	0.01	0.01	0.01
	β_1	1.33	1.33	1.33
	γ_1	9.0	9.0	9.0
	δ_1	1.5	1.5	1.5
Wave diffusion coefficient, α_w [non-dimensional]		0.19	0.5	0.8
Stratified diffusion coefficients [non-dimensional]	α_0	0.5	0.5	0.5
	β_0	0.4	0.45	0.45
Bed density parameters [non-dimensional]	$\overline{\rho}_D$ [kg/m^3]	250.3	194.4	254
	ζ_1	0.797	0.797	0.797
	ξ_1	-0.45	-0.45	-0.45
Sediment granular density [kg/m^3]		2650	2650	2650
Bed bulk density [kg/m^3]		1080	1080	1100
Water density [kg/m^3]		1000	1000	1000
Wave friction factor [non-dimensional]		0.03	0.025	0.025

Erosion rate parameters [non-dimensional]	s_{max}	0.8	0.8	0.8
	a_r	5	5	5
	b_r	1	1	1
Median particle size [m]		2.1e-6	2.1e-6	2.1e-6
Elevation of sediment sample below water surface [cm]	#1	-12.4	-8.3	-13.9
	#2	-20.7	-16.6	-22.2
	#3	-22.6	-18.5	-24.2

Table 4.8 Parameters for numerical modelling for the time-dependent erosion rate - Vermilion Bay (Kemp, 1986) and Atchafalaya Bay (Sheremet *et al.*, 2005).

		VERMILION BAY, LOUISIANA (KEMP, 1986)		ATCHAFALAYA BAY, LOUISIANA (SHEREMET *ET AL.*, 2005)
		Frontal	Post Frontal	
Wave period [s], height [m] and duration [min]		6.6;11.7;76	6.9;5.2;190	3.17;0.177;-
		5.9;10.2;46		
Water depth [m]		0.9	0.9	5.0
Mud depth [m]		0.18	0.18	0.60
Settling velocity parameters [non-dimensional]	c_1 [kg/m^3]	0.3	0.3	1.78
	w_{sf} [m/s]	1.9×10^{-6}	1.9×10^{-6}	0.000022
	α_1	0.03	0.03	0.0037
	β_1	1.33	1.33	1.33
	γ_1	9.0	9.0	2.0
	δ_1	1.5	1.5	1.5
Wave diffusion coefficient, α_w		0.3	0.3	2
Stratified diffusion coefficients [non-dimensional]	α_0	0.5	0.5	0.5
	β_0	0.33	0.33	0.2
Sediment granular density [kg/m^3]		2650	2650	2650
Bed bulk density [kg/m^3]		1270	1270	1270
Water density [kg/m^3]		1030	1030	1030
Wave friction factor [non-dimensional]		0.03	0.03	0.03
Erosion rate parameters	s_{max}	0.8	0.8	0.8
	a_r	5	5	5

	b_r	0.5	0.5	0.5
Bed density parameters [non-dimensional]	$\overline{\rho}_D$ [kg/m^3]	400	400	400
	ζ_1	0.797	0.797	0.797
	ξ_1	-0.45	-0.45	-0.45
Median particle size [m]		6e-5	6e-5	6.34e-6
Elevation of sediment sample above the bed [cm]	#1	80	80	100
	#2	55	55	200
	#3	25	25	300
	#4	0.5	0.5	

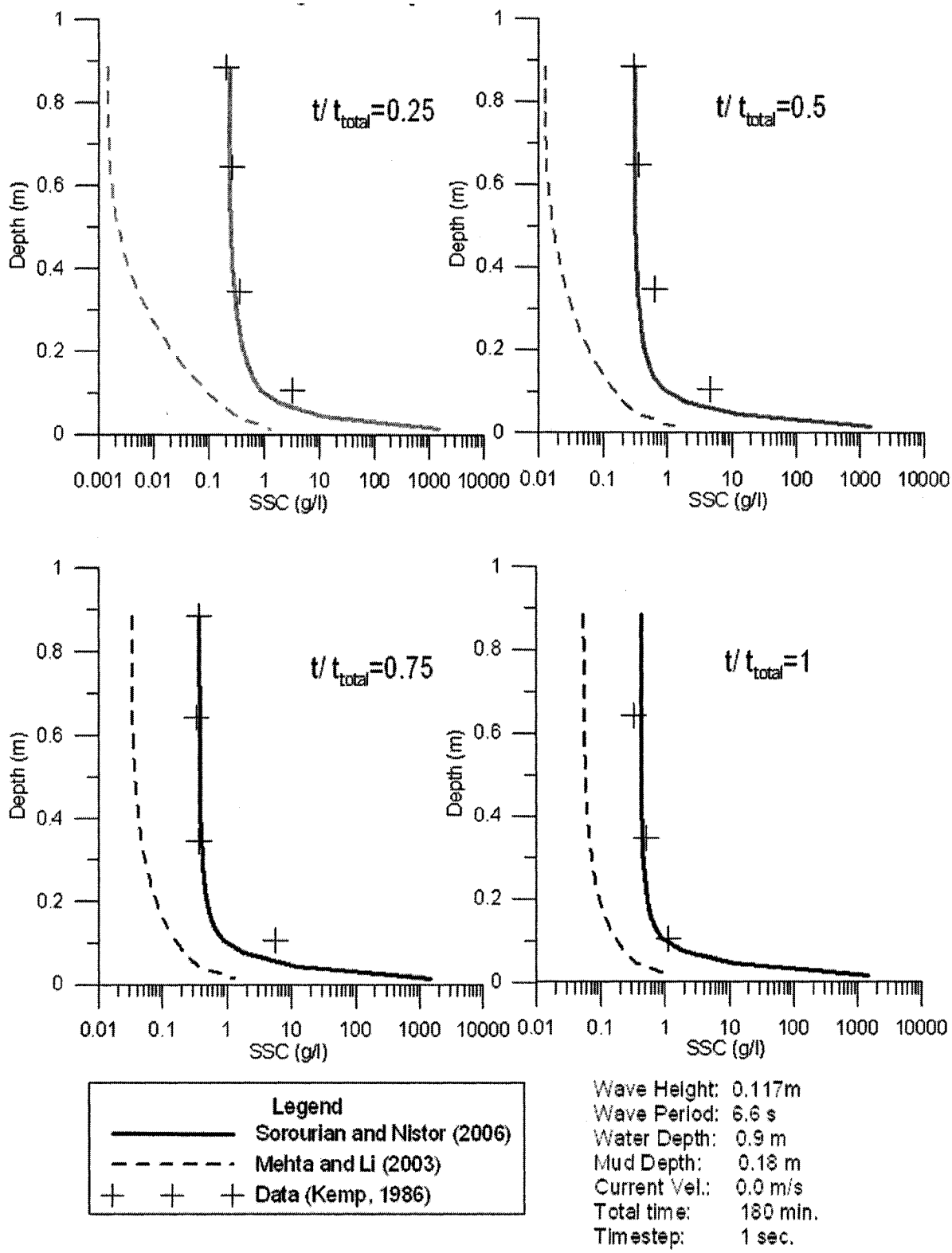

Figure 4.6 Comparison between the numerical model results and field data of Kemp (1986). - Model incorporating time-dependent erosion rate.

4.5 Model sensitivity

In this section a sensitivity analysis is provided for the proposed models. Input parameters of the models are the ones used to simulate field data of Kemp (1986) for the frontal period.

4.5.1 Electrochemical anchoring resistance

4.5.1.1 Sensitivity of the model to electrochemical anchoring coefficient

For the case of incorporating of inter-particle electrochemical forces, the sensitivity analysis is performed for two parameters: (1) electrochemical anchoring coefficient, χ, and (2) the wave friction factor, f_w. Figure 4.7 presents the variation of the mean suspended sediment concentration (SSC) at the end of wave period versus the electrochemical anchoring coefficient.

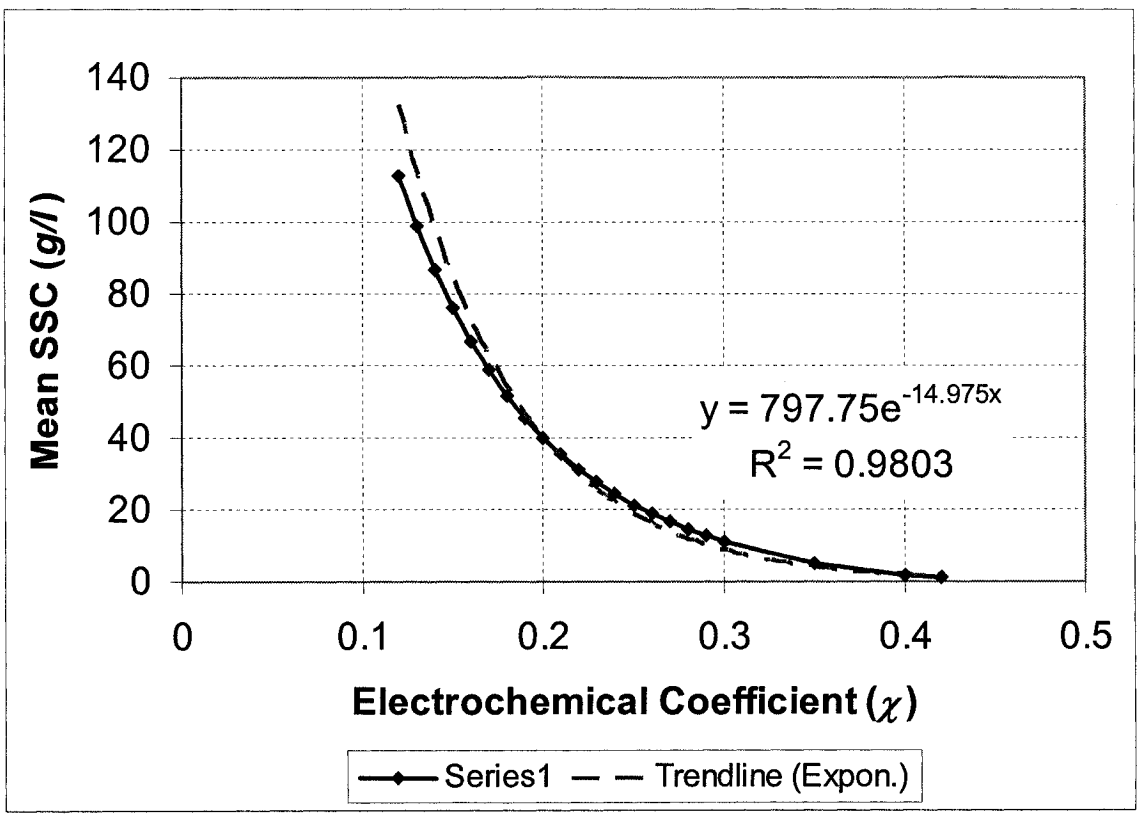

Figure 4.7 Variation of the mean suspended sediment concentration (SSC) vs. the electrochemical anchoring coefficient.

It is observed that the mean SSC decreases with an increase in the electrochemical anchoring coefficient. This relation can be approximated using an exponential expression depicted in Figure 4.7. As the electrochemical anchoring coefficient increases, the critical shear stress also increases and hence, the amount of eroded mass decreases. For the data of Kemp (1986), the erosion process ceases when the electrochemical coefficient exceeds a value of 0.4. Figure 4.8 shows the relation between the electrochemical anchoring coefficient and SSC at the water-mud interface. A sudden increase in SSC is observed when $\chi < 0.14$. This may be attributed to the mass erosion of sediments due to low strength of the bed.

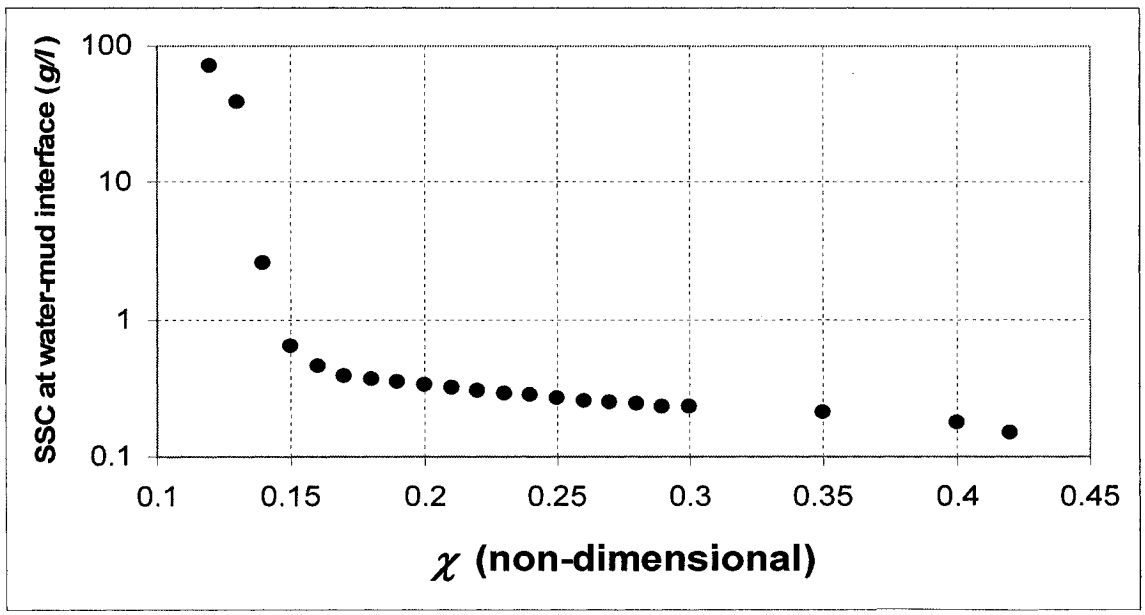

Figure 4.8 Variation of suspended sediment concentration at the water-mud interface with the varition of the electrochemical anchoring coefficient.

4.5.1.2 Sensitivity of the model with respect to the variation of the wave friction factor

As the wave friction factor increases, the bed shear stress also increases and thus, the mean suspended sediment concentration increases. The relation between mean SSC and the wave friction factor is shown in Figure 4.9. However, when the wave friction factor exceeds 0.035, the model behave s inconsistently. That is because the sudden erosion of the mud layer due to the mass erosion that is not considered in the present study.

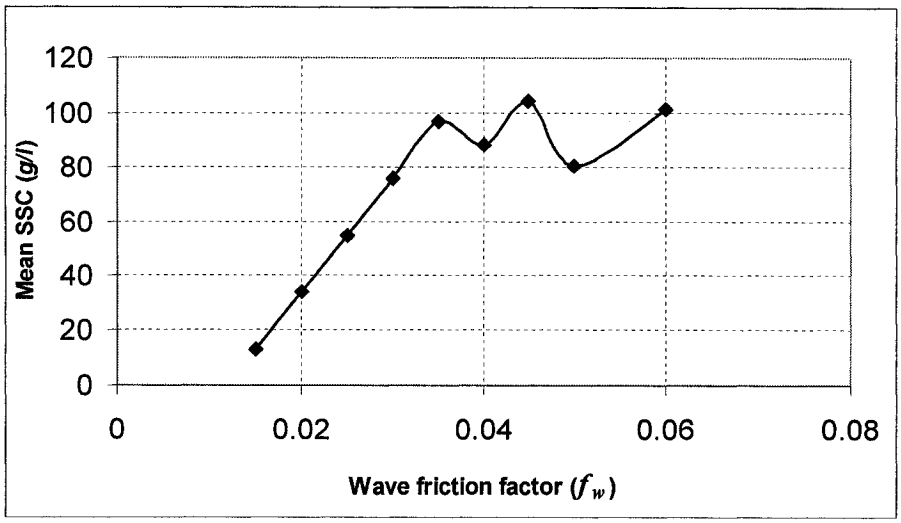

Figure 4.9 Variation of the mean SSC with the wave friction factor

4.5.2 Relating the shear resistance to the vane shear strength of the bed

The variation of the mean SSC with respect to the vane shear stress is plotted in Figure 4.10 . The mean SSC increases with an increase in the vane shear stress until the value of 0.22 Pa. With a further increase in the vane shear stress, the mean SSC decreases and reaches asymptotically to zero when the vane shear stress is about 0.6 Pa.

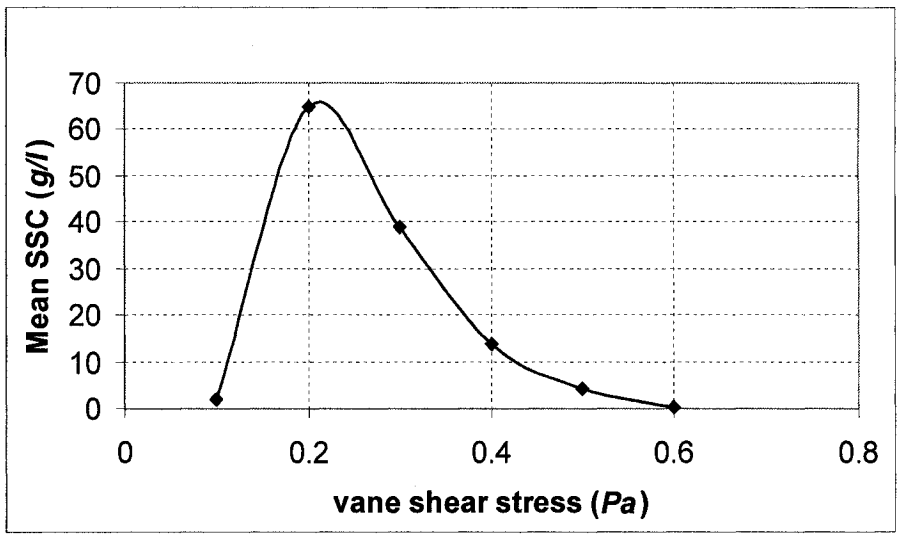

Figure 4.10 Variation of the mean SSC vs. the vane shear stress.

4.5.3 Influence of the wave friction factor

As long as the wave friction factor is expressed in terms of the bed roughness as in the formula of Jonnson (1963) and Swart (1974), the sensitivity analysis is performed for the bed roughness for both of the aforementioned models. For the case when the wave friction factor is defined as by Le Roux (2003), thenlysis is conducted based s function of the median particle diameter.

For both Jonnson (1963) and Swart (1974) formulations, the mean SSC increases as the bed roughness increases (Figure 4.11 and Figure 4.12). This relation can be approximated with a logarithmic trend-line. However, for a given value of the bed roughness, the model overpredicts the suspended sediment concentration in the case when Jonnson's equation is used.

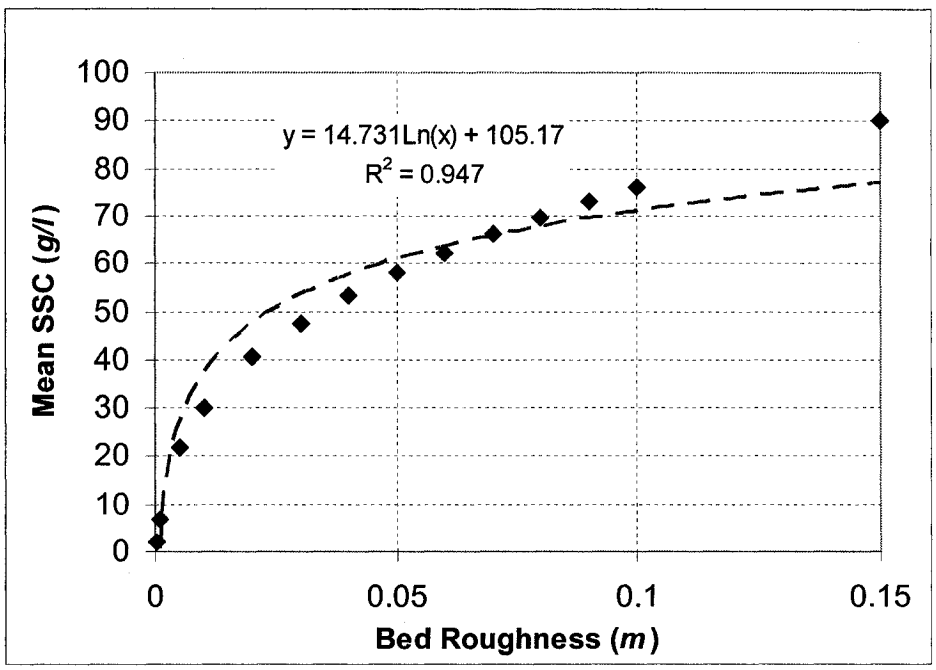

Figure 4.11 Variation of the mean SSC with the bed roughness. Model incorporating the wave friction factor using the formula of Jonsson (1963).

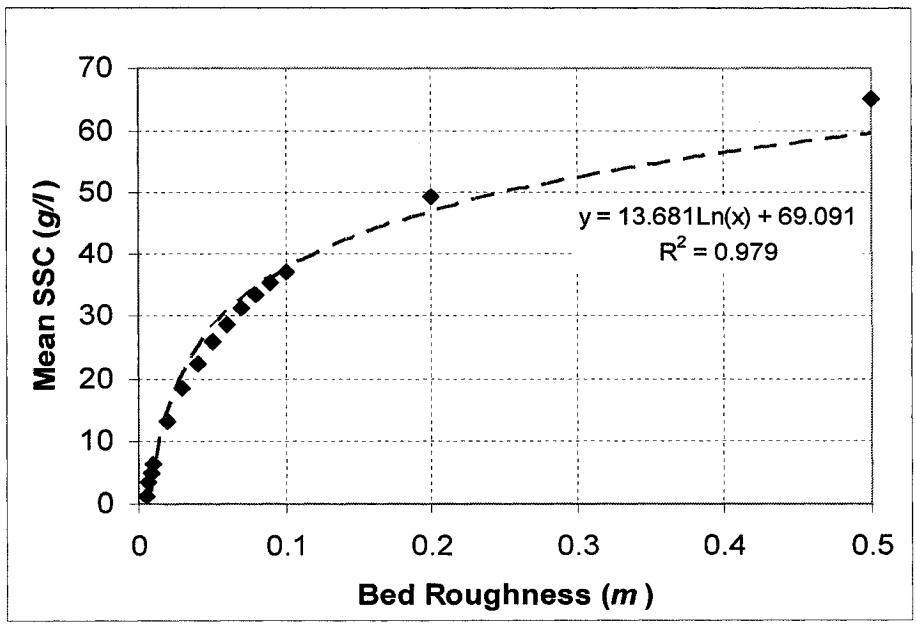

Figure 4.12 Variation of the mean SSC with the bed roughness. Model incorporating the wave friction factor using the formula of Swart (1974).

For the case of Le Roux's formula, it can be observed from Figure 4.13 that the calculated mean SSC increases with an increase in the median particle size diameter until it plateaus asymptotically to the concentration of 60 g/l corresponding to a median grain size of 60 μm.

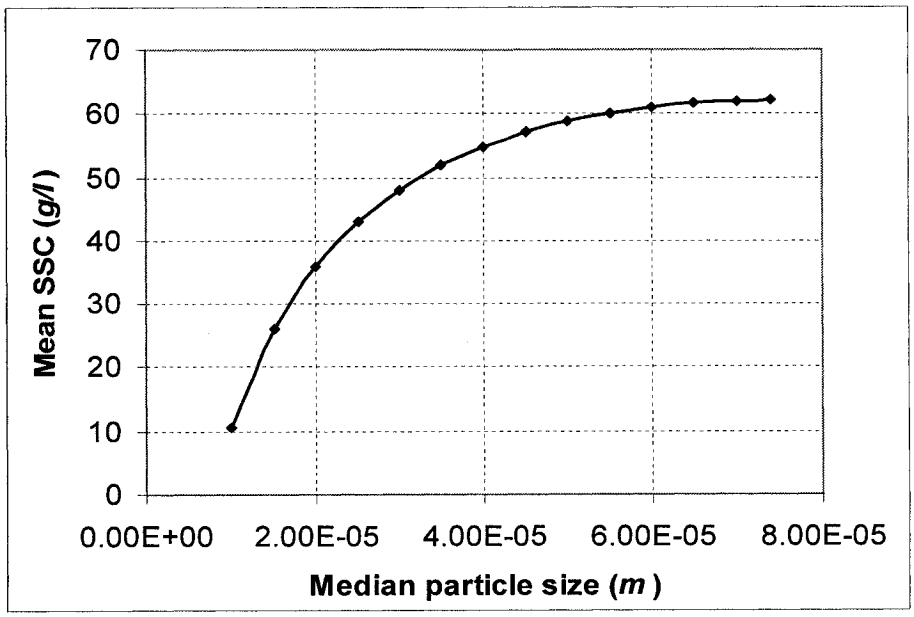

Figure 4.13 Variation of the mean SSC with the median particle size diameter. Model incorporating the wave friction factor using the formula of Le Roux (2003).

4.5.4 Time-dependent erosion rate

4.5.4.1 Sensitivity of the model to the computational timestep

According to Figure 4.14 , one can notice that the mean value of the SSC does not vary significantly with a change in computational timestep.

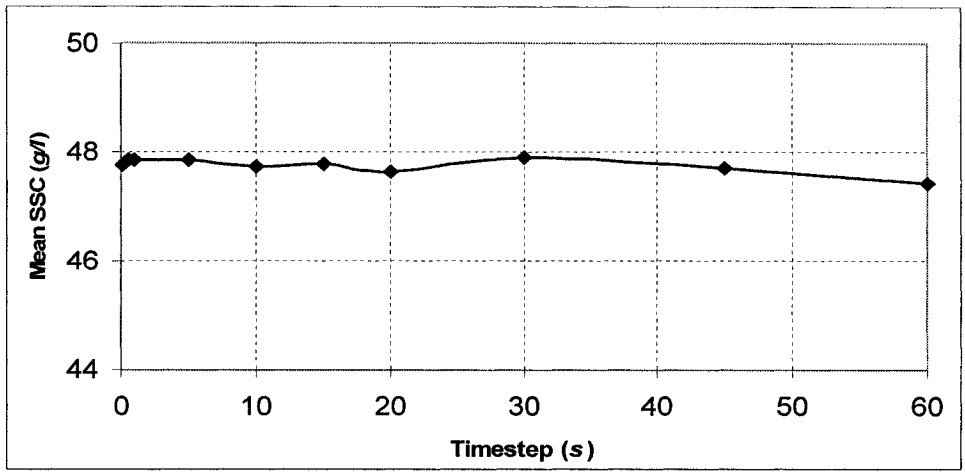

Figure 4.14 Variation of the mean SSC with computational timestep.

However, the suspended sediment concentration in the water-mud interface increases substantially when the computational timestep exceeds 20 s (Figure 4.15).

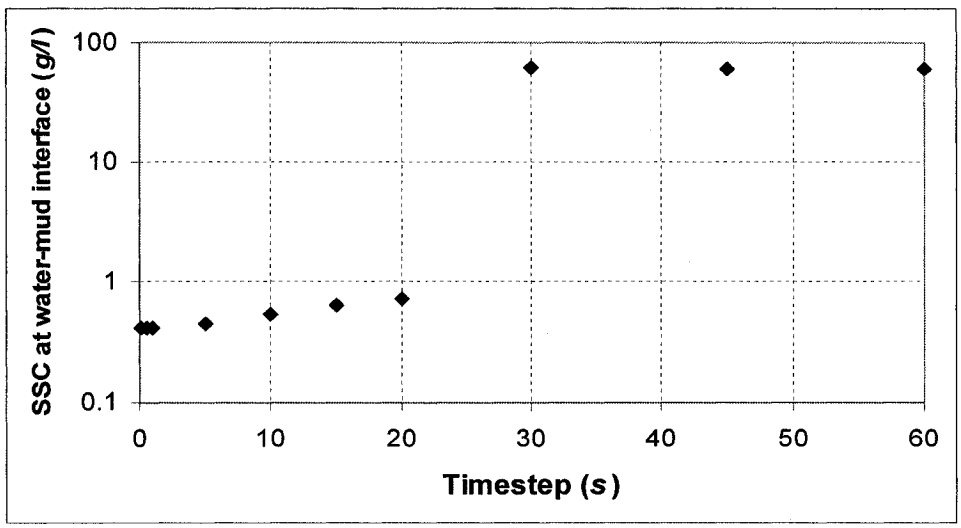

Figure 4.15 Variation of SSC at the water-mud interface with computational timestep.

4.5.4.2 Sensitivity of the model to diffusion parameters

In this part sensitivity of the model to the diffusion parameters, namely α_0, β_0 and α_w (Equations 3.14 and 3.16) is presented. As shown, the mean SSC is not sensitive to any of these three parameters (Figure 4.16 to Figure 4.18). This is because these parameters deal with diffusion of sediments in the water column and not with the process of erosion itself.

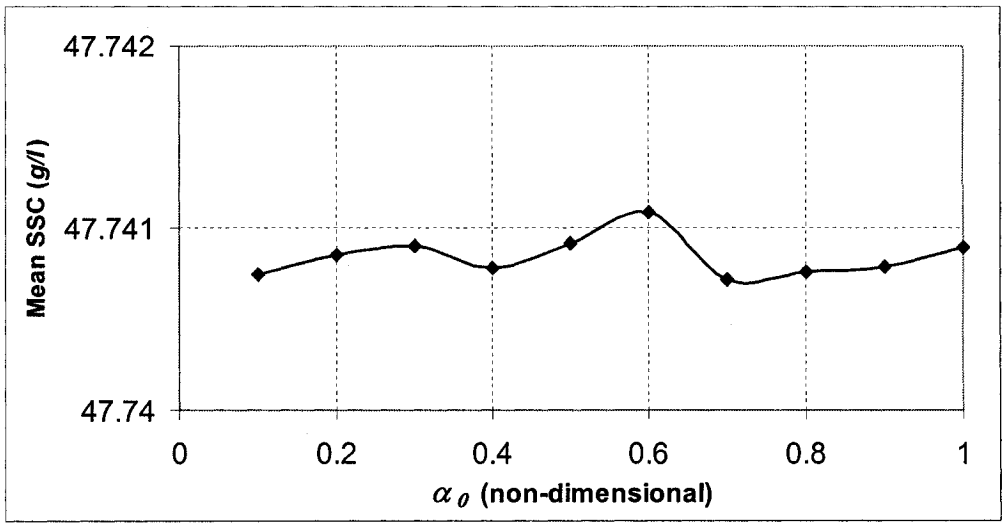

Figure 4.16 Variation of the mean SSC vs. diffusion coefficient, α_0.

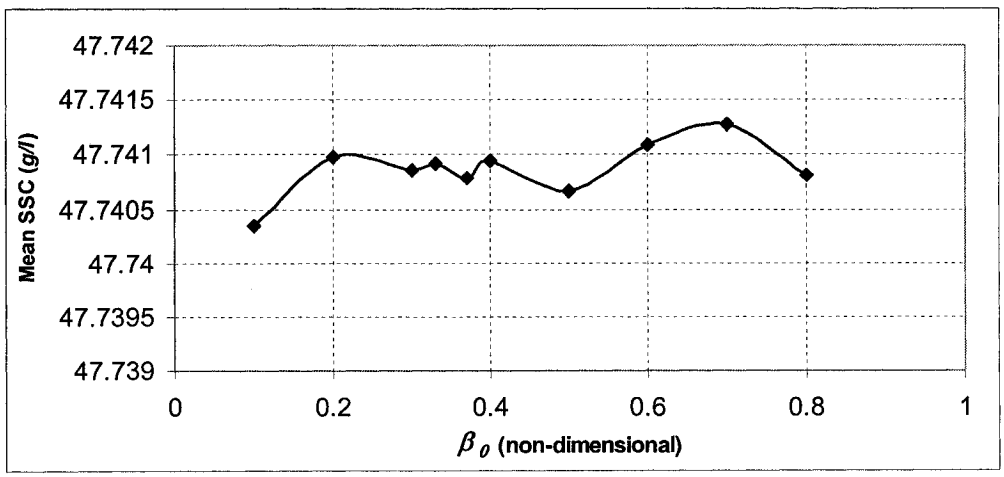

Figure 4.17 Variation of the mean SSC vs. the diffusion coefficient, β_0.

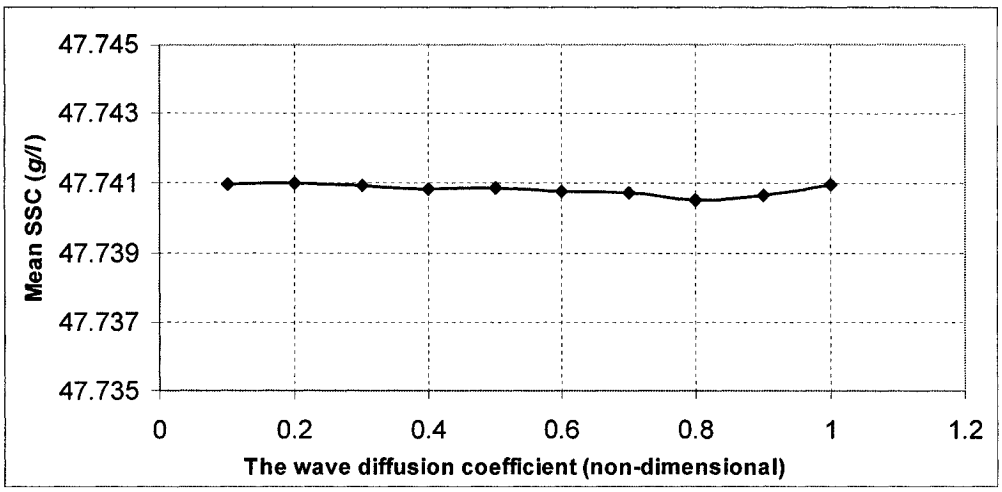

Figure 4.18 Variation of the mean SSC vs. the wave diffusion coefficient, α_w

The effect of the diffusion parameters is more important when the variation of suspended sediment concentration at a certain elevation from the bed is studied. As diffusion increases, the value of suspended sediment concentration at a specific point increases. Figure 4.19 and Figure 4.20 show the variation of suspended sediment concentration in water-mud interface with respect to α_0 and the wave diffusion coefficient, α_w. In both cases, for a value of 0.4 for both α_0 and α_w, a sudden change suspended sediment concentration. This is due to the mass erosion.

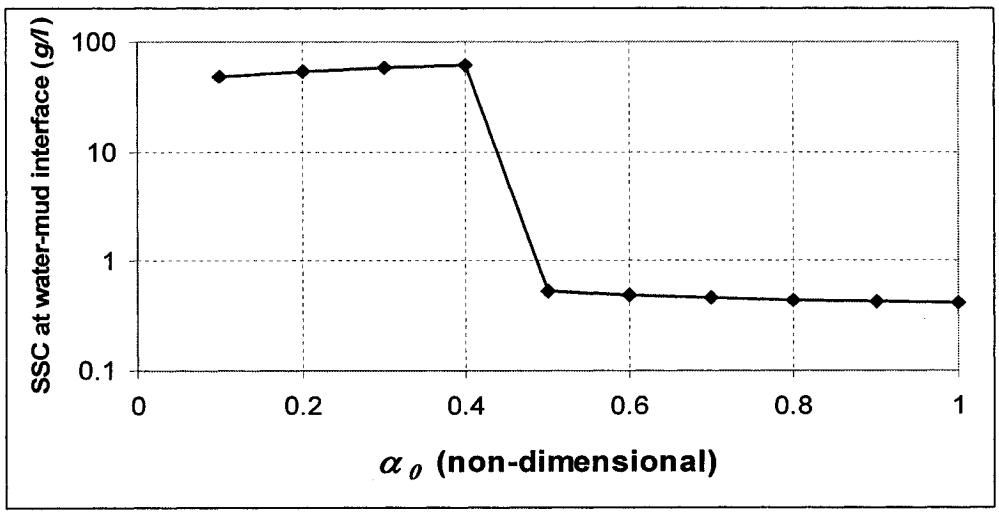

Figure 4.19 Variation of suspended sediment concentration at the water-mud interface with α_0.

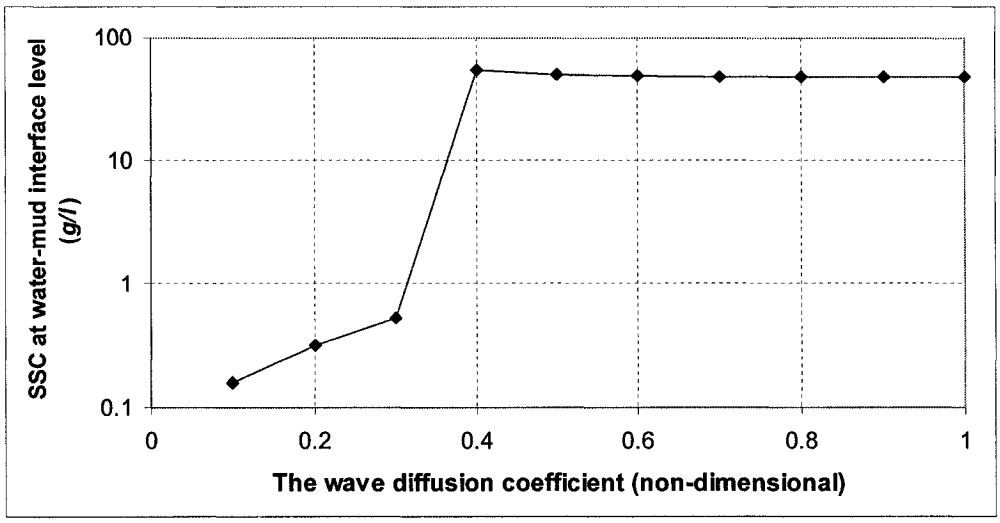

Figure 4.20 Variation of suspended sediment concentration at the water-mud interface with α_w.

For the case of β_0, the SSC at the water-mud interface decreases with an increase in β_0 and reaches a minimum value of about 0.21 g/l at the value of $\beta_0 = 0.44$; it then increases asymptotically up to a concentration of about 0.29 g/l (Figure 4.21)

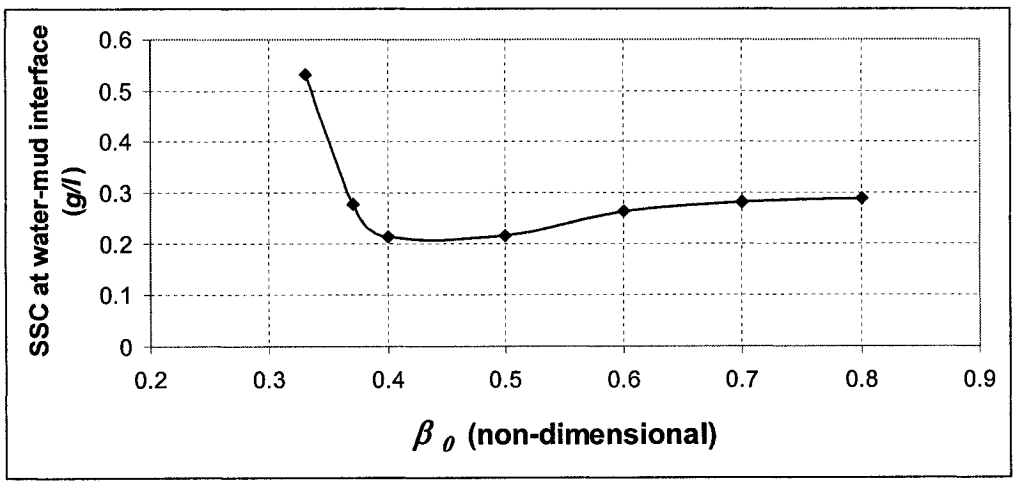

Figure 4.21 Variation of suspended sediment concentration at the water-mud interface with β_0.

4.5.4.3 Sensitivity of the model to the critical shear stress parameters

The results of the sensitivity analysis of the model with respect to the critical shear stress parameters, namely ζ and ξ (Equation 3.68) are shown in Figure 4.22 and Figure 4.23. The

relation between the mean SSC and parameter ζ follows a parabola trend. However, for the case of ξ, the mean SSC increases smoothly with an increase in ξ that can be well approximated with a polynomial.

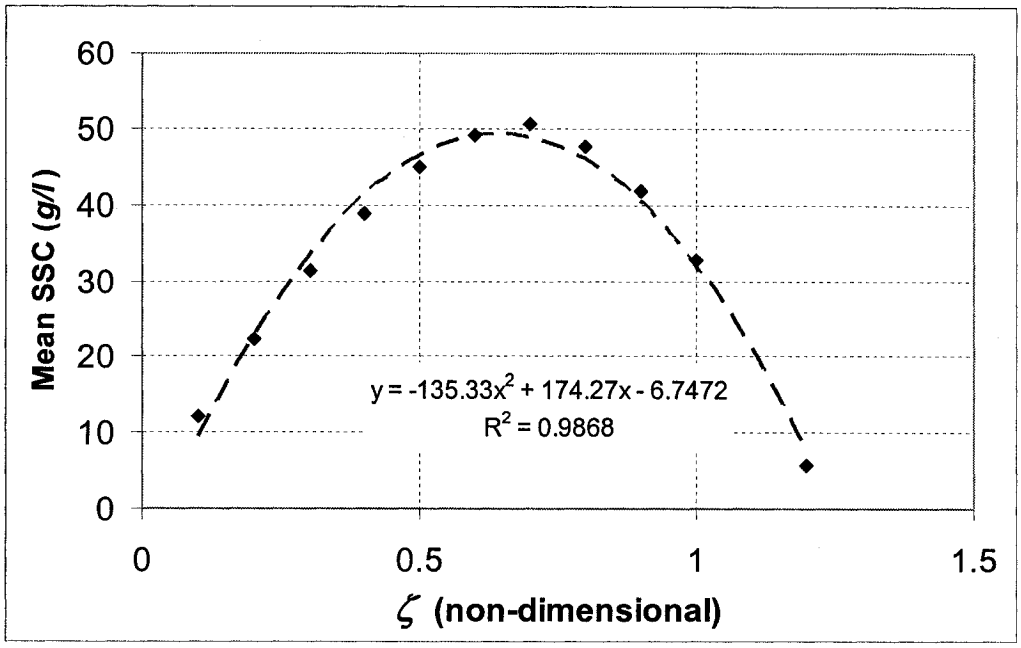

Figure 4.22 Variation of the mean SSC vs. the critical shear stress coefficient, ζ.

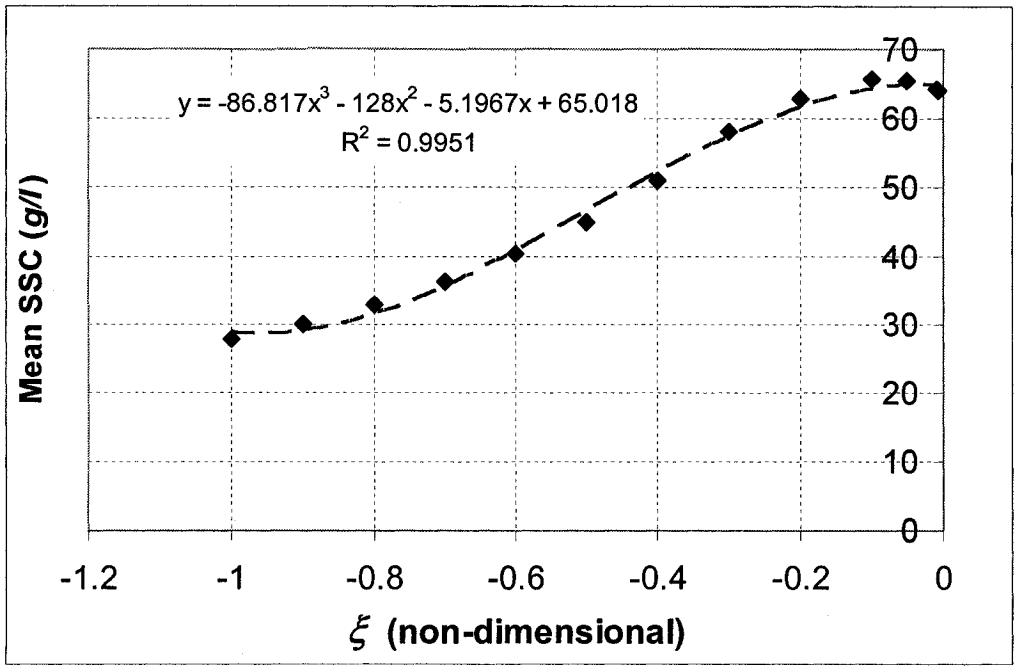

Figure 4.23 Variation of the mean SSC vs. the critical shear stress coefficient, ξ.

The variation of suspended sediment concentration at the water-mud interface is plotted in Figure 4.24. It is observed that SSC in the water-mud interface increases smoothly up to a value of $\zeta = 0.5$. Then a sudden jump is observed that is followed by a smooth decrease of SSC for values of $\zeta > 0.8$.

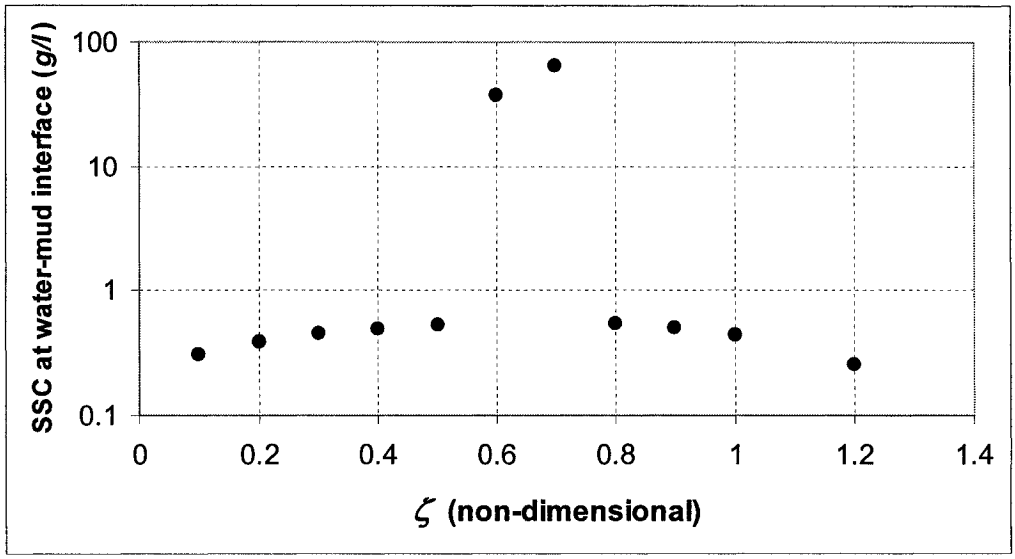

Figure 4.24 Variation of suspended sediment concentration at the water-mud interface with critical shear stress coefficient, ζ.

5 DISCUSSION, CONCLUSIONS AND RECOMMENDATIONS

5.1 Summary of the study and conclusions

Different methods have been employed to improve the sediment exchange flux at the water-mud interface and to provide more accurate predictions of suspended sediment concentration profiles for the case of cohesive sediments. In order to do so, a few new models are proposed in the present thesis in order to improve the computation of the erosion rate of cohesive sediments. These improvements are applied in three different ways: estimation of the threshold shear stress, bed shear stress, and erosion rate of cohesive sediments. Results of the numerical models are compared with laboratory and field data provided by Maa (1986), Kemp (1986) and Sheremet (2006). The models were found to perform well and they show better estimation of the sediment concentration profiles when compared with the model proposed by Mehta and Li (2003).

Two new concepts have been applied for the estimation of the threshold shear stress for the case of bed erosion. In one approach, the particle-particle electrochemical forces are taken into consideration and their inclusion is performed using the formula of Taki (2001). The second proposed concept is to relate the critical shear stress for erosion to vane shear strength of the bed by the formula of Dade and Nowell (1992). These are two of the significant contributions of the thesis as neither of these two concepts has ever been used before. In both cases, the new model provides a better estimation of the suspended sediment concentration profile when compared to the initial model of Mehta and Li (2003) and with various experimental data. Just as in the case of the Mehta and Li (2003), the suspended sediment concentration profile is underestimated in the beginning of the simulation time. This is most likely due to the fact that initial sediment concentration was not provided in the field data and was therefore not included in the model input. The model begins the computation of the sediment concentration from an initial profile which does not assume the presence of sediment in the water column. Once the numerical solution reaches steady state conditions, the numerical results are in good agreement with the experimental data for both laboratory and field data. This could also be attributed to an "inertial delay time" caused by the

differences in mass between the sediment and fluid particles. Though the mass of the mud particle may be smaller than the mass of a sand particle, inertial forces may still play a role in the differences between the numerical and experimental data. One more reason why excellent agreement with experimental data is not attained can be due to the fact that both Equation (2.53) and (2.55) are depth-independent . Therefore, the effect of the increasing bed strength due to an increase in bed depth is not captured by these formulations.

To improve the prediction of the bed shear stress, three methods are incorporated in order to relate the wave friction factor to other known parameters of the model. This factor was treated as *a priori* input in the original model of Mehta and Li (2003). In the new model, the wave friction factor is expressed in terms of other parameters of the model, such as the bed roughness and the median grain diameter. The wave friction factor is introduced using three different formulations proposed by Jonnson (1963), Swart (1974) and Le Roux (2003). The Le Roux formulation relates the wave friction factor to the median grain diameter of bed particles. Expressing the wave friction factor in terms of median grain diameter is incorporated for the first time in a cohesive sediment transport model. The other two formulas express wave friction as a function of the bed roughness. All of the formulations are proved to provide good results in the newly proposed model. The suspended sediment concentration profile shows better agreement with experimental data compared to the original model of Mehta and Li (2003). However, there is no significant difference between numerical results when using any of these three formulas for the wave friction factor. This indicates that any of these equations can be used in the model.

The third improvement to the model is performed by incorporating the time-dependent erosion rate using the concept of Sanford and Maa (2001). Again, this concept has never previously been applied in any cohesive sediment transport model. The results of the numerical model show very good agreement with experimental data in the case of both laboratory and field data. The improved model better predicts the suspended sediment concentration profile compared with the original model of Mehta and Li (2003). The author would attribute this to the additional time-dependent term in the used in the erosion rate equation. This time-dependent term provides faster erosion and allows the model to reach the equilibrium state earlier than previous models.

In all of the applied methods, the concentration near the bed is overestimated. This is because the present model does not simulate the lutocline. Incorporation of the lutocline in the model is expected to improve the estimation of near-bed concentration and could prove to be a useful model development.

5.2 Recommendations for future study

Based on the analysis of the results of the present study, its conclusions as well as its shortcomings, a number of recommendations are provided for the future study.

1. The present concepts which are used to relate critical shear strength of the bed to the vane shear stress and to the electrochemical force do not account for the mud depth. Therefore, critical shear stress does not decrease with the depth of erosion, which prolongs the time required to reach the steady state solution. One recommendation would be to include the variability of the bed thickness.

2. For bed shear stress under combined wave and current conditions, the present model uses a scalar addition for the wave and current-induced shear stresses. However, when flow is not laminar but turbulent, as in the case of wave propagation in the surf zone, this assumption is not adequate. The method introduced in Section 2.8 is therefore suggested to improve shear stress prediction.

3. For the governing equation of time-dependent erosion rate, the homogenous solution provided by Equation (2.22) is applied in the present study. This solution is difficult to validate for the case of oscillatory flows. One recommendation for further work would be the incorporation of the time-varying bed shear stress $\left(d\tau_b/dt \neq 0\right)$.

4. The local erosion constant for time-dependent erosion rate (β_e) is expressed in terms of the bed bulk density. However, this factor also depends on the salinity and sand content of the cohesive sediments (Aberle *et al.*, 2004). For a more accurate expression of this parameter, the effect of the salinity variation and of the sand content variation should be included in a future model.

5. Only the bed surface erosion is considered in the proposed model. However, mass erosion may occur, especially under wave breaking conditions. The incorporation of mass erosion and of sediment diffusion under breaking waves could be further improvements to the present model.

6. The shear stress and diffusion under breaking wave conditions was not dealt with in the present research. Just as in the case of laboratory and field data, mud beds have a strong damping effect on the wave breaking process. Hence, even though wave breaking may not always occur over muddy beds, this may still be the case in extreme weather conditions (hurricanes, extreme wave climates). In general, neglecting the effect of wave breaking leads to an under-prediction of the suspended sediment concentration in the surf zone. Calculation of the suspended sediment concentration profile under breaking waves will improve the accuracy of the model across the entire range of wave conditions.

7. The effect generated by the presence of nutrients and contaminants in the mud sediments is not included in the present model. Interdisciplinary research on the combined behaviour of fluid mud and the transport and dispersion of contained nutrients and contaminants is suggested as a possible direction of study.

REFERENCES

Aberle, J, Nikora, V, Walters, R, (2004). "Effect of Bed Material Properties on Cohesive Sediment Erosion." *Marine Geology*, Elsevier, 207, 83-93.

Allison, M.A., Kineke, G. C., Gordon, E. B., and Goni, M.A. (2000). "Development of reworking of a seasonal flood deposit on the inner continental shelf off the Atchafalaya River". *Continental Shelf. Research*, 20, 2267-2294.

Amos, C.L., Daborn, G.R., Christan, H.A., Atkinson, A., Robertson, A., (1992). "In situ erosion measurements on fine-grained sediments from the Bay of Fundy". *Marine Geology,* 108 (2), 175-196.

Amos, C.L., Feeney, T., Sutherland, T.F., Luternauer, J.L., (1997). "The stability of fine-grained sediments from the Fraser River delta". *Estuarine, Coastal and Shelf Science*, 45 (4), 507-524.

Ariathurani, R., and Arulandanan, K., (1978), "Erosion Rate of Cohesive Soils," *Journal of Hydraulic division,* ASCE, 104, HY2, 279-283, 1978.

Ariathurani, R., MacArthur R. C., and Krone, R. B., (1977). "Mathematical model of estuarial sediment transport". *Technical Report D-77-1/2*, U. S. Army Engineeri Waterways Experiment Station, Viksburg, MS.

Arnskov, M.M., Fredsøe, J., and Sumer, B.M., (1993). "Bed shear stress measurement over a smooth bed in three-dimensional wave-current motion". *Coastal Engineering*, 20, 277-316.

Atkinson, J. F., (1988). Note on "Interfacial mixing in stratified flows". *Journal of Hydraulic Research*, 26 (1), 27-31.

Black, K.S., Tolhurst, T.J., Paterson, D.M., Hagerthey, S.E., (2002). "Working with natural cohesive sediments". *Journal of Hydraulic Engineering*, 128 (1), 2-8

Bowen A.J. (1969). "The generation of longshore currents on a plane beach". *Journal of Marine Research*, Vol. 27, pp. 206-215.

Bruens, A. W., (2003) "Entraining mud suspensions". *Ph.D. Thesis*, Delft University of Technology. Report 03-1, ISSN 0169-6548.

Burban, P. Y., Xu, Y. J., McNeil, J., and Lick, W. (1990). "Settling speed of flocs in fresh water and sea water". *Journal of Geophysical Research*, Vol. 95, 18213-18220.

Burt, T. N. and Stevenson, J. R. (1983). "Field settling velocity of Thames mud". *Hydraulic Research Station*, Walling-ford, Rep. No. IT 215.

Chou, H.T., (1989). "Rheological response of cohesive sediments to water waves". *Ph.D. Dissertation,* University of California, Berkeley, 149p.

Christodoulou G. G., (1986). "Interfacial mixing in stratified flows". *Journal of Hydraulic Research*, 24, 77-92.

CTH. (1971). Estuarine navigation projects, technical bulletin 17, Corps of engineers and scientists, Printce-Hall, Englewood Cliffs, N.J.

Dade, W. B., and Nowell, A.R.M., (1991). "Moving Muds in Marine Environment." *Proc. Coastal Sediments*, ACSE, 91, 54-71.

Dade, W.B., Nowell, A.R.M., Jumars, P.A., (1992). "Predicting erosion resistance of muds". *Marine Geology*, 105 (1-4), 285-297.

Dalrymple R. A., and Lui, P. L.-F., (1978). "Wave over soft muds, a two layer fluid mud model". *Journal of Physical Oceanography*, 8, 1121-1131.

Dean R. G., and Dalrymple R. A., (2002). "Coastal Processes with Engineering Applications." Cambridge, UK : New York : Cambridge University Press, pp. 254-261.

Delo, E.A. and Burt, T. N., (1986). "The hydraulic engineering characteristics of estuarine muds". *Hydraulic Research*, Wallingford, U.K., Rep. SR 77.

Dowson, T. H., (1978). "Wave propogation over a deformable sea floor". *Ocean Engineering*, 5, 227-234.

Dunn, I. S., (1959). "Tractive Resistance of Cohesive Sediments." *Journal of Soil Mechanics and Foundations*, ASCE, 85, No. SM3, Proc. Paper 2062, 1-24.

Dyer, K.R., (1986). "Coastal and estuarine sediment dynamics". Wiley, New York, 357 p.

Dyer, K. R. and Manning, A. J., (1999). "Observation of the size, settling velocity and effective density of flocs and their fractal dimentions". *Journal of Sea Research* (41), 87-95.

El Ganaoui, O., Schaaff, E. ,Boyer, P., Amielh, M., Anselmet, F., Grenz, C., (2004) "The deposition and erosion of cohesive sediments determined by a multi-class model." *Estuarine, Coastal and Shelf Science*, Elsevier, 60, 457-475

Eugelund, F., and Wan, Z.-H., (1984). "Instability of hyperconcentrated flow". *Journal of Hydraulic Engineering*, 110 (3), 219-232.

Feng, J., (1992). "Laboratory experiments on cohesive soil bed fluidization by water waves". *M.S. Thesis*, University of Florida, Gainesville, 109p.

Foda, M. A. (1989). "Seabed damping of water beds over a soft bed". *Journal of Fluid Mechanics*, 201, 189-201.

Fennessy, M.J., Dyer, K.R., and Huntley, D.A. (1994). "INSSEV: An instrument to measure the size and settling velocity of flocs in situ". *Marine Geology* (117), 107-117.

Fredsøe, J. (1984). "Turbulent boundary layer in wave-current motion". *Journal of Hydraulic Engineering*, ASCE, 110, 1103-1120.

Fredsøe, J. and Deigaard, R., (1992). "Mechanics of coastal sediment transport". World Scientific Publishing, Advanced series on Ocean Engineering, Vol. 3.

Grant, J. and Madsen, O.S., (1979). "Combine wave and current interaction with a rough bottom". *Journal of Geophysical Research*, 84 (C4), 1797-1808.

Grim R. E., (1968). "Clay Mineralogy." McGraw-Hill, New York, NY, 596p.

Gularte, R.C., Kelly, W.E., Nacci, V.A., (1980). "Erosion of cohesive sediments as a rate process". *Ocean Engineering*. 7, 539-551.

Gust, G., Morris, M.J., (1989). "Erosion threshold and entrainment rates of undisturbed in situ sediments". *Journal of Coastal Research*, 5, 87-100 special issue.

Hayter, E.J., 1983. "Prediction of cohesive sediment transport in estuarial waters". *Ph.D. Thesis*, University of Florida, Gainesville, FL, 348 pp.

Hinze, J. O., (1959). "Turbulence". McGraw-Hill Book Company, Inc., New York, 595p.

Hsiao, W. C., and Shemdin, O. H., (1980). "Interaction of ocean waves with a soft bottom". *Journal of Physical Oceanography*, 10, 605-610.

Hunter, J. R. (1881). "Zeta potential in colloid science. Principles and applications.". Academic press, New York.

Hwang K. N. (1989). "Erodibility of fine sediments in wave-dominated environments". *M.S. Thesis*, University of 'Florida, Gainesville, FL, 159p.

Ito, I. and Matsui, T. (1975). "Plastic flow mechanism of clay". *Proceedings of the Japanese Society of civil Engineers*, Tokyo, 236, 109-123.

Jepsen R., Roberts J., and Lick W., (1997). "Effects of bulk density on the sediment erosion rates". *Water and Soil Pollution,* 99 (1-4), 21-31.

Jiang F. (1993) "Bottom mud transport due to water waves". *Ph.D. Dissertation*, University of Florida, Gainesville, FL, 222 p.

Johns, B. (1968). "The damping of the waves in shallow water by energy dissipation in a turbulent boundary layer". Tellus, Vol. XX.

Jonnson I. G., (1966). "Wave boundary layer and friction factors". *Proceeding of the 10th Coastal Engineering Conference*, Vol. 1, ASCE, New York, NY, 127-148.

Jonnson, I., G., (1963). "Measurement in the Turbulent Wave Boundary Layer." *Proc. 10th Cong.*, IAHR, pp. 85-92.

Kajiura K. (1964). "On the bottom friction in an oscillatory current". *Bull. Earthquake Res.*, Inst. Univ. of Tokyo, Vol. 42, pp. 147-174.

Kajiura K., (1968) "A model of bottom boundary layer in water waves". *Bull. Earthquake Res.*, Inst. Univ. of Tokyo, Vol. 46, pp. 75-123.

Kamphuis, J.W., (1975). "Friction factor under oscillatory waves". *Journal of Waterways, Harbours and Coastal Engineering Division*, ASCE, Vol. 101, No. WW2, pp. 135-144.

Kamphuis, J.W., (2000). "Introduction to Coastal Engineering and Management." *Advanced Series of Ocean Engineering Vol. 16, Singapore, New Jersey, London, Hong Kong: World Scientific,*

Kato, H., and Phillips, O. M. (1969), "On the penetration of a turbulent layer into a stratified fluid". *Journal of Fluid Mechanics*, 37, 753-768.

Keedwell, M. L., (1984). "Rheology and soil mechanics". Elsevier, London, 339p.

Kemp, G. P. (1986). "Mud deposition at the shore surface: Wave and sediment dynamics in the Chenier plain of Louisiana". *Ph.D. dissertation*, Louisiana State University, 159p.

Kirby R. , Hobbes, C. H., and Mehta, A. J., (1994). "Shallow stratigraphy of Lake Okeechobee Florida: a preliminary reconnaissance". *Journal of Coastal Research*, 10(2), 339-350.

Kitahara, A., Fujii, T., and Kanato, S., (1971). "Dependence of zeta potential upon particle size and capillary radius at streaming potential study in nonaqueous media" *Bulletin, Chemical Society of Japan*, 44, 3242-3245.

Kranenburg, C, (1999). "Effect of Floc Strength on Viscosity and Deposition of Cohesive Sediment Suspensions." *Continental Shelf Research*, Elsevier, 19 (13), 1665-1680

Kranenburg, C. and Wintererp, J. C., (1997). "Erosion of fluid mud layers I: Entrainment Model". *Journal of Hydraulic Engineering*, ASCE, 123 (6), 504-511.

Kranenburg, C., (1994). "An entrainment model for fluid mud". *Report 93-10*, Communications on hydraulic and geotechnical engineering, Civil Engineering Department, Delft University of Technology, the Netherlands, 10p.

Krishnappan, B., G. (2000). "In situ size distribution of suspended particles in the Fraser River". *Journal of Hydraulic Engineering*, ASCE, 126(8) 561–569.

Krishnappan, B.G., Madsen, N., Stephens, R., and Ongley, E.D. (1992). "A field instrument for measuring size distribution of suspended sediments in rivers." *In Proceedings of*

the 8th IAHR Congress (Asia and Pacific Regional Division), Pune, India, 20– 23 October 1992. IAHR, pp. F71–F81.

Krishnappan, B.G., and Engel, P. (1997). "Critical shear stresses for erosion and deposition of fine suspended sediments in the Fraser River. In Cohesive Sediments." *Proceedings of the 4th Nearshore and Estuarine Cohesive Sediment Transport Conference*, INTERCOH'94, Wallingford, UK, 11–15 July 1994. Edited by N. Burt, R. Parker, and J. Watts. John Wiley & Sons, Chichester,UK. Paper 21, pp. 279–288.

Krone R. B., (1962). "Flume studies of the transport of sediment in estuarial shoaling processes." Final *Report*, Hydraulic Engineering Laboratory and Sanitary Engineering Research Laboratory, University of California, Berkeley, CA, 118p.

Kuijper, C., Cornellise, J.M., Winterwerp, J.C. (1989). "Research on erosive properties of cohesive sediments". *Journal of Geophysical Research*, 94 (C10), 14,341-14,350.

Lau, Y.L., and Krishnappan, B.G. (1994). "Comparison of particle size measurements made with a water elutriation apparatus and a Malvern particle size analyzer." *NWRI Contribution 94-82*, National Water Research Institute (NWRI), Burlington, Ont.

Le Hir, P., (1994). "Fluid and sediment integrated modeling application to fluid mud flows in estuaries". *4th Nearshore and Estuarine Cohesive Sediment Transport Conference*, INTERCOH'94, Wallingford, England, 12p.

Le Roux, J. I., (2001). "A simple method to predict the threshold of particle transport under oscillatory waves". *Sedimentary Geology*, 143, 59-70.

Le Roux, J. P., (1992). "Settling velocity of spheres: a new approach". *Sedimentary Geology* 81, 11-16.

Le Roux, J. P., (1998). "Entrainment threshold for natural grains in liquids determined empirically from dimensionless settling velocities and other measurements of grain size". *Sedimentary Geology*, 199, 17-23.

Le Roux, J. P., (2003). "Wave friction factor as related to the Shield parameter for steady currents". *Sedimentary Geology*, 155, 37-43.

Lee S.-C., Mehta A. J., and Parchure T. M., (1994). "Cohesive sediment erosion". *Report UFL/COEL/MP-94/02*, Coastal and oceanographic Engineering Department, University of Florida, Gainesville, FL, 76 p.

Lee, S-C and Mehta, A.J. (1997). "Problems in Characterising Dynamics of Mud Shore Profiles". *Journal of Hydraulic Engineering*, 123 (4), 351-361.

Li H., (1954). "Stability of oscillatory laminar flow along the wall". *Beach Erosion Board*, ASCE, Technical Memo 47, 48 p.

Li Y., (1996). "Sediment associated constituent release at the mud-water interface due to monochromic waves". *Ph.D. Dissertation*, University of Florida, Gainesville, FL, 344 p.

Liu P. L. F. and Dalrymple R.A., (1976). "Bottom friction stresses and longshore currents due to waves with large angles of incidence". *Journal of Marine Research*, Vol. 36, No. 2, pp. 357-375.

Liu, P. L. F. and Mei, C. C., (1989). "Effects of wave-induced friction on a muddy seabed modelled as a Bingham-plastic fluid". *Journal of Coastal Research*, 5 (4), 777-789.

Loftquist, K. E. B. (1980). "Measurements of oscillatory drag on sand ripples". *Proceedings of the 17th Coastal Engineering Conference*, ASCE, Sydney, Australia, 3087-3106.

Longuet-Higgins, M.S., (1970). "Longshore currents generated by obliquely incident sea waves."1 and 2", *Journal of Geophysical Research*, vol. 75. pp. 6778-6789 and 6790-6801.

Maa, J.P.-Y, Sanfort, L.P., and Halka, J.P., (1998). "Sediment resuspension characteristics in Baltimore Harbour, Maryland". *Marine Geology*, 146, 137-145.

Maa, J.P.-Y, Wright, L.D., Lee, C.,-H, Shannon, T.W., (1993). VIMS Sea Carousel: a field instrument for studying sediment transport". *Marine Geology*, 115 (3/4), 271-287.

Maa, J. P.-Y. and Lee, C.-H., (1997). "Variation of the resuspension coefficients in the lower Chesapeake Bay". *Journal of Coastal Research*, S125, 63-75.

Maa, P.-Y. and Mehta, A. J., (1986). "mud erosion by waves: a laboratory study". *Continental Shelf Research*, 7 (11/12), 1267-1268.

Maa, P.-Y., (1986). "Erosion of Soft mud by waves". *Ph.D. Dissertation*, University of Florida, Gainesville, 296 p.

Macpherson, H., (1980). "The attenuation of water waves over a non-rigid bed". *Journal of Fluid Mechanics*, 97 (4), 721-742.

Mathew, J., (1992). "Wave-mud interaction in mudbanks". *Ph.D. Dissertation*, Cochin University of Science and Technology, Cochin, Kerala, India, 139 p.

McAnally, W. H. (2000). "Aggregation and deposition of fine sediment." Technical Rep. No. ERDC/CHL TR-00-8, U.S. Army Corps of Engineers Research and Development Center, Vicksburg, Miss.

McAnally, W. H., and Mehta, A. J., (2002). "Significance of Aggregation of Fine Sediment Particles in Their Deposition." *Estuarine, Coastal, and Shelf Science*, Elsevier, 54 (4), 643-653.

McAnally, W. H., Friedrichs, C., Hamilton, D., Hayter, E., Shrestha, P., Rodriguez H., Sheremet, A., Teeter A. (2007). "Management of fluid mud in estuaries, bays, and lakes. I: Present state understanding on character and behaviour". *Journal of Hydraulic Engineering*, 133 (1), 9-23.

Mehta A. J., (1978). Bed friction characteristics of three tidal entrances. *Coastal Engineering*, 2, 69-83.

Mehta A. J., (1985). "On Estuarine Cohesive Sediment Behaviour." *Journal of Geographic Research*, 94, C10, 14, 303-314.

Mehta A. J., (1988). "Laboratory studies on cohesive sediment deposition and erosion." *Physical Processes in Estuaries*, J. Dronkers and W. van Leussen, eds., Springer-Verlag, Berlin, 427-445.

Mehta A. J., (1991). "Characterization of cohesive soil bed surface erosion, with special reference to the relationship between erosion shear strength and bed density." *Report UFL/COEL/MP-91/4*, Coastal and Oceanographic Engineering Department, University of Florida, Gainesville, 83p.

Mehta A. J., (1991b). "Understanding fluid mud in dynamic environment". *Geo-Marine Letters*, 11 (3/4), 113-118.

Mehta, A.J and Li , Y., (2003). "Principles and process-modeling of cohesive sediment transport". University of Florida, Gainesville, FL. 86 pp

Mehta A. J., and Srinivas R.,(1993). "Observation on the entrainment of fluid-mud by shear flow". *Nearshore and estuarine cohesive sediment transport*, A. J. Mehta (ed.) American Geophysical Union, Washington, DC, 224-246.

Mehta A. J., Parchure T. M., Dixit J. G. and Ariathurai R. (1982). "Resuspension potential of deposited cohesive sediment beds." In: *Estuarine Comparisons. V. S. Kennedy ed., Academic Press*, New York, NY, 591-609.

Mehta, A. J. (1986). "Characterization of cohesive sediment properties and transport processes in estuaries". *Estuarine Cohesive Sediment Dynamics*, A. J. Mehta (ed.), Springer-Verlag, 290-325.

Mehta, A. J. (1989). "On estuarine cohesive sediment suspension behaviour". *Journal of Geophysical Research*, 94 (C4), 14303-14314.

Mehta, A. J. (1998). "Laboratory studies on cohesive sediment deposition and erosion." In: Dronker, J., van Leussen, W. (Eds.), *Physical Processes in Estuaries*. Springer, Berlin, pp. 427-445.

Mehta, A.J., and McAnally, W. H. (2002). "Fine-grained cohesive sediment transport." *Sedimentation engineering*, ASCE manual 54, Chapter 4, Vol. 2, ASCE, New York.

Mei, C.C., Fan, S.-J., Jin, K.-R., (1997). "Resuspension and transport of fine sediments by waves". *Journal of Geophysical Research*, 102 (C7), 15807-15821.

Miamura, N. (1993). "Rates of erosion and deposition of cohesive sediments under wave wave action". *Nearshore and estuarine cohesive sediment transport*, A. J. Mehta (ed.), American Geophysical Union, Washington, DC, 247-264.

Migniot, C., (1968). "Étude des Propriétés Physiques de Différents Sédiments Très Fins et de Leur Comportement Sous des Actions Hydrodynamiques. " La Houille Blanche, 12, 169-187.

Moore, M. J., and Long, R. R., (1971). "An experimental investigation of turbulent stratified shearing flow". *Journal of Fluid Mechanics*, 10, 496-508.

Munk W. H. and Anderson E. R., (1948). "Notes on a theory of the thermocline." *Journal of Marine Research*, 1, 276-295.

Myrhaug (1995). "Bottom friction beneath random waves". *Coastal Engineering*, 24, 259-273.

Myrhaug, (1989). "A rational approach to wave friction coefficient for rough, smooth and transitional turbulent flow". *Coastal Engineering*, 13, 11-21.

Neilson, P. (1992). "Coastal Boundary layer and sediment transpoprt". World Scientific Publishing, Singapore, Advanced Series on Ocean Engineering, vol., 4.

Nishimura, H. (1982). "Numerical simulation of wave-induced circulation". *Proc. 29th Japanese Int. Conf. on Coastal Eng.*, JSCE, pp. 333, 227.

Oveisy, A. and Soltanpor M., (2005). "Simulation of wave transformation on muddy coast". *Proceeding of 5th International Conference on Coastal Dynamics*, Barcelona, 196-197.

Overbeek, J. Th. G., (1991). "Stability of hydrophobic colloids and emulsions". *In Colloid Science, H. R. Kruyt ed.*, Elsevier, Amsterdam, 302-341.

Parchure, T.M., Mehta, A.J., (1985). "Erosion of soft sediment deposits". *Journal of Hydraulic Engineering*, 111 (10), 1308-1326.

Parker, W. R., and Kirby, R. (1982). "Time dependent properties of cohesive sediment relevant to sedimentation management –European experience". Estuarine Comparisons, V.S. Kennedy, ed., Academic, NewYork.

Partheniades, E., (1965). "Erosion and Deposition of Cohesive Soils". *Journal of Hydraulic Division*, ASCE 91 (HY1), 105-139.

Partheniades, E., (1965). "Unified view of wash load and bed material load". *Journal of Hydraulic Engineering*, 103 (9), 1037-1057.

Piedra-Cueva, I., Mory, M., (2001). "Erosion of a deposited layer of cohesive sediment". In: McAnally and Mehta (Eds.), *Coastal and Estuarine Fine Sediment Transport Processes*. Elsevier, Amesterdam, pp.41-52.

Raudkivi, A. J., (1998). "Loose Boundary Conditions." A. A. Balkema, Rotterdam, Brookfield., pp.171-312.

Ravens, T.M., Gschwend, P.M., (1999). "Flume measurements of sediment erodibility in Boston Harbout". *Journal of Hydraulic Engineering*,. ASCE 125 (10), 998-1005.

Reidel H.P., Kamphuis, J.W. and Brebner, A. (1973). "Measurement of bed shear stresses under waves". *Proceedings of 13th International Conference on Coastal Engineering*, ASCE, pp. 587-603.

Ren, R. S. and Zheng, X. C., (1986). "Experiment studies on settling velocity and rheological properties of cohesive sediment from Changjiang estuary". *Scientific Information of Hohai University*, 11, (in Chinese), 10-18.

Richardson J. F. and Zaki W. N., (1954). "The sedimentation of a suspension of uniform spheres under conditions of viscous flow." *Chemical Engineering Science*, 3, 65-72.

Roberts, J., Jepsen, R., Gotthard, D., and Lick, W. (1998). "Effects of particle size and bulk density on erosion of quartz particles". J. Hydraulic Eng. 124 (12), 1261-1268.

Ross, M. A., (1988). "Vertical structure of estuarine fine sediment suspensions". *Ph.D. Dissertation*, University of Florida, Gainesville, 206p.

Sakakiyama, T., and Bijker, E. W., (1989). "Mass transport velocity in mud layer due to progressive waves". *Journal of Waterway, Port, Coastal and Ocean Engineering*, 115 (5), 614, 633.

Sanford, L.P., and Maa, J.P.-Y, (2001) "A unified erosion formulation for fine sediments". *Marine Geology*, 179, 9-23.

Sanford, L.P. and Helka, J.P., (1993). "assessing a paradigm of mutually exclusive erosion and deposition of mud, with examples from upper Chesapeake Bay". *Marine Geology*, 114, 37-57.

Sanford, L.P., Panageotou, W., and Helka, J.P., (1991). "Tidal resuspension of sediments in northern Chesapeake Bay". *Marine Geology*, 97, 87-103.

Sawaragi, T. (1995). "Coastal Engineering Waves, Beaches, Wave Structure Interactions." *Development in Geotechnical Engineering*, 78, Amsterdam, Lausanne, New York, Oxford, Shannon, Tokyo: Elsevier, pp. 151-159.

Sawaragi, T., Deguchi, I. and Taruno, T. (1978). "Study on bottom shear stress under waves and longshore current". *Proc. 25th Japanese Int. Conf. on Coastal Eng.*, JSCE, pp. 42-45.

Scarlatos, P. D., and Mehta, A. J., (1993). "Instability and entrainment mechanisms at the stratified fluid mud-water interface". *Nearshore and estuarine cohesive sediment transport*, R. T. Cheng (ed.), Springer-Verlag, New York, 321-332.

SFWMD. (2004). "Indian river lagoon restoration feasibility study". South Florida Water Management District, http://www.sfwmd.gov/org/wrp/wrp_ce/projects/muck.html.

Schlichting, H., (1968). "Boundary layer theory". McGraw-Hill, 6th ed. New York.

Sheikh, A., Ruff, J. F., and Abt, S., R., (1988). "Erosion rate of compacted Na-montmorillonite soils". *Journal of Geotechnical Engineering*, 114 (3), 296-305

Sheng Y. P., (1986). "Modeling bottom boundary layer and cohesive sediment dynamics in estuarine and coastal waters". *Estuarine cohesive sediment dynamics*, A. J. Mehta (ed.), Springer-Verlag, Berlin, 360-400.

Sheremet, A. and Stone, G.W. (2003). "Observations of nearshore wave dissipation over muddy sea beds". *Journal of Geophysical Research*, Vol 108 (C11), 3357, doi: 10.1029/2003JC001885.

Sheremet, A., (2006). Personal communication.

Sheremet, A., Mehta, A.J., Liu, B., and Stone G.W., (2005). "Wave-sediment interaction on a muddy inner shelf during Hurricane Claudette". *Estuarine, Coastal and Shelf Science* 63, 225-233.

Shibayama, T., Okuno, M., and Sato, S., (1990). "Mud transport in mud layer due to waves: a viscoplastic model". *Proceedigs of the 22nd Coastal Engineering Conference*, ASEC, New York, 3, 3037-3049.

Shybayama, T., Takikawa, H., and Horikawa, K., (1986). "Mud mass transport due to waves". *Coastal Engineering in Japan*, 29, 151-161.

Sisko A. W., (1958). "The flow of lubricating greases". *Industrial Engineering Chem.*, 50, 1789-1792.

Soltanpour, M., T. Shibayama and T. Noma, (2003). "Cross-Shore Mud Transport and Beach Deformation Model." *Coastal Engineering Journal*, JSCE, 45(3), 363-386.

Soulsby R.L., Hamm, L., Klopman, G., Myrhaung, D., Simons, R.R. and Thomas, G.P., (1993). "Wave-current interaction within and outside bottom boundary layer". *Coastal Engineering*, Elsevier, 21, 41-69

Soulsby, R.L., (1997). "Dynamics of Marine sands". *A manual for practical applications*. Tomas Telford, London.

Srinivas R., and Mehta, A. J. (1989). "Observations on estuarine fluid mud entrainment". *International Journal of Sedimentary Research*, 5 (1), 15-22.

Stone, G. W., Zhang, X.P., Gibson, W., and Fredericks, R. A., (2001). " New Wave-current On-line Information System for Oil Spill Contingency Planning (WAVCIS)". *Proceedings of the 24th Arctic and Marine Oilspill Program Technical Seminar*, Edmonton, Alberta, Canada, pp. 410-425.

Suhayda, J.N., (1986). "Interaction between surface waves and muddy bottom sediments". In: *Estuarine cohesive sediment dynamics*, A. J. Mehta (ed.), Springer-Verlag, Berlin, 401-428.

Swart, D.H., (1974). "Offshore sediment transport and equilibrium beach profiles". Delft Hydraulic Laboratory publication, 131 pp.

Taki, K. (1986). "Rheological behaviour on high density mud ". *Proceedings of the 30th Japanese Conference on Hydraulics*, Japanese Society of Civil Engineers, Tokyo, 475-498.

Taki, K. (1990). "Hydraulic study on the rate of resuspension of mud due to free surface water flow". *Ph. D. Thesis*, Chuo University, Tokyo, 180p. (in Japanese).

Taki, K., (1991) "Critical shear stress on cohesive mud particles in river". *Proceedings of the 3rd IAWPRC Conference Asian Waterqual'91*, Development and Water Pollution Control, F. Wang, T. Deng, and X., Li eds., IAWPRC, Shanghai, China, V71-V76.

Taki, K., (2001). "Critical Shear Stress For Cohesive Sediment Transport." *Coastal and Estuarine Fine Sediment Processes*, McAnally and Mehta eds., Elsevier, Amsterdam, Boston, Heidelberg, London, New York, Oxford, Paris, San Diego, San Francisco, Singapore, Sydney, Tokyo., pp. 53-61.

Teleki P.G., and Anderson, M. W. (1970). "Bottom boundary shear stress on a model beach". *Proc. 12th Conf. on Coastal Engr.*, Washington, D.C., 269-288.

Teeter, A. M., Fagerburg, T., Walker, T., Benson, H., Brister, D., and McAdory, R. (2003). Factors affecting fluff and fluid mud accumulation in the Atchafalaya bar channel. U.S. Army Corps of Engineers Research and Development Center, Vicksburg, Miss.

Thorn, M.F.C. (1981). "Physical processes of siltation in tidal channels", *Proc. Hydraulic Modeling Applied to Maritime Engineering Problems*, I. C. E., London, 47-55.

Thorn, M.F.C. and Parsons, J.G. (1980). "Erosion of cohesive sediments in estuaries: An Engineering guide". In Proc. Third Intl. Conf. on Dredging Tech., Ed. H. S. Stephens BHRA, Bordeaux, France, 349-358.

Tolhurst, T.J., Black, K.S., Paterson, D.M., Mitchener, H.J., Termaat, G.R., Shayler, S.A., (2000a). A comparison and measurement standarization of four in situ devices for determining the erosion shear stress of intertidal sediments". *Continental Shelf Research*, 20 (10-11), 1397-1418.

Tolhurst, T.J., Riehmuller, R., Paterson, D.M., (2001b). "In situ versus laboratory analysis of sediment stability from intertidal mudflats". *Continental Shelf Research,* 20 (10-11), 1317-1334.

Torfs, H. (1997). "Erosion of mixed cohesive/non-cohesive sediments in uniform flow. In Cohesive Sediments." *Proceedings of the 4th Nearshore and Estuarine Cohesive Sediment Transport Conference*, INTERCOH'94, Wallingford, UK, 11–15 July 1994.

Edited by N. Burt, R. Parker, and J. Watts. John Wiley & Sons,Chichester, UK. Paper 16, pp. 245–252.

U.S. Army Corps of Engineers, (2002), "CEM: Coastal Engineering Manual." Chapter 3, [Cited April 19, 2006] Available from the World Wide Web: http://users.coastal.ufl.edu/~sheppard/eoc6430/Coastal_Engineering_Manual.htm.

van Leussen, W. (1988). "Aggregation of Particles, Settling Velocity of Mud Flocs. in Physical Processes in Estuaries." Edited by J. Dronkers and W. van Leussen. Springer-Verlag, New York.

van Leussen, W., and Winterwerp, J.C., (1990). "Laboratory experiments on sedimentation of fine-grained sediments: a state-of-the-art review in the light of experiments with the Delft tidal flume". In: Cheng, R.T., Barber, R.T., Moores, C.N.K., Raven, J.A. (Eds.), *Residual Currents and Long-term Transport.* Coastal and Estuarine Studies. Springer, New York, pp. 241-259.

Van Rijn, L. C. (1989). "Handbool Sediment Transport By Currents and Waves." Delf Hydraulics, Rept. H. 461, 12.1-12.24.

Vanoni V. A. ed., (1975). "Sedimentation Engineering." American Society of Civil Engineers, New York, 761p.

Walker, N.D., and Hammack, A.B., Impact of winter storms on circulation and sediment transport: Atchafalaya-Vermillion Bay region, Louisiana, USA". *Journal of Coastal Research*, 16, 996-1010.

Whitehouse, R., Soulsby, R.R., Roberts, W., Mitchener, H., (2000). "Dynamics of Estuarine Muds." H. R. Wallingford, UK, 210p.

Wilkinson, W. L. (1960). "Non-Newtonian fluid: Fluid mechanics, Mixing and Heat transfer". Pergamon Press, New York, 152p.

Williams D. J. A., and Williams, P. R., (1992). "Laboratory experiments on cohesive soil be fluidization by water waves, Part II: In-situ rheometry for determining dynamic response of bed. *Report UFL/COEL-92-015*, Coastal and Oceanographic Engineering Department, University of Florida, Gainesville, FL, 28p.

Willis, D. H., and Krishnappan B. G., (2004), "Numerical Modeling of Cohesive Sediment Transport in Rivers." *Canadian Journal of Civil Engineering,* NRC Canada, 31(5), 749-758.

Willis, D., H., and Krishnappan, B., G., (2004). "Numerical modeling of cohesive sediment transport in rivers". *Canadian Journal of Civil Engineering,* 31: 749-758.

Winterwerp, J., C. and van Kesteren, W., G.M., (2004). "Introduction to the physics of Cohesive sediment in the marine environment". *Development in sedimentology*, vol. 56, T. van Loon (ed.), Elsevier, p.462.

Winterwerp, J., C., (1994), "On the erosion of fluid mud layers by entrainment". *4th Nearshore and Estuarine Cohesive Sediment Transport Conference*, INTERCOH'94, Wallingford, England, 11p.

Wolanski E. J., Gibbes, R. J., Mazda, Y., Mehta, A. J., and King, B., (1992). "The role of turbulence in settling of mud flocs". *Journal of Coastal Research*, 8(1), 35-46.

Wolanski, E. J., Chappel, P. R., and Bertessy, R., (1988). "Fluidization of mud in estuaries". *Journal of Geophysical Research*, 8 (1), 35-46.

Wolanskim, E. J., Chappel, P. R., and Bertessy, R., (1988). "Fluidization of mud in estuaries". *Journal of Geophysical Research*, 93(C3), 2351-2361.

Wright, L. D., Sherwood, C. R., and Sternberg, R. W., (1997). "Field measurements of fair-weather bottom boundary layer processes and sediment suspension on Louisiana inner continental shelf". *Marine Geology*, 140, 245-329.

You, Z. J., (2004). "The Effect of Suspended Sediment Concentration on the Settling Velocity of Cohesive Sediment in Quiescent Water." *Ocean Engineering*, Elsevier, 31, 1955-1965.

Young, R.N., Southard, J.B., (1978). "Erosion of fine-grained marine sediments: sea-floor and laboratory experiments". *Geol. Soc. Am. Bull.*, 89, 663-672.

Zreik, D.A., Krishnappan, B.G., Germaine, J.T., Madson, O.S., Ladd, C.C., (1998). "Erosional and mechanical strength of deposited cohesive sediments". *Journal of Hydraulic Engineering*, 124 (11), 1076-1085.

APPENDICES

A- Simulated and experimental suspended sediment concentration profiles

A.1- Comparison between numerical model and lab data of Maa (1986)

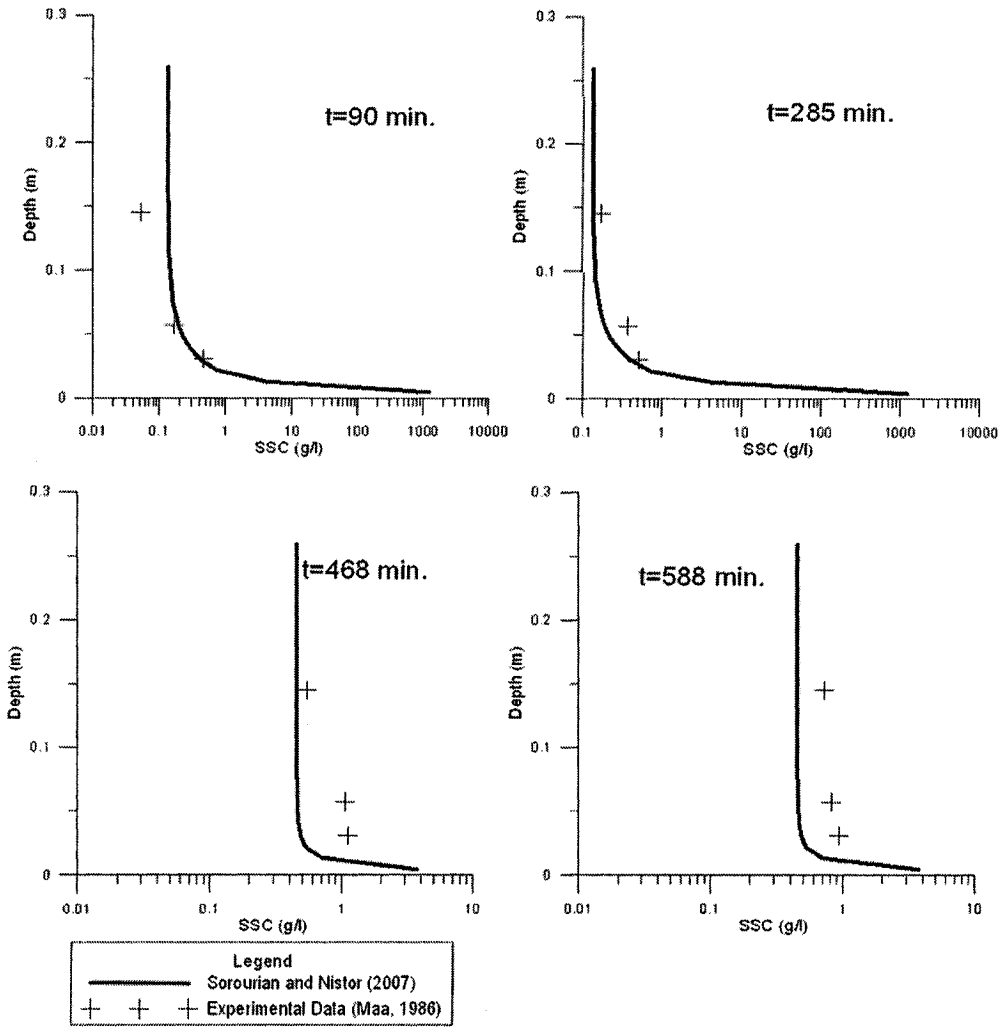

Figure A.01 Comparison of the numerical model results with laboratory data - Run 4 of the data of Maa (1986) - Model modified for including electrochemical particle resistance.

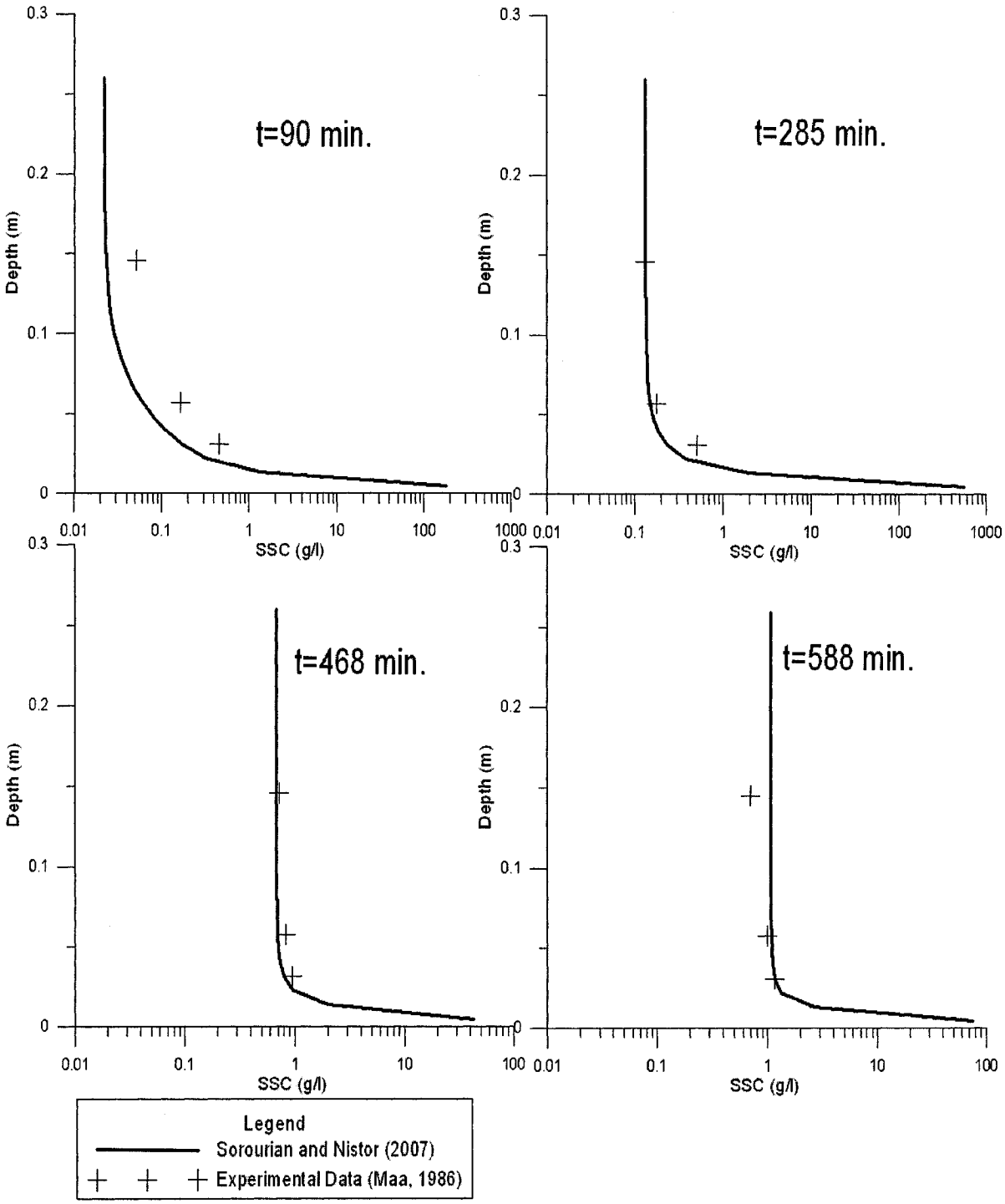

Figure A.2 Comparison of the numerical model results with laboratory data - Run 4 of the data of Maa (1986) - Model including the concept of the vane shear strength.

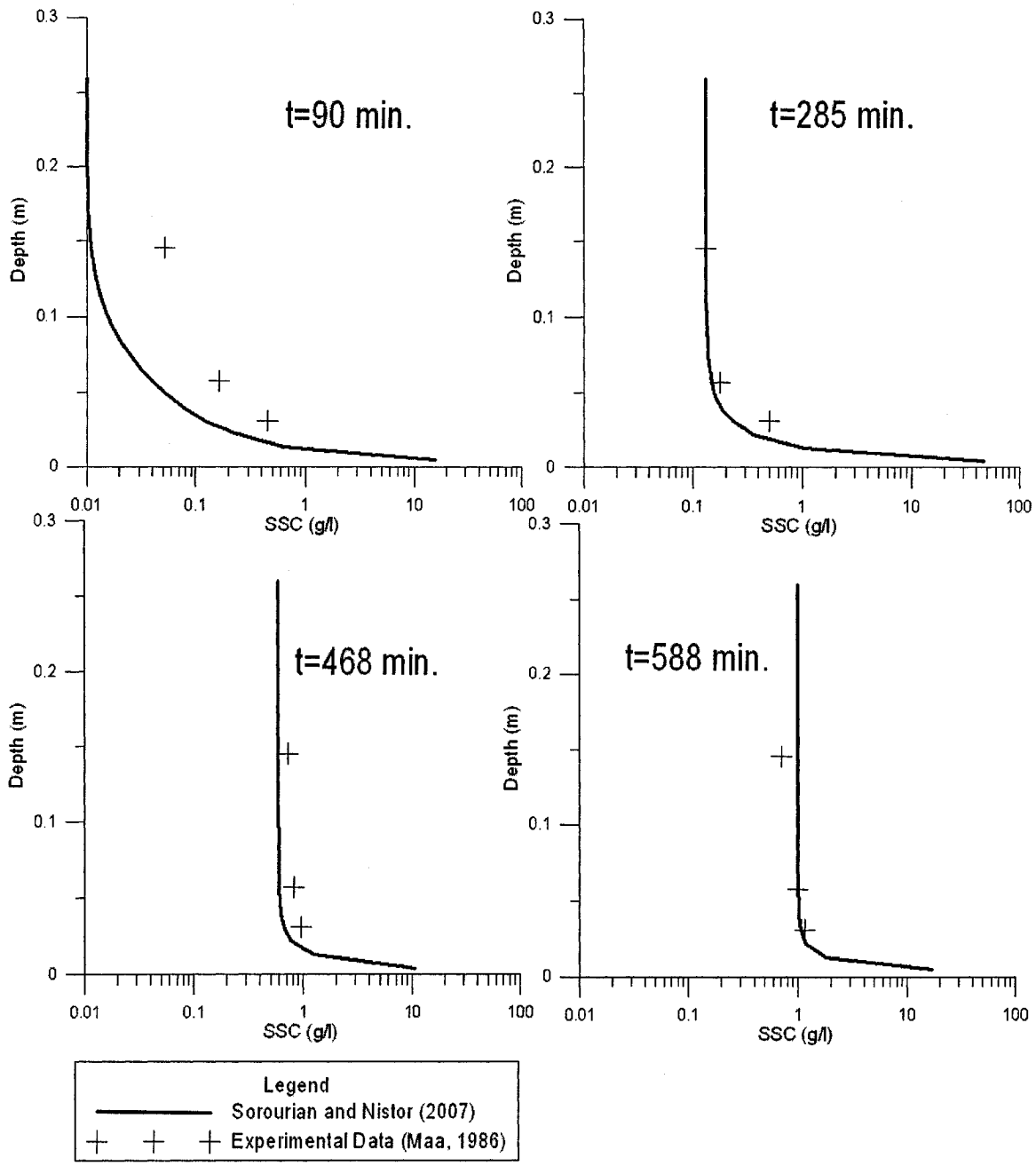

Figure A.3 Comparison of the numerical model results with laboratory data - Run 4 of the data of Maa (1986) - Model incorporating the wave friction factor using the formula of Jonsson (1963).

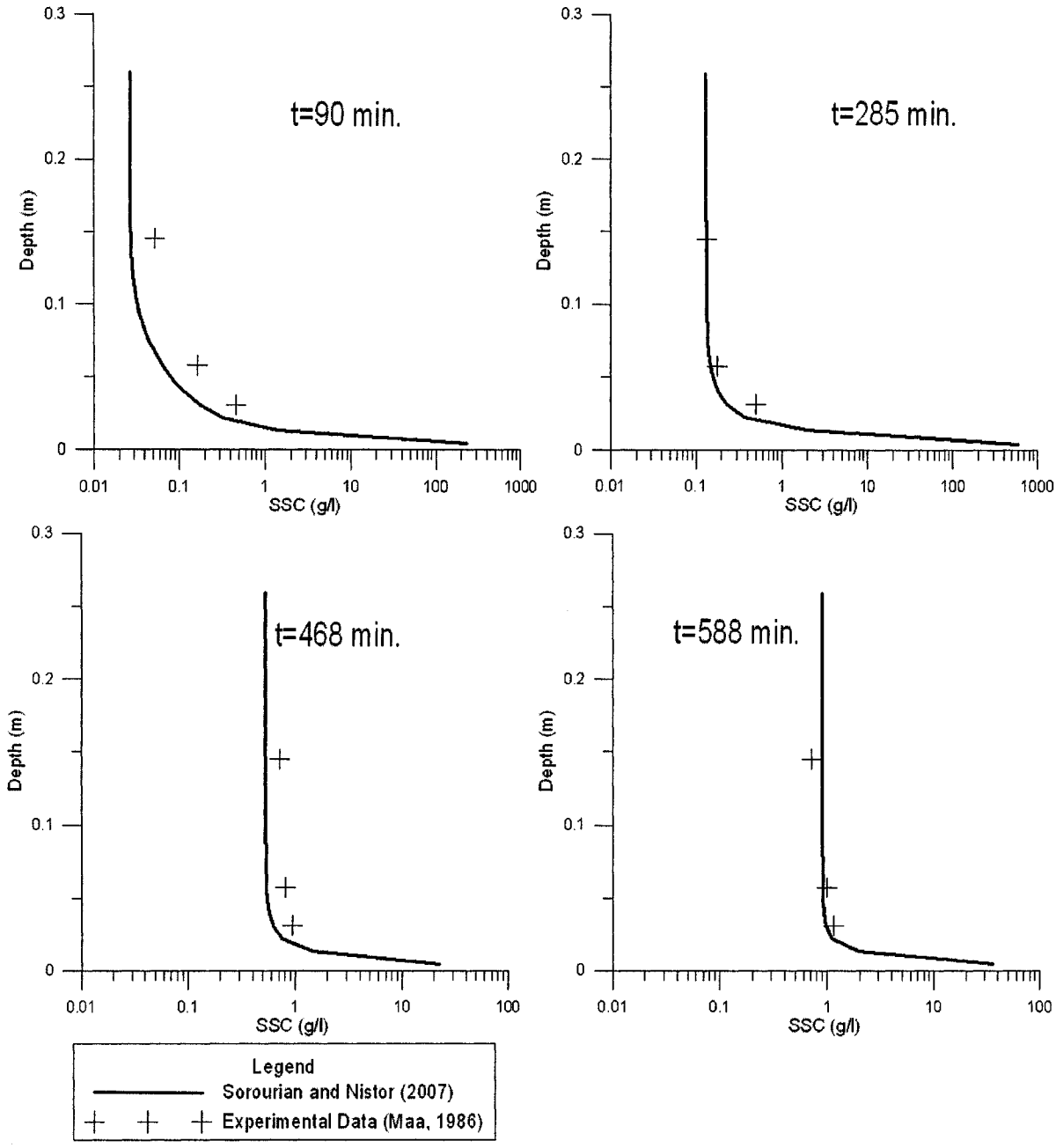

Figure A.4 Comparison of the numerical model results with laboratory data - Run 4 of the data of Maa (1986) - Model incorporating the wave friction factor using the formula of Swart (1974).

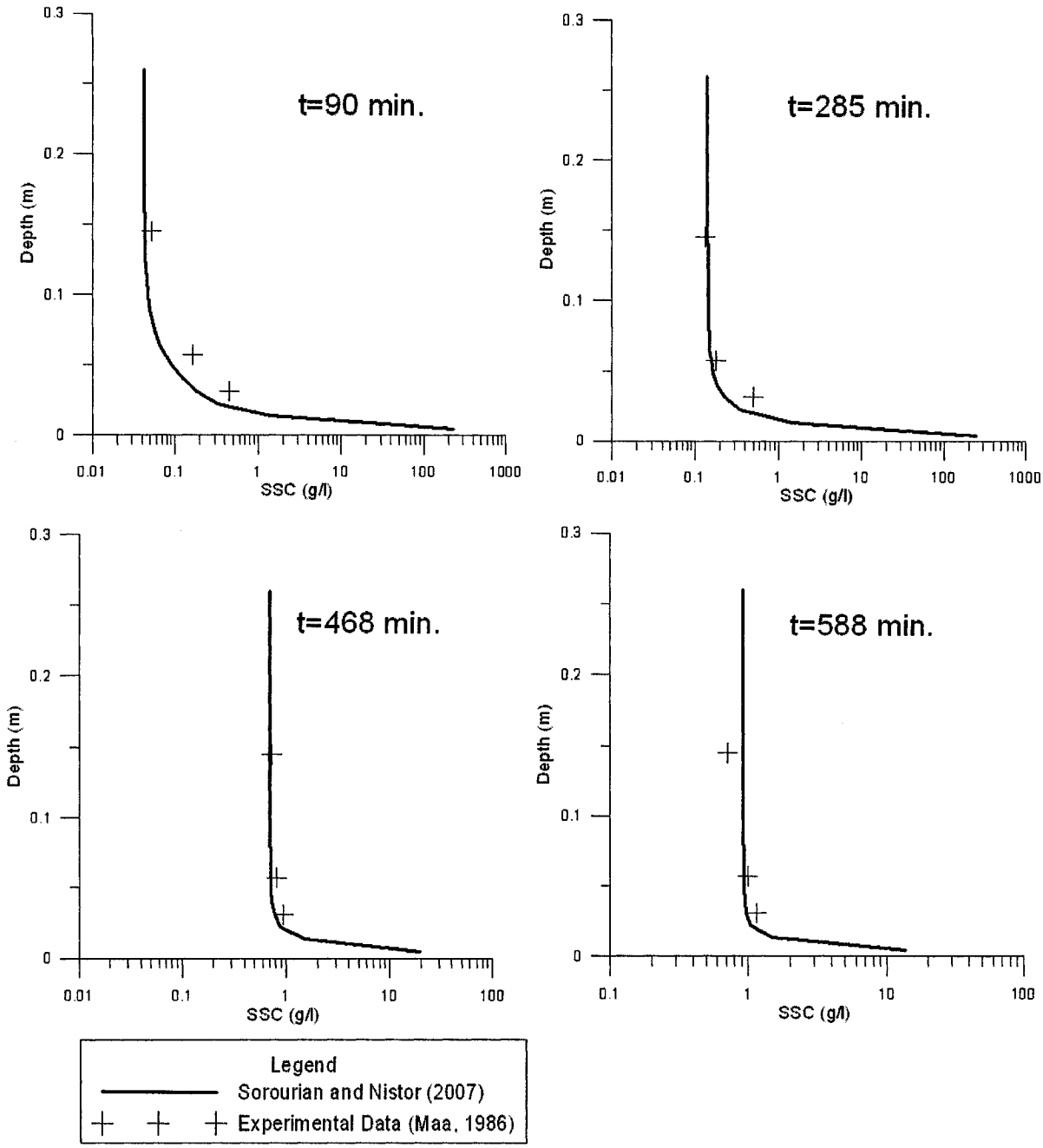

Figure A.5 Comparison of the numerical model results with laboratory data - Run 4 of the data of Maa (1986) - Model incorporating the wave friction factor using the formula of Le Roux (2003).

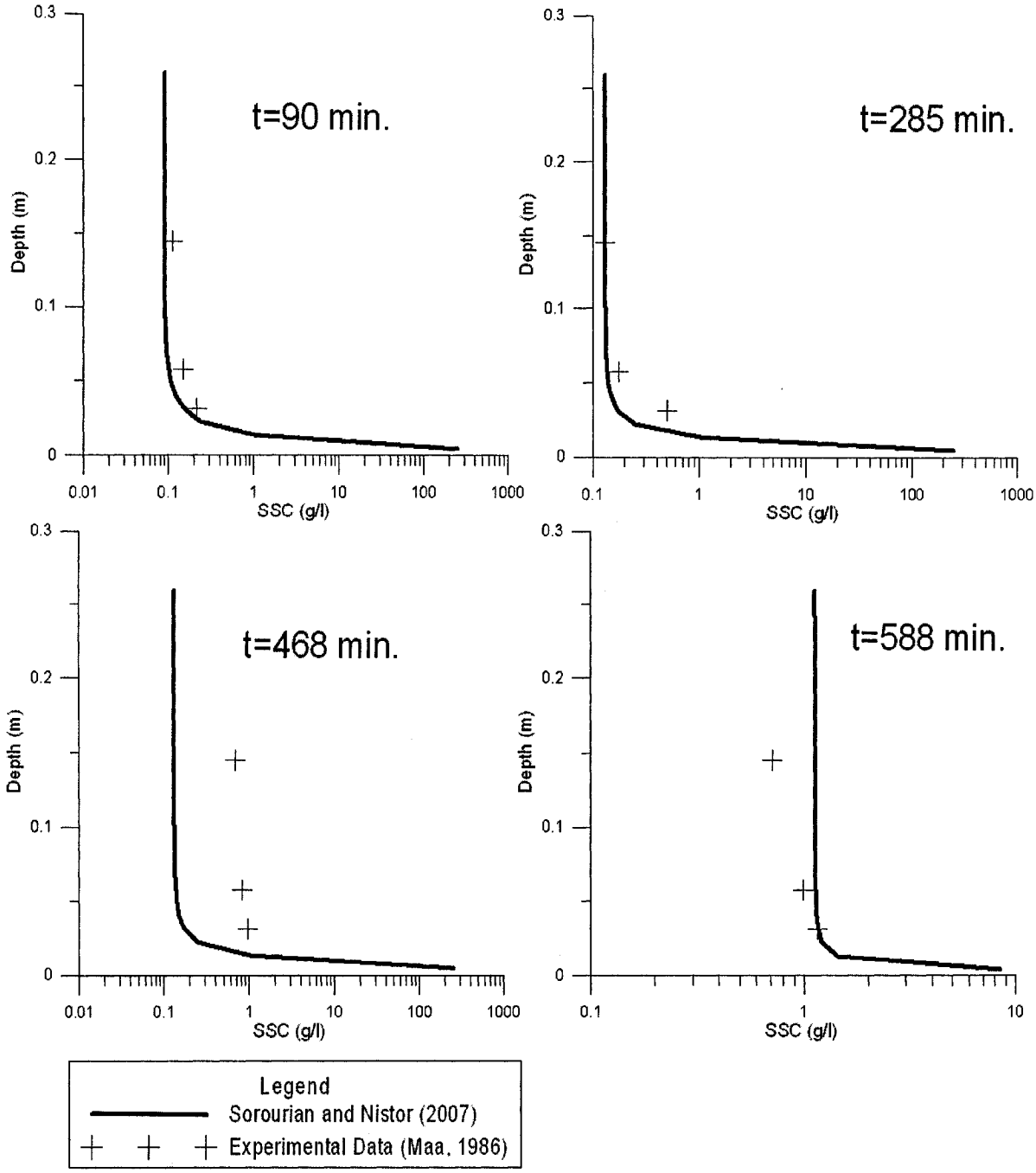

Figure A.6 Comparison of the numerical model results with laboratory data - Run 4 of the data of Maa (1986) - Model incorporating time-dependent erosion rate.

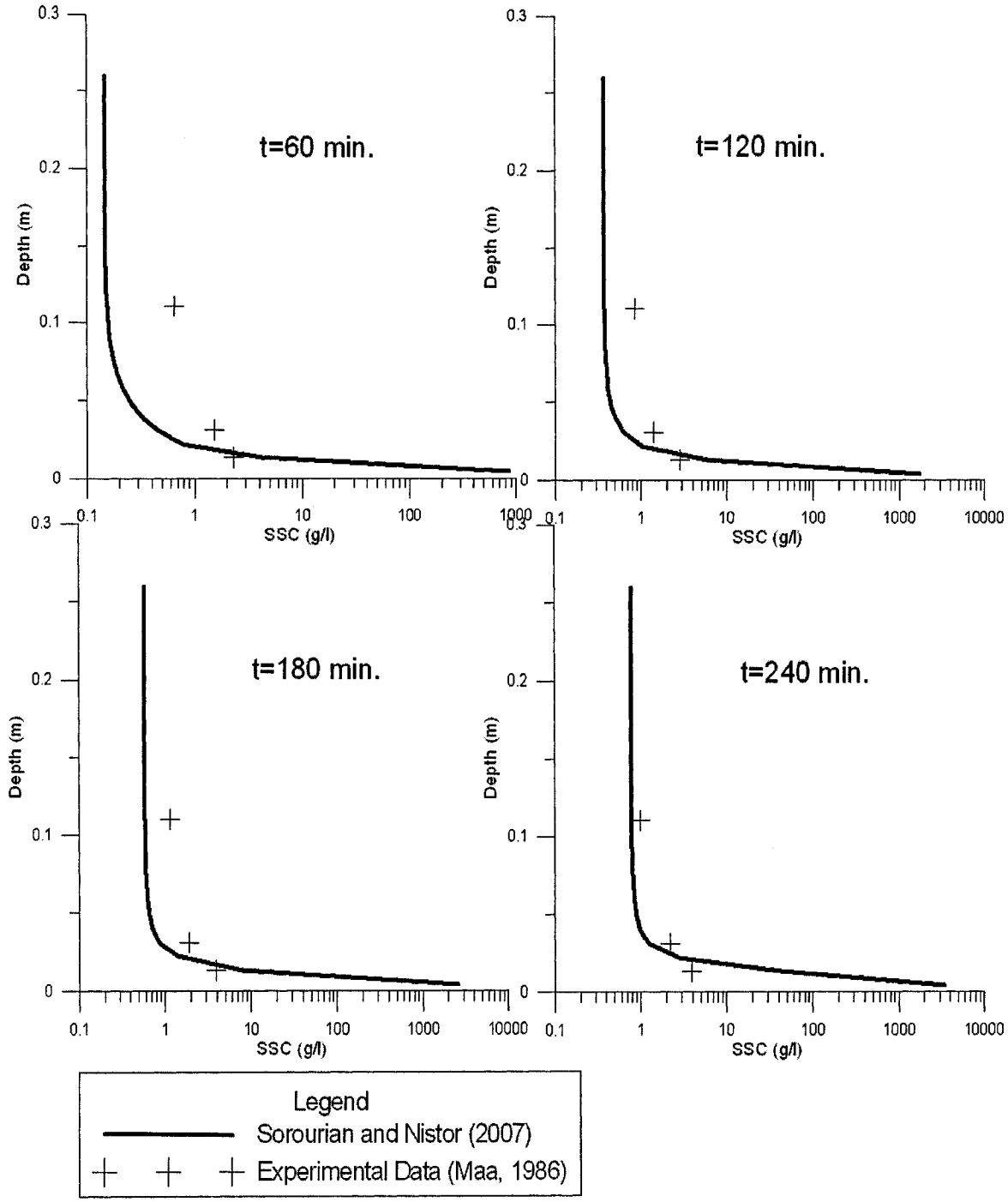

Figure A.7 Comparison of the numerical model results with laboratory data - Run 5 of the data of Maa (1986) - Model modified for including electrochemical resistance.

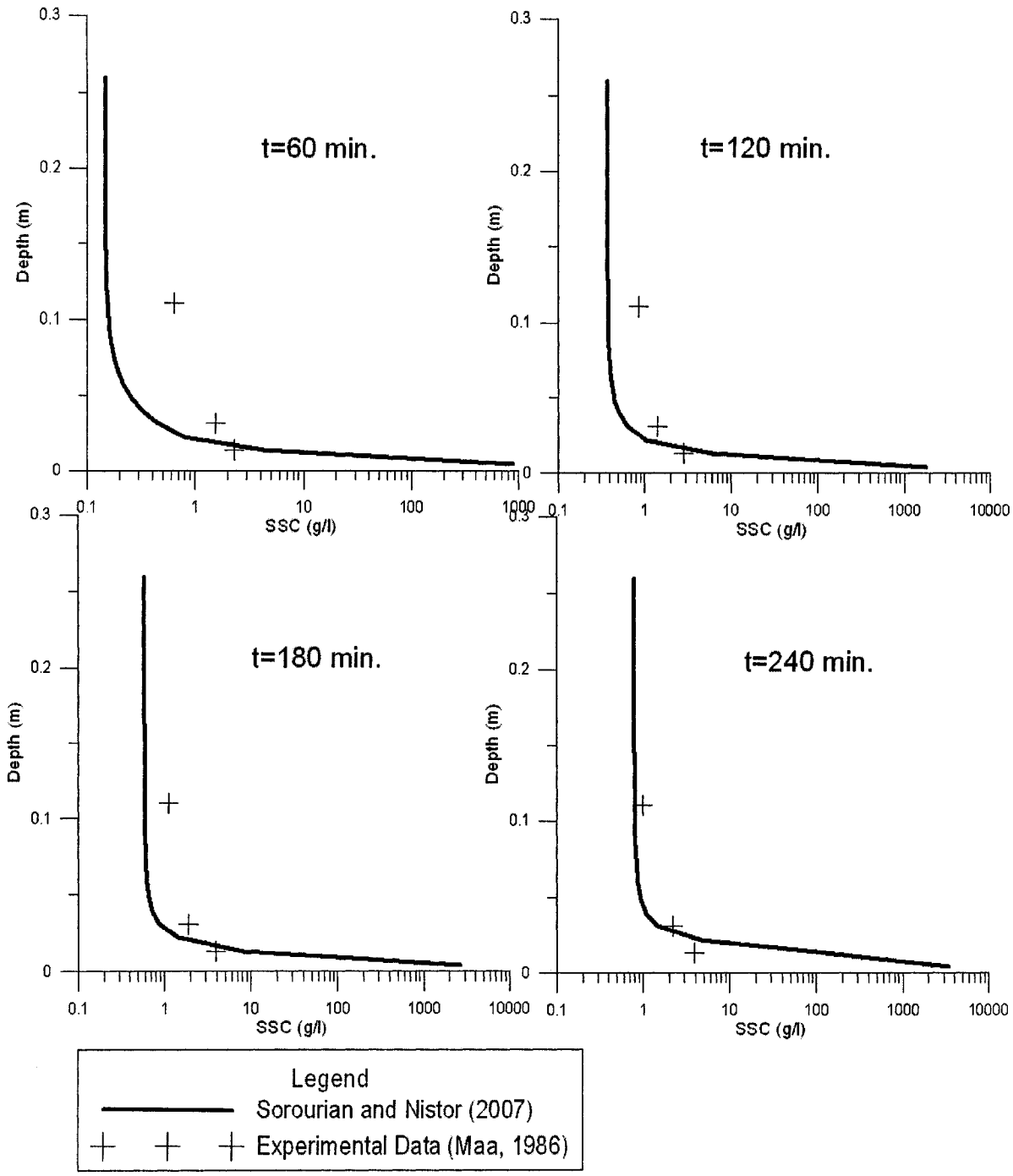

Figure A.8 Comparison of the numerical model results with laboratory data - Run 5 of the data of Maa (1986) - Model including the concept of the vane shear strength.

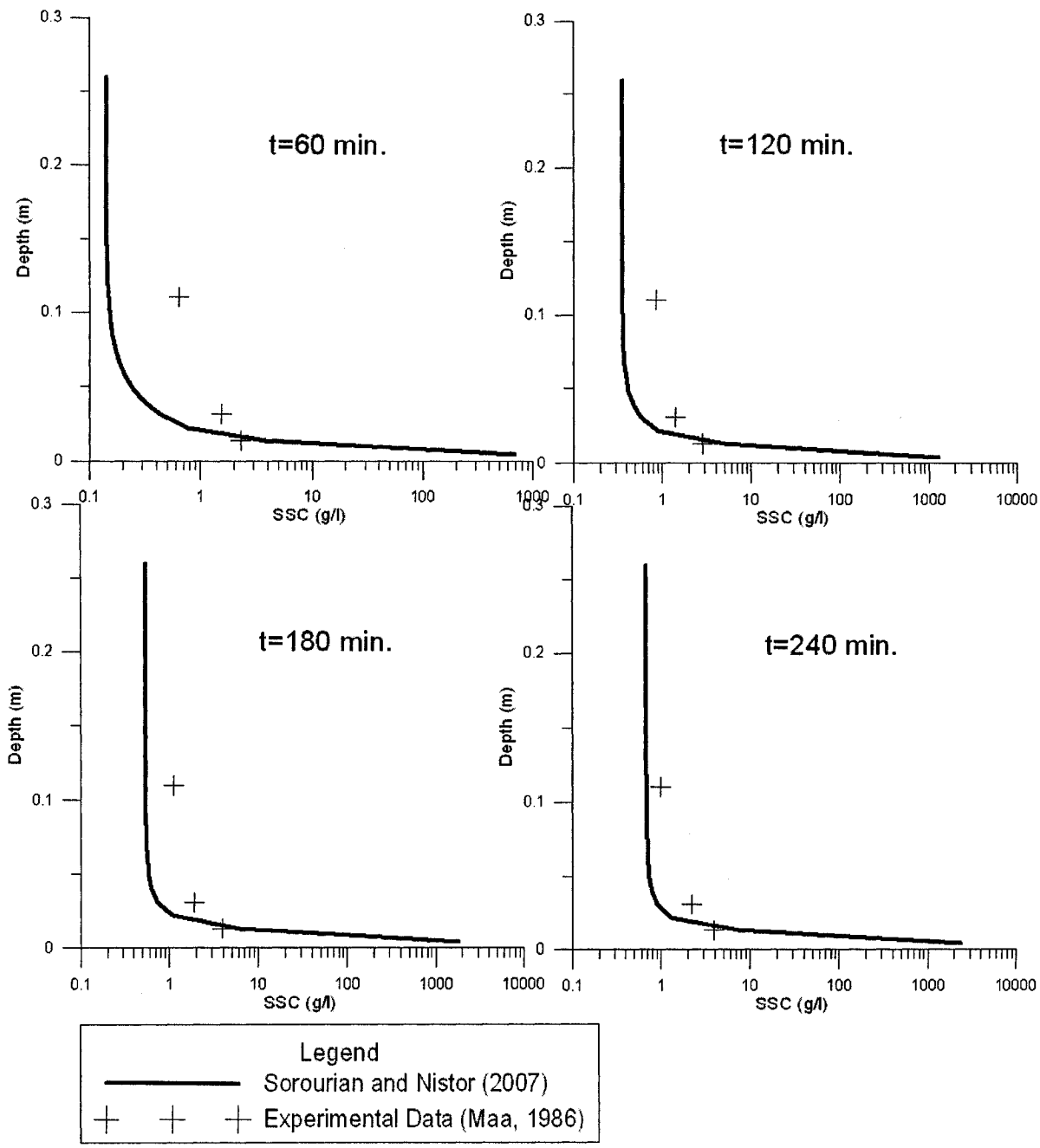

Figure A.9 Comparison of the numerical model results with laboratory data - Run 5 of the data of Maa (1986) - Model incorporating the wave friction factor using the formula of Jonsson (1963).

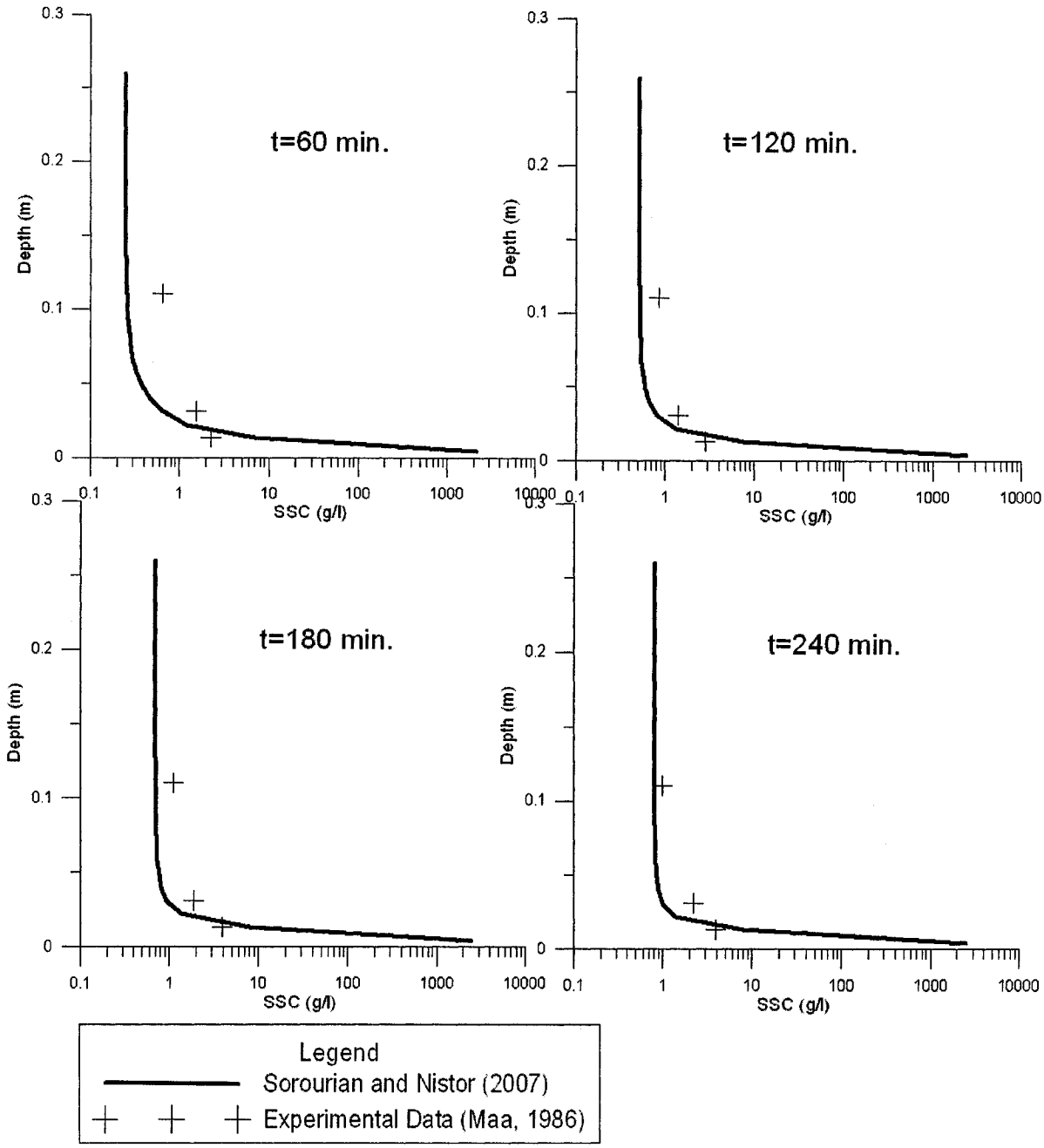

Figure A.10 Comparison of the numerical model results with laboratory data - Run 5 of the data of Maa (1986) - Model incorporating the wave friction factor using the formula of Swart (1974).

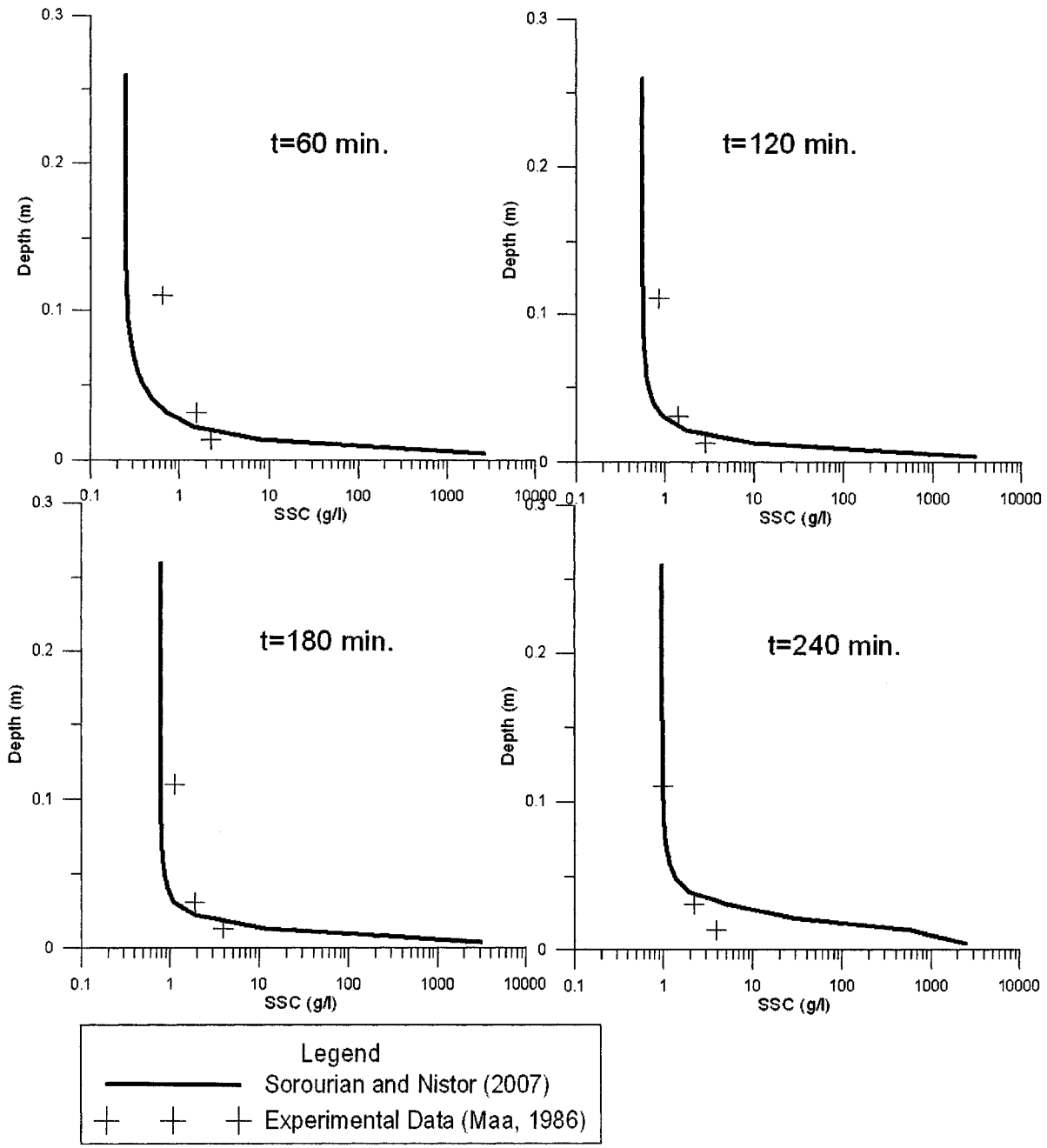

Figure A.11 Comparison of the numerical model results with laboratory data - Run 5 of the data of Maa (1986) - Model incorporating the wave friction factor using the formula of Le Roux (2003).

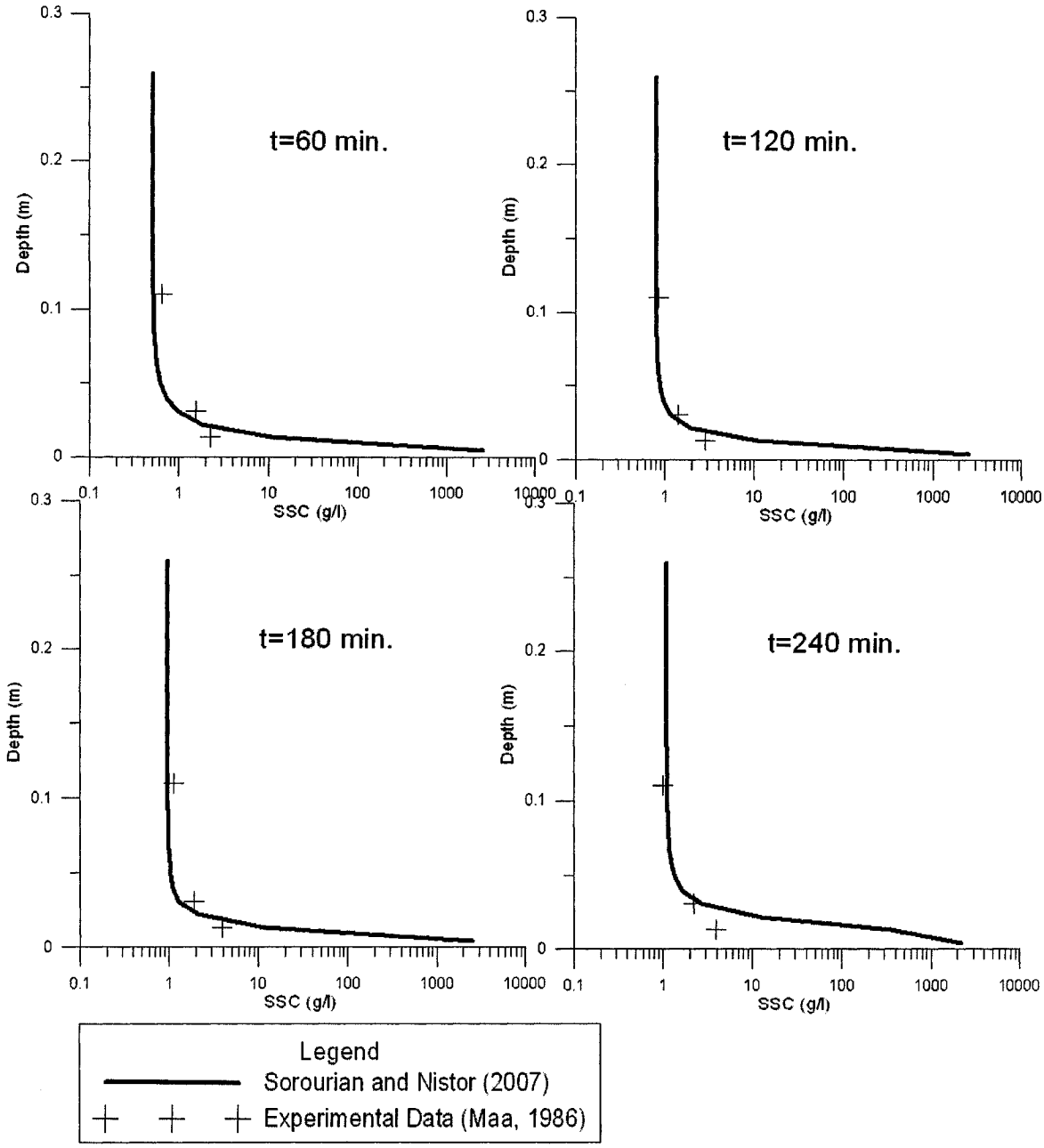

Figure A.12 Comparison of the numerical model results with laboratory data - Run 5 of the data of Maa (1986) - Model incorporating time-dependent erosion rate.

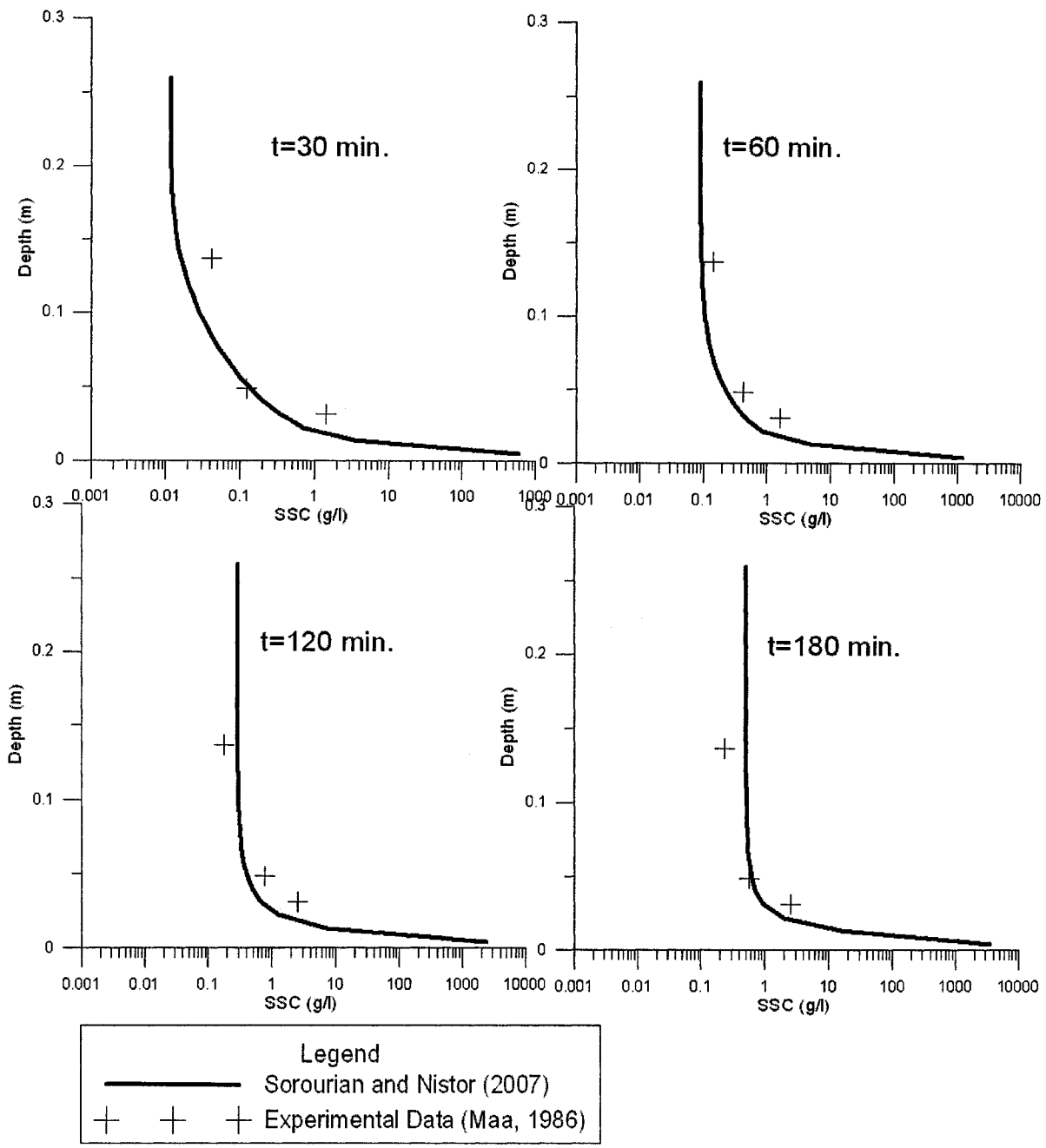

Figure A.13 Comparison of the numerical model results with laboratory data - Run 6 of the data of Maa (1986) - Model modified for including electrochemical resistance.

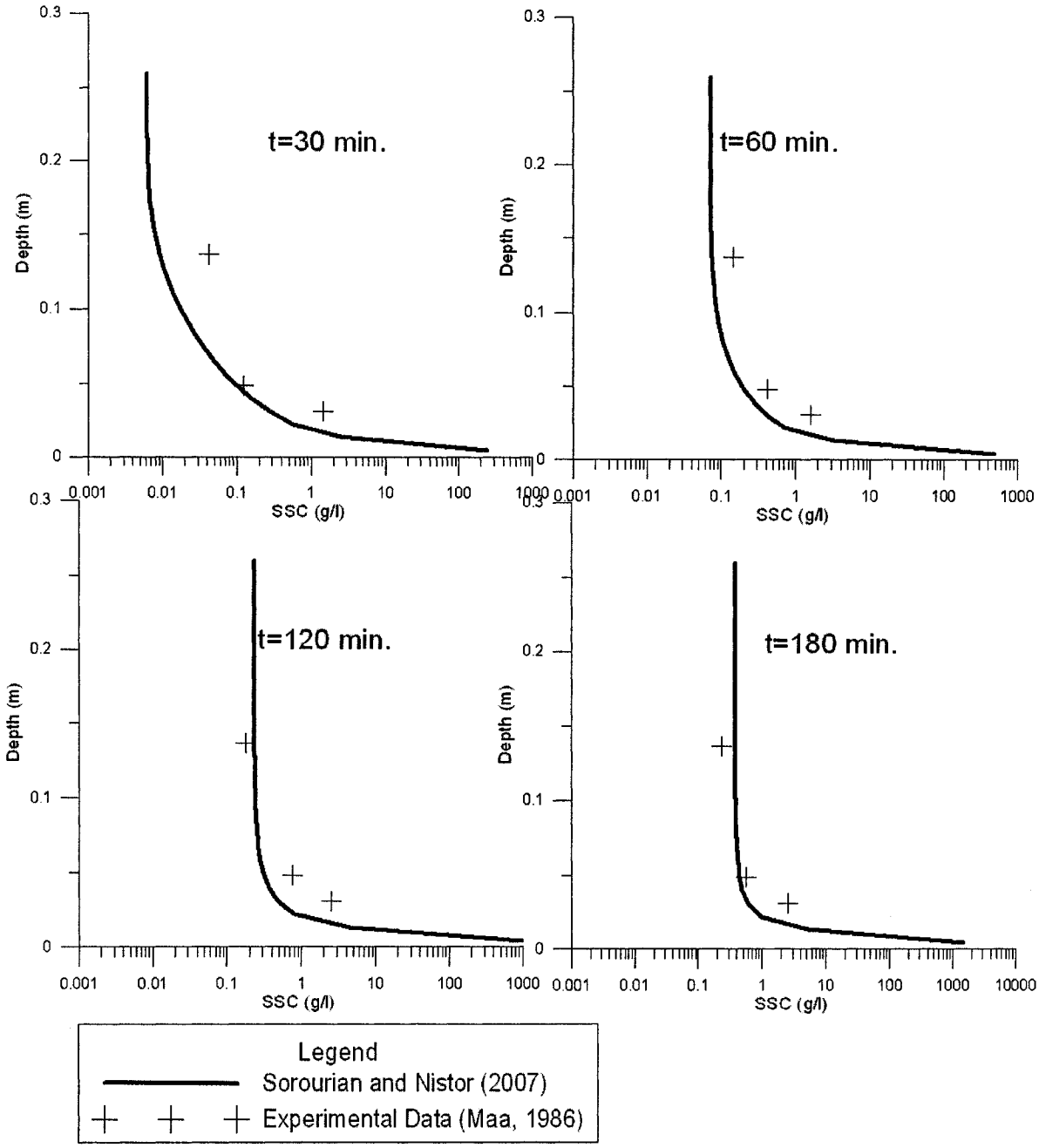

Figure A.14 Comparison of the numerical model results with laboratory data - Run 6 of the data of Maa (1986) - Model including the concept of the vane shear strength.

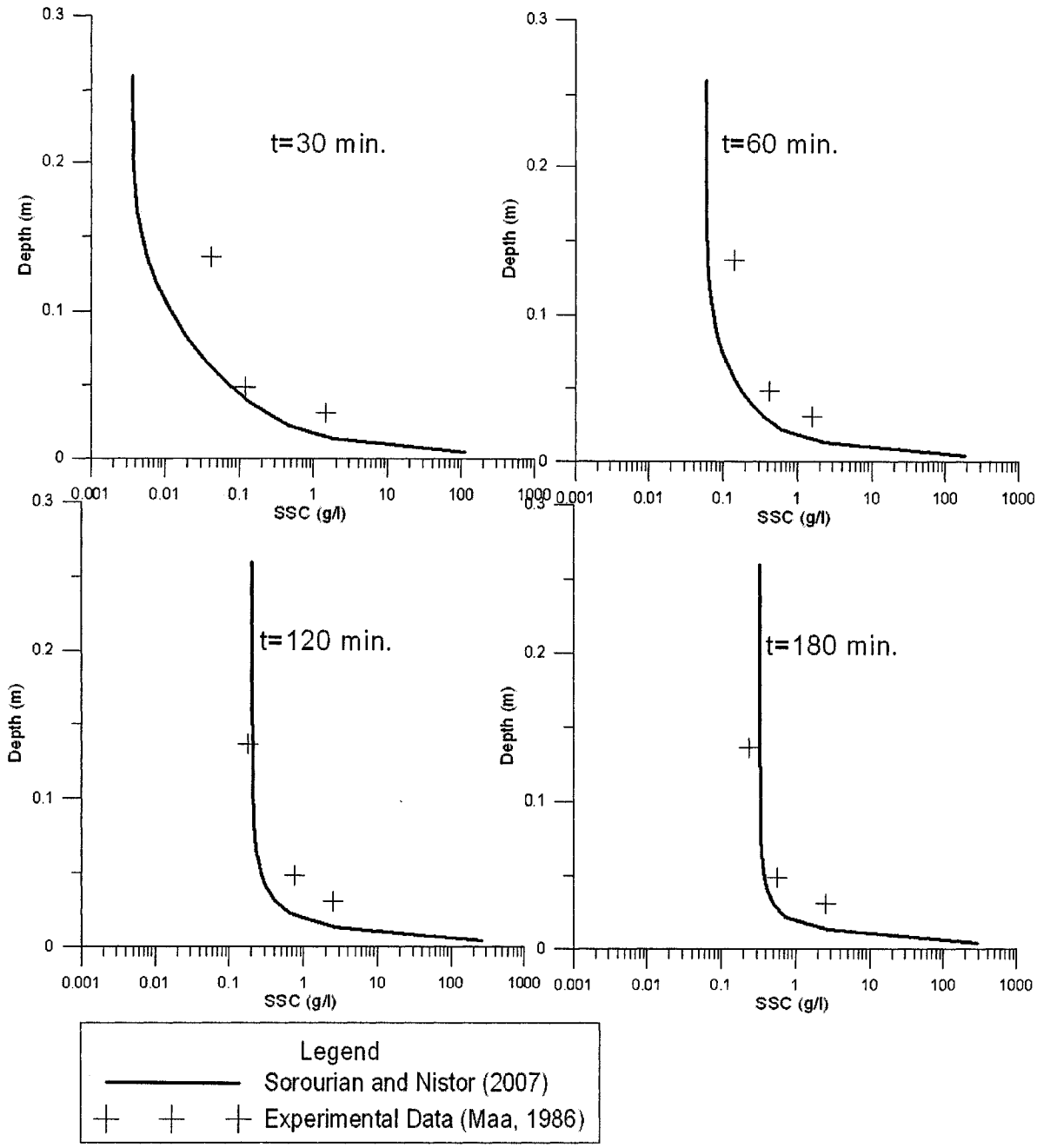

Figure A.15 Comparison of the numerical model results with laboratory data - Run 6 of the data of Maa (1986) - Model incorporating the wave friction factor using the formula of Jonsson (1963).

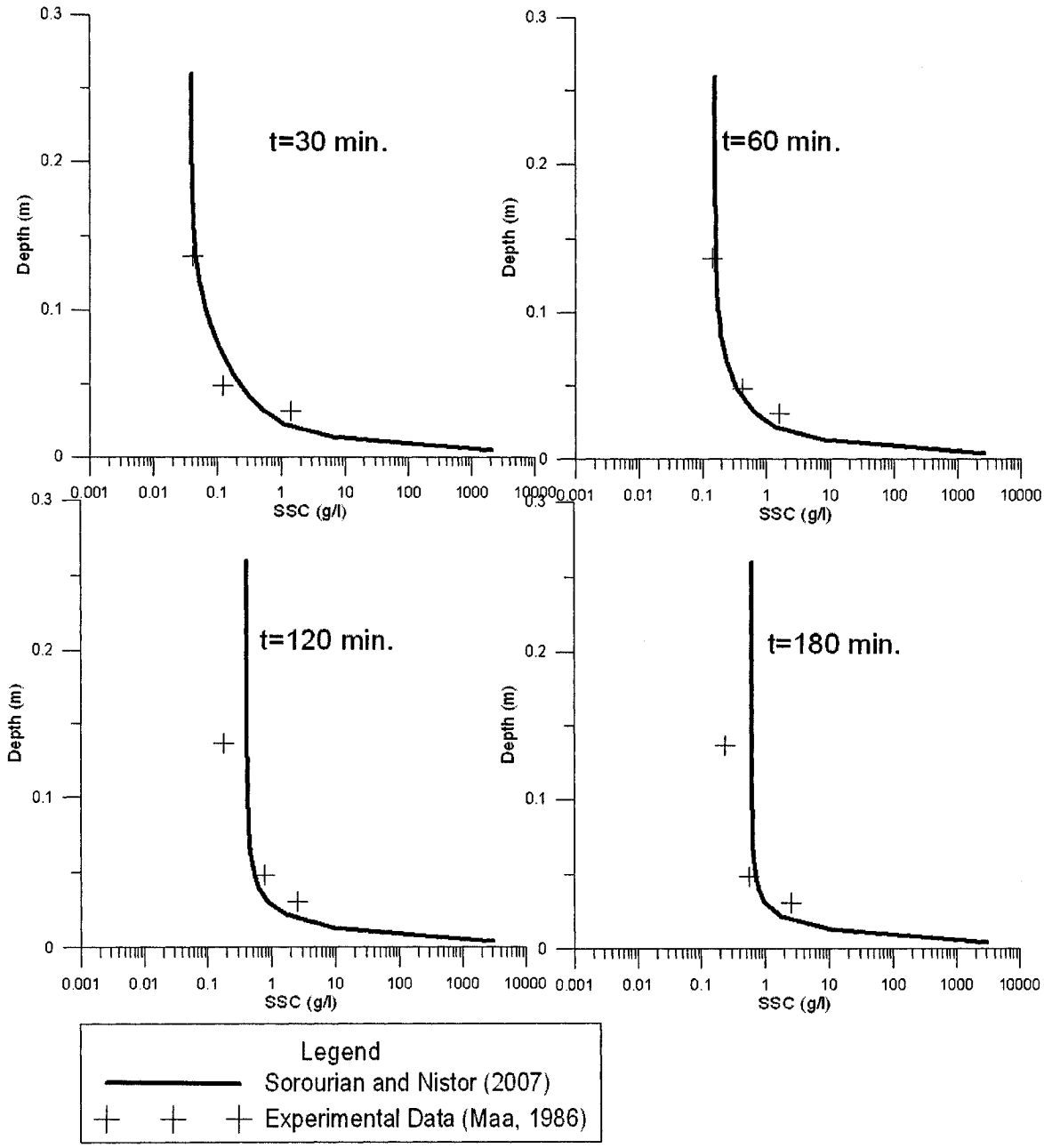

Figure A.16 Comparison of the numerical model results with laboratory data - Run 6 of the data of Maa (1986) - Model incorporating the wave friction factor using the formula of Swart (1974).

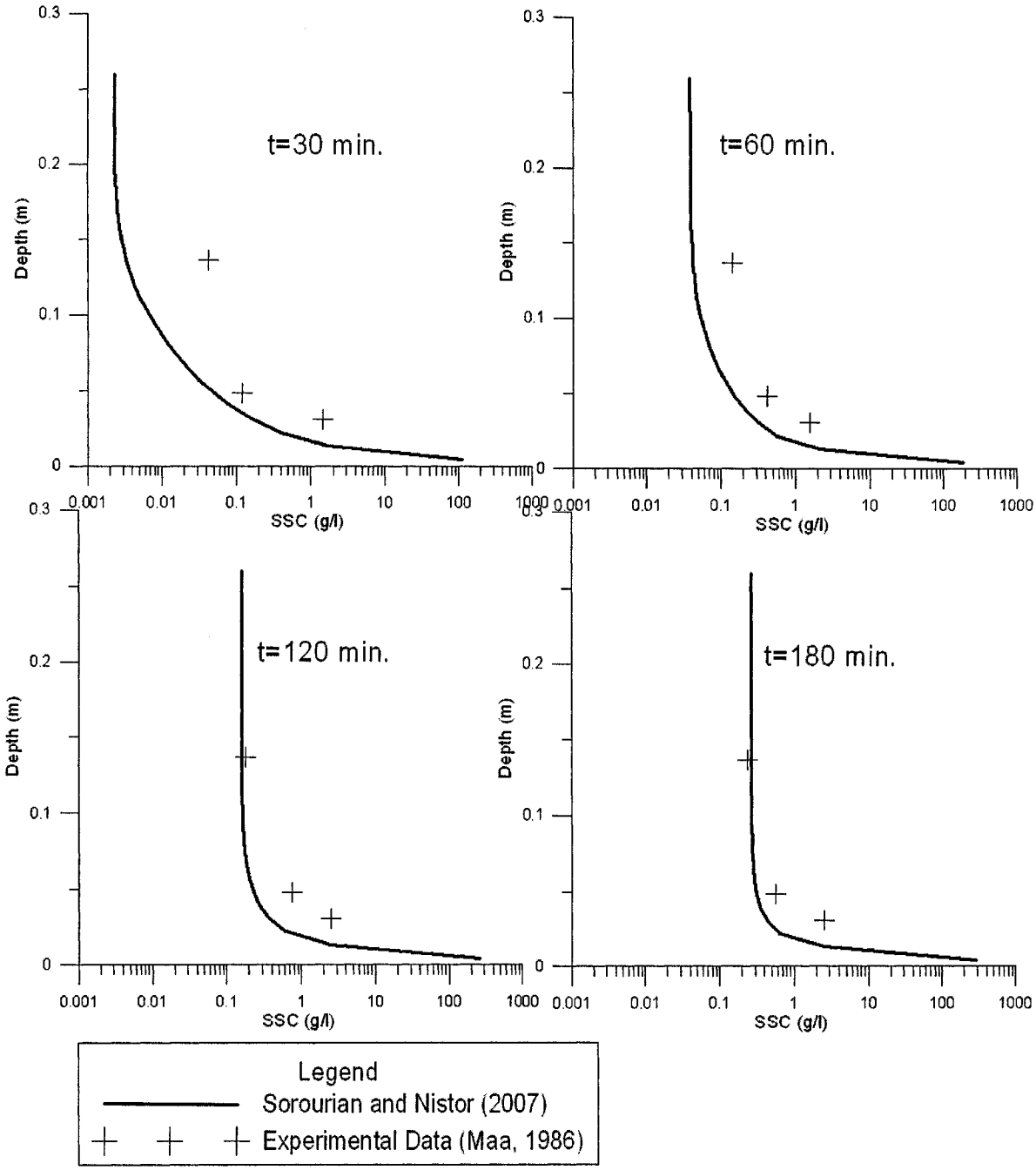

Figure A.17 Comparison of the numerical model results with laboratory data - Run 6 of the data of Maa (1986) - Model incorporating the wave friction factor using the formula of Le Roux (2003).

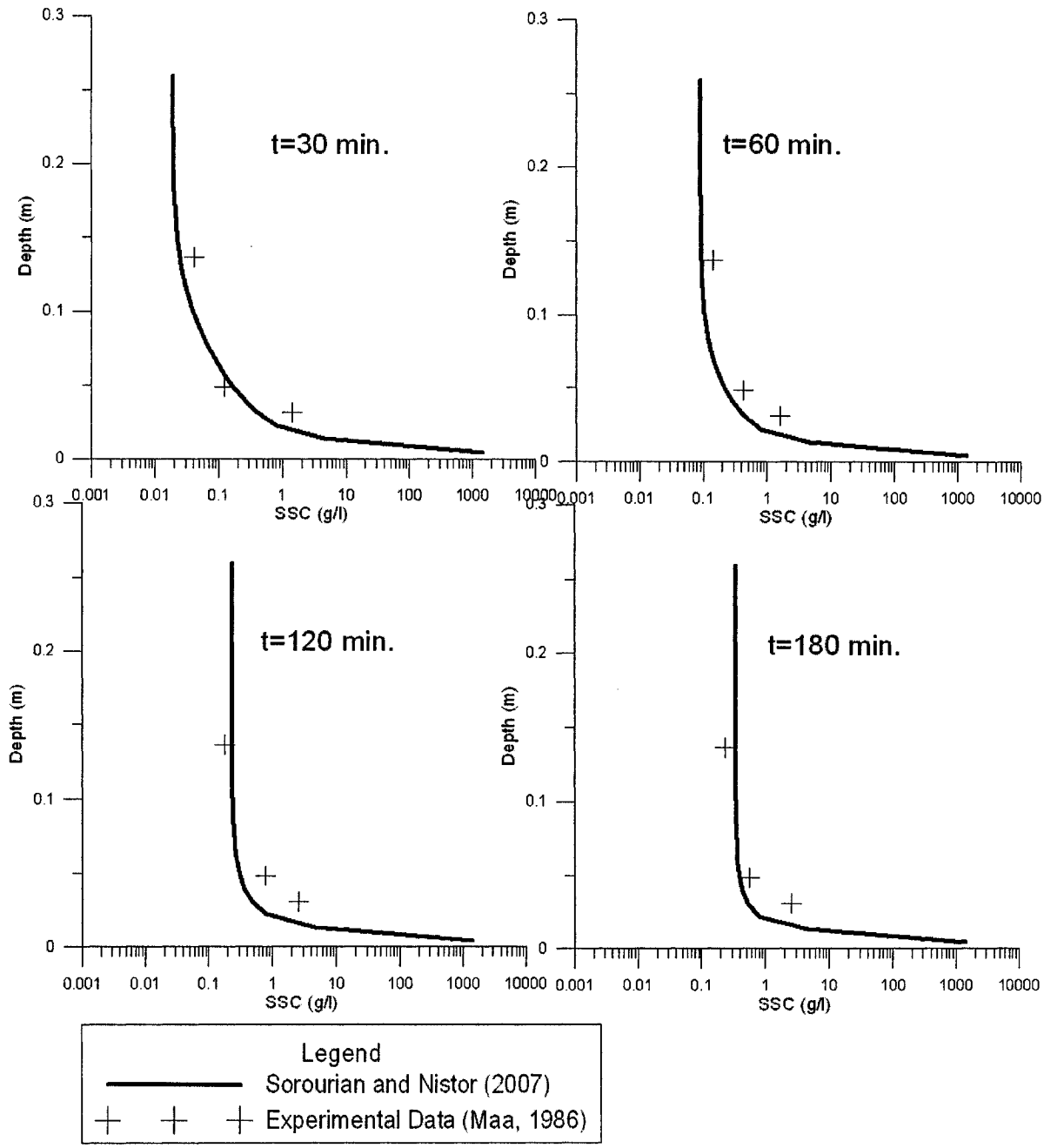

Figure A.18 Comparison of the numerical model results with laboratory data - Run 6 of the data of Maa (1986) - Model incorporating time-dependent erosion rate.

A.2- Comparison between numerical model and field data of Kemp (1986) for Vermilion Bay, Louisiana, post frontal period

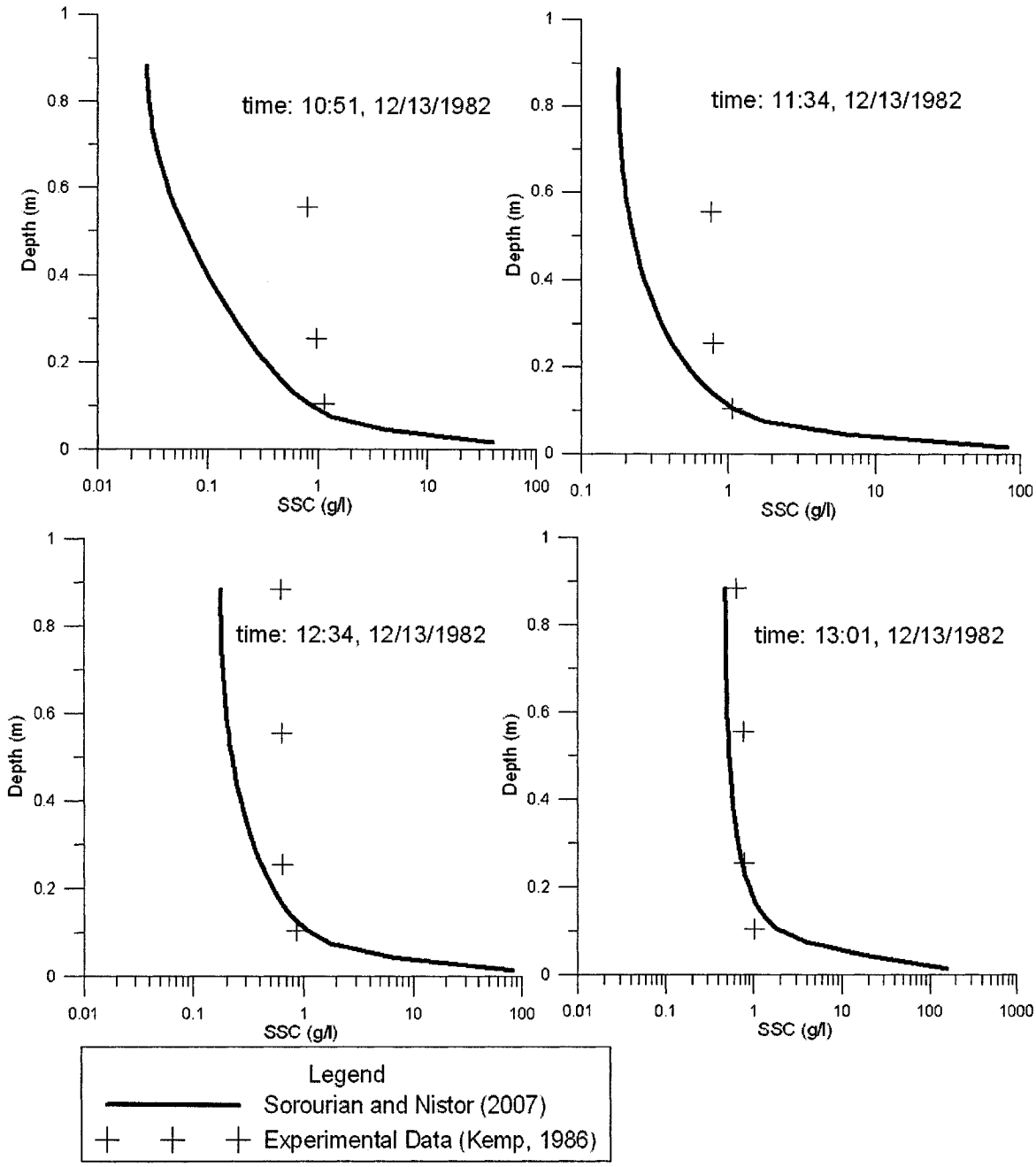

Figure A.19 Comparison of the numerical model results with field data of Kemp (1986) - Model modified for including electrochemical resistance.

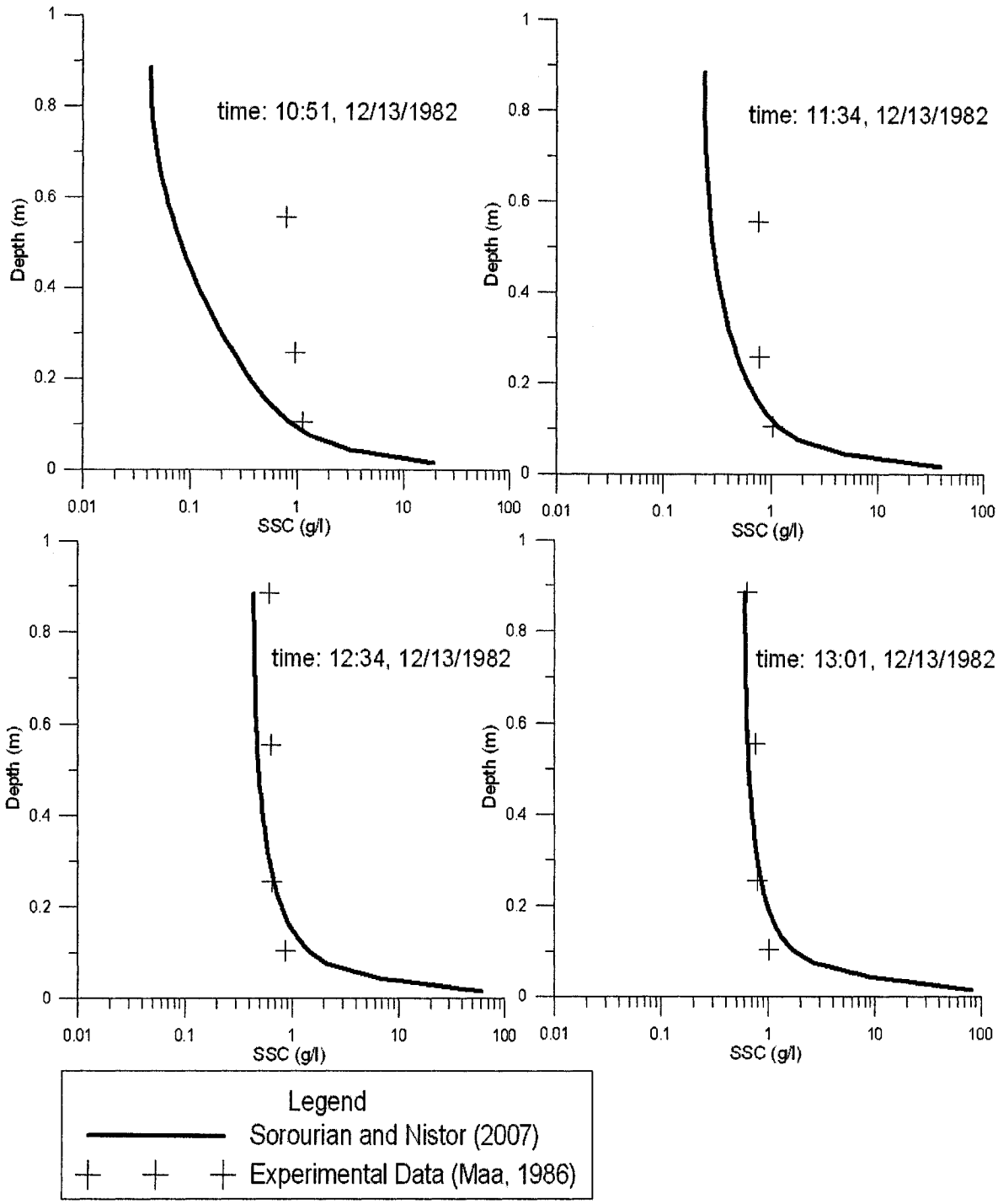

Figure A.20 Comparison of the numerical model results with field data of Kemp (1986) - Model including the concept of the vane shear strength.

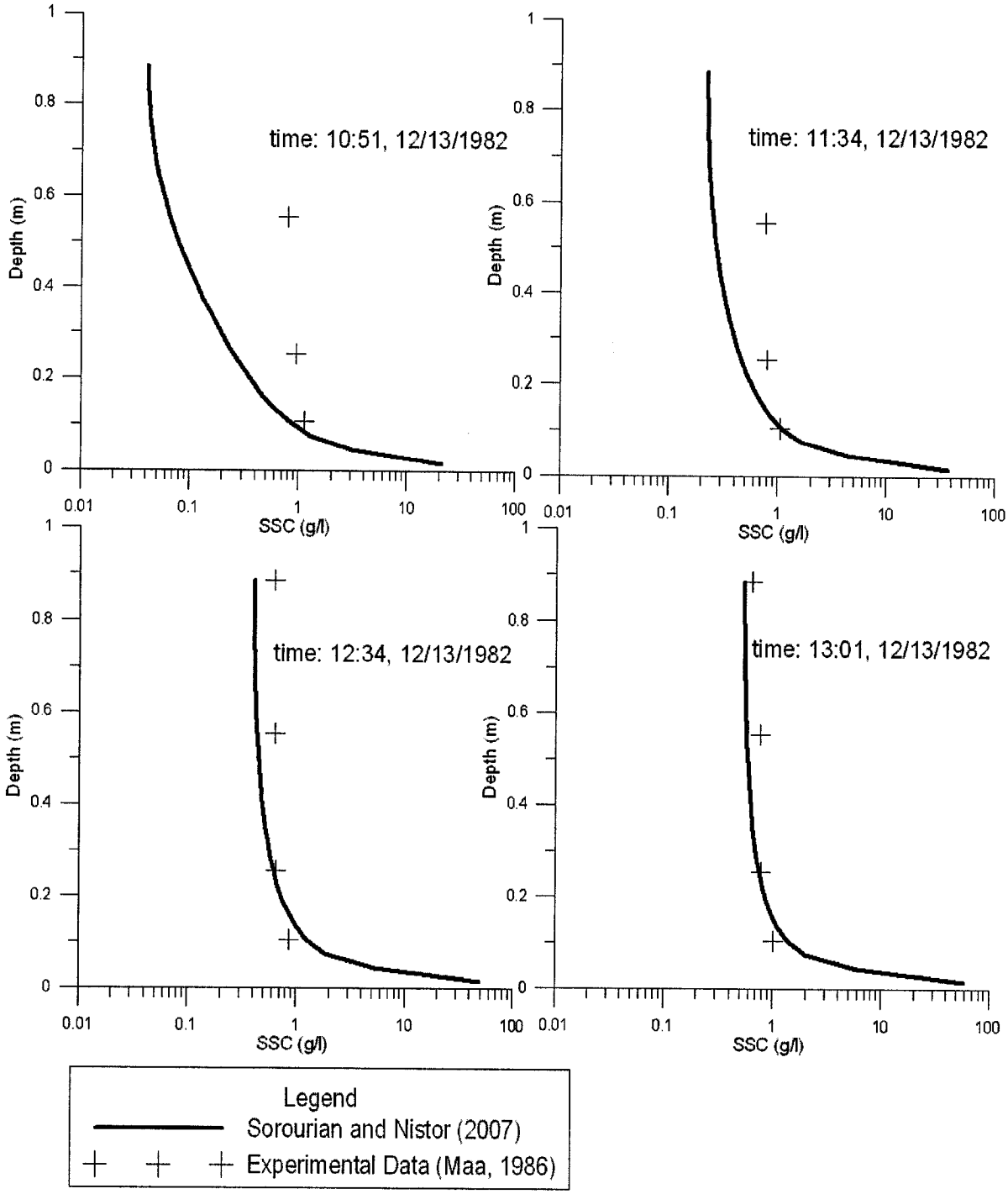

Figure A.21 Comparison of the numerical model results with field data of Kemp (1986) - Model incorporating the wave friction factor using the formula of Jonsson (1963).

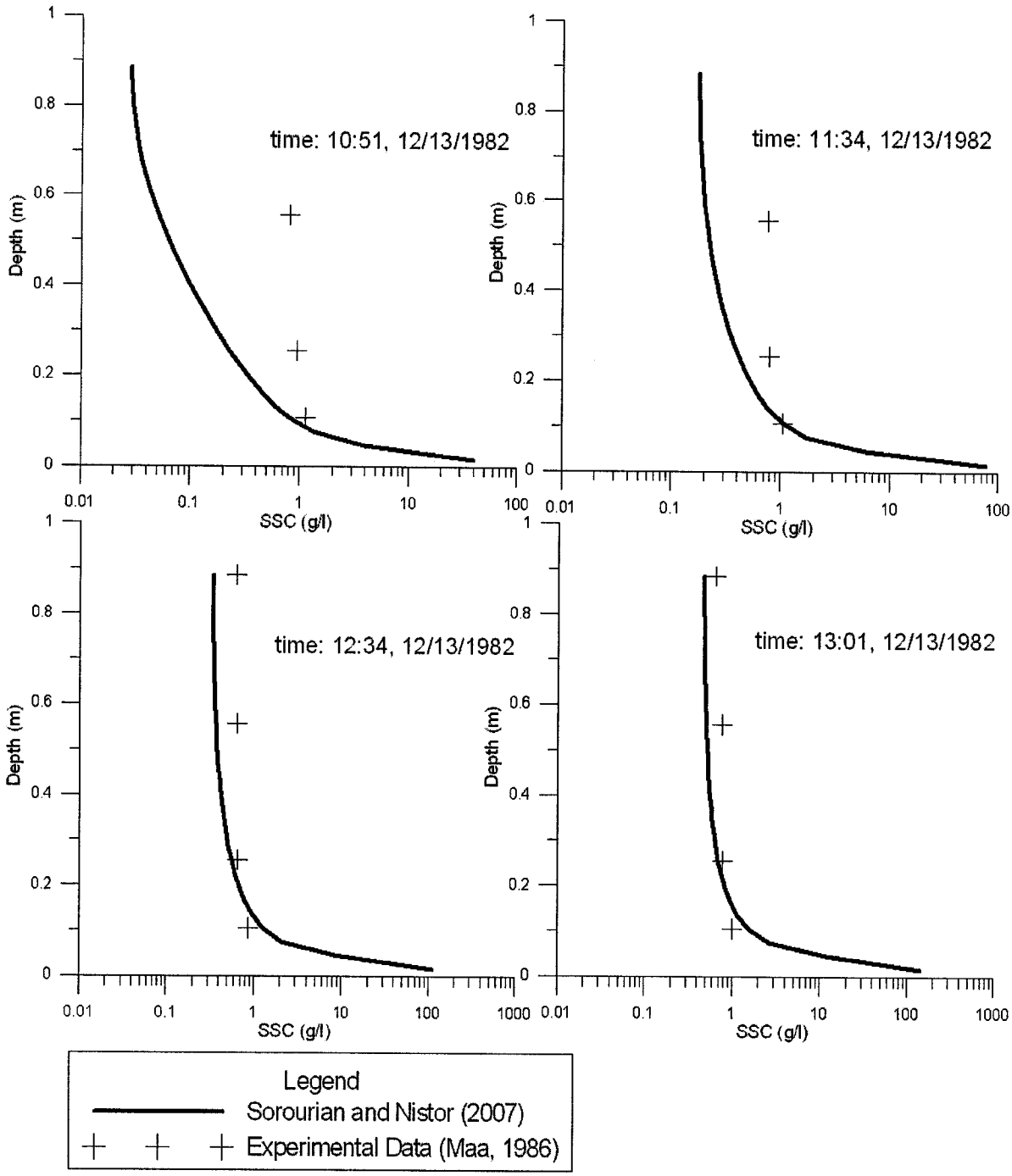

Figure A.22 Comparison of the numerical model results with field data of Kemp (1986) - Model incorporating the wave friction factor using the formula of Swart (1974).

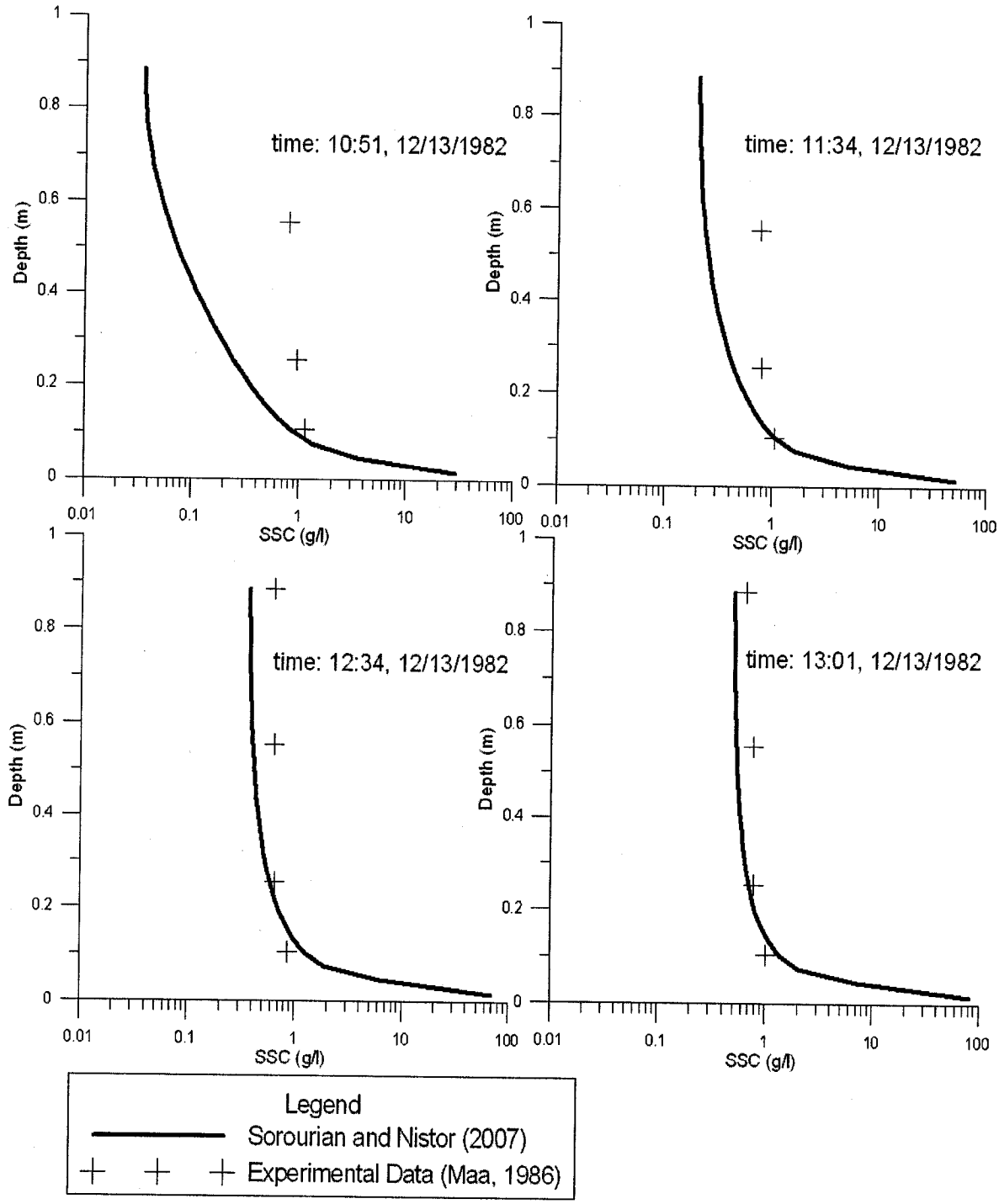

Figure A.23 Comparison of the numerical model results with field data of Kemp (1986) - Model incorporating the wave friction factor using the formula of Le Roux (2003).

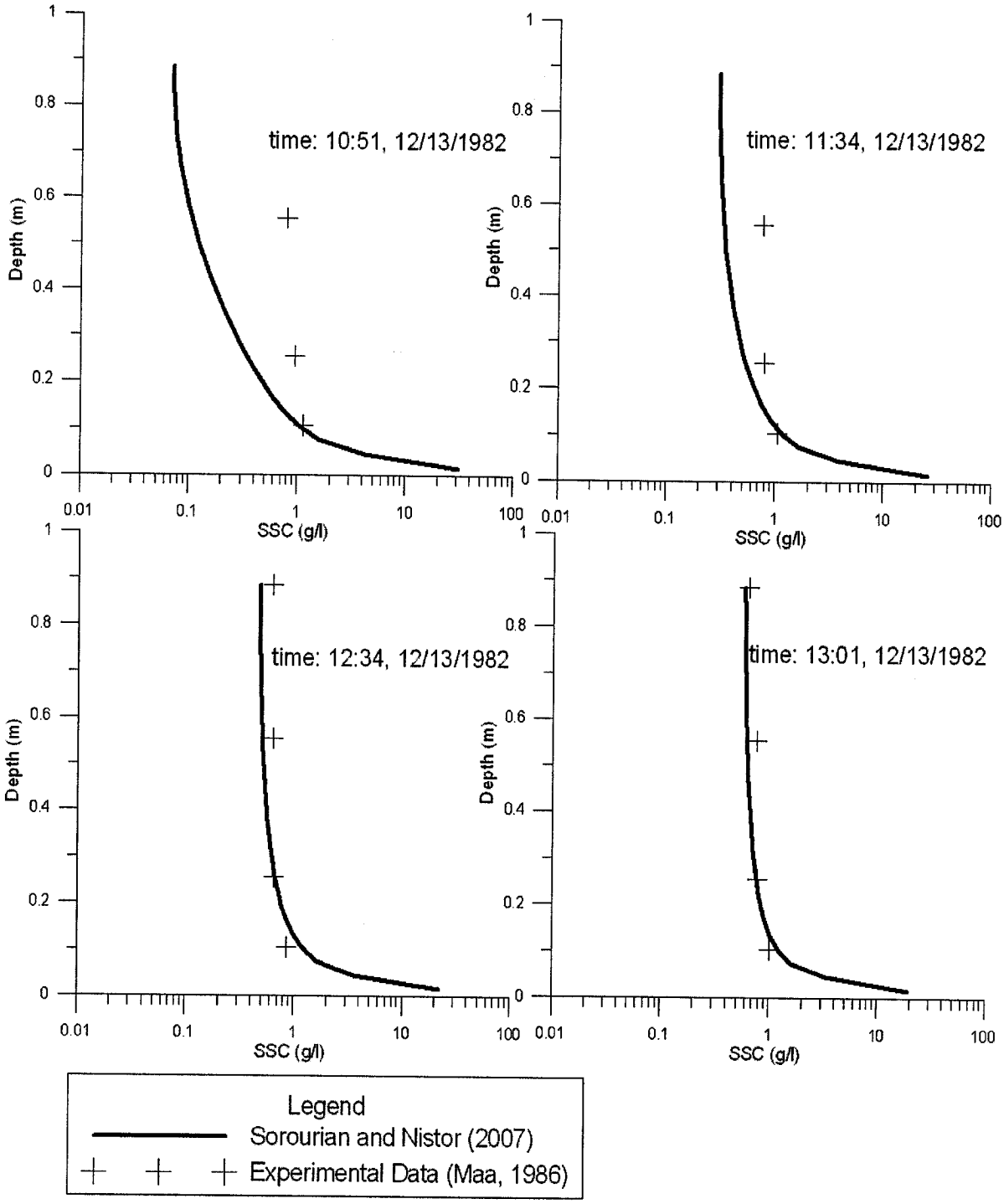

Figure A.24 Comparison of the numerical model results with field data of Kemp (1986) - Model incorporating time-dependent erosion rate.

A.3- Comparison between numerical model and field data of Sheremet (2006) for Atchafalaya Bay, Louisiana

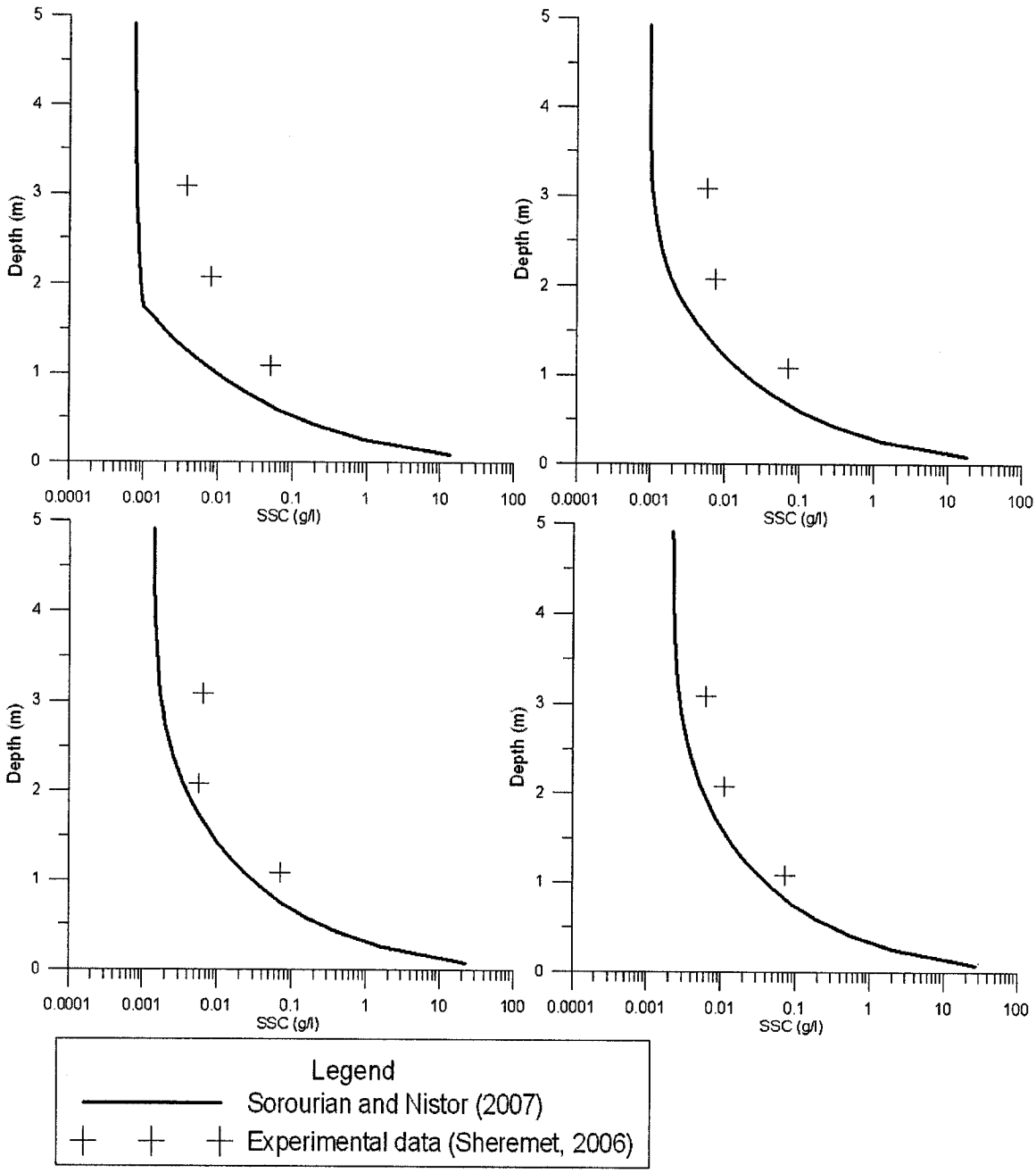

Figure A.25 Comparison of the numerical model results with field data of Sheremet (2006) - Model modified for including electrochemical resistance.

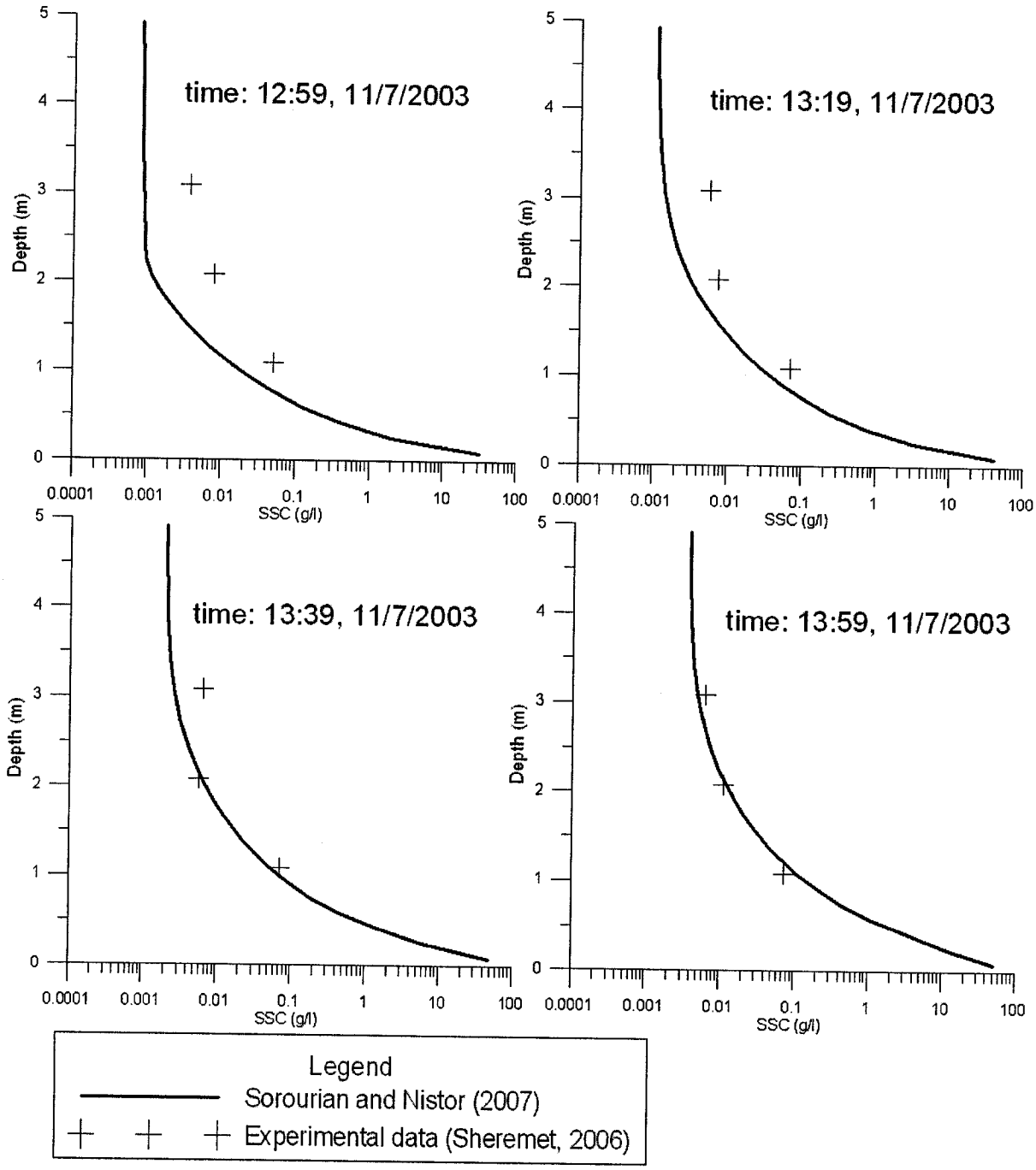

Figure A.26 Comparison of the numerical model results with field data of Sheremet (2006) - Model including the concept of the vane shear strength.

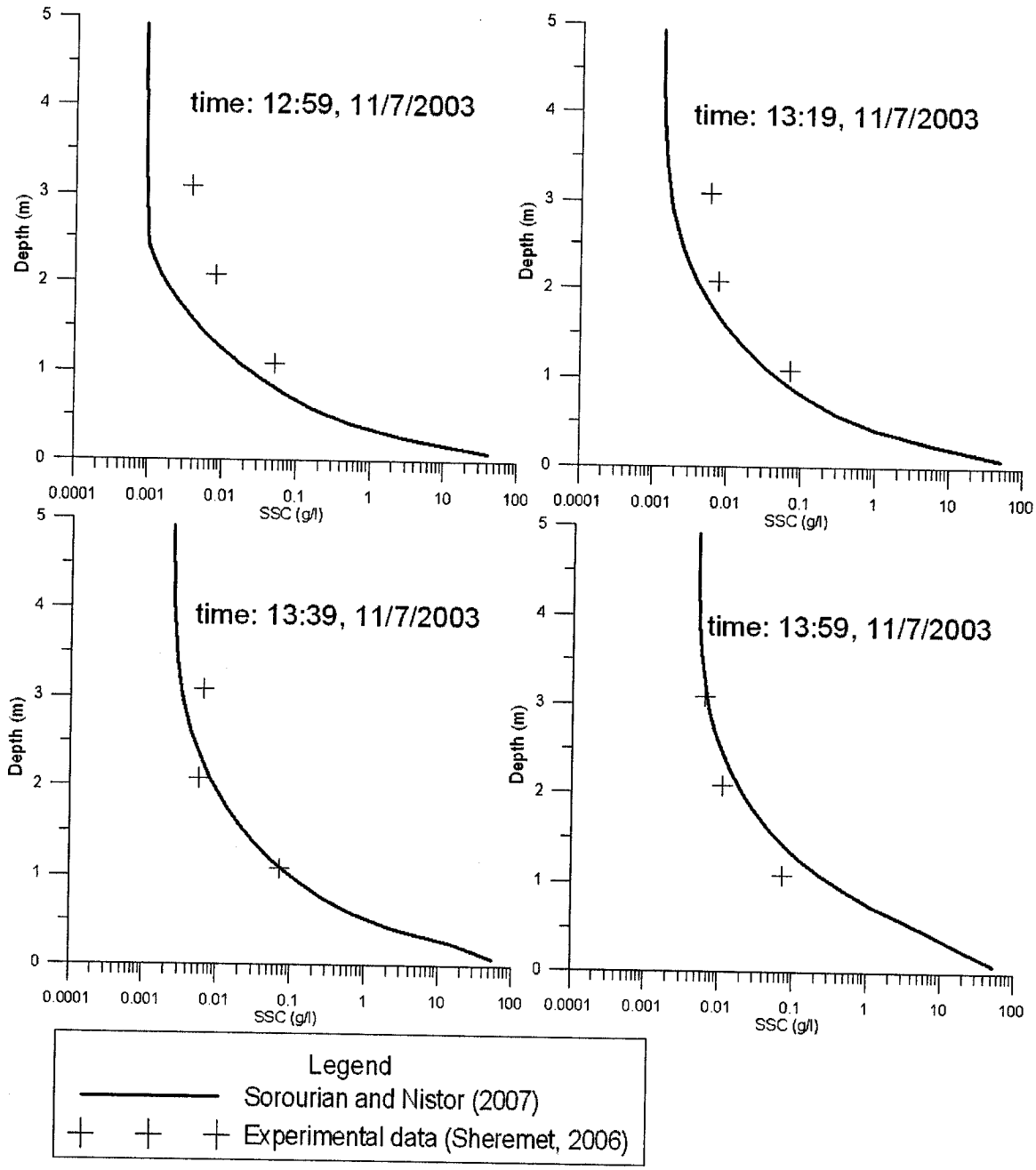

Figure A.27 Comparison of the numerical model results with field data of Sheremet (2006) - Model incorporating the wave friction factor using the formula of Jonsson (1963).

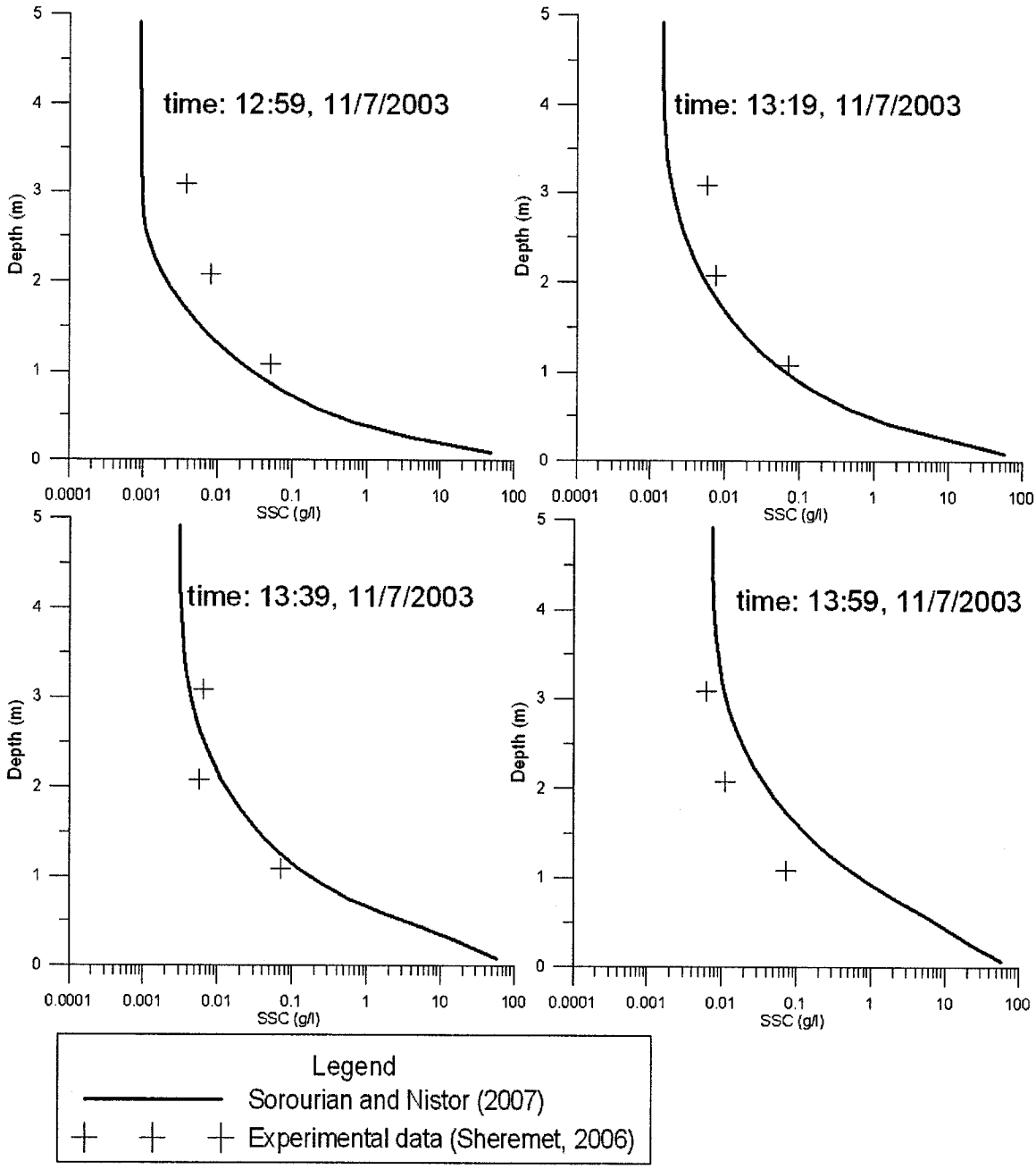

Figure A.28 Comparison of the numerical model results with field data of Sheremet (2006) - Model incorporating the wave friction factor using the formula of Swart (1974).

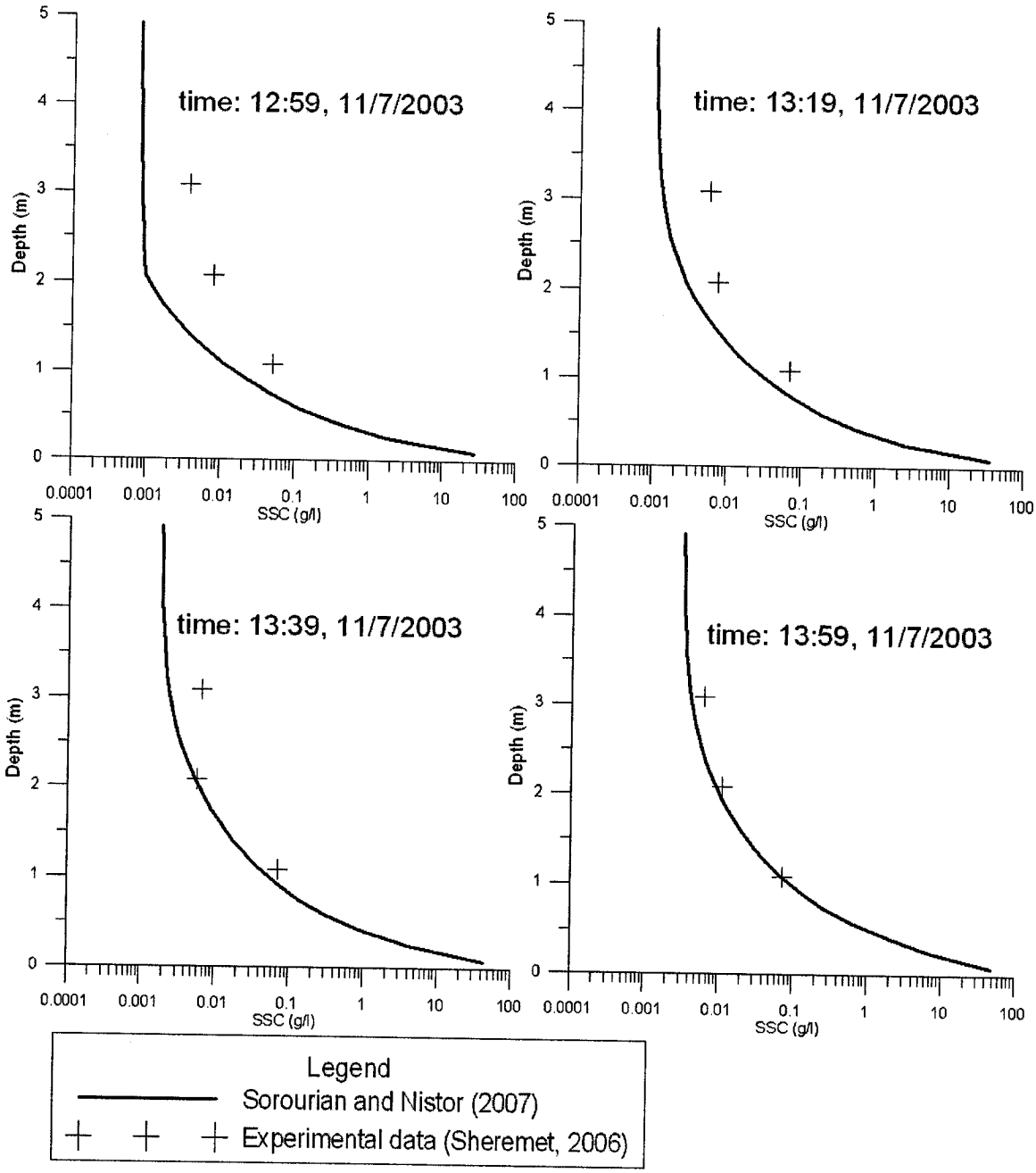

Figure A.29 Comparison of the numerical model results with field data of Sheremet (2006) - Model incorporating the wave friction factor using the formula of Le Roux (2003).

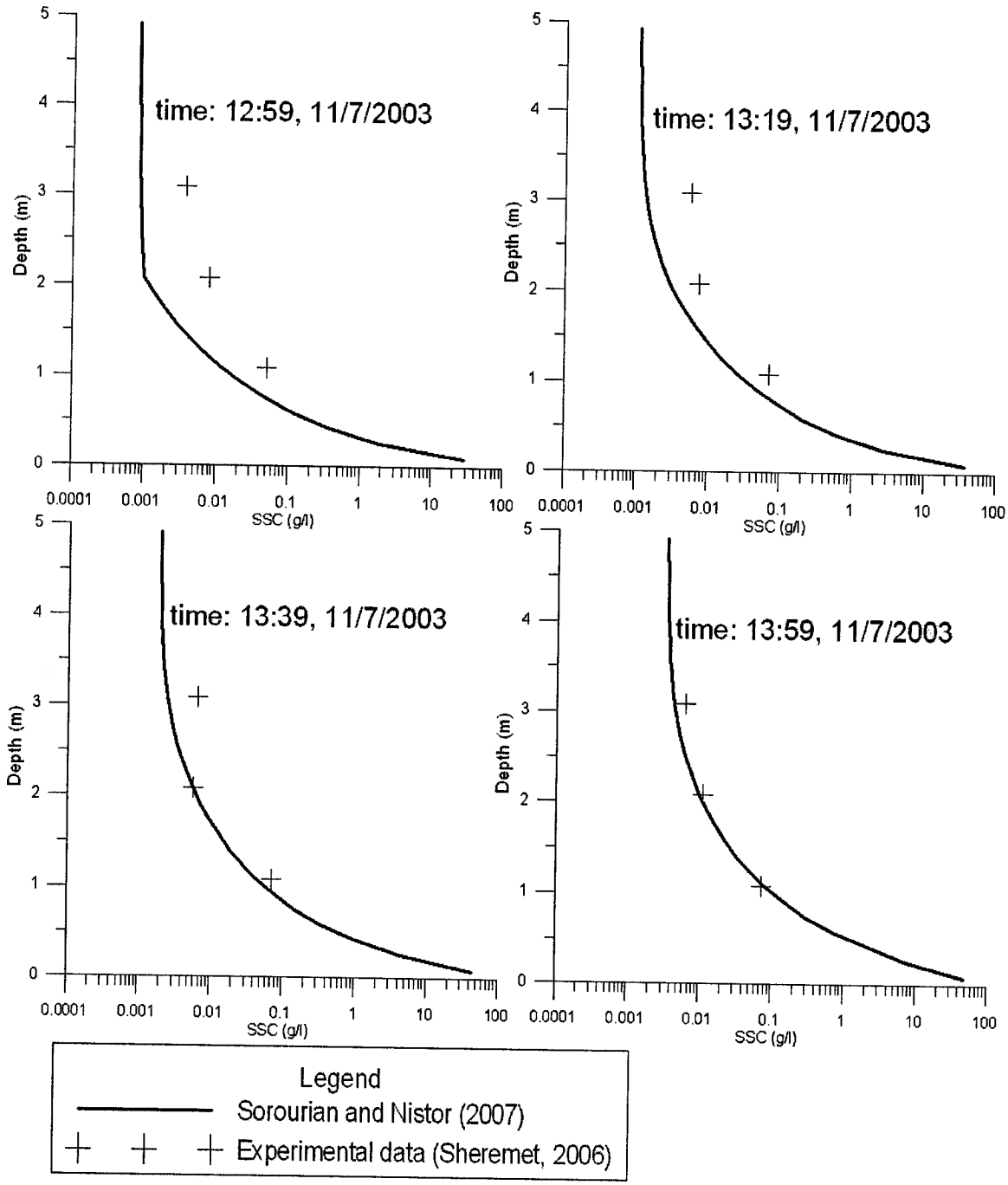

Figure A.30 Comparison of the numerical model results with field data of Sheremet (2006) - Model incorporating time-dependent erosion rate.

B- Input files for numerical model

B.1- Input file for model incorporating the electrochemical resistance force

The data are saved from screen input

Give output file name

takiout.out

Give graphics file name

takigra.gra

Information file name

takiinfo.inf

Description of input data

test

Water depth: h0(m), Bed depth: m0(m), Grid points in water: ngrids.

9.000000E-01 1.800000E-01 30

Starting time, End time, Time step, Output time

0.000000E+00 180.000000 10.000000000000000 45.000000

Settling velocity parameters

C1=?, wsf=?, a=?, b=?, m=?, n=?

3.000000E-01 1.90000E-06 3.000000E-02 9.000000

1.500000 1.330000

Stratified diffusion parameters

alpha0 = ?, beta0 = ?

5.000000E-01 3.300000E-01

Selection for external hydrodynamics: mode = ?

1==CURRENT, 2==WAVE, 3==WAVE+WEAK CURRENT.

2

Wave height:H(m), Wave period:T(sec), Wave diffusion coefficient: alphaw

0.117 6.600000 3.000000E-01

Granular density,rhos, Bed bulk density,rhom, Water density, rhow (kg/m^3).

2650.000000 1270.000000 1030.000000

Choose 1 or 2 for input: mchoo = ?

Fluid mud == 1, Bed == 2

2

Critical stress of deposition: tauc = ?(Pa)

1.000000E-01

Wave bottom friction coefficient: fw = ?

3.000000E-02

Bed density parameters: zeta=?, xi=?, rhodbar=?

0.797 -0.45 400.000000

Erosion critical stress parmeters: D_s=?, nu_b=?

6.000000E-05 0.03

Electrochemical anchoring coefficient

.15

Erosion rate parameters: ersmax, ar & br = ?

8.000000E-01 8.000000 5.000000E-01

Number of points for initial concentration input(Integer)

2

Elevation: zi(i)(m), Concentration ci(i)(kg/m^3)

(i from 1 to jn; zi(i) must be in an increasing order from water bottom)

.1 0.000000

Elevation: zi(i)(m), Concentration ci(i)(kg/m^3)

(i from 1 to jn; zi(i) must be in an increasing order from water bottom)

5.000000E-01 0.000000E+00

B.2- Input file for model incorporating the vane shear stress

The data are saved from screen input

Give output file name

dadeout.out

Give graphics file name

dadegra.gra

Information file name

dadeinfo.inf

Description of input data

experiment

Water depth: h0(m), Bed depth: m0(m), Grid points in water: ngrids.

9.000000E-01 1.800000E-01 30

Starting time, End time, Time step, Output time

0.000000E+00 180.000000 10.000000000000000 45.000000

Settling velocity parameters

C1=?, wsf=?, a=?, b=?, m=?, n=?

3.000000E-01 1.900000E-06 3.000000E-02 9.000000

1.500000 1.330000

Stabilized diffusion parameters

alpha0 = ?, beta0 = ?

5.000000E-01 3.300000E-01

Selection for external hydrodynamics: mode = ?

1==CURRENT, 2==WAVE, 3==WAVE+WEAK CURRENT.

2

Wave height:H(m), Wave period:T(sec), Wave diffusion coefficient: alphaw

0.117 6.600000 3.000000E-01

Granular density,rhos, Bed bulk density,rhom, Water density, rhow (kg/m^3).

2650.000000 1270.000000 1030.000000

Choose 1 or 2 for input: mchoo = ?

Fluid mud == 1, Bed == 2

2

Critical stress of deposition: tauc = ?(Pa)

1.000000E-01

Wave bottom friction coefficient: fw = ?

3.000000E-02

Bed density parameters: zeta=?, xi=?, rhodbar=?

0.797 -0.45 400.000000

Particle Diameter: D_s=?, friction angle(DEG): Phie=? Vane shear stress: Tau_y

=?

6.00000e-5 65.0000 0.5

Erosion rate parameters: ersmax, ar & br = ?

8.000000E-01 8.000000 5.000000E-01

Number of points for initial concentration input(Integer)

2

Elevation: zi(i)(m), Concentration ci(i)(kg/m^3)

(i from 1 to jn; zi(i) must be in an increasing order from water bottom)

1.0000E-01 0.000000E+00

Elevation: zi(i)(m), Concentration ci(i)(kg/m^3)

(i from 1 to jn; zi(i) must be in an increasing order from water bottom)

5.000000E-01 0.000000E+00

B.3- Input file for model incorporating Jonnson(1966) formula for the wave friction factor

The data are saved from screen input

Give output file name

jonssonout.out

Give graphics file name

jonssongra.gra

Description of input data

test

Water depth: h0(m), Bed depth: m0(m), Grid points in water: ngrids.

9.000000E-01 1.800000E-01 30

Starting time, End time, Time step, Output time

0.000000E+00 180.000000 10.000000000000000 45.000000

Settling velocity parameters

C1=?, wsf=?, a=?, b=?, m=?, n=?

3.000000E-01 1.90000E-06 3.000000E-02 9.000000

1.500000 1.330000

Stabilized diffusion parameters

alpha0 = ?, beta0 = ?

5.000000E-01 3.300000E-01

Selection for external hydrodynamics: mode = ?

1==CURRENT, 2==WAVE, 3==WAVE+WEAK CURRENT.

2

Wave height:H(m), Wave period:T(sec), Wave diffusion coefficient: alphaw

0.117 6.600000 3.000000E-01

Granular density,rhos, Bed bulk density,rhom, Water density, rhow (kg/m^3).

2650.000000 1270.000000 1030.000000

Choose 1 or 2 for input: mchoo = ?

Fluid mud == 1, Bed == 2

2

Critical stress of deposition: tauc = ?(Pa)

1.000000E-01

Roughness: K_s = ?

0.05

Bed density parameters: zeta=?, xi=?, rhodbar=?

0.797 -0.45 400.000000

Erosion critical stress parmeters: phie=?, alphae=? & betae=?

5.000000E-02 2.85 1.000000

Erosion rate parameters: ersmax, ar & br = ?

8.000000E-01 8.000000 5.000000E-01

Number of points for initial concentration input(Integer)

2

Elevation: zi(i)(m), Concentration ci(i)(kg/m^3)

(i from 1 to jn; zi(i) must be in an increasing order from water bottom)

1.810000E-01 0.000000E+00

Elevation: zi(i)(m), Concentration ci(i)(kg/m^3)

(i from 1 to jn; zi(i) must be in an increasing order from water bottom)

5.000000E-01 0.000000E+00

B.4- Input file for model incorporating Swart(1974) formula for the wave friction factor

The data are saved from screen input

Give output file name

swartout.out

Give graphics file name

swartgra.gra

Description of input data

test

Water depth: h0(m), Bed depth: m0(m), Grid points in water: ngrids.

9.000000E-01 1.800000E-01 30

Starting time, End time, Time step, Output time

0.000000E+00 180.000000 10.000000000000000 45.000000

Settling velocity parameters

C1=?, wsf=?, a=?, b=?, m=?, n=?

3.000000E-01 1.90000E-06 3.000000E-02 9.000000

1.500000 1.330000

Stabilized diffusion parameters

alpha0 = ?, beta0 = ?

5.000000E-01 3.300000E-01

Selection for external hydrodynamics: mode = ?

1==CURRENT, 2==WAVE, 3==WAVE+WEAK CURRENT.

2

Wave height:H(m), Wave period:T(sec), Wave diffusion coefficient: alphaw

1.200000E-01 6.600000 3.000000E-01

Granular density,rhos, Bed bulk density,rhom, Water density, rhow (kg/m^3).

2650.000000 1270.000000 1030.000000

Choose 1 or 2 for input: mchoo = ?

Fluid mud == 1, Bed == 2

2

Critical stress of deposition: tauc = ?(Pa)

1.000000E-01

Roughness K_s:

0.05000000

Bed density parameters: zeta=?, xi=?, rhodbar=?

0.797 -0.45 400.000000

Erosion critical stress parmeters: phie=?, alphae=? & betae=?

5.000000E-02 5.000000 1.000000

Erosion rate parameters: ersmax, ar & br = ?

8.000000E-01 8.000000 5.000000E-01

Number of points for initial concentration input(Integer)

2

Elevation: zi(i)(m), Concentration ci(i)(kg/m^3)

(i from 1 to jn; zi(i) must be in an increasing order from water bottom)

1.810000E-01 0.000000E+00

Elevation: zi(i)(m), Concentration ci(i)(kg/m^3)

(i from 1 to jn; zi(i) must be in an increasing order from water bottom)

5.000000E-01 0.000000E+00

B.5- Input file for model incorporating Le Roux (2003) formula for the wave friction factor

The data are saved from screen input

Give output file name

rouxout.out

Give graphics file name

rouxgra.gra

Description of input data

test

Water depth: h0(m), Bed depth: m0(m), Grid points in water: ngrids.

9.000000E-01 1.800000E-01 30

Starting time, End time, Time step, Output time

0.000000E+00 180.000000 10.000000000000000 45.000000

Settling velocity parameters

C1=?, wsf=?, a=?, b=?, m=?, n=?

3.000000E-01 1.190000E-06 3.000000E-02 9.000000

1.500000 1.330000

Stabilized diffusion parameters

alpha0 = ?, beta0 = ?

5.000000E-01 3.300000E-01

Selection for external hydrodynamics: mode = ?

1==CURRENT, 2==WAVE, 3==WAVE+WEAK CURRENT.

2

Wave height:H(m), Wave period:T(sec), Wave diffusion coefficient: alphaw

0.117 6.600000 3.000000E-01

Granular density,rhos, Bed bulk density,rhom, Water density, rhow (kg/m^3).

2650.000000 1270.000000 1030.000000

Choose 1 or 2 for input: mchoo = ?

Fluid mud == 1, Bed == 2

2

Critical stress of deposition: tauc = ?(Pa)

1.000000E-01

prticle sizein meter: D

6.000000E-05

Bed density parameters: zeta=?, xi=?, rhodbar=?

0.797 -.45 400.000000

Erosion critical stress parmeters: phie=?, alphae=? & betae=?

0.05 2.000000 1.000000

Erosion rate parameters: ersmax, ar & br = ?

8.000000E-01 8.000000 5.000000E-01

Number of points for initial concentration input(Integer)

2

Elevation: zi(i)(m), Concentration ci(i)(kg/m^3)

(i from 1 to jn; zi(i) must be in an increasing order from water bottom)

1.810000E-01 0.000000E+00

Elevation: zi(i)(m), Concentration ci(i)(kg/m^3)

(i from 1 to jn; zi(i) must be in an increasing order from water bottom)

5.000000E-01 0.000000E+00

B.6- Input data for the time dependent erosion rate

The data are saved from screen input

Give output file name

fileout.out

Give graphics file name

filegra.gra

Description of input data

test

Water depth: h0(m), Bed depth: m0(m), Grid points in water: ngrids.

0.9 0.18 30

Starting time, End time, Time step, Output time

0.000000E+00 180.000000 10.000000000000000 45

Settling velocity parameters

C1=?, wsf=?, a=?, b=?, m=?, n=?

3.000000E-01 1.90000E-06 3.000000E-02 9.000000

1.500000 1.330000

Stabilized diffusion parameters

alpha0 = ?, beta0 = ?

5.000000E-01 3.300000E-01

Selection for external hydrodynamics: mode = ?

1==CURRENT, 2==WAVE, 3==WAVE+WEAK CURRENT.

2

Wave height:H(m), Wave period:T(sec), Wave diffusion coefficient: alphaw

0.117 6.600000 3.000000E-01

Granular density,rhos, Bed bulk density,rhom, Water density, rhow (kg/m^3).

2650.000000 1270.000000 1030.000000

Choose 1 or 2 for input: mchoo = ?

Fluid mud == 1, Bed == 2

2

Critical stress of deposition: tauc = ?(Pa)

1.000000E-01

Wave bottom friction coefficient: fw = ?

3.000000E-02

Bed density parameters: zeta=?, xi=?, rhodbar=?

0.797 -0.45 400.000000

Erosion critical stress parmeters: phie=?, alphae=? & betae=?

5.000000E-02 4.000000 1.000000

Erosion rate parameters: ersmax, ar & br = ?

8.000000E-01 5.000000 0.500000

Number of points for initial concentration input(Integer)

2

Elevation: zi(i)(m), Concentration ci(i)(kg/m^3)

(i from 1 to jn; zi(i) must be in an increasing order from water bottom)

0.00000E-00 0.000000

Elevation: zi(i)(m), Concentration ci(i)(kg/m^3)

(i from 1 to jn; zi(i) must be in an increasing order from water bottom)

1.790000E-01 0.000000

C- FORTRAN program code for the case of time-dependent erosion rate

```
C*********************************************************************
C  PROGRAME NAME:  VEST.FOR                              *
C                                                        *
C  ONE-DIMENSIONAL NON-EQUILIBRIUM SUSPENSION PROFILE MODELING    *
*                    *                                                  *
C                                                        *
C    Originally by: MEHTA AND LI (2003)                                 *
C    Modified by: SOROUSH SOROURIAN (2006-2007)              *
C    Advisor: Prof. Dr. IOAN NISTOR, Dr. RONALD TOWNSEND        *
C                                                        *
C    DEPARTMENT OF CIVIL ENGINEERING                     *
C    UNIVERISTY OF OTTAWA                                *
C*********************************************************************

      parameter (nd=500)
      character DESCR*60,FILEIN*30,FILEOUT*30,FILEGRA*30
      real*8 mmc,mmt,tt,ctt,dt
      real m0, kk, ks, kn, kkss
      dimension c0t(nd),dvel(nd),c0(nd),c(nd),z(nd),
     *      ws(nd),kn(nd),ks(nd)
      dimension zi(500),ci(500),ddtout(500)
      dimension p(nd),q(nd),r(nd)
      common/com/h0,m0,g,pi,kk,rhow,visc,kkss,
     *       mode,ngrids,dz,dtrun,dtout,dt,stt,dps,mchoo
```

```
      common/wave/wheight,wperiod,wdiffk,wlength,ub,wfric
      common/flow/uu,qn
      common/tide/qqn,umax,ptide
      common/mud/rhosed,rhom,ric,rig,dudb,ent0,enn
      common/mr/gg1,gg2,uu2
      common/out/wsc0,ws0,wsa,wsb,wsm,wsn,dsk1,dsk2
      common/cal/suspmas,eromas
      common/bed/ dzb,taudep,bdp1,bdp2,rhbbar,phic,tcp1,tcp2,
     *            ersmax,erp1,erp2,tauero
          dzb=0
          dzbt=0
c
      data g, pi, kk, visc                !Program Constants
     *    / 9.81, 3.14159, 0.4, 1e-06 /
c
      write(*,*)'Non-Equilibrium Suspension Profile Simulation'
      write(*,*)'  '
      write(*,*)'Which option would you like to use for input data?'
      write(*,*)'file input == 1 ; screen input ==2 '
      read(*,*) ifile
ccc
      if(ifile.eq.1) then
ccc
      write(*,*)'You are using file input.'
      write(*,*)'Please give input file name '
      read(*,*) FILEIN
      open(1,file=FILEIN,status='unknown')
      read(1,*)
      read(1,*)
      read(1,*) FILEOUT
      write(*,*)fileout
      read(1,*)
      read(1,*) FILEGRA
      open(2,file=FILEOUT,status='unknown')
      open(3,file=FILEGRA,status='unknown')
c
      read(1,*)
```

```
      read(1,*) descr
      read(1,*)
      read(1,*) h0, m0, ngrids              !Discretization Parameters
      read(1,*)
      read(1,*) stt,dtrun,dt,dtout          !Time Parameters
      if(dtout.le.0.000001) then
        read(1,*)
        read(1,*) idt
        read(1,*)
        read(1,*) (ddtout(i),i=1,idt)
      end if
      read(1,*)
      read(1,*)
      read(1,*) wsc0, ws0, wsa, wsb, wsm, wsn !Settling Velocity Parameters
      read(1,*)
      read(1,*)
      read(1,*) dsk1, dsk2                  !Stabilized Diffusion Constants.
c     read(1,*) dps                         !Deposition rate
      dps=1.0
c
      read(1,*)
      read(1,*)
      read(1,*) mode                        !Define: Program Logic
      if(mode.eq.1) then
        read(1,*)
        read(1,*) uu, qn                    !Current Hydrodynamics
      else if(mode.eq.2) then
        read(1,*)
        read(1,*) wheight,wperiod,wdiffk    !Wave Hydrodynamics
      else if(mode.eq.3) then
        read(1,*)
        read(1,*) uu, qn                    !Current Hydrodynamics
        read(1,*)
        read(1,*) wheight,wperiod,wdiffk    !Wave Hydrodynamics
c     else if(mode.eq.4) then
c       read(1,*) umax, ptide, qqn          !Tidal Hydrodynamics
      else
```

```
      write(*,*) '"mode" input is wrong! "mode" must 1, 2 or 3'
      stop
    end if
c
    read(1,*)
    read(1,*) rhosed, rhom, rhow          !Density
    read(1,*)
    read(1,*)
    read(1,*)mchoo
    if(mchoo.eq.1) then
      read(1,*)
C       read(1,*) ric, ent0, enn        !Entrainment parameter
      read(1,*) ric, ent0               !Entrainment parameter
      enn=1.0
      read(1,*)
      read(1,*)
      read(1,*) gg1,gg2,uu2             !Mud Reology
    else if(mchoo.eq.2) then
      read(1,*)
      read(1,*) taudep                  !Critical Stress of deposition
      read(1,*)
      read(1,*) wfric                   !Wave friction coefficient
      read(1,*)
      read(1,*) bdp1, bdp2, rhbbar      !Bed density parameters
      read(1,*)
      read(1,*) phic, tcp1, tcp2        !Critical stress parameters
      read(1,*)
      read(1,*) ersmax, erp1, erp2      !Erosion rate coefficient parameters
    else
      write(*,*)'Inappropriate choice for bottom sediment!'
      stop
    end if
c
    read(1,*)
    read(1,*) jn                        !Initial concentration points
    do i =1,jn
    read(1,*)
```

```
      read(1,*)
      read(1,*) zi(i),ci(i)              !Initial concentration profile
      end do
      close(1)
ccc
      else if (ifile.eq.2) then
ccc
      write(*,*)'You are using screen input'
      write(*,*)'Input data from screen will be saved in an input file'
      write(*,*)'Give file name to save your input data (Characters)'
      read(*,*) FILEIN
c
      write(*,*)
      write(*,*)'Give output file name (Characters)'
      read(*,*) FILEOUT
      write(*,*)
      write(*,*)'Give graphics file name (Characters)'
      read(*,*) FILEGRA
c
      open(unit=1,file=FILEIN,status='unknown')
      open(unit=2,file=FILEOUT,status='unknown')
      open(unit=3,file=FILEGRA,status='unknown')


c
      write(1,*)'The data are saved from screen input'
      write(1,*)'Give output file name'
      WRITE(1,*) FILEOUT
      write(1,*)'Give graphics file name'
      WRITE(1,*) FILEGRA
c
      write(*,*)
      write(*,*)'Give description of input data'
      read(*,*) descr
      write(1,*)'Description of input data'
      WRITE(1,*) descr
c
      write(*,*)
```

```
      write(*,*)'Water depth: h = ?(m)'
      read(*,*) h0
      write(*,*)
      write(*,*)'Bed (or fluid mud) depth: hb = ?(m)'
      read(*,*) m0
      write(*,*)
      write(*,*)' Number of vertical grid points in water:  ngrids = ?
     *(Integer)'
      read(*,*) ngrids
      write(1,*)'Water depth: h0(m), Bed depth: m0(m), Grid points in
     *water: ngrids.'
      WRITE(1,*) h0, m0, ngrids
c
      write(*,*)
      write(*,*)'Starting time of simulation: stt =  ?(min)'
      read(*,*) stt
      write(*,*)
      write(*,*)'End time of simulation, ett = ?(min)'
      read(*,*) dtrun
      write(*,*)
      write(*,*)'Time step for calculation: dt = ?(sec)'
      read(*,*) dt
      write(*,*)
      write(*,*)'Output time step: ott = ?(min)'
c     write(*,*)'If you select dtout < 0, the selected output time will
c     * be stated'
      read(*,*) dtout
      write(1,*)'Starting time,  End time,  Time step,  Output time'
      WRITE(1,*) stt,dtrun,dt,dtout

      write(*,*)
      write(*,*)'Settling velocity parameters'
      write(*,*)' C1=?, wsf=?, a=?, b=?, m=?, n=?'
      read(*,*) wsc0, ws0, wsa, wsb, wsm, wsn
      write(1,*)'Settling velocity parameters'
      write(1,*)' C1=?, wsf=?, a=?, b=?, m=?, n=?'
      WRITE(1,*) wsc0, ws0, wsa, wsb, wsm, wsn
```

```
C
      write(*,*)
      write(*,*)' Stabilized diffusion parameters'
      write(*,*)' alpha0 = ?, beta0 = ?'
      read(*,*) dsk1, dsk2
      write(1,*)' Stabilized diffusion parameters'
      write(1,*)' alpha0 = ?, beta0 = ?'
      WRITE(1,*) dsk1, dsk2
c     read(1,*) dps                    !Deposition rate
      dps=1.0
c
402   write(*,*)'Selection of external hydrodynamic mode'
      write(*,*)'mode: 1==CURRENT, 2==WAVE, 3==WAVE+WEAK CURRENT.'
      read(*,*) mode
      write(*,*)
      write(1,*)'Selection for external hydrodynamics: mode = ?'
      write(1,*)'1==CURRENT, 2==WAVE, 3==WAVE+WEAK CURRENT.'
      WRITE(1,*) mode
C
      if(mode.eq.1) then
      write(*,*)
        write(*,*)'Mean current velocity: U = ?(m/s)'
        read(*,*) uu
      write(*,*)
        write(*,*)'Manning`s coefficient, n = ?'
        read(*,*) qn
      write(1,*)'Mean current velocity: U(m/s),Manning`s coefficient: n'
        WRITE(1,*) uu, qn
C
      else if(mode.eq.2) then
      write(*,*)
        write(*,*)'Wave height: H = ? (m)'
        read(*,*) wheight
      write(*,*)
        write(*,*)'Wave period: T = ?(sec)'
        read(*,*) wperiod
      write(*,*)
```

```
        write(*,*)'Wave diffusion coefficient: alphaw = ?'
        read(*,*) wdiffk
       write(1,*)'Wave height:H(m), Wave period:T(sec), Wave diffusion
     * coefficient: alphaw'
        WRITE(1,*) wheight,wperiod,wdiffk
C
      else if(mode.eq.3) then
      write(*,*)
        write(*,*)'Mean current velocity: U = ?(m/s)'
        read(*,*) uu
      write(*,*)
        write(*,*)'Manning`s coefficient, n = ?'
        read(*,*) qn
      write(1,*)'Mean current velocity: U(m/s),Manning`s coefficient: n'
        WRITE(1,*) uu, qn
      write(*,*)
        write(*,*)'Wave height: H = ? (m)'
        read(*,*) wheight
      write(*,*)
        write(*,*)'Wave period: T = ?(sec)'
        read(*,*) wperiod
      write(*,*)
        write(*,*)'Wave diffusion coefficient: alphaw = ?'
        read(*,*) wdiffk
       write(1,*)'Wave height:H(m), Wave period:T(sec), Wave diffusion
     * coefficient: alphaw'
        WRITE(1,*) wheight,wperiod,wdiffk    !Wave Hydrodynamics
c
c     else if(mode.eq.4) then
c       read(1,*) umax, ptide, qqn          !Tidal Hydrodynamics
      else
      write(*,*)
        write(*,*)'"mode" input is wrong! "mode" must 1, 2 or 3'
        write(*,*)'Please choose again!'
        write(1,*)'"mode" input is wrong! "mode" must 1, 2 or 3'
        write(1,*)'Please choose again!'
C
```

```
      goto 402
    end if
    write(*,*)
    write(*,*)'Granular density: rhos = ?(kg/m^3)'
    read(*,*) rhosed
    write(*,*)
    write(*,*)'Bed bulk density: rhom = ?(kg/m^3)'
    read(*,*) rhom
    write(*,*)
    write(*,*)'Water density: rhow = ?(kg/m^3)'
    read(*,*) rhow
    write(1,*)'Granular density,rhos, Bed bulk density,rhom, Water
   *density, rhow (kg/m^3).'
    WRITE(1,*) rhosed, rhom, rhow

C
403   if(rhom.gt.1300.0.and.rhom.lt.2200.0) then
    write(*,*)
      write(*,*)'Bed density > 1,300 kg/m^3'
     write(*,*)'Bottom sediment should be considered as a bed'
    write(*,*)
      write(*,*)'Bed == 2, fluid mud == 1'
    else if(rhom.lt.1200.0.and.rhom.gt.1050.0) then
    write(*,*)
      write(*,*)'Bed density <1,200 kg/m^3'
      write(*,*)'Bottom sediment should be considered as fluid mud'
      write(*,*)
      write(*,*)'Fluid mud == 1, Bed == 2'
    else if((rhom.ge.1200.0).and.(rhom.le.1300.0)) then
    write(*,*)
      write(*,*)'Bed density > 1,200 kg/m^3 and < 1,300 kg/m^3'
     write(*,*)'Bottom sediment can be bed or fluid mud'
    write(*,*)
      write(*,*)'Fluid mud == 1, Bed == 2'
    else
      write(*,*)'Incorrect choice for bed density!!!'
      stop
```

```
      end if
      write(*,*)
      write(*,*)'Choose 1 or 2 for input:'
      read(*,*)mchoo
      write(1,*)'Choose 1 or 2 for input: mchoo = ?'
      write(1,*)'Fluid mud == 1, Bed == 2'
      WRITE(1,*)mchoo
c
      if(mchoo.eq.1) then
      write(*,*)
        write(*,*)'Critical Richardson number for entrainment:Ric'
        read(*,*) ric
      write(*,*)
C       write(*,*)'Two entrainment rate coefficients.: ent0 and enn'
C       read(*,*) ent0, enn
        write(*,*)'entrainment rate coefficient: Beta = ?'
        read(*,*) ent0
        enn=1.0
C       write(1,*)'Critical Ri:ric,Entrainment rate coefficients: ent0 & enn.'
C       WRITE(1,*) ric, ent0, enn          !Entrainment parameter
        write(1,*)'Critical Ri:Ric,Entrainment rate coefficient: Beta'
        WRITE(1,*) ric, ent0         !Entrainment parameter
C
      write(*,*)
      write(*,*)'Bottom sediment rheological parameters:G1, G2 and mu2'
        write(*,*)'(G1 and G2 in Pa and mu2 in Pa.s)'
        write(*,*)'(Note: if G1>0: three-parameter rheological model'
        write(*,*)'       if G1<0: two-parameter rheological model'
        write(*,*)'       if G1 < 0 and G2 = 0: viscous model)'
        write(*,*)' G1 = ?, G2 = ?, mu2 =?'
        read(*,*) gg1,gg2,uu2            !Mud Reology
      write(1,*)'Bottom sediment rheological parameters: G1, G2 and mu2'
        write(1,*)'(G1 and G2 in Pa and mu2 in Pa.s)'
        WRITE(1,*) gg1,gg2,uu2           !Mud Reology
C
      else if(mchoo.eq.2) then
        write(*,*)
```

```
        write(*,*)'Critical stress for deposition: tauc = ?(Pa)'
        read(*,*) taudep
        write(1,*)'Critical stress of deposition: tauc = ?(Pa)'
        WRITE(1,*) taudep
C
      write(*,*)
        write(*,*)'Wave bottom friction coefficient: fw = ?'
        read(*,*) wfric
        write(1,*)'Wave bottom friction coefficient: fw = ?'
        WRITE(1,*) wfric
C
      write(*,*)
        write(*,*)'Bed density parameters: zeta=?, xi=?, rhodbar=?'
        read(*,*) bdp1, bdp2, rhbbar
        write(1,*)'Bed density parameters: zeta=?, xi=?, rhodbar=?'
        WRITE(1,*) bdp1, bdp2, rhbbar
C
      write(*,*)
      write(*,*)'Erosion critical stress parameters: phie=?, alphae=? &
     * betae=?'
        read(*,*) phic, tcp1, tcp2
       write(1,*)'Erosion critical stress parmeters: phie=?, alphae=? &
     * betae=?'
        WRITE(1,*) phic, tcp1, tcp2
C
      write(*,*)
        write(*,*)'Erosion rate parameters: smax, ar & br = ?'
        read(*,*) ersmax, erp1, erp2
        write(1,*)'Erosion rate parameters: ersmax, ar & br = ?'
        WRITE(1,*) ersmax, erp1, erp2
C
      else
      write(*,*)
        write(*,*)'Inappropriate choice for bottom sediment!'
        write(*,*)'Reselect mchoo: ( == 1 or 2 )'
        write(1,*)'Inappropriate choice for bottom sediment!'
        write(1,*)'Reselect mchoo: ( == 1 or 2 )'
```

```
C
       goto 403
     end if
c
     write(*,*)
401   write(*,*)'Number of points for initial concentration input:'
     write(*,*)'  jn = ? (must be integer, up to',ngrids,')'
     read(*,*) jn
     write(*,*)
          write(1,*)'Number of points for initial concentration input
    *(Integer)'
     WRITE(1,*) jn                    !Initial concentration points
C
     write(*,*)
     write(*,*)'Elevation: zi(i)(m), Concentration ci(i)(kg/m3)'
      write(*,*)'Elevations must be in an increasing order from water
    *bottom'
     do idt1=1,jn
     write(*,*) 'For i = ',idt1,',give,  zi = ? , ci = ?'
     read(*,*) zi(idt1),ci(idt1)
     write(1,*)'Elevation: zi(i)(m), Concentration ci(i)(kg/m3)'
      write(1,*)'(i from 1 to jn; zi(i) must be in an increasing order
    *from water bottom)'
     WRITE(1,*) zi(idt1),ci(idt1)        !Initial concentration
     end do
C
ccc
     else
ccc
     write(*,*)
     write(*,*)'Incorrect selection for input data!!!'
     write(1,*)'Incorrect selection for input data!!!'
C
     stop
ccc
     end if
ccc
```

```
      write(3,*) h0, ngrids
      write(*,*) h0, ngrids
      if(dtout.le.0.000001) then
        iii=idt+1
        write(3,*)iii,dtout
        write(*,*)iii,dtout
      else
        iii=int((dtrun-stt)/dtout)+1
        write(3,*) iii,dtout
      end if
c
      if(wheight.lt.1e-10) then
        wheight=1e-10
      end if
      dz=h0/float(ngrids)
      st=stt*60.0
      mmc=dtout*60.0
      mmt=dtrun*60.0
c*    initial data **
      do 1 i=1,ngrids
        z(i)=(float(i)-0.5)/float(ngrids)*h0
1     continue
c
      if(jn.eq.1) then
        do 2 i=1,ngrids
          c0(i)=ci(1)
2       continue
      end if
c
      if(jn.gt.1.and.jn.lt.ngrids) then
        do i=1,jn-1
          if(zi(i+1).le.zi(i)) then
      write(*,*)'Incorrect selection for initial concentration input.'
            write(*,*)'The zi(i) is not in an increasing order.'
            stop
          end if
        end do
```

```
      do 3 j=1,jn-1
       do 4 i=1,ngrids
        ss=(float(i)-0.5)*dz
        if(z(i).le.zi(1)) then
         c0(i)=ci(1)
        else if(z(i).ge.zi(jn)) then
         c0(i)=ci(jn)
        else
         if(z(i).gt.zi(j).and.z(i).lt.zi(j+1)) then
          c0(i)=ci(j)+(ci(j+1)-ci(j))
     *              *(z(i)-zi(j))/(zi(j+1)-zi(j))
         else if(z(i).eq.zi(j)) then
          c0(i)=ci(j)
         else if(z(i).eq.zi(j+1)) then
          c0(i)=ci(j+1)
         end if
        end if
4       continue
3      continue
    end if
c
    if(jn.eq.ngrids) then
       do 5 i=1,ngrids
          c0(i)=ci(i)
5      continue
    end if
c
c
    tt=st-dt
    ctt=-dt
    eromas=0.0
c
    do i=1,ngrids
       c(i)=c0(i)
    end do
c
    if(mode.eq.1) then
```

```
      if(mchoo.eq.1) then
        write(*,*)'For entrainment of fluid mud under current,'
        write(*,*)'This case is not appropriate for practical use.'
        write(*,*)'Sorry!!!'
        stop
c        call hydroflow1(dvel,kn)
c        ustar=uu
      else if(mchoo.eq.2) then
        call hydroflow2(dvel,kn,taubed)
      else
      end if
      end if
c
      if(mode.eq.2) then
c     call prowmita(PWD1,PWD2,PDEN1,PDEN2,PWP,PAMP1,
c    *                PMU1,Puu,PGG1,PGG2,ip,RRR,rr2)
      if(mchoo.eq.1) then
        pmu1=visc*rhow
        ip=10
        call prowmita(h0,m0,rhow,rhom,wperiod,wheight,
     *                pmu1,uu2,gg1,gg2,ip,rrr,rr2)
        dudb=rrr
        call hydrowave1(dvel,kn,rr2)
        ustar=ub
      else if(mchoo.eq.2) then
        call hydrowave2(dvel,kn,taubed)
      else
      end if
      end if
c
      if(mode.eq.3) then
c     call prowmita(PWD1,PWD2,PDEN1,PDEN2,PWP,PAMP1,
c    *                PMU1,Puu,PGG1,PGG2,ip,RRR,rr2)
      if(mchoo.eq.1) then
        pmu1=visc*rhow
        ip=10
        call prowmita(h0,m0,rhow,rhom,wperiod,wheight,
```

```
     *                pmu1,uu2,gg1,gg2,ip,rrr,rr2)
          dudb=rrr
          call wavecurrent1(dvel,kn,rr2)
          ustar=ub
        else if(mchoo.eq.2) then
          rr2=0.0
          call wavecurrent2(dvel,kn,taubed)
        else
        end if
        end if
999   tt=tt+dt
        ctt=ctt+dt
c
        do 6 i=1,ngrids
         if(c0(i).lt.0.000001) then
           c0(i)=0.000001
         end if
6       continue
c
c       if(mode.eq.4) then
c         call hydrotide(dvel,kn,tt,ustar)
c       end if
c
       do 12 i=2,ngrids
c*     settling velocity        *****
         ccc=abs((c0(i)-c0(i-1))/(c0(i)+c0(i-1)))
         if(ccc.gt.0.7) then
           cc=c0(i)
         else
         cc=(c0(i)+c0(i-1))/2.0
         end if
c        cc=(c0(i)+c0(i-1))/2.0
         if(cc.lt.wsc0) then
           ws(i)=(wsa*wsc0**wsn)/(wsc0*wsc0+wsb*wsb)**wsm
         else
           ws(i)=(wsa*cc**wsn)/(cc*cc+wsb*wsb)**wsm
         end if
```

```
c*   diffusion coefficient      *****
      if(mode.eq.1) then
       vcc=0.01
      elseif (mode.eq.2.) then
       vcc=0.0001
      elseif (mode.eq.3) then
       vcc=0.01
      end if
      vcc=0.001
      if(cc.lt.vcc.or.dvel(i).le.0.0)then
       ri=0.0
      else
       if((-c0(i)+c0(i-1)).lt.0.0) then
        ri=-0.5/dsk1
       else
        ri=(g/cc)*((-c0(i)+c0(i-1))/dz)/(dvel(i))**2.0
       end if
      end if
      ks(i)=kn(i)/(1.0+dsk1*ri)**dsk2
12    continue
c*   Bottom boundary condition       **********
     if(c(1).lt.wsc0) then
      wsbb=(wsa*wsc0**wsn)/(wsc0*wsc0+wsb*wsb)**wsm
     else
      wsbb=(wsa*c0(1)**wsn)/(c0(1)*c0(1)+wsb*wsb)**wsm
     end if
     if(mchoo.eq.1) then
        call bedflux1(wsbb,c0(1),ustar,fs)
     else
        call bedflux2(wsbb,c0(1),taubed,fs)
     end if
      eromas=eromas+fs*dt
c*   initial conditions            **********
     if(abs(tt).le.(st+1.0e-6)) then
      call result(tt,c,descr,FILEIN,taubed)
     end if
c*   implicit calculation          **********
```

```
      r(1)=-dt/(dz*dz)*ks(2)
      p(1)=1.0-r(1)
      c0t(1)=c0(1)+dt/dz*fs
      do 13 i=2,ngrids
       q(i-1)=r(i-1)-dt/dz*ws(i)
       r(i)=-dt/(dz*dz)*ks(i+1)
       p(i)=1.0-q(i-1)-r(i)
        c0t(i)=c0(i)
13    continue
      call stm(ngrids,c,c0t,p,q,r)
C*    output results              **********
      if(mmc.gt.0.0001) then
         if(abs(ctt-mmc).le.0.00001.and.tt.gt.0.00001) then
          call result(tt,c,descr,FILEIN,taubed)
          ctt=ctt-mmc
         end if
      else
         do i=1,idt
         if(abs(tt/60.0-ddtout(i)).lt.0.001) then
          call result(tt,c,descr,FILEIN,taubed)
         end if
         end do
      end if
      do 14 i=1,ngrids
       c0(i)=c(i)
14    continue
      if(tt.lt.mmt) then
      goto 999
      end if
      stop
      end
C
C     Following is program VESTSUB.FOR
C
C
C     Subroutine for tri-diagonal matrix equations **
C
```

```
      subroutine stm(n,x,z,a,b,c)
      dimension x(n),z(n),a(n),b(n),c(n)
      dimension y(500),p(500),q(500),r(500)
      q(1)=a(1)
      do 1 i=1,n-1
       r(i)=b(i)
       p(i)=c(i)/q(i)
       q(i+1)=a(i+1)-p(i)*b(i)
1     continue
      y(1)=z(1)
      do 2 i=1,n-1
       y(i+1)=z(i+1)-y(i)*p(i)
2     continue
      x(n)=y(n)/q(n)
      do 3 i=n-1,1,-1
       x(i)=(y(i)-r(i)*x(i+1))/q(i)
3     continue
      end
C
C              BEDFLUX Subroutine for Fluid Mud
C
      subroutine bedflux1(wsbb,c0bb,ustar,fs)
      real*8 dt
      real m0, kk, kkss, ustar
     common/com/h0,m0,g,pi,kk,rhow,visc,kkss,
     *          mode,ngrids,dz,dtrun,dtout,dt,stt,dps,mchoo
     common/mud/rhosed,rhom,ric,rig,dudb,ent0,enn
c
     if(rig.ge.ric) then
       fen=0.0
     else
       fen=rhom*ustar*ent0*(ric*ric/rig-rig)**enn
     end if
     fse=-1.0*dps*wsbb*c0bb
     fs=fen+fse
     return
     end
```

```
C
C               BEDFLUX Subroutine for Bed
C
      subroutine bedflux2(wsbb,c0bb,taubed,fs)
      real*8 dt, wtt
      real m0,kk,kkss
         real tauero0, gama
      common/com/h0,m0,g,pi,kk,rhow,visc,kkss,
     *          mode,ngrids,dz,dtrun,dtout,dt,stt,dps,mchoo
      common/mud/rhosed,rhom,ric,rig,dudb,ent0,enn
      common/bed/ dzb,taudep,bdp1,bdp2,rhbbar,phic,tcp1,tcp2,
     *           ersmax,erp1,erp2,tauero
c*      bed density          *****
      if(dzb.ge.m0) then
       write(*,*)'All the sediment at the bottom is eroded!'
     write(*,*)'Your bed depth is incorrect or time step is too large!'
       stop
      else if(dzb.lt.0.0) then
       rhob=rhbbar*bdp1
      else
       rhob=rhbbar*bdp1*((m0-dzb)/m0)**bdp2
      end if
c*      eosion shear strength     *****
      tauero=tcp1*(rhob/rhosed-phic)**tcp2
c*      Erosion or depsition rate        *****
      if(taubed.lt.taudep) then
       fs=-1.0*wsbb*c0bb*(1.0-taubed/taudep)
      else if(taubed.ge.tauero) then
c       fs=ersmax*exp(-erp1*tauero**erp2)*(taubed-tauero)
                tauero0=tcp1*(rhbbar*bdp1/rhosed-phic)**tcp2
                 gama=-tcp1*tcp2*rhbbar*bdp1*bdp2/rhosed/m0*
        *        ((m0-dzb)/m0)**(bdp2-1.0)*(rhob/rhosed-phic)**(tcp2-1.0)
                 fs=rhob*0.0012*(taubed-tauero0)
        *        *EXP(-gama*0.0007*(wtt-(stt*60)))
      else
      fs=0.0
      end if
```

```
c*      Bed change        ** ?????  ******
       dzbt=dzb+dt*fs/rhob
c         write (*,*) fs, wtt
       if(dzbt.le.m0) then
        dzb=dzbt
       else
        fs=(m0-dzb)*rhob/dt
        dzb=m0
       end if
          wtt=wtt+dt
       return
       end
C
C
       subroutine hydroflow2(dvel,kn,taubed)
       real*8 dt
       real m0, kk, kn, kkss
       dimension dvel(1), kn(1)
       common/com/h0,m0,g,pi,kk,rhow,visc,kkss,
     *          mode,ngrids,dz,dtrun,dtout,dt,stt,dps,mchoo
       common/flow/uu,qn
       kkss=3.15*100000.0*9.8**3.0*qn**6.0
       y0=kkss/30.1
       ff=8.0*9.8*qn**2.0/h0**(1.0/3.0)
       taubed=rhow*ff*uu**2.0/8.0
       do 2 i=2,ngrids+1
        z=(float(i-1))*dz
        dvel(i)=uu/z/(alog(h0/y0)-1.0)
        kn(i)=(kk*kk*uu)/(alog(h0/y0)-1.0)*z*(h0-z)/h0
2      continue
       return
       end
C
C      HYDRODYNAMICS Subroutine--WAVE for fluid mud
C
       subroutine hydrowave1(dvel,kn,rd)
```

```
      real*8 dt
      real m0, kk, kn, kkss, rd
      dimension dvel(1), kn(1)
     common/com/h0,m0,g,pi,kk,rhow,visc,kkss,
     *          mode,ngrids,dz,dtrun,dtout,dt,stt,dps,mchoo
     common/wave/wheight,wperiod,wdiffk,wlength,ub,wfric
     common/mud/rhosed,rhom,ric,rig,dudb,ent0,enn
c
      sig=2.0*3.14159265/wperiod
      qkk=(sig*sig)/9.8
1     qk=sig**2.0/(9.8*tanh(qkk*h0))
      if(abs(qk-qkk).gt.0.000001) then
       qkk=0.5*(qk+qkk)
       goto 1
      end if
      wnu=0.5*(qk+qkk)
      wlength=2.0*3.14159265/wnu
       wfr=2.0*pi/wperiod
      do 2 i=2,ngrids+1
       z=(float(i-1))*dz
       dvel(i)=wheight/2.0*wfr*wnu
     *          *sinh(wnu*z)/sinh(wnu*h0)
c      kn(i)=wdiffk*wfr*wheight**2.0*(sinh(wnu*z))**2.0
c     *                          /(2.0*(sinh(wnu*h0))**2.0)
      kn(i)=wdiffk*wfr*wheight**2.0*sinh(wnu*h0/(h0+rd)*(z+rd))
     *       *cosh(wnu*z)/(2.0*(sinh(wnu*h0))**2.0)
2     continue
      rig=g*(visc*wperiod)**0.5*(rhom-rhow)/rhow/(dudb*dudb)
      ub=sig/2.0*wheight/(sinh(wnu*h0))
      return
      end
C
C     HYDRODYNAMICS Subroutine--WAVE for bed
C
      subroutine hydrowave2(dvel,kn,taubed)
      real*8 dt
      real m0, kk, kn, kkss
```

```
      dimension dvel(1), kn(1)
     common/com/h0,m0,g,pi,kk,rhow,visc,kkss,
     *          mode,ngrids,dz,dtrun,dtout,dt,stt,dps,mchoo
     common/wave/wheight,wperiod,wdiffk,wlength,ub,wfric
      sig=2.0*3.14159265/wperiod
      qkk=(sig*sig)/9.8
1     qk=sig**2.0/(9.8*tanh(qkk*h0))
      if(abs(qk-qkk).gt.0.000001) then
       qkk=0.5*(qk+qkk)
       goto 1
      end if
      wnu=0.5*(qk+qkk)
      wlength=2.0*3.14159265/wnu
       wfr=2.0*pi/wperiod
      do 2 i=2,ngrids+1
       z=(float(i-1))*dz
       dvel(i)=wheight/2.0*wfr*wnu*sinh(wnu*z)/sinh(wnu*h0)
       kn(i)=wdiffk*wfr*wheight**2.0*(sinh(wnu*z))
     *        *cosh(wnu*z)/(2.0*(sinh(wnu*h0))**2.0)
2     continue
      taubed=rhow*wfric/2.0*(wheight/2.0*wfr/sinh(wnu*h0))**2.0
      return
      end
C
C     HYDRODYNAMICS Subroutine--WAVE + WEAK CURRENT
C                        for fluid mud
C     WAVE -- entrainment and WAVE + WEAK CURRENT -- diffusion
      subroutine wavecurrent1(dvel,kn,rd)
      real*8 dt
      real m0, kk, kn, kkss,knc,knw,rd
      dimension dvel(1), kn(1)
      dimension knc(500), knw(500), dvelc(500), dvelw(500)
     common/com/h0,m0,g,pi,kk,rhow,visc,kkss,
     *          mode,ngrids,dz,dtrun,dtout,dt,stt,dps,mchoo
     common/wave/wheight,wperiod,wdiffk,wlength,ub,wfric
     common/flow/uu,qn
     common/mud/rhosed,rhom,ric,rig,dudb,ent0,enn
```

```
c
      kkss=3.15*100000.0*9.8**3.0*qn**6.0
      y0=kkss/30.1
      do 1 i=2,ngrids+1
       z=(float(i-1))*dz
       aatt=alog(h0/y0)
       dvelc(i)=uu/z/(aatt-1.0)
       knc(i)=(kk*kk*uu)/(aatt-1.0)*z*(h0-z)/h0
1     continue
c
      sig=2.0*3.14159265/wperiod
      qkk=(sig*sig)/9.8
2     qk=sig**2.0/(9.8*tanh(qkk*h0))
      if(abs(qk-qkk).gt.0.000001) then
       qkk=0.5*(qk+qkk)
       goto 2
      end if
      wnu=0.5*(qk+qkk)
      wlength=2.0*3.14159265/wnu
       wfr=2.0*pi/wperiod
      do 3 i=2,ngrids+1
       z=(float(i-1))*dz
       dvelw(i)=wheight/2.0*wfr*wnu
     *          *sinh(wnu*h0/(h0+rd)*(z+rd))/sinh(wnu*h0)
c     kn(i)=wdiffk*wfr*wheight**2.0*(sinh(wnu*z))**2.0
c    *                          /(2.0*(sinh(wnu*h0))**2.0)
      knw(i)=wdiffk*wfr*wheight**2.0*sinh(wnu*h0/(h0+rd)*(z+rd))
     *       *cosh(wnu*z)/(2.0*(sinh(wnu*h0))**2.0)
      dvel(i)=dvelw(i)+dvelc(i)
      kn(i)=knw(i)+knc(i)
3     continue
      rig=g*(visc*wperiod)**0.5*(rhom-rhow)/rhow/(dudb*dudb)
      ub=sig/2.0*wheight/(sinh(wnu*h0))
      return
      end
C
C     HYDRODYNAMICS Subroutine--WAVE + WEAK CURRENT
```

```
C                       for bed
C
      subroutine wavecurrent2(dvel,kn,taubed)
      real*8 dt
      real m0, kk, kn, kkss,knc,knw
      dimension dvel(1), kn(1)
      dimension knc(500), knw(500), dvelc(500), dvelw(500)
     common/com/h0,m0,g,pi,kk,rhow,visc,kkss,
     *          mode,ngrids,dz,dtrun,dtout,dt,stt,dps,mchoo
     common/wave/wheight,wperiod,wdiffk,wlength,ub,wfric
     common/flow/uu,qn
c
      kkss=3.15*100000.0*9.8**3.0*qn**6.0
      y0=kkss/30.1
      do 1 i=2,ngrids+1
       z=(float(i-1))*dz
       aatt=alog(h0/y0)
       dvelc(i)=uu/z/(aatt-1.0)
       knc(i)=(kk*kk*uu)/(aatt-1.0)*z*(h0-z)/h0
1     continue
     ff=8.0*9.8*qn**2.0/h0**(1.0/3.0)
     taubedc=rhow*ff*uu**2.0/8.0
c
     sig=2.0*3.14159265/wperiod
     qkk=(sig*sig)/9.8
2     qk=sig**2.0/(9.8*tanh(qkk*h0))
     if(abs(qk-qkk).gt.0.000001) then
      qkk=0.5*(qk+qkk)
      goto 2
     end if
     wnu=0.5*(qk+qkk)
     wlength=2.0*3.14159265/wnu
     wfr=2.0*pi/wperiod

     do 3 i=2,ngrids+1
      z=(float(i-1))*dz
      dvelw(i)=wheight/2.0*wfr*wnu
```

```
     *          *sinh(wnu*z)/sinh(wnu*h0)
c      kn(i)=wdiffk*wfr*wheight**2.0*(sinh(wnu*z))**2.0
c     *                          /(2.0*(sinh(wnu*h0))**2.0)
       knw(i)=wdiffk*wfr*wheight**2.0*sinh(wnu*z)
     *       *cosh(wnu*z)/(2.0*(sinh(wnu*h0))**2.0)
       dvel(i)=dvelw(i)+dvelc(i)
       kn(i)=knw(i)+knc(i)
3      continue
       taubedw=rhow*wfric/2.0*(wheight/2.0*wfr/sinh(wnu*h0))**2.0
       taubed=taubedw+taubedc
       return
       end
cC
C
C          OUTPUT Subroutine
C
       subroutine result(tt,c,descr,FILEIN,taubed)
       character descr*60, FILEIN*30
       real*8 tt,dt
       real m0, kk, kkss
       dimension c(1)
      common/com/h0,m0,g,pi,kk,rhow,visc,kkss,
     *          mode,ngrids,dz,dtrun,dtout,dt,stt,dps,mchoo
      common/wave/wheight,wperiod,wdiffk,wlength,ub,wfric
      common/flow/uu,qn
      common/tide/qqn,umax,ptide
      common/mud/rhosed,rhom,ric,rig,dudb,ent0,enn
      common/mr/gg1,gg2,uu2
      common/out/wsc0,ws0,wsa,wsb,wsm,wsn,dsk1,dsk2
      common/cal/suspmas,eromas
      common/bed/ dzb,taudep,bdp1,bdp2,rhbbar,phic,tcp1,tcp2,
     *          ersmax,erp1,erp2,tauero
c
      if(abs(tt-stt*60.0).gt.0.01) goto 30
       WRITE(*,*) 'Program IN PROGRESS - DO NOT TOUCH KEYBOARD'
       WRITE(2,'(a30)') DESCR
       WRITE(2,*) 'Input Filename is: ', FILEIN
```

```
      WRITE(2,*) 'MODE =',mode, ' (1=Current, 2=Wave, 3=Wave+Cur)'
      WRITE(2,*) 'The time step used is: ', dt, ' (sec)'
      WRITE(2,*) 'Discretization Parameters Follow'
      WRITE(2,*) 'NGRIDS=',ngrids,' DTSEC=',dt,'(sec) DZ=',dz,'(m)'
      WRITE(2,*) 'Depth of Water (m) is:', h0
      WRITE(2,*) 'Depth of Bottom sediment(m) is:', m0
      WRITE(2,*) 'Fluid Mud Density (kg/m^3) is:',rhom
      WRITE(2,*) 'Water Density (kg/m^3) is:',rhow
      WRITE(2,*) 'Sediment Granular Density(kg/m^3) is:',rhosed
      WRITE(2,*) 'Settling Velocity Parameters Follow'
      WRITE(2,*) ' wsc0 ws0 wsa wsb wsm
     *  wsn'
      WRITE(2,'(6(1x,e10.3))') wsc0,ws0,wsa,wsb,wsm,wsn
      WRITE(2,*) 'Stabilized Diffusion Parameters Follow'
      WRITE(2,*) ' alpha0 beta0 '
      WRITE(2,'(2(2x,e12.4))') dsk1, dsk2
     if(mode.eq.1.or.mode.eq.3) then
      WRITE(2,*) 'Flow Hydrodynamic Parameters Follow'
      WRITE(2,*) 'Flow ave. velo.(m/s) , Manning`s coefficient'
      WRITE(2,'(2(10x,F10.4))') uu, qn
     end if
     if(mode.eq.2.or.mode.eq.3) then
     WRITE(2,*) 'Wave Hydrodynamic Parameters Follow'
     WRITE(2,*)'WHeight(m),WPeriod(s),WLength(m),WDiff Coef,WFric Coef'
     WRITE(2,'(5(e10.4,1x))')wheight,wperiod,wlength,wdiffk,wfric
     end if
c     if(mode.eq.3) then
c      WRITE(2,*) 'Tidal Hydrodynamic Parameters Follow'
c      WRITE(2,*) 'Max. Tidal Velocity, Tidal Period, Manning`s coefficient'
c      WRITE(2,'(3(1x,e10.4))') umax, ptide, qqn
c     end if
     if(mchoo.eq.1) then
      WRITE(2,*) 'Fluid mud Parameters Follow'
      WRITE(2,*) 'Mud Reological Parameters'
      WRITE(2,*) ' GG1 , GG2 , uu2 , DUDB '
      WRITE(2,'(4(1x,e10.4))') gg1,gg2,uu2,dudb
      WRITE(2,*) 'Entrainment Rate Coefficient Parameters Follow'
```

```
      WRITE(2,*) '  ent0   ,  enn   ,  entad'
      WRITE(2,'(3(1x,e10.4))') ent0, enn, ric*ric
      WRITE(2,*) 'Critical Global Richarson Number is:',ric
     else if(mchoo.eq.2) then
      WRITE(2,*) 'Bed Parameters Follow'
      WRITE(2,*) 'Bed Density Parameters Follow'
      WRITE(2,*) '  bdp1,    bdp2,     rhbbar'
      WRITE(2,'(3F10.4)') bdp1,bdp2,rhbbar
      WRITE(2,*) 'Bed Shear Strength '
      WRITE(2,*) '   phic ,   tcp1 ,   tcp2 '
      WRITE(2,'(3F10.4)') phic, tcp1, tcp2
      WRITE(2,*) 'Erosion Rate Parameters Follow'
      WRITE(2,*) '  ersmax  ,  erp1  ,  erp2  '
      WRITE(2,'(3F10.4)') ersmax, erp1, erp2
      WRITE(2,*) 'taudep = ', taudep, '(Pa)'
     else
     end if
30    suspmas = 0.0
      WRITE(*,*) 'Program in Progress: Time=',tt/60.0,'(min)'
      WRITE(2,*)
      WRITE(2,*) 'CONCENTRATIONS (kg/m^3) for time=',tt/60.0, '(min)'
      write(2,*) 'Elevation from bed      Concentrtion (kg/m^3)'
     do 11 i=ngrids,1,-1
      zz=(float(i)-0.5)*dz
      write(2,'(2(4x,f15.5))') zz, c(i)
      write(3,*) zz, c(i)
      suspmas=suspmas+c(i)*dz
11    continue
      WRITE(2,*)
     WRITE(2,*)'Total Sediment Now In Suspension: ',suspmas,' (kg/m^2)'
     WRITE(2,*)'Total Sediment Added From Bed Erosion: ',eromas,
    *' (kg/m^2)'
     if(mchoo.eq.1) then
      WRITE(2,*) 'Global Richarson Number :', rig
     else if(mchoo.eq.2) then
     WRITE(2,*)'Total Sediment Lost From Bed Deposition:', dzb, '(m)'
      WRITE(2,*) 'taubed = ', taubed, '(Pa), '
```

```
      WRITE(2,*) 'tauero = ', tauero, '(Pa)'
      else
      end if
9999  return
      end
C
C     VEST1>FOR
C
C
C     MAIN PROGRAM FOR WAVE-MUD INTERACTION
C
      subroutine prowmita(PWD1,PWD2,PDEN1,PDEN2,PWP,PAMP1,
     *                    PMU1,Puu,PGG1,PGG2,ip,RRR,rr2)
      integer ip
      real*4   PWD1,PWD2,PDEN1,PDEN2,PWP,PAMP1,
     *                    PMU1,Puu,PGG1,PGG2,RRR
c         REAL*8 V1(101),V2(101),V1S(101),V2S(101),
c     *      U1(101),U2(101),U1S(101),U2S(101),
c     *      P1(101),P2(101),P1S(101),P2S(101),
c     *      Z1(101),Z2(101)
c         REAL*8 VA1(101),VA2(101),VA1S(101),VA2S(101),
c     *      UA1(101),UA2(101),UA1S(101),UA2S(101),
c     *      PA1(101),PA2(101),PA1S(101),PA2S(101)
c      real*8 u1,u2

         REAL*8 DEN1,DEN2,WP,AMP1,SIGN,SIGN2,PI
         REAL*8 WD1,WD2,CRIT,WDY1,WDY2
         REAL*8 MU1,NU1
         REAL*8 GG1,GG2,UU2,AQ1,BQ0,BQ1

         COMPLEX*16 LSINH,LCOSH

         COMPLEX*16 A2,B2,C2,D2,E2,F2,G2,H2,AMP2,BAMP2
         COMPLEX*16 MU2,NU2
         COMPLEX*16 A1,B1,C1,D1,E1,F1,G1,H1,BAMP1,WN
         COMPLEX*16 VY1,VY2,UY1,UY2,PY1,PY2
c        COMPLEX*16 VY1S,VY2S,UY1S,UY2S,PY1S,PY2S
```

```
      COMPLEX*16 II,LAM1,LAM2,BET1,BET2

    PI=DACOS(-1.0D0)
      II=(0.0,1.0)
      SIGN=.1D1
      SIGN2=.1D1
      CRIT=1.0D-15

      WD1=DBLE(PWD1)
      WD2=DBLE(PWD2)
      DEN1=DBLE(PDEN1)
      DEN2=DBLE(PDEN2)
      WP=DBLE(PWP)
      AMP1=DBLE(PAMP1)
      MU1=DBLE(PMU1)
    GG1=DBLE(PGG1)
      GG2=DBLE(PGG2)
      uu2=dble(puu)

C     OPEN(1,FILE='LI.IN',STATUS='UNKNOWN')
C     READ(1,*)WD1,WD2,DEN1,DEN2,WP,AMP1,MU1,uu2,GG1,GG2,ip
C     CLOSE(1)

C***** MUD RHEOLOGICAL MODEL  ***************
    IF(PGG1.GE.0.0) THEN
      AQ1=uu2/(GG1+GG2)
      BQ0=(GG1*GG2)/(GG1+GG2)
      BQ1=(uu2*GG1)/(GG1+GG2)

      MU2=((6.2832D0/WP*(BQ1-BQ0*AQ1))
     *     +II*(BQ0+AQ1*BQ1*(6.2832D0/WP)**2.0))
     *    /(6.2832D0/WP*(1.0D0+(AQ1*6.2832D0/WP)**2.0))
    ELSE
    MU2=uu2+II*(GG2*dble(wp/(2.0*3.14159265)))
    END IF

      NU1=MU1/DEN1
```

```
      NU2=MU2/DEN2

C*****  CALL JIANG'S (1993) SUBROUTINE  ******************
      CALL CWAVE2ND(WD1,WD2,DEN1,DEN2,MU1,MU2,WP,AMP1,SIGN,
     #          SIGN2,WN,A1,B1,C1,D1,E1,F1,G1,H1,BAMP1,
     #          A2,B2,C2,D2,E2,F2,G2,H2,BAMP2,AMP2,CRIT)

c     OPEN(2,FILE='LI.OUT',STATUS='UNKNOWN')
c     WRITE(2,203)WN,A1,B1,C1,D1,E1,F1,G1,H1,BAMP1,
c    *          A2,B2,C2,D2,E2,F2,G2,H2,BAMP2,AMP2
c
c     WRITE(2,203)SIGN,SIGN2,WP,AMP1,WD1,WD2,
c    *            DEN1,DEN2,MU1,NU1,MU2,NU2
c203  FORMAT(2(3X,D15.9,3X,D15.9))

      LAM1=SIGN*(WN*WN-II*(0.62832D1/WP)/NU1)**0.5
      LAM2=SIGN*(WN*WN-II*(0.62832D1/WP)/NU2)**0.5
      BET1=SIGN2*(4.0D0*WN*WN-2.0D0*II*(0.62832D1/WP)/NU1)**0.5
      BET2=SIGN2*(4.0D0*WN*WN-2.0D0*II*(0.62832D1/WP)/NU2)**0.5

c     WRITE(2,204) LAM1,LAM2,BET1,BET2
c204  FORMAT(2(3X,D15.9,3X,D15.9))
c     CLOSE(2)
C*****************************************************************

      WDY1=dsqrt(nu1*wp/2.0d0/pi/2.0d0)
      WDY2=WD2
      UY1=II*(A1*LCOSH(WN*WDY1)+B1*LSINH(WN*WDY1)
     *   +C1*LAM1/WN*CDEXP(LAM1*(WDY1-WD1))
     *   -D1*LAM1/WN*CDEXP(-LAM1*WDY1))
      UY2=II*(E1*LCOSH(WN*WDY2)+F1*LSINH(WN*WDY2)
     *   +G1*LAM2/WN*CDEXP(LAM2*(WDY2-WD2))
     *   -H1*LAM2/WN*CDEXP(-LAM2*WDY2))
    rr2=sngl(cdabs(bamp1))

    WDY1=dsqrt(nu1*2.0d0*wp/2.0d0/pi)
      UY1=II*(A1*LCOSH(WN*WDY1)+B1*LSINH(WN*WDY1)
```

```
*     +C1*LAM1/WN*CDEXP(LAM1*(WDY1-WD1))
*     -D1*LAM1/WN*CDEXP(-LAM1*WDY1))
      RRR=SNGL(CDABS(UY1-UY2))

      RETURN
      END

      FUNCTION LSINH(X)
      COMPLEX*16 LSINH
      COMPLEX*16 X
      LSINH=(CDEXP(X)-CDEXP(-X))/0.2D1
      RETURN
      END

      FUNCTION LCOSH(X)
      COMPLEX*16 LCOSH
      COMPLEX*16 X
      LCOSH=(CDEXP(X)+CDEXP(-X))/0.2D1
      RETURN
      END
C
C   VEST2.FOR
C
C*************************************************************************C
C       This subroutine is solving for the coefficients:              C
C   A2,CB2,C2,D2,E2, F2,G2,H2,AMP2,B2 for second order solution       C
C       SH1=sinh(2*k*h1), CH1=cosh(2*k*h1)                            C
C       SH2=sinh(2*k*h2), CH2=cosh(2*k*h2)                            C
C       need subroutine  WNIST1.FOR                                   C
C       need subroutine  SINHCOSH.FOR                                 C
C*************************************************************************C
C
      SUBROUTINE CWAVE2ND(WD1,WD2,DEN1,DEN2,MU1,MU2,WP,AMP1,SIGN,
     #          SIGN2,WN,A1,B1,C1,D1,E1,F1,G1,H1,BAMP1,
     #          A2,B2,C2,D2,E2,F2,G2,H2,BAMP2,AMP2,CRIT)
C.....
      COMPLEX*16 Y1,Y2,Y3,Y4,Y5,Y6,Y7,Y8
```

```
      COMPLEX*16 W1,W2,W3,W4,W5,W6,W7,W8,W9,W10
      COMPLEX*16 W11,W12,W13,W14,W15,W16,W17,W18,W19,W20
     COMPLEX*16 W21,W22,W23,W24,W25,W26,W27
      COMPLEX*16 A2,B2,C2,D2,E2,F2,G2,H2,AMP2,BAMP2
      COMPLEX*16 BETA1,BETA2,SH1,SH2,CH1,CH2,SINH1,SINH2,COSH1,COSH2
      COMPLEX*16 AN1,AN2,DA1,DA2
      COMPLEX*16 A1,B1,C1,D1,E1,F1,G1,H1,BAMP1,WN,DWN
      REAL*8 DEN1,DEN2,WP,SMA,AMP1,SIGN,SIGN2
      REAL*8 WD1,WD2,WD,DWD1,DWD2,CRIT
      REAL*8 MU1,NU1,RBAMP1,RBAMP2,RAMP2
      COMPLEX*16 MU2,NU2
C.....
C     OPEN(UNIT=10,FILE='OUT.DAT',STATUS='NEW')
C.....
      WD=WD1+WD2
      NU1=MU1/DEN1
      NU2=MU2/DEN2
      SMA=.628D1/WP
C.....
      CALL WN1ST1(WD1,WD2,DEN1,DEN2,MU1,MU2,WP,AMP1,SIGN,
     #     WN,A1,B1,C1,D1,E1,F1,G1,H1,BAMP1,CRIT)
C.....
C     PRINT *,'SIGN2='
C     READ *,SIGN2
      DWN=(.2D1,0.)*WN
      BETA1=SIGN2*CDSQRT(DWN**2-(0.,.2D1)*SMA/NU1)
      BETA2=SIGN2*CDSQRT(DWN**2-(0.,.2D1)*SMA/NU2)
C.....
      AN1=(0.,.1D1)*DEN1*SMA/WN-(.4D1,0.)*WN*MU1
      AN2=(0.,.1D1)*DEN2*SMA/WN-(.4D1,0.)*WN*MU2
C.....
      DWD1=.2D1*WD1
      DWD2=.2D1*WD2
      CALL SINHCOSH(WN,DWD1,SH1,CH1)
      CALL SINHCOSH(WN,DWD2,SH2,CH2)
      CALL SINHCOSH(WN,WD1,SINH1,COSH1)
      CALL SINHCOSH(WN,WD2,SINH2,COSH2)
```

```
      DA1=SIGN*CDSQRT(WN**2-(0.,.1D1)*SMA/NU1)
      DA2=SIGN*CDSQRT(WN**2-(0.,.1D1)*SMA/NU2)
C.....
      Y1=AMP1*(WN*A1*COSH1+WN*B1*SINH1+DA1*C1)
      Y2=AMP1*MU1*(((.2D1,0.)+DA1**2/WN**2)*(WN**2*(
     #  A1*SINH1+B1*COSH1)+DA1**2*C1)-(WN**2*(
     #  A1*SINH1+B1*COSH1)+DA1**4*C1/WN**2))
      Y3=-(.2D1,0.)*AMP1*((.2D1,0.)*WN**3*(A1*COSH1+
     #  B1*SINH1)+DA1*(WN**2+DA1**2)*C1)
      Y4=BAMP1*(WN*A1-DA1*D1)
      Y5=(.2D1,0.)*BAMP1*(WN**2*(E1*SINH2+F1*COSH2)+
     #  DA2**2*G1-WN**2*B1-DA2**2*D1)
      Y6=AMP1*(WN*(E1*COSH2-F1*SINH2)+DA2*G1-WN*A1+DA1*D1)
      Y7=AMP1*(-MU2*(WN**2+DA2**2)*(E1*SINH2+F1*COSH2)-
     #  MU2*(.2D1,0.)*DA2**2*G1+MU1*(WN**2+DA1**2)*B1
     #  +(.2D1,0.)*MU1*DA1**2*D1)
      Y8=AMP1*(MU2*((.4D1,0.)*WN**3*(E1*COSH2+F1*SINH2)+
     #  (.2D1,0.)*DA2*(DA2**2+WN**2)*G1)-MU1*((.4D1,0.)*
     #  WN**3*A1-(.2D1,0.)*DA1*(DA1**2+WN**2)*D1))
C.....
      W1=BETA2*SH1/DWN-CH1
      W2=BETA2*CH2-DWN*SH2
C.....
      W3=AN1*CH1-(0.,.1D1)*DEN1*.98D1*SH1/SMA/(.2D1,0.)
      W4=AN1*SH1-(0.,.1D1)*DEN1*.98D1*CH1/SMA/(.2D1,0.)
C.....
      W5=DWN*((.2D1,0.)*MU1*BETA1+(0.,.1D1)*
     #  DEN1*.98D1/SMA/(.2D1,0.))
      W6=(W2*W3+DWN*W1*W4)/W5
      W7=BETA2*W3/W5
      W8=(BETA1*W3-DWN*W4)/W5
      W9=(W3*Y5+DWN*W4*Y6-DWN*(Y2+
     #  (0.,.1D1)*DEN1*.98D1*Y1/SMA/(.2D1,0.)))/W5
C.....
      W10=(.8D1,0.)*WN**2*(W2*SH1/DWN+W1*CH1)+
     #  W6*(BETA1**2+DWN**2)
      W11=(.8D1,0.)*WN**2*BETA2*SH1/DWN+
```

```
     #    W7*(BETA1**2+DWN**2)
          W12=(.8D1,0.)*WN**2*(BETA1*SH1/DWN-CH1)+
     #    W8*(BETA1**2+DWN**2)
          W13=Y3-(.8D1,0.)*WN**2*(SH1*Y5/DWN+CH1*Y6)
     #    -W9*(BETA1**2+DWN**2)
C.....
          W14=W2*AN1/DWN-BETA2*AN2*CH2/DWN+
     #    AN2*SH2+(0.,.1D1)*(DEN2-DEN1)*.98D1*W1/SMA/(.2D1,0.)
          W15=BETA2*AN1/DWN+(.2D1,0.)*MU2*BETA2*AN2
          W16=BETA1*AN1/DWN+(.2D1,0.)*MU1*BETA1
          W17=Y7-(0.,.1D1)*(DEN2-DEN1)*.98D1*(Y6+Y4)/SMA/(.2D1,0.)
     #    -AN1*Y5/DWN
C.....
          W18=(.8D1,0.)*MU1*WN**2*W1-(.8D1,0.)*MU2*WN**2*(BETA2
     #    *SH2/DWN-CH2)
          W19=-(.8D1,0.)*MU2*WN**2*(BETA2**2+DWN**2)
          W20=MU1*(BETA1**2-DWN**2)
          W21=Y8-(.8D1,0.)*MU1*Y6*WN**2
C.....
          W22=W11*W14-W15*W10
          W23=W12*W14-W16*W10
          W24=W13*W14-W17*W10
          W25=W11*W18-W19*W10
          W26=W12*W18-W20*W10
          W27=W13*W18-W21*W10
C.....
          D2=(W24*W25-W27*W22)/(W23*W25-W26*W22)
          G2=(W24-W23*D2)/W22
          H2=(W13-W11*G2-W12*D2)/W10
C.....
          F2=-H2
          E2=BETA2*H2/DWN
          BAMP2=(0.,.1D1)*(W1*H2+Y6+Y4)/SMA/(.2D1,0.)
          B2=W1*H2-D2+Y6
          A2=(H2*W2+BETA2*G2+BETA1*D2+Y5)/DWN
          C2=W6*H2+W7*G2+W8*D2+W9
          AMP2=(0.,.1D1)*(A2*SH1+B2*CH1+C2+Y1)/SMA/(.2D1,0.)
```

```
C.....
      RBAMP1=DREAL(BAMP1)
      RBAMP2=DREAL(BAMP2)
      RAMP2=DREAL(AMP2)
C     WRITE(10,140) WD1,WD2,WP,DEN1,DEN2,MU1,MU2
C     WRITE(10,150) WN
C     WRITE(10,200) AMP1,RBAMP1
C     WRITE(10,300) RAMP2,RBAMP2
140   FORMAT(2X,'WD1=',F10.5,2X,'WD2=',F10.5,2X,'WP=',F10.5,2X,
     #      'DEN1=',F10.5,2X,'DEN2=',F10.5,2X,'MU1=',F10.5,2X,
     #    'MU2=',F10.5)
150   FORMAT(2X,'WAVE NUMBER=',F10.6,5X,F10.6)
200   FORMAT(2X,'AMP1=',F10.5,5X,'BAMP1=',F10.6)
300   FORMAT(2X,'AMP2=',F10.6,5X,'BAMP2=',F10.6)
C.....
      RETURN
      END
C
C**************************************************************************C
C     WN1ST1.FOR                                                 C
C     The solutions to second-order wave over soft mud are       C
C   composed of two parts: first order part and second           C
C     order part. This program is for solving (complex) wave number  C
C    using the secant method, and all coefficients               C
C   A1,CB1,C1,D1,E1,F1,G1,H1,B1 for the first part.              C
C   Units are in Metric system, Double precision                 C
C     Need subroutines AIRY,FUNC1ST1,SINHCOSH.                   C
C**************************************************************************C
      SUBROUTINE WN1ST1(WD1,WD2,DEN1,DEN2,MU1,MU2,WP,AMP1,SIGN,
     #          WN,A1,B1,C1,D1,E1,F1,G1,H1,SAMP1,CRIT)
C.....
      COMPLEX*16 WFUN1,WFUNX,WN1,WN2,WN,DX
      COMPLEX*16 X,FOLD,FNEW,TED,TEG,TEH
      COMPLEX*16 A1,B1,C1,D1,E1,F1,G1,H1,SAMP1
      COMPLEX*16 DA1,DA2,SINH1,COSH1,SINH2,COSH2
      REAL*8 WP,SMA,WD1,WD2,DEN1,DEN2,WDTEP
      REAL*8 WD,MU1,NU1,AMP1,SIGN,CRIT
```

```
      COMPLEX*16 MU2,NU2
C.....
      WD=WD1+WD2        ! TOTAL DEPTH
      NU1=MU1/DEN1
      NU2=MU2/DEN2
      SMA=.628D1/WP
C.....
      WDTEP=WD1+WD1          ! FOR ITERATION PURPOSE
      CALL AIRY(WP,WD1,WN1)          !WN1>WN2
      CALL AIRY(WP,WDTEP,WN2)
C     CALL AIRY(WP,WD,WN2)
C     PRINT *,'WN1=',WN1
C     PRINT *,'WN2=',WN2
C.....
      DX=WN2-WN1
      X=WN2
      CALL FUNC1ST1(WD1,WD2,DEN1,DEN2,MU1,MU2,WP,SIGN,
     #          AMP1,WN1,WFUN1,TED,TEG,TEH,H1,
     #          DA1,DA2,SINH1,COSH1,SINH2,COSH2)
      FOLD=WFUN1
      N=0
100   CALL FUNC1ST1(WD1,WD2,DEN1,DEN2,MU1,MU2,WP,SIGN,
     #          AMP1,X,WFUNX,TED,TEG,TEH,H1,
     #          DA1,DA2,SINH1,COSH1,SINH2,COSH2)
      N=N+1
      IF(N.GT.100) GO TO 200
      FNEW=WFUNX
      DX=-FNEW*DX/(FNEW-FOLD)
      X=X+DX
C     PRINT *,'N=',N,',   ','WAVE NUMBER=',X
      IF(CDABS(DX).GT.CRIT) THEN
       FOLD=FNEW
       GO TO 100
      ENDIF
C.....
200   WN=X
C.....
```

```
      PRINT *,'N=',N
      D1=TED*H1
      G1=-TEG*H1
      F1=-H1
      E1=DA2*H1/WN
      SAMP1=(0.,.1D1)*(E1*SINH2+F1*COSH2+G1)/SMA
C       FIRST ORDER INTERFACIAL AMPLITUDE
      B1=E1*SINH2+F1*COSH2+G1-D1
      A1=(E1*WN*COSH2+F1*WN*SINH2+G1*DA2+D1*DA1)/WN
      C1=-(.2D1,0.)*NU1*AMP1*WN**2
C.....
      RETURN
      END
C
C
C*****************************************************************C
C   The following approximate solution to the dispersion    C
C   relation was proposed by Hunt (1979)                C
C   Units are in Metric System                          C
C*****************************************************************C
    SUBROUTINE AIRY(PERIOD,DEPTH,WN)
    COMPLEX*16 WN
    REAL*8 GRAV,SUM,PERIOD,DEPTH,Y,CGM,DUM,D(10),KH
    GRAV=.98D1
    CGM=.62832D1/PERIOD
    Y=CGM**2*DEPTH/GRAV
    D(1)=0.066666666D1
    D(2)=0.035555555D1
    D(3)=0.01608465608D1
    D(4)=0.00632098765D1
    D(5)=0.00217540484D1
    D(6)=0.00065407983D1
    SUM=.1D1
C.....
    DO J=1,6
    DUM=Y**J
    SUM=SUM+D(J)*DUM
```

```
      END DO
C.....
C     KH=SQRT(Y**2+Y/SUM)
      KH=DSQRT(Y**2+Y/SUM)
      WN=KH/DEPTH
C.....
      RETURN
      END
C
C*********************************************************************C
C*    This subroutine is for preparing the function for the     *C
C*    secant method for solving the first order problem         *C
C*    Units are in Metric system, Double precision              *C
C*    Input information:                                        *C
C*      WD1=WATER DEPTH IN UPPER LAYER                          *C
C*      WD2=WATER DEPTH IN LOWER LAYER                          *C
C*      DEN1=DENSITY IN UPPER LAYER                             *C
C*      DEN2=DEMSITY IN LOWER LAYER                             *C
C*      MU1=DYNAMIC VISCOSITY IN UPPER LAYER                    *C
C*      MU2=DYNAMIC VISCOSITY IN LOWER LAYER                    *C
C*      WP=INCOMING WAVE PERIOD                                 *C
C*      AMPL1=FIRST ORDER WAVE AMPLITUDE                        *C
C*      WN=WAVE NUMBER (COMPLEX)                                *C
C*      RETURNED INFORMATION:                                   *C
C*      FUNCTION WHICH WILL BE USED FOR SECANT THE METHOD       *C
C*********************************************************************C
      SUBROUTINE FUNC1ST1(WD1,WD2,DEN1,DEN2,MU1,MU2,WP,SIGN,
     #          AMP1,WN,WFUN,TED,TEG,TEH,H1,
     #          DA1,DA2,SINH1,COSH1,SINH2,COSH2)
C.....
      COMPLEX*16 DA1,DA2,S2,Q2,TED,TEG,TEH,WN
      COMPLEX*16 AM1,AM2,SINH1,SINH2,COSH1,COSH2
      COMPLEX*16 WFUN,H1
      REAL*8 WP,SMA,WD1,WD2,DEN1,DEN2,NU1
      REAL*8 MU1,AMP1,SIGN
      COMPLEX*16 MU2,NU2
C.....
```

```
      NU1=MU1/DEN1
      NU2=MU2/DEN2
      SMA=.628D1/WP
C.....
      CALL SINHCOSH(WN,WD1,SINH1,COSH1)
      CALL SINHCOSH(WN,WD2,SINH2,COSH2)
C.....
      DA1=SIGN*CDSQRT(WN**2-(0.,0.1D1)*SMA/NU1)  ! `+' OR `-'
      DA2=SIGN*CDSQRT(WN**2-(0.,0.1D1)*SMA/NU2)
      S2=SINH2-COSH2*DA2/WN
      Q2=COSH2-SINH2*DA2/WN
      AM1=(0.,.1D1)*SMA*DEN1/WN-.2D1*WN*MU1
      AM2=(0.,.1D1)*SMA*DEN2/WN-.2D1*WN*MU2
      TEG=(.2D1*DA1*(MU2*Q2-MU1*Q2)+
     #     (AM2-AM1)*S2-(0.,.1D1)*(DEN2-DEN1)*.98D1*Q2
     #    /SMA)/(.2D1*MU1*DA1+DA2*AM1/WN
     # +.2D1*MU2*DA2+(0.,.1D1)*(DEN2-DEN1)*.98D1/SMA
     # -DA1*MU2*(DA2**2+WN**2)/WN/WN)
      TED=(.2D1*WN**2*(MU2*Q2-MU1*Q2)-TEG*
     #    (.2D1*MU1*WN**2-MU2*(DA2**2+
     #     WN**2)))/SMA/DEN1/(0.,.1D1)
      TEH=(DA1*COSH1/WN-SINH1)*TED-
     #    TEG*(DA2*COSH1/WN+SINH1)-
     #    S2*COSH1-Q2*SINH1
      H1=(DEN1*.98D1*AMP1-.4D1*DEN1*(NU1**2)*AMP1*
     #   (WN**2)*DA1)/AM1/TEH
C.....
      WFUN=(DA1*SINH1/WN-COSH1)*TED*H1-
     #    (DA2*SINH1/WN+COSH1)*TEG*H1-
     #    (S2*SINH1+Q2*COSH1)*H1+
     #    AM1*WN*AMP1/DEN1
C.....
      RETURN
      END

C*******************************************************C
C    This subroutine is for calculation of functions    C
```

```
C      sinh(x) and cosh(x) with double precision       C
C      complex variables                               C
C*************************************************************C
       SUBROUTINE SINHCOSH(WN,WD,SINHX,COSHX)
       COMPLEX*16 XKH,WN,TEMP1,TEMP2,SINHX,COSHX
       REAL*8 WD
C.....
       XKH=WN*WD
       TEMP1=CDEXP(XKH)
       TEMP2=CDEXP(-XKH)
       SINHX=(TEMP1-TEMP2)/.2D1
       COSHX=(TEMP1+TEMP2)/.2D1
C      PRINT *,'KH=',XKH,',   ','COSH(KH)=',COSHX
C.....
       RETURN
       END
C.....
```

Subroutine for incorporating electrochemical force

```
subroutine bedflux2(wsbb,c0bb,taubed,fs)
      real*8 dt
      real m0,kk,kkss
      common/com/h0,m0,g,pi,kk,rhow,visc,kkss,
     *        mode,ngrids,dz,dtrun,dtout,dt,stt,dps,mchoo
      common/mud/rhosed,rhom,ric,rig,dudb,ent0,enn
      common/bed/ dzb,taudep,bdp1,bdp2,rhbbar,phic,tcp1,tcp2,
     *         ersmax,erp1,erp2,tauero
c*      bed density          *****
      if(dzb.ge.m0) then
       write(*,*)'All the sediment at the bottom is eroded!'
     write(*,*)'Your bed depth is incorrect or time step is too large!'
       stop
      else if(dzb.lt.0.0) then
       rhob=rhbbar*bdp1
      else
       rhob=rhbbar*bdp1*((m0-dzb)/m0)**bdp2
      end if
```

```
c*      eosion shear strength     *****
       tauero=tcp1*(rhob/rhosed-phic)**tcp2
c*      Erosion or depsition rate        *****
       if(taubed.lt.taudep) then
        fs=-1.0*wsbb*c0bb*(1.0-taubed/taudep)
       else if(taubed.ge.tauero) then
        fs=ersmax*exp(-erp1*tauero**erp2)*(taubed-tauero)
       else
       fs=0.0
       end if
c*      Bed change        ** ?????  ******
       dzbt=dzb+dt*fs/rhob
       if(dzbt.le.m0) then
        dzb=dzbt
       else
        fs=(m0-dzb)*rhob/dt
        dzb=m0
       end if
       return
       end
```

C.1- Subroutine for incorporating the electrochemical force

```
       subroutine bedflux2(wsbb,c0bb,taubed,fs)
       real*8 dt
       real m0,kk,kkss
          real s,eta
       common/com/h0,m0,g,pi,kk,rhow,visc,kkss,
     *         mode,ngrids,dz,dtrun,dtout,dt,stt,dps,mchoo
       common/mud/rhosed,rhom,ric,rig,dudb,ent0,enn
       common/bed/ dzb,taudep,bdp1,bdp2,rhbbar,phic,tcp1,tcp2,
     *           ersmax,erp1,erp2,tauero, betta
c*      bed density          *****
       if(dzb.ge.m0) then
        write(*,*)'All the sediment at the bottom is eroded!'
      write(*,*)'Your bed depth is incorrect or time step is too large!'
        stop
       else if(dzb.lt.0.0) then
```

```
      rhob=rhbbar*bdp1
     else
      rhob=rhbbar*bdp1*((m0-dzb)/m0)**bdp2
     end if
c*     eosion shear strength     *****
c      tauero=tcp1*(rhob/rhosed-phic)**tcp2
                  s=rhosed /rhow
                  eta= tcp1/((s-1)*9.81*phic**3)**0.5
        tauero=0.05+betta/(3.1415/6/(1+32*s*tcp2*eta**(-0.4))**3-1)**2

c*     Erosion or depsition rate        *****
     if(taubed.lt.taudep) then
      fs=-1.0*wsbb*c0bb*(1.0-taubed/taudep)
     else if(taubed.ge.tauero) then
      fs=ersmax*exp(-erp1*tauero**erp2)*(taubed-tauero)
     else
     fs=0.0
     end if
c*     Bed change        ** ?????  ******
     dzbt=dzb+dt*fs/rhob
     if(dzbt.le.m0) then
      dzb=dzbt
     else
      fs=(m0-dzb)*rhob/dt
      dzb=m0
     end if
     return
     end
```

C.2- Subroutine for incorporating the vane shear stress

```
     subroutine bedflux2(wsbb,c0bb,taubed,fs)
     real*8 dt
     real m0,kk,kkss
        real a1,b1,c1
     common/com/h0,m0,g,pi,kk,rhow,visc,kkss,
    *         mode,ngrids,dz,dtrun,dtout,dt,stt,dps,mchoo
     common/mud/rhosed,rhom,ric,rig,dudb,ent0,enn
```

```
      common/bed/ dzb,taudep,bdp1,bdp2,rhbbar,phic,tcp1,tcp2,
     *            ersmax,erp1,erp2,tauero
c*      bed density          *****
      if(dzb.ge.m0) then
       write(*,*)'All the sediment at the bottom is eroded!'
     write(*,*)'Your bed depth is incorrect or time step is too large!'
       stop
      else if(dzb.lt.0.0) then
       rhob=rhbbar*bdp1
      else
       rhob=rhbbar*bdp1*((m0-dzb)/m0)**bdp2
      end if
c*      eosion shear strength     *****
        a1=(1.0+3.0*(1+cosd(tcp1)))*tcp2/9.81/(rhosed-rhow)/phic
     b1=9.81*(rhosed-rhow)*phic**3*(tand(tcp1))**(2.0)
        * /240.0/rhow/visc**(2.0)
     c1=40.0*rhow*visc**(2.0)/tand(tcp1)/phic**(2.0)
     tauero=c1*(sqrt(b1*a1+1.0)-1.0)
c*      Erosion or depsition rate        *****
      if(taubed.lt.taudep) then
       fs=-1.0*wsbb*c0bb*(1.0-taubed/taudep)
      else if(taubed.ge.tauero) then
       fs=ersmax*exp(-erp1*tauero**erp2)*(taubed-tauero)
      else
      fs=0.0
      end if
c*      Bed change        ** ?????  ******
      dzbt=dzb+dt*fs/rhob
      if(dzbt.le.m0) then
       dzb=dzbt
      else
       fs=(m0-dzb)*rhob/dt
       dzb=m0
      end if
      return
      end
C
```

C.3- Subroutine for incorporating Jonnson (1966) formula for the wave friction factor

```
      subroutine hydrowave2(dvel,kn,taubed)
      real*8 dt
      real m0, kk, kn, kkss

         real delta

      dimension dvel(1), kn(1)
     common/com/h0,m0,g,pi,kk,rhow,visc,kkss,
     *          mode,ngrids,dz,dtrun,dtout,dt,stt,dps,mchoo
     common/wave/wheight,wperiod,wdiffk,wlength,ub,wfric, wK_s
      sig=2.0*3.14159265/wperiod
      qkk=(sig*sig)/9.8
1     qk=sig**2.0/(9.8*tanh(qkk*h0))
      if(abs(qk-qkk).gt.0.000001) then
       qkk=0.5*(qk+qkk)
       goto 1
      end if
      wnu=0.5*(qk+qkk)
      wlength=2.0*3.14159265/wnu
       wfr=2.0*pi/wperiod
      do 2 i=2,ngrids+1
       z=(float(i-1))*dz
       dvel(i)=wheight/2.0*wfr*wnu*sinh(wnu*z)/sinh(wnu*h0)
       kn(i)=wdiffk*wfr*wheight**2.0*(sinh(wnu*z))
     *        *cosh(wnu*z)/(2.0*(sinh(wnu*h0))**2.0)
2     continue

         delta=6.5*(visc*wperiod/2.0/3.141592)**0.5
     wfric=0.0604/Alog10((30.0*delta/wK_s)**(2.0))

      taubed=rhow*wfric/2.0*(wheight/2.0*wfr/sinh(wnu*h0))**2.0
      return
      end
```

C.4- Subroutine for incorporating Swart (1974) formula for the wave friction factor

```
      real*8 dt
      real m0, kk, kn, kkss

c       real delta, k_s

      dimension dvel(1), kn(1)
     common/com/h0,m0,g,pi,kk,rhow,visc,kkss,
     *          mode,ngrids,dz,dtrun,dtout,dt,stt,dps,mchoo
     common/wave/wheight,wperiod,wdiffk,wlength,ub,wfric, wK_s
      sig=2.0*3.14159265/wperiod
      qkk=(sig*sig)/9.8
1     qk=sig**2.0/(9.8*tanh(qkk*h0))
      if(abs(qk-qkk).gt.0.000001) then
       qkk=0.5*(qk+qkk)
       goto 1
      end if
      wnu=0.5*(qk+qkk)
      wlength=2.0*3.14159265/wnu
       wfr=2.0*pi/wperiod
      do 2 i=2,ngrids+1
       z=(float(i-1))*dz
       dvel(i)=wheight/2.0*wfr*wnu*sinh(wnu*z)/sinh(wnu*h0)
       kn(i)=wdiffk*wfr*wheight**2.0*(sinh(wnu*z))
     *       *cosh(wnu*z)/(2.0*(sinh(wnu*h0))**2.0)
2     continue

         ub=sig/2.0*wheight/(sinh(wnu*h0))
         wfric= exp(-5.977+5.213*(ub/sig/wK_s)**(-0.194))

      taubed=rhow*wfric/2.0*(wheight/2.0*wfr/sinh(wnu*h0))**2.0
      return
      end
```

C.5- Subroutine for incorporating Le Roux (2003) formula for the wave friction factor

```
      subroutine hydrowave2(dvel,kn,taubed)
      real*8 dt
      real m0, kk, kn, kkss
           real Dd, mu, Wds, beta, tetawc, a1, Uwcr
      dimension dvel(1), kn(1)
     common/com/h0,m0,g,pi,kk,rhow,visc,kkss,
     *          mode,ngrids,dz,dtrun,dtout,dt,stt,dps,mchoo
     common/wave/wheight,wperiod,wdiffk,wlength,ub,wfric,wD
          common/mud/rhosed,rhom,ric,rig,dudb,ent0,enn
      sig=2.0*3.14159265/wperiod
      qkk=(sig*sig)/9.8
1     qk=sig**2.0/(9.8*tanh(qkk*h0))
      if(abs(qk-qkk).gt.0.000001) then
       qkk=0.5*(qk+qkk)
       goto 1
      end if
      wnu=0.5*(qk+qkk)
      wlength=2.0*3.14159265/wnu
       wfr=2.0*pi/wperiod
      do 2 i=2,ngrids+1
       z=(float(i-1))*dz
       dvel(i)=wheight/2.0*wfr*wnu*sinh(wnu*z)/sinh(wnu*h0)
       kn(i)=wdiffk*wfr*wheight**2.0*(sinh(wnu*z))
     *       *cosh(wnu*z)/(2.0*(sinh(wnu*h0))**2.0)
2     continue

         mu=rhow*visc
         Dd=wD*(rhow*g*(rhosed-rhow)/mu**2.0)**(1.0/3.0)
         if (Dd<=1.2538) then
                 Wds=(0.2354*Dd)**(2.0)
         else if (Dd> 1.2538 .AND. Dd<=2.9074) then
                 Wds=(0.208*Dd-0.0652)**(1.5)
         else if (Dd>2.9074 .AND. Dd<=22.9866) then
                 Wds=(0.2636*Dd-0.37)
```

```
    else if (Dd>22.9866 .AND. Dd<=134.92150) then
            Wds=(0.8255*Dd-5.4)**(2.0/3.0)
    else if (Dd>134.92150 .AND. Dd<=1750) then
            Wds=(2.531*Dd+160)**(0.5)
    else
            Write (*,*) 'There is something wrong with your input data!!!'
    stop
    end if

    ! ****calculating Shield parameter****

    if (Wds<=2.5) then
            beta= -0.717*log10(Wds)+0.0625
    else if (Wds>2.5 .AND. Wds<=11) then
            beta= 0.0171*log10(Wds)+0.0272
    else
            beta=0.045
    end if

    tetawc=0.0246*Wds**(-0.55)
    a1=(tetawc*g*wD*(rhosed-rhow)/(rhow*mu/wperiod)**(0.5))*100.0
    Uwcr=(-0.01*a1**(2.0)+1.3416*a1-0.6485)/100.0


    ! ****calculating wave friction factor****

    wfric=(2.0)*beta*g*(rhosed-rhow)*wD/Uwcr**(2.0)/rhow

taubed=rhow*wfric/2.0*(wheight/2.0*wfr/sinh(wnu*h0))**2.0
return
end
```